EXPERIMENTAL VERIFICATION OF DISCRETE-ELEMENT SOLUTIONS FOR PLATES AND PAVEMENT SLABS

by

Sohan L. Agarwal
W. Ronald Hudson

Research Report Number 56-15

Development of Methods for Computer Simulation
of Beam-Columns and Grid-Beam and Slab Systems

Research Project 3-5-63-56

conducted for

The Texas Highway Department

in cooperation with the
U. S. Department of Transportation
Federal Highway Administration
Bureau of Public Roads

by the

CENTER FOR HIGHWAY RESEARCH
THE UNIVERSITY OF TEXAS AT AUSTIN

APRIL 1970

The opinions, findings, and conclusions expressed in this publication are those of the authors and not necessarily those of the Bureau of Public Roads.

PREFACE

Research Report No. 56-15 describes a series of test programs for an experimental study of plates and slabs for the verification of the discrete-element solution. It is the fifteenth in a series of reports on the work in Research Project 3-5-63-56, "Development of Methods for Computer Simulation of Beam-Columns and Grid-Beam and Slab Systems." It is the first report dealing with experimental verification based on the results of carefully controlled tests, and considers plates on rigid supports under a variety of load and stiffness conditions and a slab on a clay subgrade under two loading conditions. Results of static loading on the plates and slab are presented as well as experimental results of some cyclic loadings on the slab together with a preliminary interpretation of the data.

Our thanks are extended to Professor Hudson Matlock for his suggestions at various stages of the work, Messrs. Harold H. Dalyrmple and Fred Koch for their help in instrumentation, and Mr. Marlin Bakke for the fabrication of the necessary test equipment.

We are grateful to the entire staff of the Center for Highway Research at The University of Texas, who provided support during the preparation of this report. Particular thanks are due Mrs. Joye Linkous for typing the drafts of the manuscript and Mr. Art Frakes for his great pains in coordinating the report preparation.

We wish to thank the sponsors of this research study, the Texas Highway Department and the U. S. Department of Transportation Bureau of Public Roads, for their support and assistance.

Sohan L. Agarwal
W. Ronald Hudson

August 1969

LIST OF REPORTS

Report No. 56-1, "A Finite-Element Method of Solution for Linearly Elastic Beam-Columns" by Hudson Matlock and T. Allan Haliburton, presents a finite-element solution for beam-columns that is a basic tool in subsequent reports.

Report No. 56-2, "A Computer Program to Analyze Bending of Bent Caps" by Hudson Matlock and Wayne B. Ingram, describes the application of the beam-column solution to the particular problem of bent caps.

Report No. 56-3, "A Finite-Element Method of Solution for Structural Frames" by Hudson Matlock and Berry Ray Grubbs, describes a solution for frames with no sway.

Report No. 56-4, "A Computer Program to Analyze Beam-Columns under Movable Loads" by Hudson Matlock and Thomas P. Taylor, describes the application of the beam-column solution to problems with any configuration of movable non-dynamic loads.

Report No. 56-5, "A Finite-Element Method for Bending Analysis of Layered Structural Systems" by Wayne B. Ingram and Hudson Matlock, describes an alternating-direction iteration method for solving two-dimensional systems of layered grids-over-beams and plates-over-beams.

Report No. 56-6, "Discontinuous Orthotropic Plates and Pavement Slabs" by W. Ronald Hudson and Hudson Matlock, describes an alternating-direction iteration method for solving complex two-dimensional plate and slab problems with emphasis on pavement slabs.

Report No. 56-7, "A Finite-Element Analysis of Structural Frames" by T. Allan Haliburton and Hudson Matlock, describes a method of analysis for rectangular plane frames with three degrees of freedom at each joint.

Report No. 56-8, "A Finite-Element Method for Transverse Vibrations of Beams and Plates" by Harold Salani and Hudson Matlock, describes an implicit procedure for determining the transient and steady-state vibrations of beams and plates, including pavement slabs.

Report No. 56-9, "A Direct Computer Solution for Plates and Pavement Slabs" by C. Fred Stelzer, Jr., and W. Ronald Hudson, describes a direct method for solving complex two-dimensional plate and slab problems.

Report No. 56-10, "A Finite-Element Method of Analysis for Composite Beams" by Thomas P. Taylor and Hudson Matlock, describes a method of analysis for composite beams with any degree of horizontal shear interaction.

Report No. 56-11, "A Discrete-Element Solution of Plates and Pavement Slabs Using a Variable-Increment-Length Model" by Charles M. Pearre, III, and W. Ronald Hudson, presents a method of solving for the deflected shape of freely discontinuous plates and pavement slabs subjected to a variety of loads.

Report No. 56-12, "A Discrete-Element Method of Analysis for Combined Bending and Shear Deformations of a Beam" by David F. Tankersley and William P. Dawkins, presents a method of analysis for the combined effects of bending and shear deformations.

Report No. 56-13, "A Discrete-Element Method of Multiple-Loading Analysis for Two-Way Bridge Floor Slabs" by John J. Panak and Hudson Matlock, includes a procedure for analysis of two-way bridge floor slabs continuous over many supports.

Report No. 56-14, "A Direct Computer Solution for Plane Frames" by William P. Dawkins and John R. Ruser, Jr., presents a direct method of solution for the computer analysis of plane frame structures.

Report No. 56-15, "Experimental Verification of Discrete-Element Solutions for Plates and Slabs," by Sohan L. Agarwal and W. Ronald Hudson, presents a comparison of discrete-element solutions with the small-dimension test results for plates and slabs along with some cyclic data on the slab.

ABSTRACT

To obtain test results for use in verifying discrete-element analytical methods for slabs-on-foundation, a study of small-dimension plates and slabs was conducted, with the basic approach divided into two parts:

(1) a check of the modeling and method of solution for plates on simple supports for a variety of stiffness and load conditions and

(2) an investigation of the modeling of the soil-structure interaction problem of a slab-on-foundation using linear and nonlinear characteristics according to the Winkler assumption.

For the first part, tests were conducted on thin plates of two materials and under simple support conditions. These included isotropic plates under several loading patterns, isotropic plates with discontinuity, and orthotropic plates. The loads in all cases were restricted in order to keep the deflections small.

For the second part of the study, tests were conducted on a slab resting on a clay subgrade under two different loading conditions. Plate load tests were performed to determine linear and nonlinear characteristics for representing the soil subgrade. These characteristics were also determined from stress-strain relations of the soil, obtained from unconfined compression tests.

Measured deflections and principal stresses obtained for the plates in the first group of tests were compared with the analytical solutions using independently determined material properties of the plates concerned. From the study of all cases dealing with the variety of loadings, supports, and stiffnesses, verification of the method of solution within acceptable accuracy was established.

From comparison of the second group of tests with the analytical results, it was observed that for small loads, good agreement exists between experimental and analytical solutions using linear or nonlinear springs; however, for larger loads only nonlinear soil characteristics produce good agreement.

Based on the experimental evidence, the discrete-element model methods provide satisfactory analytical solution for two-dimensional problems.

In addition to the results of static loading, experimental results of some cyclic loadings on the slab are presented and a preliminary attempt is made to interpret the data, modify the soil representation for cyclic loading, and compare the experimental results with the analytical solutions thus obtained.

KEY WORDS: Analysis, discrete-element, instrumentation, plate, orthotropic plate, slab, testing, soil modulus, nonlinear support, experimental verification, cyclic loading, soil-structure, pavement slab.

TABLE OF CONTENTS

CHAPTER 1. INTRODUCTION

Problem

A general discrete-element method for solution of discontinuous plates and slabs has been described by Hudson and Matlock (Ref 19) and Stelzer and Hudson (Ref 43). The principal feature of the method is a physical model representation of the plate or slab by bars, springs, and torsion bars which are grouped in a system of orthogonal beams. The initial development utilized an alternating-direction iterative technique to solve for the deflections of the plate or slab, and a subsequent development utilized a direct matrix manipulation technique. The direct solution method has been shown to be more efficient computationally.

The method was subsequently modified by Panak for more precise modeling of orthotropic plates (Ref 29); and Pearre and Hudson further modified it to handle variable increment lengths between stations, permitting more precise modeling near abrupt changes, without excessive computer storage (Ref 30). These early solutions could handle only linearly elastic supports but Kelly (Ref 20) modified the method to include nonlinear support characteristics.

The method was checked by comparing solutions using it with data existing for problems previously solved, but more complete checks were desired. Since validity of analytical solutions can best be established by comparing them with results of carefully controlled tests, an experimental study of plates and slabs under a variety of load, support, and stiffness conditions appeared to be needed; and this study of small-dimensioned plates and slabs was conducted.

Research

The objectives of this study were to verify use of the discrete-element model as a satisfactory analytical tool for two-dimensional problems such as elastic plates under transverse loads, and to investigate the use of the discrete-element model to reach a satisfactory solution for soil-structure interaction problems, e.g., slabs on a soil subgrade.

The research was divided into two parts, one to check the modeling and method of solution for plates on simple supports for a variety of stiffness and load conditions and the second to investigate the modeling of a slab on soil foundation, using linear and nonlinear Winkler foundation models.

Tests for the first part of the study were conducted on both aluminum and Plexiglas model plates, 25 inches square and resting on four points. Test loading was done in increments of 10 pounds with a maximum of 40 pounds, plus a seating load of 10 pounds. Deflections were measured by 0.0001-inch dial gages, and strains, where obtained, were measured by rosettes. Preliminary tests involving four-edge support were conducted also, but because of shortcomings in the test set-up they were not continued. The four-point support tests were performed to find

(1) deflections and strains on aluminum plate under center loading,
(2) deflections and strains on aluminum plate under off-center loading,
(3) deflections and strains on aluminum plate with a slot cut in the plate,
(4) deflections for isotropic Plexiglas plate, and
(5) deflections for orthotropic Plexiglas plate.

The second group of tests used an instrumented aluminum slab 9 by 9 by 1/8 inches resting on a clay subgrade compacted in a 2-foot cubic box. The subgrade material was prepared by extrusion at an average density of 116 lb/ft^3 and a moisture content of 38 percent. Load was applied by a mechanical screw jack, measured by a load cell, and recorded on a digital voltmeter. Deflections of the slab were measured by linear variable differential transformers and dial gages, and strains were measured by rosettes. Tests were conducted for center load and two-point corner loads. Load was applied continuously up to 255 pounds for center load and 208 pounds for corner loads and records for loads, strains, and LVDT's were obtained at regular intervals on a 40-channel voltmeter with a digital scanning system. Testing was done under static as well as cyclic loading.

Characteristics of the soil subgrade, for use in the computer program, were determined by tests conducted on circular rigid plates of different diameters (Ref 37), and from stress-strain relationships of the soil, obtained from unconfined compression tests.

Report

This report describes the tests carried out to accomplish the study objectives. Chapter 2 presents a brief discussion of the basic equations connected with the theory of elastic plates and slabs, the main contributions by various researchers, and the limitations of their approaches. A brief history and description of the discrete-element method is included.

Chapter 3 describes the instrumentation techniques used to measure and record strain, deflection, and load in performing the tests.

Chapter 4 describes the procedure to investigate the modeling of plate behavior, including the tests conducted, materials used, and the loading conditions, and presents an analysis of the data, including a comparison of the experimental and analytical solutions for deflections and principal stresses.

Chapter 5 describes the test program for slabs resting on clay soil for two loading conditions. Data analysis, including representation of the soil subgrade with linear and nonlinear characteristics, is briefly described, and the comparison between experimental and analytical solutions using both types of soil springs is included.

Chapter 6 presents some of the test results from cyclic loading on the slab and includes discussion interpreting the data, modifying the soil representation for cyclic loading, and comparing the experimental results with the analytical solutions thus obtained.

Chapter 7 presents conclusions, suggestions for further research, and a section on application of results.

CHAPTER 2. EXISTING ANALYTICAL SOLUTIONS AND RECENT DEVELOPMENTS

Existing Analytical Solutions

Elastic Plate Problem Solutions

Analytical solutions for two-dimensional plate problems have been discussed by Timoshenko (Ref 47) and others who characterize three kinds of plate bending: (1) thin plates with small deflections, (2) thin plates with large deflections, and (3) thick plates. This report deals only with the first of these, using the following assumptions:

(1) There is no deformation in the plate's middle plane.

(2) Points of the plate which initially lie normal to the middle surface of the plate remain normal to the middle surface of the plate after bending.

(3) The normal stresses in the direction transverse to the plate can be disregarded.

With these assumptions, the deflected surface of an isotropic plate is described by the biharmonic equation

$$D\left(\frac{\partial^4 w}{\partial x^4} + 2\frac{\partial^4 w}{\partial x^2 \partial y^2} + \frac{\partial^4 w}{\partial y^4}\right) = q \qquad (2.1)$$

where

D = the bending stiffness of the plate,

w = the deflection (positive upwards),

q = the lateral load.

A complete discussion of this equation is given in Chapter 2 of Ref 47.

For a given set of boundary conditions, solution of this differential equation gives all the information necessary for calculating the stresses at any point in the plate. Closed-form solutions of this equation are available for a number of special cases, including homogeneous, isotropic plates, which

are generally round with a finite radius, or square with infinite dimensions in the x and y-directions. The loading conditions in most closed-form solutions are either uniform over the entire plate or concentrated in the center of the plate. Solutions of isotropic plates for specific cases are readily accomplished by hand calculation, but computers must be used for solutions of homogeneous orthotropic plates. As the problem becomes involved, with various combinations of load, support, and stiffness conditions, closed-form solutions are generally not available and an approximate numerical method must be used to solve the problem.

Slab-on-Foundation Problem Solutions

For solving slabs-on-foundations, subgrade soil has been represented by the Winkler assumption and the semi-infinite elastic-isotropic solid. In the Winkler assumption (Ref 55), soil strata are approximated by a series of infinitely closely-spaced independent springs. Spring stiffness k , known as modulus of subgrade reaction, is defined as

$$k = \frac{q}{w} \tag{2.2}$$

where

q = soil reaction at any point, in lb/in^2;

w = deflection at that point, in inches.

Soil type and size of loaded area are the main influences on k . Determination of k has been discussed in detail by Terzaghi, Skempton, Barkan, Chopane, and Vesic and Saxena (Refs 45, 40, 1, 6, and 50, respectively).

In the semi-infinite elastic-isotropic solid concept, Hogg, Holl, Pickett and others, and Vesic and Saxena (Refs 15, 16, 32 and 33, and 50, respectively) represented the subgrade soil as a semi-infinite elastic half space, characterized by modulus of deformation E_S and Poisson's ratio ν_S .

Solutions involving the Winkler assumption were developed by Westergaard and formulas are available which can be used to find deflections, moments, and stresses for three special-case loadings: corner, edge, and center (Refs 51 through 54). These solutions are subject to severe limiting assumptions, which are not realistic.

(1) The slab is assumed to be infinite, whereas in reality it is always finite.

(2) The subgrade, assumed to have uniform and linearly elastic support, is not always uniform for many reasons, including differential settlement and local loss of support. The nonlinear characteristics of the soil are totally ignored.

(3) The concrete slab assumed to be homogeneous, isotropic, and elastic material of uniform thickness is not so in reality, since the subgrade is generally not perfectly level when the slab is poured. No provision is made for cracks or discontinuities.

Extensions of this work are discussed by Hudson and Matlock (Ref 19) and Pickett and others (Refs 32 and 33).

For the semi-infinite elastic-isotropic solid, Pickett and others (Refs 32 and 33) developed the fundamental equation of Hogg (Ref 15) into influence charts. Vesic and Saxena (Ref 50) developed equations for deflections and pressure by extending Biot's theory of bending of plates (Ref 2) and the equations of Holl (Ref 16) and Hogg (Ref 15) with the help of Bessel's functions. Lee (Ref 21) also discussed the solutions obtained using this approach. The semi-infinite elastic-isotropic solid approach is also subject to the following limitations:

(1) The soil subgrade represented by the elastic constants according to this concept ignore the nonlinear characteristics of the subgrade.

(2) The problem of limitations imposed for plates according to elastic theory is also unresolved for slabs.

(3) These solutions are almost inapplicable when a discontinuity in the slab or subgrade is encountered.

Need for Another Analytical Method

After considering the various methods available for the solution of plates and slabs and the severe limitations imposed by them, it was considered desirable to develop an analytical method capable of the following:

(1) allowing freely discontinuous variation of input parameters, including bending stiffness and load;

(2) providing for combination loading, including lateral loads, in-plane forces, and applied couples or moments;

(3) handling freely variable foundation conditions, including the nonlinear characteristics of the subgrade; and

(4) application to orthotropic plates.

Recent Developments Based on Numerical Methods

The theories and solutions discussed above are based on infinitesimal calculus, but since many complex engineering problems do not properly fulfill the conditions governing the use of such calculus and cannot be solved by resorting to it, so-called "numerical" methods have been developed in the past few years. Two major numerical methods are of interest.

Discrete-Element Method

The discrete-element method presented by Matlock, Hudson, and others (Refs 23, 19, and 43), is capable of meeting most of the requirements of a new method. The subgrade soil in this approach is represented by the Winkler foundation.

Matlock (Ref 23) presented a discrete-element model (Fig 1) which satisfied the differential equation for a beam-column, using infinitesimal increments. The model is a system of rigid bars connected by springs which represent the stiffness F of the beam.

Hudson and Matlock (Ref 19) extended this bar-spring model to a slab, using an alternating-direction iterative method to solve for the deflected shape of the slab. This method depends on an estimate of the closure parameter, which is difficult to make in certain practical slab and plate problems. Stelzer and Hudson (Ref 43) utilized a direct matrix manipulation technique to obtain the deflections, and this has been shown to be more efficient computationally for most problems than the alternating-direction technique.

Figure 2 is a pictorial representation of the discrete-element model of the slab as suggested by Hudson and Stelzer (Refs 19 and 43). The slab is replaced by an analogous mechanical model representing all stiffness and support properties of the actual slab. The joints of the model are connected by rigid bars which are in turn interconnected by torsion bars representing the plate twisting stiffness C. The flexible joint models the concentrated bending stiffness D and the effects of Poisson's ratio ν. The equations shown are normally used to compute the stiffness properties D and C involving modulus of elasticity E, thickness t of plate or slab, and ν. The soil support is represented by independent elastic springs, i.e., the Winkler foundation, and concentrated at the joints. Figure 3 shows a typical joint representing rigid bars, springs, and torsion bars.

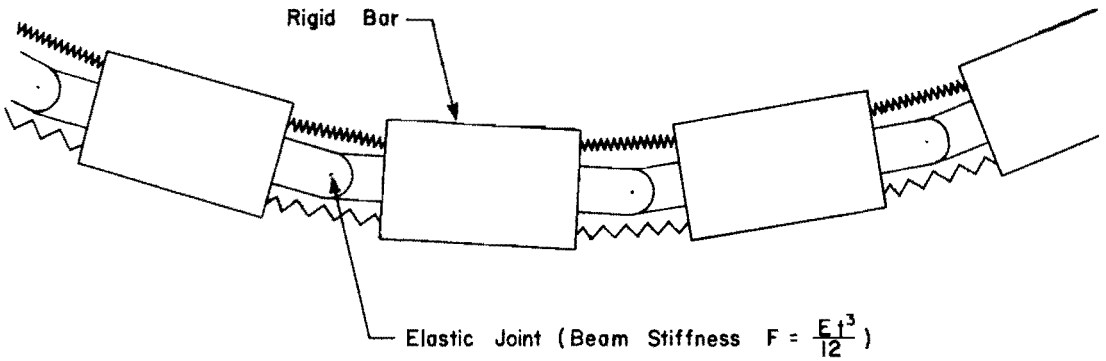

Fig 1. Discrete-element beam model (Ref 23).

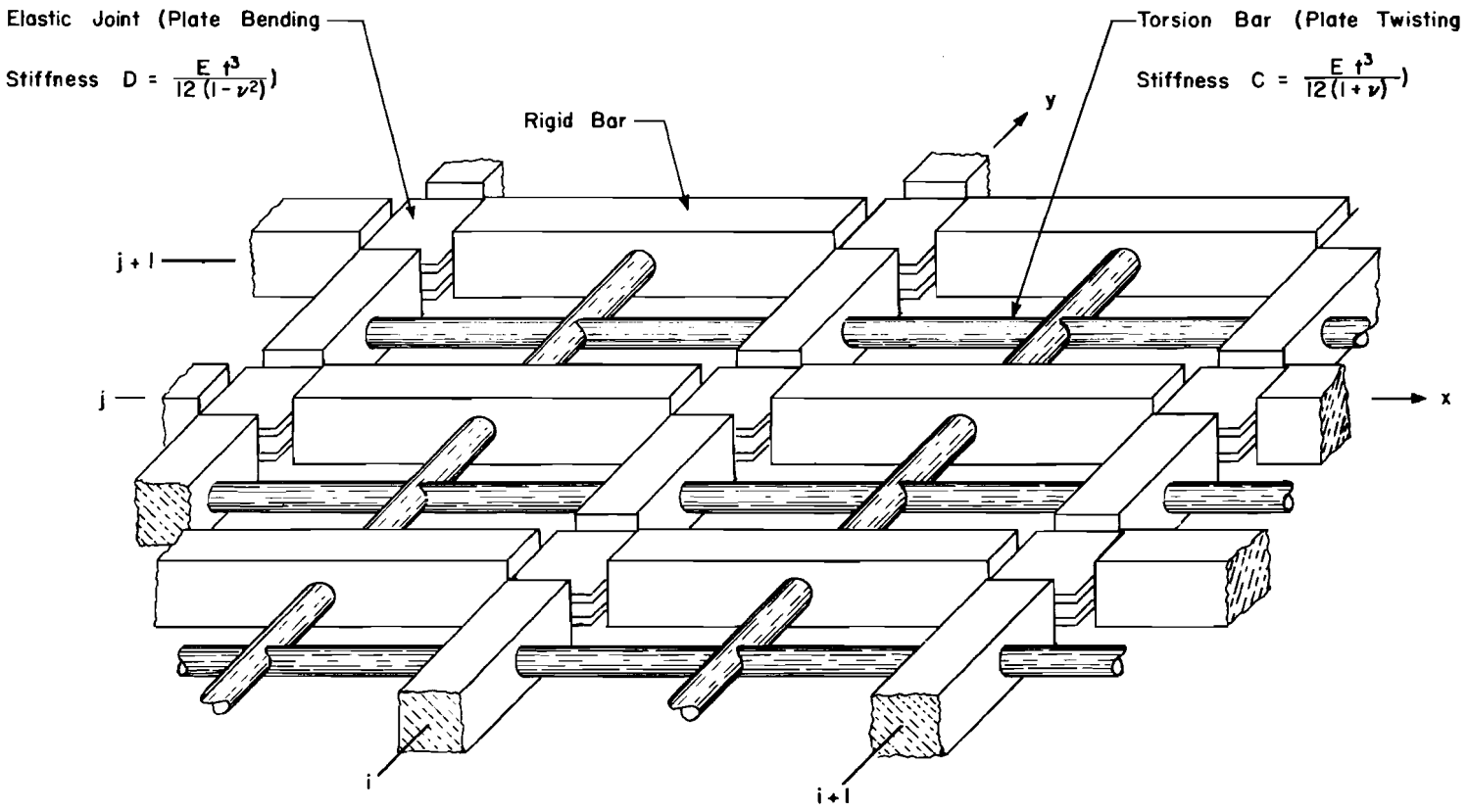

Fig 2. Discrete-element model of a plate or slab (Ref 19).

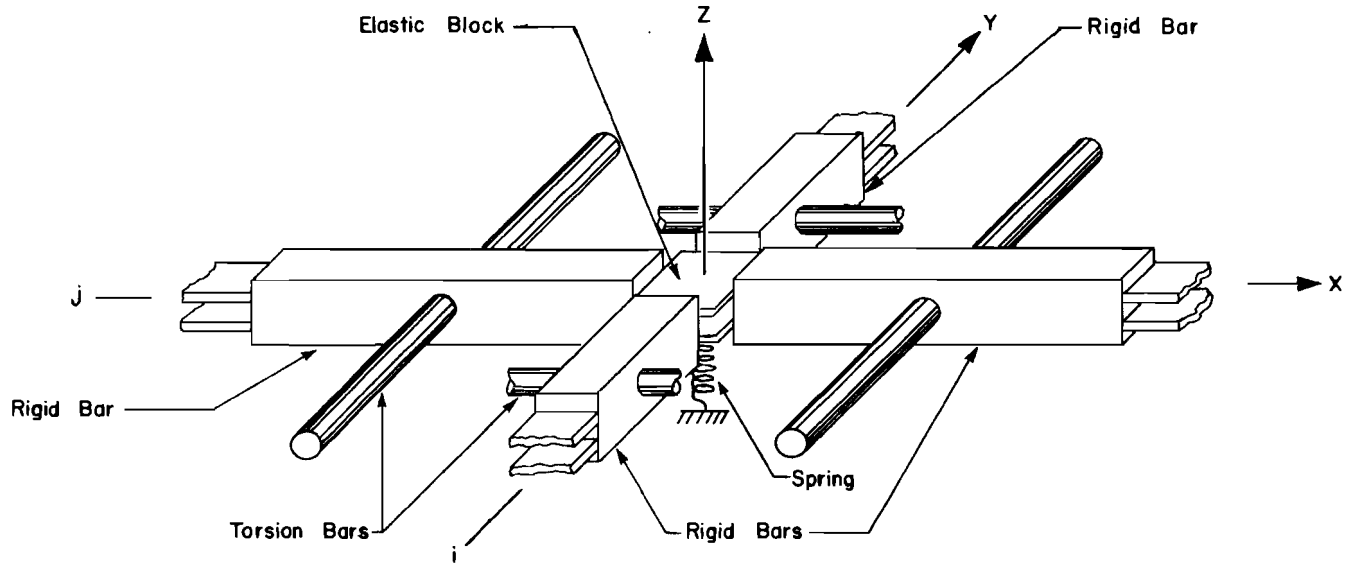

Fig 3. Typical joint i,j taken from discrete-element slab model (Ref 19).

The deflection at each joint is the unknown. The basic equilibrium equations are derived from the free-body of the slab joint with all appropriate internal and external forces and reactions. These equations include summing the vertical forces at each joint and summing the moments about each individual bar. A complete derivation of these equations and the fourth-difference equations can be found in Ref 43.

The equations resulting are arranged in matrix form, as shown in Fig 4 and represented by

$$[K][W] = [Q]$$

where

$[K]$ = stiffness matrix, symmetrical about its major diagonal and banded (with the central band five terms wide, the bands on either side of the central band three terms wide, and the two extreme bands only one term wide);

$[W]$ = deflection vector (unknown);

$[Q]$ = load vector.

The stiffness matrix is partitioned into submatrices, which are shown by dashed lines. A back and forth recursive technique analogous to Matlock's method of solving beams and columns (Ref 23) is applied to the submatrices to solve for the deflections; and slopes, moments, shears, and reactions are computed using the difference-equation relations. A computer program, DSLAB 5 (Ref 43), has been developed and written in FORTRAN computer language for the Control Data Corporation 6600 digital computer.

Subsequent developments include (1) DSLAB 19 and 21 (Refs 11 and 28), modified versions of DSLAB 5 requiring less computer storage and computation time, (2) VISAB 3 (Ref 30), which handles variable increment lengths in the model, permitting more precise modeling near abrupt changes in load, support, or stiffness of the plate or slab; and (3) DSLAB 30 (Ref 29), which models orthotropic plates more precisely, considering a constant relationship between bending stiffness in one orthogonal direction and the Poisson's ratio in the opposing direction and vice versa according to Maxwell's theorem of reciprocity (Ref 48). The early solutions could handle only linearly elastic supports, but Kelly (Ref 20) modified the method to include nonlinear support characteristics.

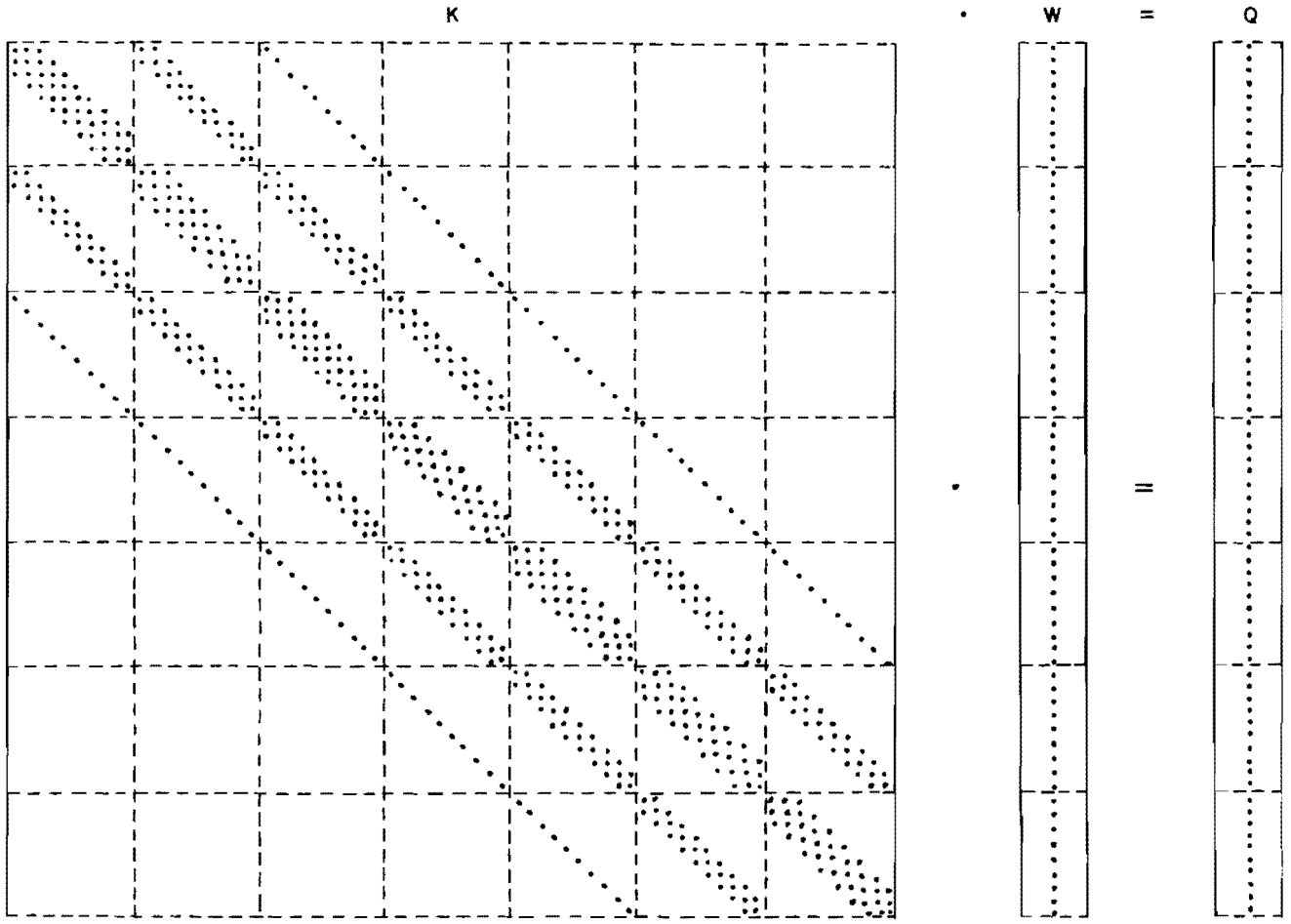

Fig 4. Form of the equations showing partitioned stiffness matrix (Ref 43).

Finite-Element Method

In the second major numerical method, a given continuum is divided into a finite number of pieces, called finite elements (Refs 7, 56, 14, and 5). These elements are assumed to be joined together by certain displacement functions at a number of intersections called nodal points. The finite elements in general should be simple to arrange in an orderly fashion and should be adaptable to variations of size and shape. Triangular, rectangular, quadrilateral, and other shapes have been used. The conditions of static equilibrium and compatibility are satisfied in forming the set of simultaneous equations. Details of this method for structural problems in general are given in Refs 7 and 56, for plate problems in Ref 14, and for slabs-on-elastic-foundations in Ref 5.

The difficulty in making the proper choice for the shape of the element and displacement functions has been a limitation to this method; improper choice of a displacement function can introduce considerable error.

Application of this method to soil-structure interaction problems for footings, considering the nonlinear behavior of soils, was utilized successfully by Desai and Radhakrishnan (Refs 9 and 35, respectively). With increased use of this method, a rational approach may be evolved for all soil problems, and it may then be possible to apply this method to slab-on-foundation problems in which linear and nonlinear characteristics of the subgrade can be studied.

CHAPTER 3. INSTRUMENTATION

A brief description of the techniques used to measure and record strain, deflection, and load for the tests is presented in this chapter.

Strain Measurements

For plate and slab problems, strains are measured in at least three directions at the same location so that the principal strains and stresses can be computed. For this study, rectangular rosettes oriented at 0, 45, and 90° were used, as shown in Fig 5. Their specifications are given in the following table.

TABLE 1. ROSETTE SPECIFICATIONS (from Ref 12)

Make	BLH Electronics
Type	FABR-25-12S13
Gage factor	2.08 ± 1 percent
Resistance	120.0 ± 0.5
Gage length	0.25 inch
Grid dimensions	0.36 x 0.16 inch
Carrier material	phenolic glass

At least one rosette was fixed to measure the maximum strains close to the loading point and the remaining rosettes were located at other significant positions. For the plate problem, rosettes were fixed at identical positions on the top and bottom of the plate so that one could serve as a check on the other and to eliminate the effects of in-plane forces.

For the corner loads slab test single strain gages were fixed as near the edge of the slab as possible. Their specifications are shown in the following table.

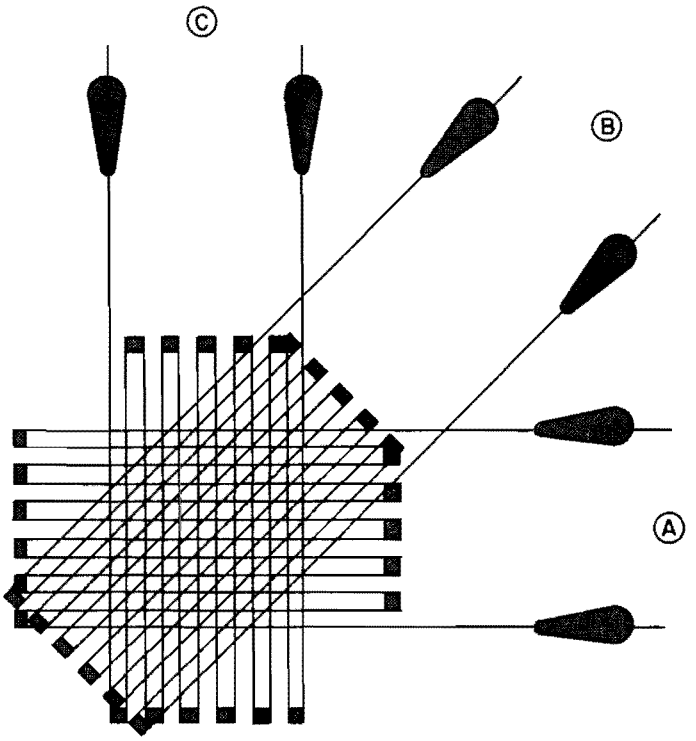

Gage A oriented at 0°
Gage B oriented at 45°
Gage C oriented at 90°

Fig 5. Rectangular rosette.

TABLE 2. STRAIN GAGE SPECIFICATIONS (from Ref 25)

Make	Micro-measurements
Type	EA-13-250BG-120
Gage factor	2.095 ± 0.5 percent
Resistance	120.0 ± 0.15 percent
Grid dimensions	0.25 × 0.125 inch

To find the elastic properties of the materials, i.e., modulus of elasticity E and Poisson's ratio ν, SR-4 epoxy foil general purpose strain gages oriented at 90° to each other were located on 2 by 18-inch straps of each material at a considerable distance from the load.

For the tests the gages were fixed to the specified locations, which had been precisely marked. The surface of the plate, slab, or strap was cleaned with emery paper or sand blasting and methyl ethyl ketone (MEK), and the back of the gage was also cleaned with MEK. Approximately 24 hours after curing the gages at the temperature specified by the manufacturer, the lead wires were soldered, and the gages were tested for continuity, leakage, and resistance. Finally the gages were protected from moisture and weather variations by several coats of a moisture proofing material.

A Wheatstone bridge circuit with a single active arm was used as the hookup for strain measurement. A compensating gage of similar type, mounted on an unstrained plate of the same material, was used to provide temperature compensation. Figure 6 shows a typical connection for this half-bridge connection.

Deflection Measurements

Dial gages with 0.0001-inch resolution and 0.5-inch range were used to measure deflection in plate tests, and as checks in slab tests. They were also used to measure deflection in testing rigid plates in connection with the slab tests and in preliminary slab testing.

Deflections on instrumented slabs were measured by direct current linear variable differential transducers, referred to as DCDT or LVDT. Two models of Hewlett-Packard deflection transducers (Ref 10) were used in the slab

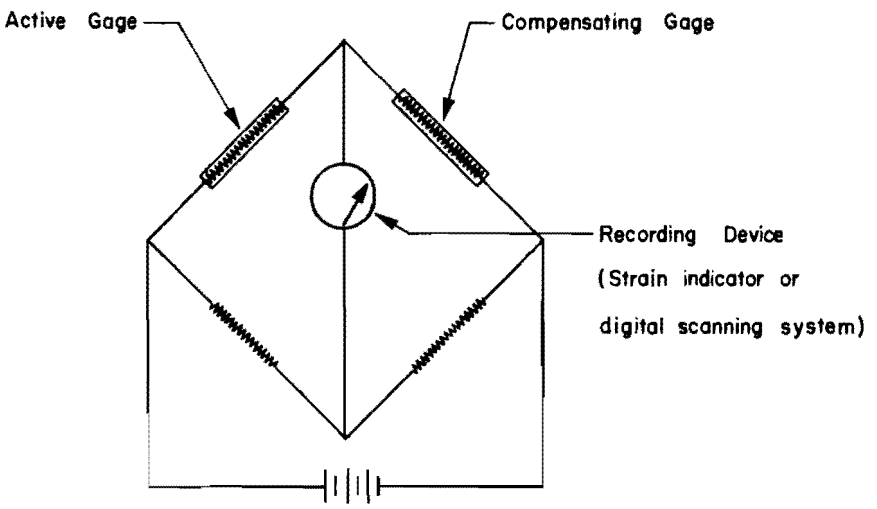

Fig 6. Connections for Wheatstone half-bridge.

tests. A 7-volt DCDT provided approximately ± 5.0 volts DC output for a ± 0.5-inch displacement of the core. A 24-volt DCDT provided approximately ± 20.0 volts DC output for a ± 0.5-inch deflection or ± 1.0-inch deflection, depending on the range of the particular unit. Quoted specifications are for 0.5 percent linearity and hysteresis with infinite resolution.

Load Application and Measurement

Dead weights on a hanger were used for all the tests on plates. Loading for the slab tests was done with a mechanical screw jack and was measured by a load cell and recorded on the digital voltmeter. The mechanical jack, of 20-ton capacity and driven by a variable stepping motor, was mounted on the crossbeam of a loading frame anchored to the test bed. Ormond load cells having 2 milivolts/volt output and 0.25 percent accuracy were used. The capacities and resolutions of the different load cells used are given in the following table.

TABLE 3. SPECIFICATIONS OF LOAD CELLS

Test Series	Capacity (kips)	Resolution (lb)
320	4	1
330	20	5
340	10	2

Load for the preliminary slab test and plate load tests was measured with a 400-pound double proving ring. Its calibration constants were 12 divisions per pound up to 100 pounds and 2.25 divisions per pound from 100 to 400 pounds.

Recording Equipment

Portable Strain Indicator

A portable Budd strain indicator was used to record strains for all aluminum plate tests. A Budd switch and balance unit was used where strains for more than one gage were desired. Half bridge connections were used (see

Fig 6). The specifications of the strain indicator are shown in the following table.

TABLE 4. STRAIN INDICATOR SPECIFICATIONS (from Ref 4)

Make	Budd
Model	P-350
Instrument serial No. 1834	
Resolution	1 microinch/inch
Range extender	±20
Gage factor	1.77 to 2.20

A strain indicator was also used to take preloading data for slab tests as well as to find the elastic properties during testing of straps.

Digital Scanning System

Data from the slab tests were recorded in digital form with a Honeywell Data Logging System (Ref 8), shown in block diagram in Fig 7 with only one recording channel used at a time during the test. For strain measurement the gages were connected, as a half bridge, into the strain gage balancing circuit, where the Wheatstone bridge was completed by two 120-ohm precision resistors. The temperature coefficient of the precision resistors was 10 parts per million per degree centigrade. Initial balance of each circuit was accomplished with a 10K-ohm, 25-turn potentiometer. Gage power was supplied from an electronic power supply with 0.01 percent regulation adjusted to 6.0 volts. The output of each circuit was connected to the scanner input of the data logger.

For deflection measurements the DCDT's used were powered with 0.01 percent regulated supplies adjusted for the particular model DCDT. The output of each DCDT was connected to one channel of the scanner input.

The load measured by an Ormond load cell was connected to the scanner on all odd numbered channels; this provided a reading of load immediately preceding each of the other measurements. This procedure allowed each measurement to be associated with an applied load taken in close time proximity in order to minimize interpolation. Had the load been applied at a faster rate the sequential readings would not have been acceptable.

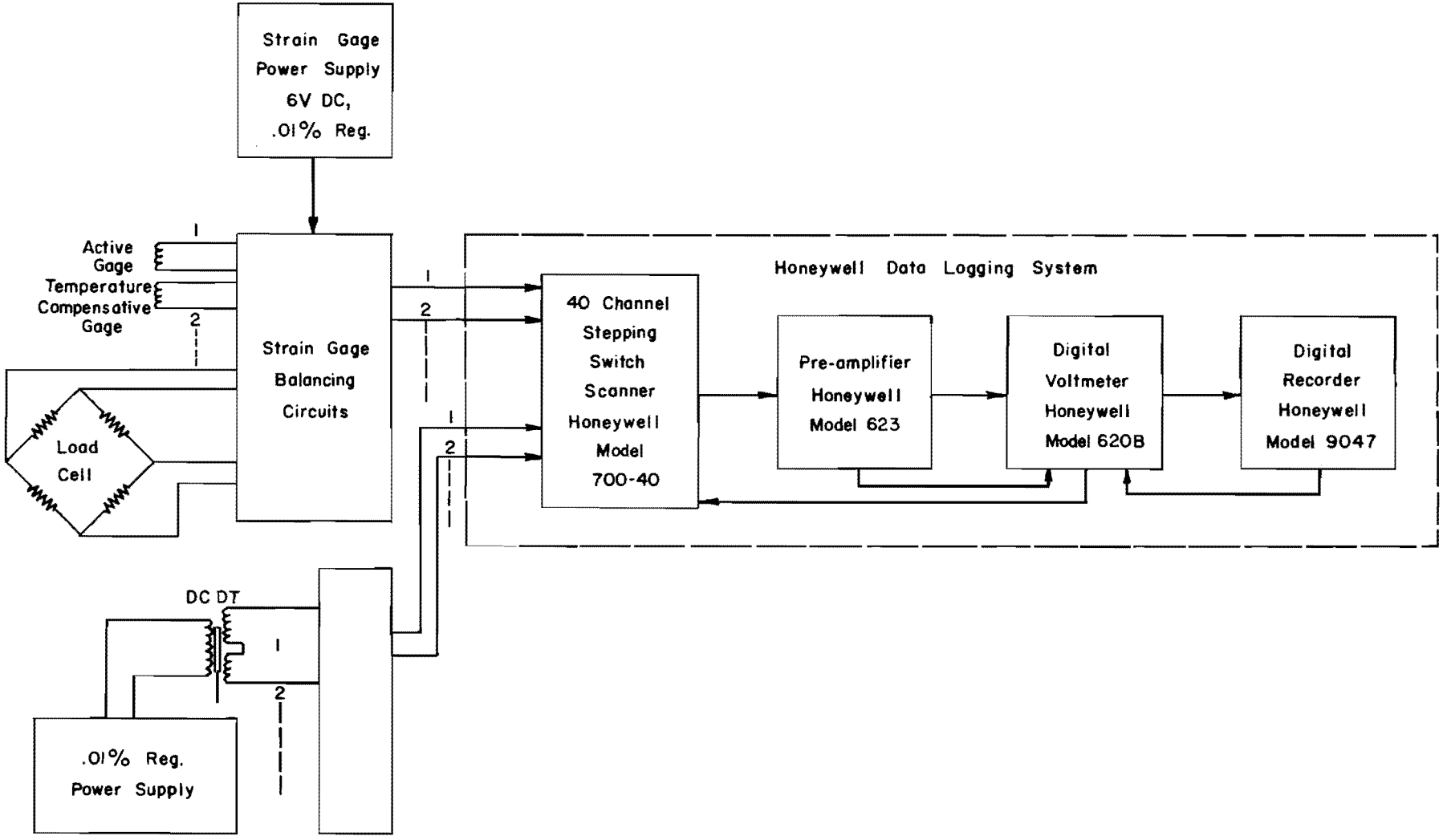

Fig 7. Data recording system.

Each recording channel was connected to one of the 40 inputs to the data logging system scanner. When recording started, the scanner stepped to the first channel. This input was connected to the preamplifier where it was scaled to the proper level for the digital voltmeter. The digital voltmeter sampled this signal and converted the voltage to a 10-line decimal number which was sent to the print modules in the printer followed by a "print" command. When printing was completed a "print complete" command was returned to the voltmeter and the meter transfered a "step" command to the scanner causing it to advance one channel. This process repeated at approximately one reading per second until all inputs had been read.

The quoted accuracy of the data logging system was ±0.03 percent of the reading ±0.02 percent of full scale for the range in use. For the 100 mv range the system accuracy would be about ±20 microvolts.

The system provides four decimal digits in the ranges and associated resolutions given in the following table.

TABLE 5. SCALES AND RESOLUTIONS OF LOGGING SYSTEM

Resolution (mv)	Full-Scale Voltage
0.001	9.999 mv
0.010	99.990 mv
0.100	999.900 mv
1.000	9.999 v
10.000	99.990 v
100.000	750.000 v

The digital voltmeter automatically ranges up when the reading exceeds 118 percent of any scale and ranges down when 10.5 percent of any range is reached.

Data printout is provided in the following format on 4-inch adding machine tape:

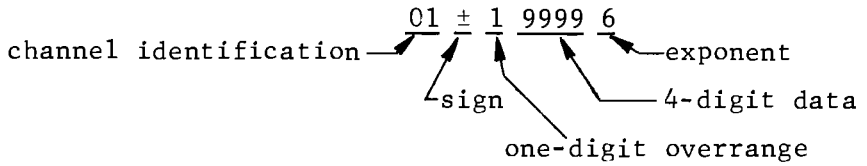

An example of typical data printout is shown on page 209 in Appendix 3.

Visual display of channel identification is provided on the scanner front panel and visual data, sign, and range are displayed on the front panel of the digital voltmeter.

Calibration of Deflections and Strains in the Slab Tests

For deflections the DCDT's were used over a very limited range (±0.2 inch or less); therefore it was necessary to calibrate each transducer in place for each test against the digital voltmeter of the scanning system. Calibration was accomplished by mounting the transducers in test position and adjusting for the "null" or center zero position and displacing the core with locally machined gage blocks of known thickness. The output for each position was recorded from the digital voltmeter and plotted to develop calibration curves. The sensitivity of the transducers was decreased by shunting different resistances so that the deflections at various points could be adjusted within the anticipated range. Each transducer was calibrated at least twice to check reproducibility within 2 percent.

This procedure was completed on all DCDT's immediately prior to each test to assure the most accurate calibration possible with the transducers available. However, data over the ±0.2-inch range could have been taken with more facility and better accuracy using the transducers with a range of ±0.2 inch.

The voltage to power the transducers was provided by electronically regulated power supplies with 0.01 percent line and load regulation.

For strains, each strain channel was calibrated by shunting a known resistance in the gage circuit and recording the output, first on the digital voltmeter and then on the strain indicator. The calibration was also accomplished with the following equation (Ref 4):

$$E_o = k\epsilon v \tag{3.1}$$

where

E_o = output voltage in microvolts;

k = gage factor = 2.05;

$\epsilon = \frac{\epsilon_1 - \epsilon_2 + \epsilon_3 - \epsilon_4}{4}$, average strain per arm in microinches/inch for a four-gage circuit;

$= \frac{\epsilon}{4}$ for one gage circuit under use;

v = voltage = 6 volts.

Thus, $\epsilon = 0.325\ E_o$ was established as the calibration constant for all gages, agreeing well with the actual calibration described above.

CHAPTER 4. STUDY OF PLATES

To achieve the first objective of this study, to check the method of solution based on the discrete-element model, tests were conducted on small-dimension plates under a variety of support, load, and stiffness conditions.

To design the apparatus for the test it was necessary to study the variables involved in the problem:

(1) plate properties and dimensions,
(2) support and boundary conditions,
(3) nature and position of load, and
(4) range of deflections.

The test program was developed for the same conditions as the analytical solutions, which were applicable to thin plates with small deflections and neglected horizontal movement. In all cases the test loads were static and restricted to produce small deflections. Center and off-center loadings were used. The plates tested were 25 by 25 by 0.25-inch aluminum plates with and without a discontinuity and 25 by 25 by 0.50-inch Plexiglas plates unstiffened and stiffened by 0.50 by 25 by 0.25-inch ribs on one side.

Two types of support conditions were considered: four edge and four point. The test arrangements, test procedures, and comparisons of test results with analytical solutions are presented below.

Elastic properties, i.e., modulus of elasticity E and Poisson's ratio ν were determined for each material by testing 2 by 18-inch straps of each under tension. Longitudinal and transverse strains were measured using foil strain gages oriented at 90 degrees, and bending stiffness EI was determined by testing the straps as cantilevers. The values of E and ν thus obtained and computations of bending and twisting stiffnesses for each plate are given in Appendix 1. The plate properties, independently determined, were as follows:

(1) for aluminum plate

$D_x = D_y = 1.6 \times 10^4$ lb-in

$C_x = C_y = 1.061 \times 10^4$ lb-in

$\nu = 0.336$

(2) for Plexiglas plate

$D_x = D_y = 4.950 \times 10^3$ lb-in

$C_x = C_y = 3.12 \times 10^3$ lb-in

$\nu = 0.375$

(3) for Plexiglas plate with ribs

$D_x = 10.825 \times 10^3$ lb-in

$D_y = 7.560 \times 10^3$ lb-in

$C_x = C_y = 6.440 \times 10^3$ lb-in

$\nu_{yx} = 0.329$

Four-Edge Support Tests

The four-edge support tests were a preliminary series conducted to establish a suitable procedure for the study. Testing revealed shortcomings in the test set-up, however, and its use was not continued. Instead, the

four-point support test procedure was developed and was used during the investigation.

The four-edge support test arrangements (Ref 27) are shown in Figs 8(a) and 9. A 25 by 25-inch plate was supported near all four edges between two angles, one above and one below the plate. The two angles were held tightly together by bolts through timber pieces between them. Pressure could be uniformly applied between the angles by tightening each bolt by the same amount of torque. Before testing, this pressure was released by the same amount at each bolt so that the plate could not become wedged between the angles when its slope changed under load. The plate was thus hinged for zero deflection at all edges. The plate was placed on the supports, which were arranged as a 24-inch square, so that it overhung 0.5 inch at each edge as shown in Fig 8(b). The supports and plate were placed on a wooden table which had leveling screws in the legs and a hole in the center. No hole was made in the plate for loading, in order to avoid any change in its properties. Instead, a hook was attached to the bottom of the test plate with epoxy and a hanger for dead weights was added. Testing was done under center loading with a concentrated load. Deflections were measured at various points by 0.0001-inch dial gages. The supports of the beams carrying the dial gages were fixed on the table (Fig 8).

For the testing, the table was leveled, the angle supports with the plate inserted between them placed on the table, and the level of the plate rechecked. The bolts connecting the angles were tightened equally to a torque of 10 lb/in^2. Supports of the beams carrying the dial gages were fixed on the table, and the dial gages were set at the correct positions. A seating load of 10 pounds was placed on the hanger for a day before the actual testing. Loading was done in increments of 10 pounds with a maximum load of 50 pounds. Deflections were recorded after every load increment. The plate was unloaded the same way and deflections were recorded. The test was repeated three more times to check the reproducibility of the results.

Deflections for different points on the plate calculated for each load increment are given in Ref 26.

Comparison of Analytical and Experimental Results

Analytical solutions based on the discrete-element model were found with DSLAB 21 (Ref 28), using 1/2-inch increment lengths in both directions. The

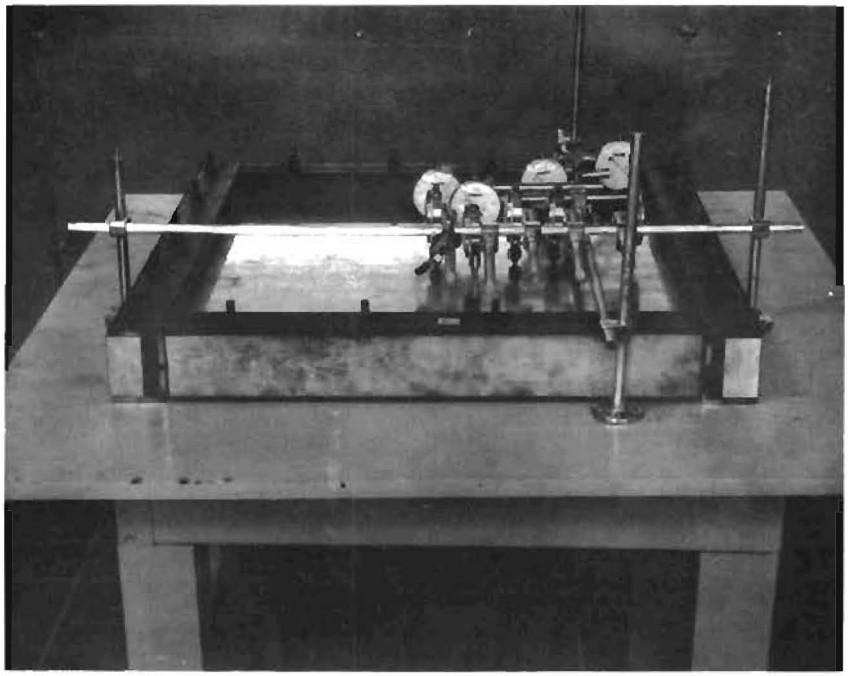

(a) Test set-up.

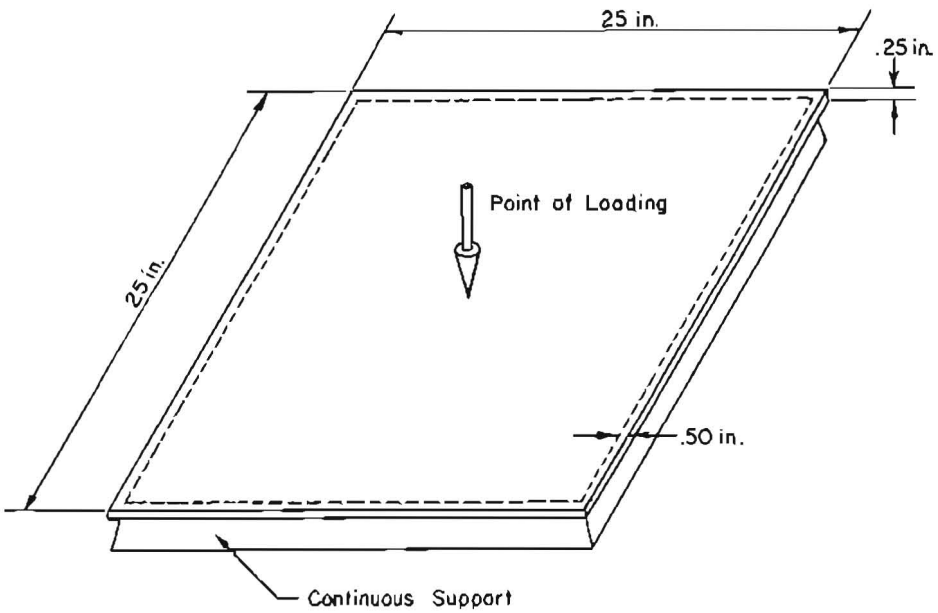

(b) Dimensions.

Fig 8. Arrangements for four-edge support test.

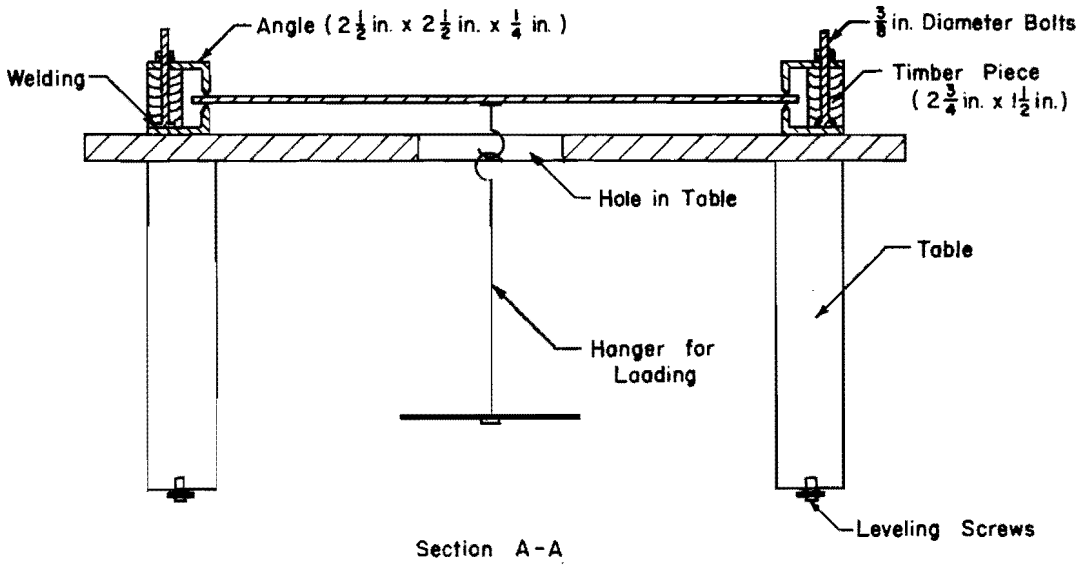

Section A-A

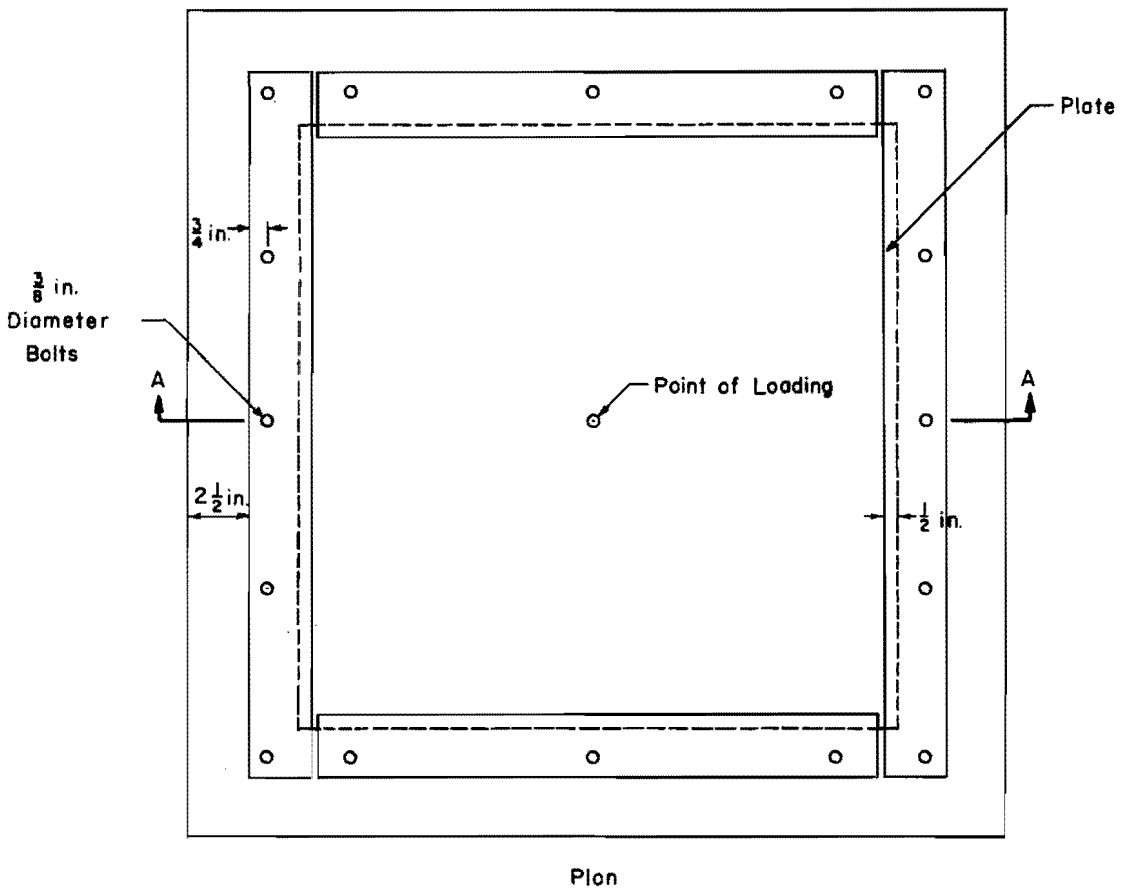

Plan

Fig 9. Details of the set-up for four-edge support test.

measured and computed deflections for a particular load were compared and the error was calculated as percentage of maximum measured deflection as shown below:

$$\text{Percentage error} = \frac{w_{mi} - w_{ci}}{(w_{max})_m} \times 100 \qquad (4.1)$$

where

w_{mi} = measured deflection at point i,

w_{ci} = computed deflection at point i,

$(w_{max})_m$ = maximum measured deflection for the load under consideration.

Figure 10 shows the positions of dial gages and load. A plot between the measured and computed deflections was made for the center line (Fig 11) and for the diagonal (Fig 12). Percentage error was calculated for all points for 10, 20, 30, 40, and 50 pounds for Test 211, as given in Table 6. Similar calculations were done for other tests and plots were drawn which are given in Ref 26. However, the observations as discussed below cover the entire series.

The comparison between the measured and computed deflections showed a discrepancy of 1.3 to 11.6 percent and indicated that the error increased with the load increase.

Shortcomings of the test set-up which were pointed out include the following:

(1) Under a load of 50 pounds the frame supporting the plate moved down, by magnitudes shown in Fig 13, and on unloading came back to its original position, all in respect to the top of the plate.

(2) With the torque of 10 lb/in^2 on all the bolts there was a gap of 0.0004 between the top angle and the plate at the places shown in Fig 13, indicating that the hinged-edge support was not uniform.

(3) The table supporting the set-up was not sufficiently rigid and its top not perfectly smooth.

(4) The beams supporting the dial gages were not sufficiently rigid.

(5) The edge supports were not relieved of all restraining moments.

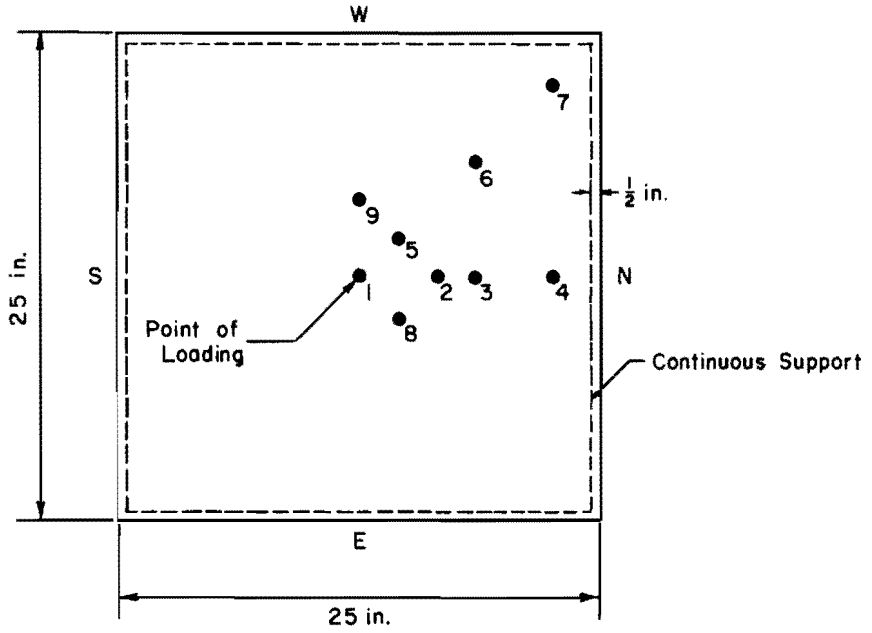

Dial Number	Distance from Center
1	at center (point of loading)
2	4 in. N on Center Line
3	6 in. N on Center Line
4	10 in. N on Center Line
5	2.83 in. NW on Diagonal
6	8.5 in. NW on Diagonal
7	14.14 in. NW on Diagonal - Support
8	2.83 in. NE (Check for Dial 5)
9	4 in. W (Check for Dial 2)

Fig 10. Positions of load and dial gages for four-edge support test.

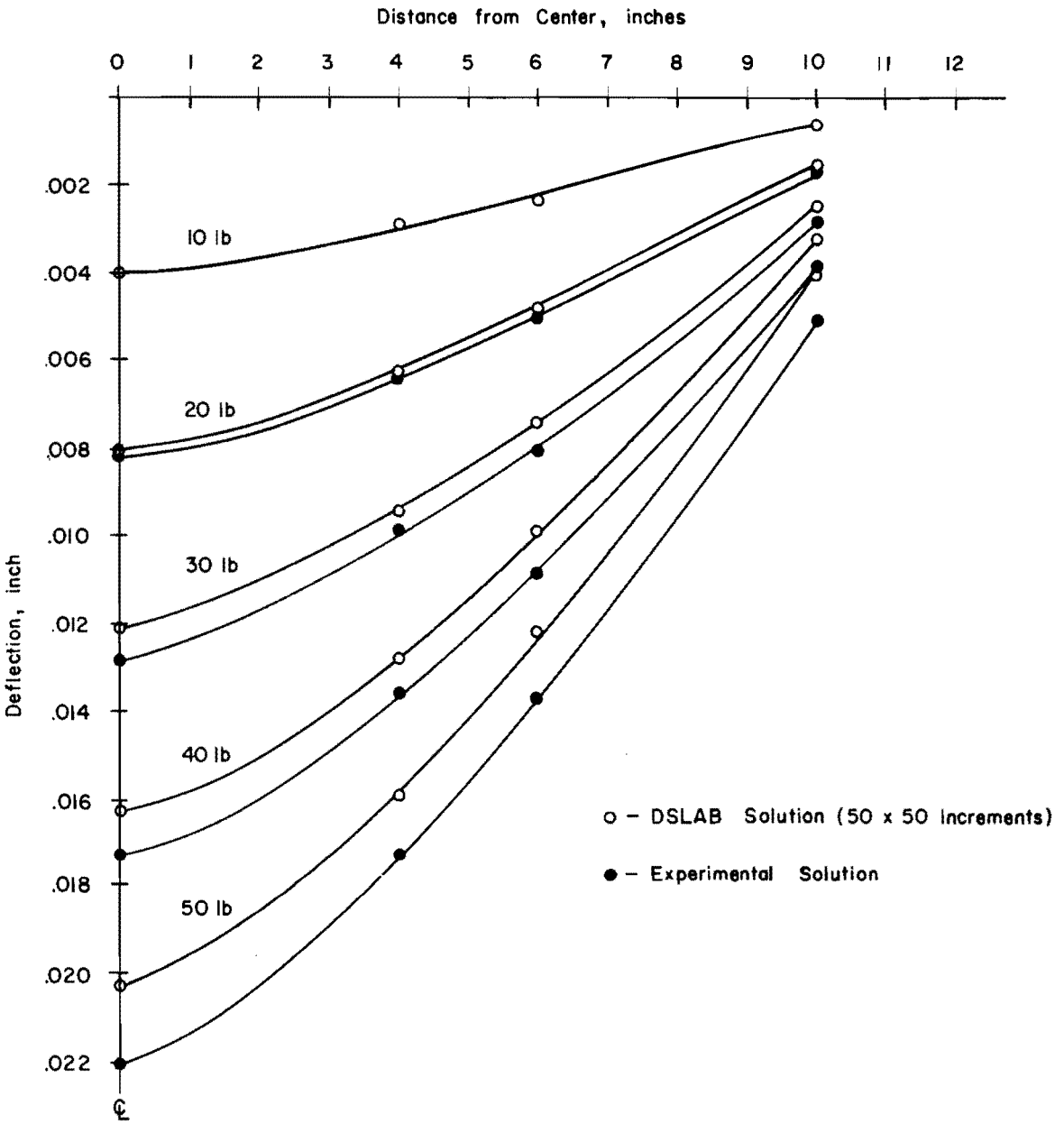

Fig 11. Experimental and analytical deflections on center line for aluminum plate on four-edge support (see Table 6).

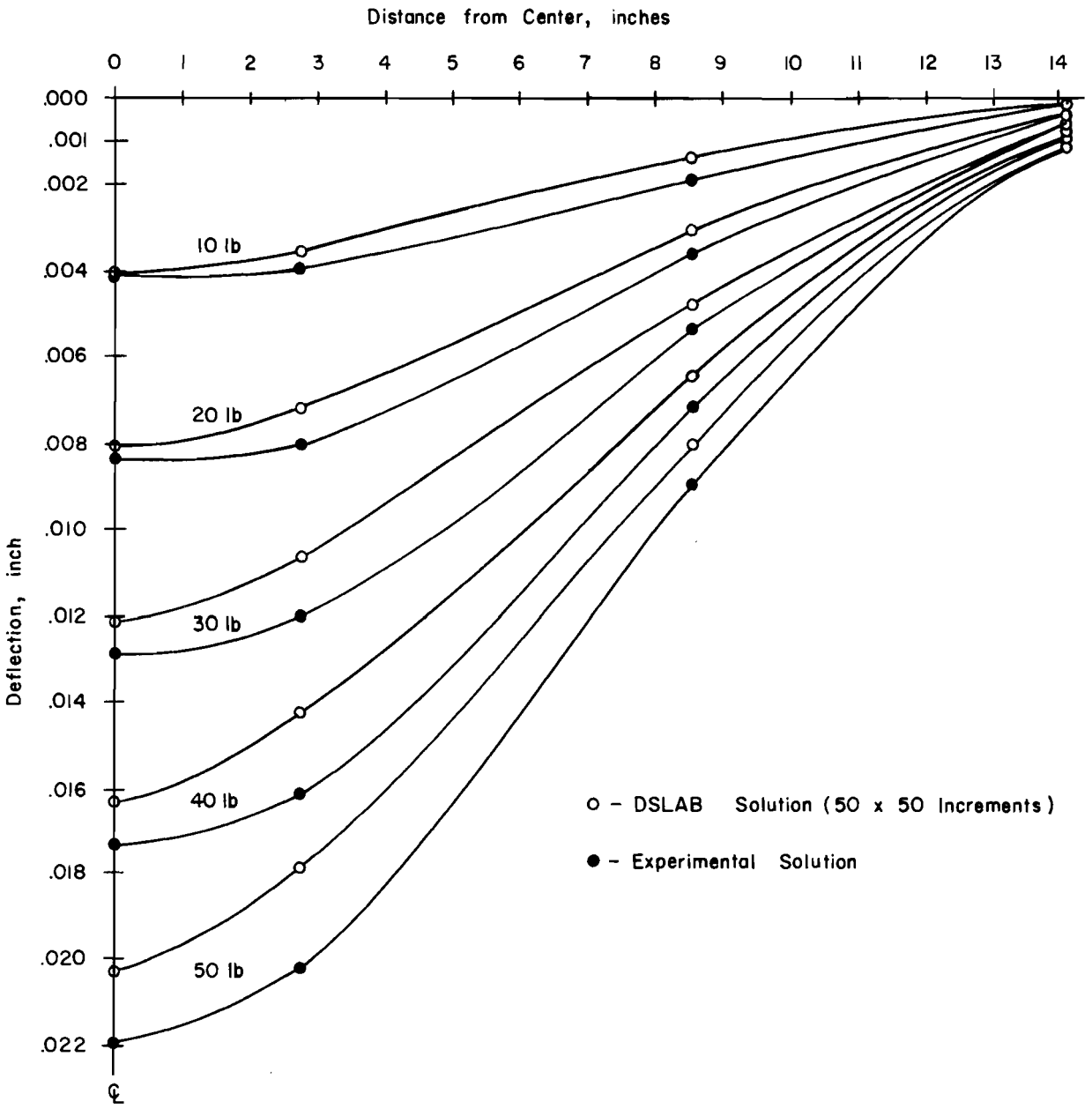

Fig 12. Experimental and analytical deflections on diagonal for aluminum plate on four-edge support (see Table 6).

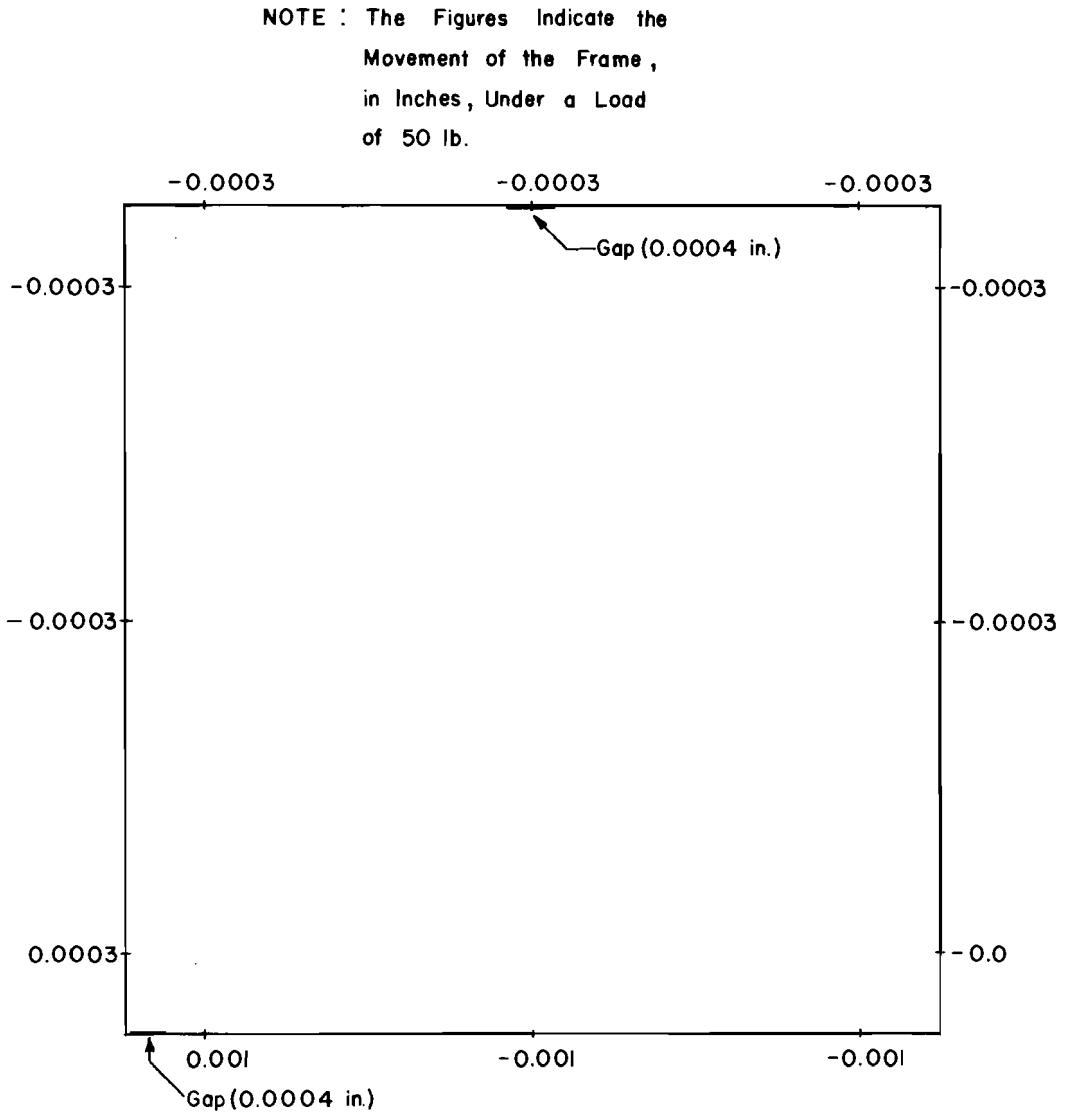

Fig 13. Shortcomings of the set-up for four-edge support test.

TABLE 6. COMPARISON BETWEEN ANALYTICAL AND EXPERIMENTAL DEFLECTIONS FOR ALUMINUM PLATE ON FOUR-EDGE SUPPORT

Load: in center (test 211)

Program: DSLAB 21 (50 x 50 increments)

Load (lb)		Deflections at Points (inch) 1	2	3	4	5	6	7	8	9	Remarks
10	DSLAB	-0.00404	-0.00317	-0.00246	-0.00083	-0.00354	-0.00163	-0.00020	-0.00354	-0.00317	Error calculated as percentage of maximum deflection
	Exptl	-0.00400	-0.00310	-0.00240	-0.00080	-0.00390	-0.00180	-0.00030	-0.00400	-0.00300	
	% Error	-1.00	-1.85	-1.38	-0.83	9.08	4.30	2.50	11.57	-4.35	
20	DSLAB	-0.00808	-0.00635	-0.00491	-0.00167	-0.00707	-0.00326	-0.00040	-0.00707	-0.00635	
	Exptl	-0.00830	-0.00630	-0.00510	-0.00180	-0.00790	-0.00360	-0.00050	-0.00810	-0.00630	
	% Error	2.65	-0.58	2.29	1.63	9.95	4.14	1.19	12.36	-0.58	
30	DSLAB	-0.01212	-0.00952	-0.00737	-0.00250	-0.01061	-0.00488	-0.00601	-0.01061	-0.00952	
	Exptl	-0.01280	-0.00980	-0.00800	-0.00290	-0.01200	-0.00530	-0.00800	-0.01210	-0.00990	
	% Error	5.31	2.17	4.96	3.14	10.85	3.25	15.55	11.63	2.95	
40	DSLAB	-0.01616	-0.01270	-0.00982	-0.00333	-0.01415	-0.00651	-0.00080	-0.01415	-0.01270	
	Exptl	-0.17200	-0.01350	-0.01080	-0.00400	-0.01600	-0.00700	-0.00100	-0.01620	-0.01360	
	% Error	6.05	4.67	5.70	3.89	10.77	2.84	1.16	11.93	5.26	
50	DSLAB	-0.02020	-0.01587	-0.01228	-0.00416	-0.01769	-0.00814	-0.00100	-0.01769	-0.01587	
	Exptl	-0.02200	-0.01720	-0.01360	-0.00500	-0.02010	-0.00880	-0.00130	-0.02030	-0.01740	
	% Error	8.18	6.05	6.02	3.80	10.98	3.00	1.35	11.89	6.95	

Note: Plots along center line and diagonal are given in Figs 11 and 12.

Further study indicated that it would be difficult to overcome these shortcomings and achieve a completely uniform edge support; and therefore, testing with four-edge support was not continued.

Four-Point Support Test Set-Up and Procedure

The set-up for the four-point support condition is shown in Fig 14(a). The point supports were short aluminum rods 3/8 inch in diameter with rounded ends which could be adjusted for leveling and locked in position on 1-inch-diameter aluminum rods 2 inches long fixed on a steel frame. The frame was made as a single unit by welding 2 by 2 by 1/4-inch angle iron pieces on all four sides. It was fixed on a rigid testing bed by bolts through slots and could be moved between the slots and the testing bed as necessary for positioning in relationship to the hole used for loading. A hanger was suspended through the hole, which was directly under the point of loading, and loads were added on the floor below. The point supports were placed 22 inches apart and a 25 by 25-inch plate was rested on them symmetrically as shown in Fig 14(b).

An independent deflection reference frame was built to support dial gages without touching the frame supporting the plate. This unit was made of beams and vertical supports stiffened by vertical, diagonal, and horizontal pieces which made it act like a truss.

Tests were carried out under interior loading by a concentrated load. Each plate was tested under different loads, with the stresses kept within the elastic limit and deflections kept small.

Loading was done in increments of 10 pounds with a seating load of 10 pounds and a maximum of 40 pounds. Deflections were measured by 0.0001-inch dial gages at various points on the plates after each load increment was added. Unloading was accomplished in the same way as loading and deflections for that were measured also. Deflections obtained are given in Ref 26.

Strains were measured in three directions, with rectangular rosettes fixed on the top and bottom of the aluminum plate at two locations (Fig 15), and were recorded by a strain indicator. Strain data for the various tests are given in Ref 26. With the strains measured by the rosettes, the principal stresses were determined using the following formulas (Ref 31).

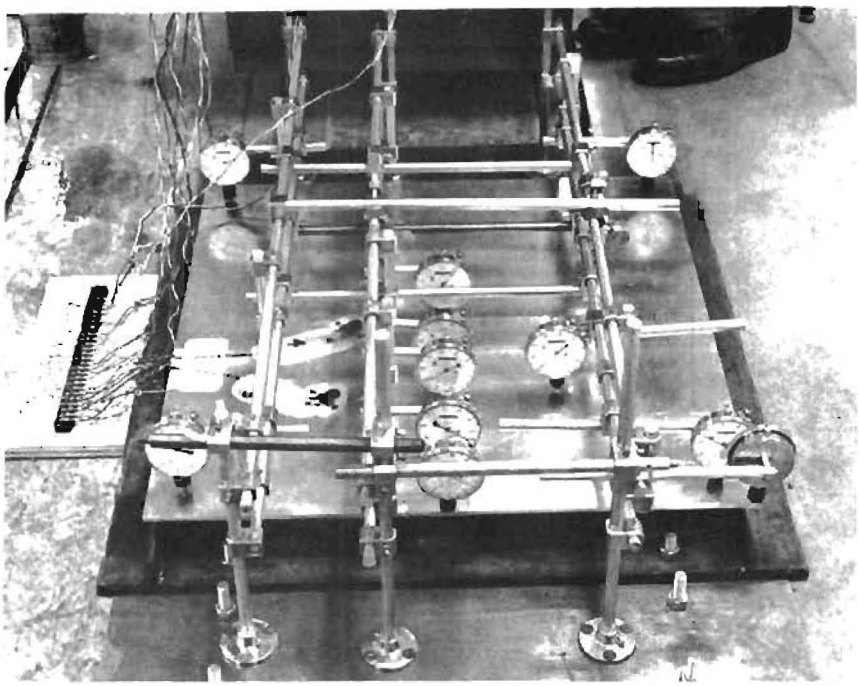

(a) Test set-up.

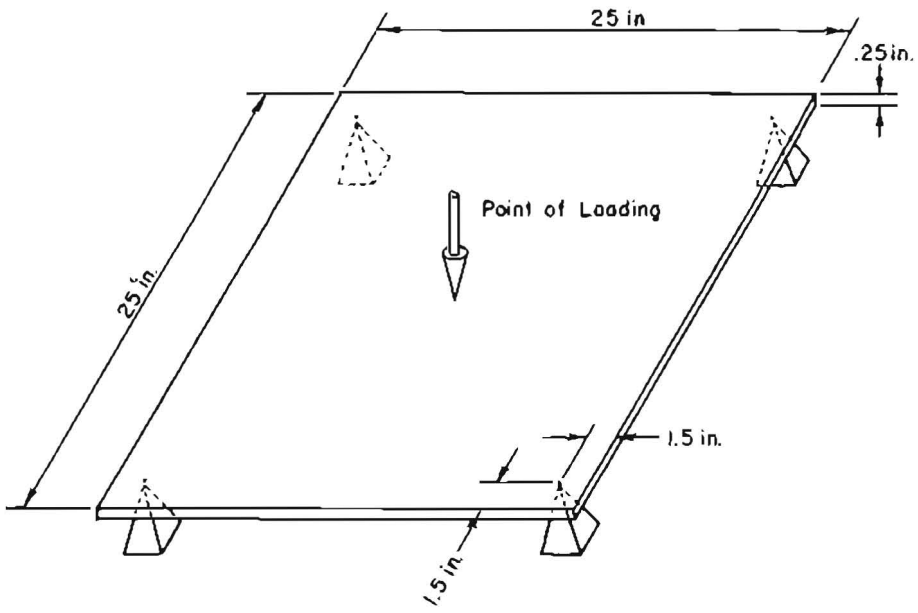

(b) Dimensions.

Fig 14. Arrangements for four-point support test.

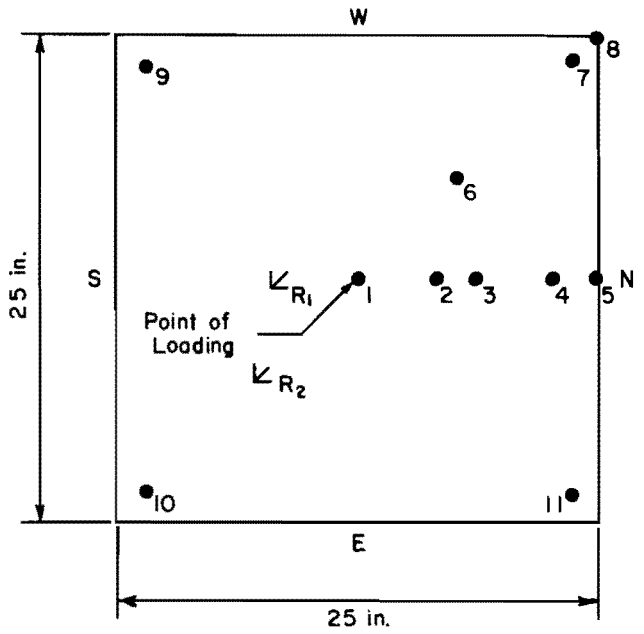

Dial Number	Distance from Center
1	at center (Point of Loading)
2	4 in. N on Center Line
3	6 in. N on Center Line
4	10 in. N on Center Line
5	12.5 in. N on Center Line
6	7.1 in. NW on Diagonal
7	15.6 in. NW on Diagonal - Support
8	17.7 in. NW
9	15.6 in. SW on Diagonal - Support
10	15.6 in. SE on Diagonal - Support
11	15.6 in. NE on Diagonal - Support
Rosettes	
R_1 (Gages 1,2,3)	4 in. S on Center Line - Bottom
R_2 (Gages 4,5,6)	7.1 in. SE on Diagonal - Bottom
R_3 (Gages 7,8,9)	4 in. S on Center Line - Top
R_4 (Gages 10,11,12)	7.1 in. SE on Diagonal - Top

Fig 15. Positions of dial gages and rosettes for four-point support tests.

$$\sigma_{max} = \frac{E}{2}\left[\frac{\varepsilon_a + \varepsilon_c}{1 - \nu} + \frac{1}{1 + \nu}\sqrt{(\varepsilon_a - \varepsilon_c)^2 + \left(2\varepsilon_b - (\varepsilon_a + \varepsilon_c)\right)^2}\right] \quad (4.2)$$

$$\sigma_{min} = \frac{E}{2}\left[\frac{\varepsilon_a + \varepsilon_c}{1 - \nu} - \frac{1}{1 + \nu}\sqrt{(\varepsilon_a - \varepsilon_c)^2 + \left(2\varepsilon_b - (\varepsilon_a + \varepsilon_c)\right)^2}\right] \quad (4.3)$$

where

σ_{max} = maximum principal stress,

σ_{min} = minimum principal stress,

E = modulus of elasticity of plate material,

ν = Poisson's ratio of plate material,

ε_a, ε_b, ε_c = strains measured by the strain gages of the rosette.

Every test was repeated to check the reproducibility of results. The tests are summarized in Table 7.

Comparison of Analytical and Experimental Results

Analytical solutions based on the discrete-element model were found by use of three computer programs: (1) DSLAB 21 (Ref 28) for isotropic plates using equal increment lengths, (2) DSLAB 30 (Ref 29) for orthotropic plates using equal increment lengths, and (3) VISAB 3 (Ref 30) for isotropic plates using variable increment lengths.

Percentage error for deflections was calculated as a function of the maximum measured value using Eq 4.1 in the same way as for four-edge support, but calculations were made for the deflections obtained under the maximum load applied, i.e., 40 pounds.

TABLE 7. TESTS CONDUCTED ON FOUR-POINT SUPPORTS

Test No.	Material of Plate	Loading Position	Parameters Measured	Repeated Test Nos.
286	Aluminum	Center	Deflections and strains	287 and 288
292	Aluminum	Off-center	Deflections and strains	293
294	Aluminum with 6 x 1/2-inch slot	Center	Deflections and strains	295 and 296
281	Plexiglas	Center	Deflections	282 and 283
298 (a)	Plexiglas with stiffeners (orthrotropic)	Center	Deflections	298(b) and 298(c)

There was settlement of the supports under the load, as discussed later, and the average value of support settlement was deducted from the measured deflections at all points. The resulting deflections were again compared with the analytical solution and percentage error calculated.

The principal stresses were determined from the strains obtained from the rosette readings, as described earlier. They were compared with the computed principal stresses and the percentage error computed. As the strains were measured at only two points, near the center, the percentage error was computed as a function of the respective measured value and not as a function of the maximum value, as was done for the deflection. The error was calculated as follows:

$$\text{Percentage error} = \frac{\sigma_{1m} - \sigma_{1c}}{\sigma_{1m}} \times 100 \tag{4.4}$$

where

σ_{1m} = maximum principal stress obtained from measured strains,

σ_{1c} = maximum principal stress computed.

A similar procedure was adopted in determining the percentage error for the minimum principal stresses. As the rosettes were used at identical positions on the top and bottom of the plate, averages of the strain values were taken in order to cancel any possible effects of in-plane forces. These average values were slightly different from the top and bottom values. Principal stresses and percent errors were again calculated.

Aluminum Plate under Center Load

Figure 15 shows the positions of dial gages, rosettes, and supports with load in the center at point 1. The measured deflections and the analytical deflections, from DSLAB 21 (Ref 28), are plotted in Figs 16 and 17 along the center line and diagonal, respectively. Computations for percent error are given in Table 8. It was observed that the computed deflections compared well with the experimental values, within 1 percent of maximum measured deflection. Comparison of the principal stresses as given in Table 9 showed that the maximum difference between experimental and computed values was 6.1 percent, using

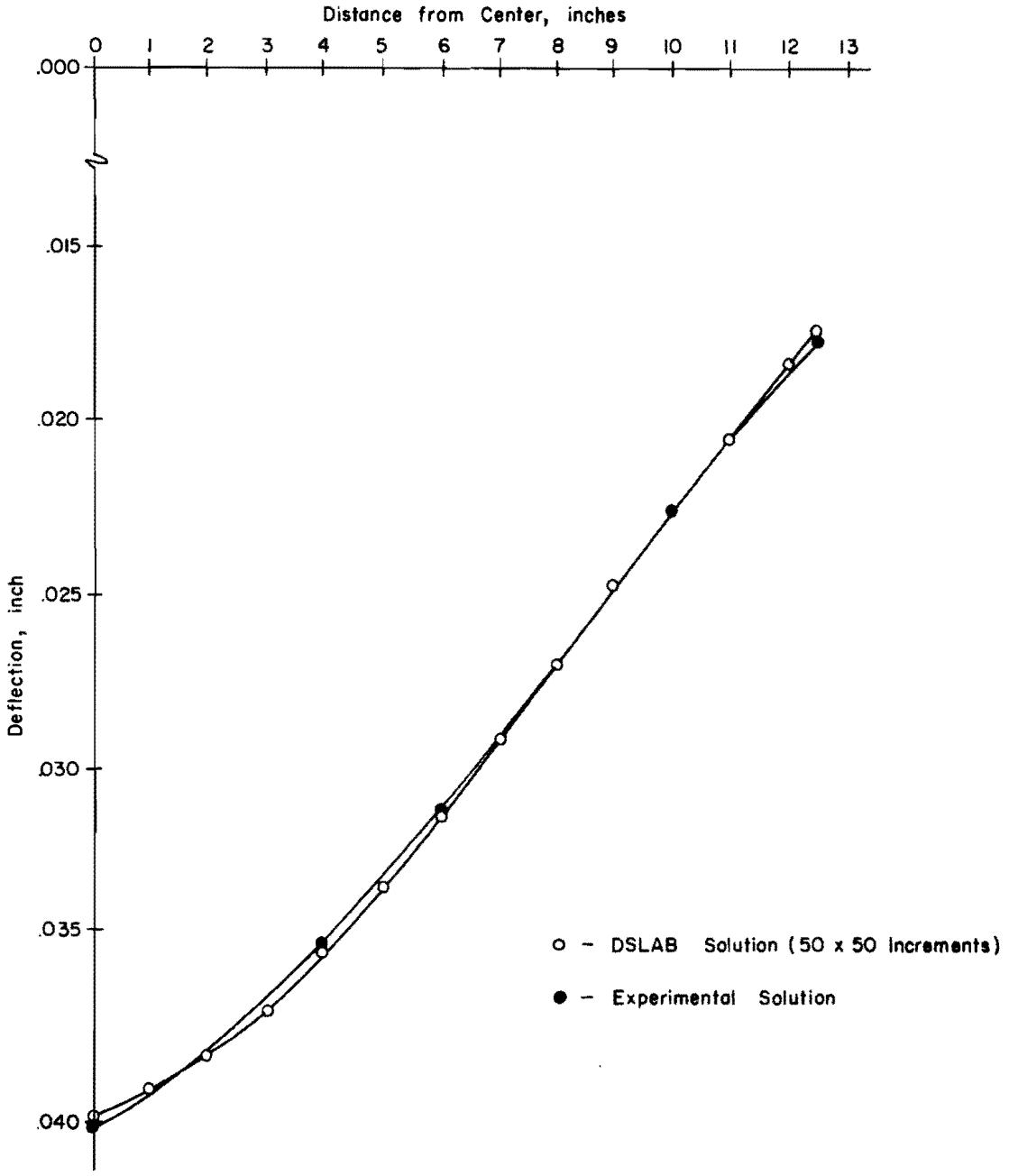

Fig 16. Experimental and analytical deflections on center line for aluminum plate on four-point support under center load (see Table 8).

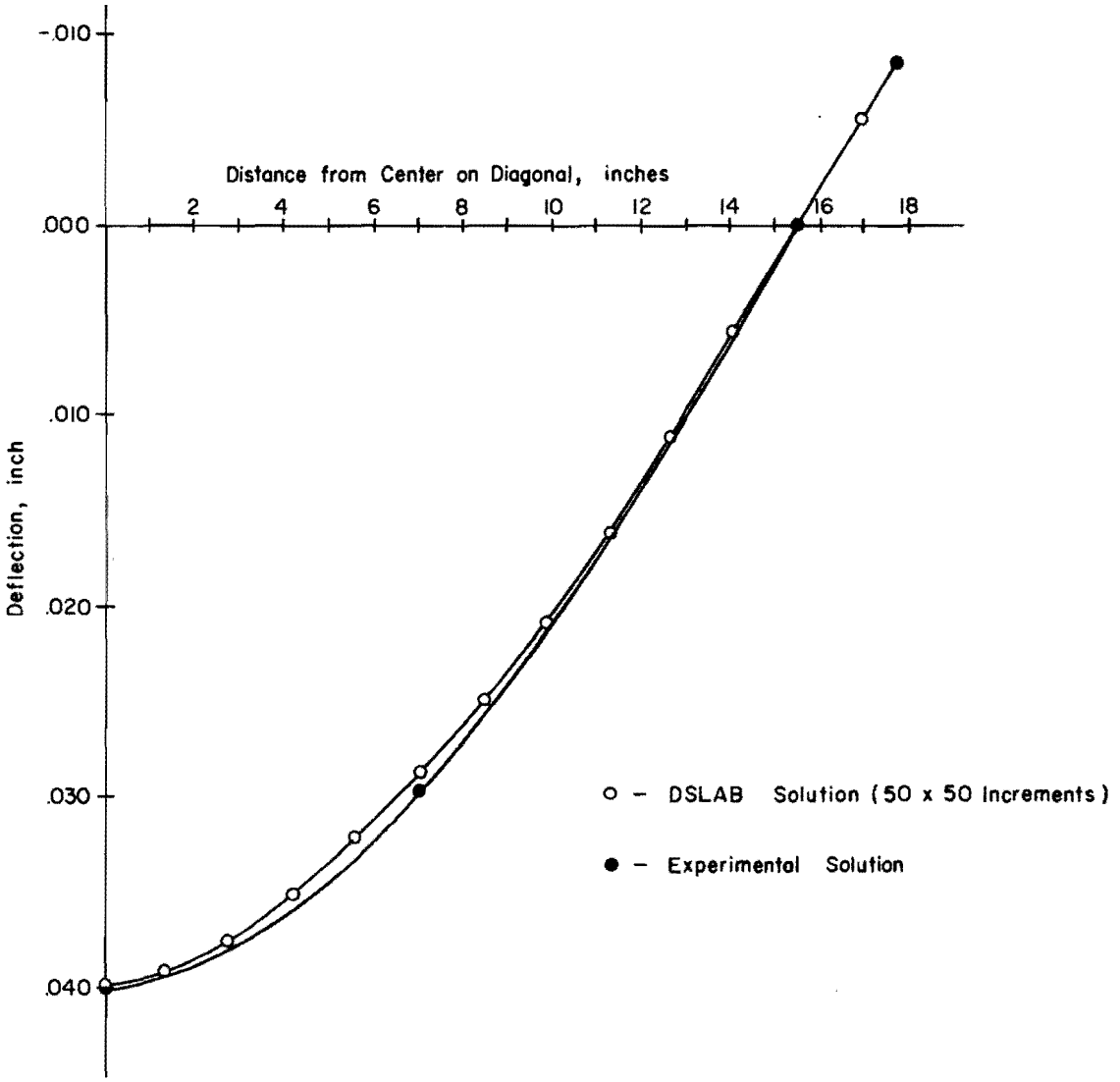

Fig 17. Experimental and analytical deflections on diagonal for aluminum plate on four-point support under center load (see Table 8).

TABLE 8. COMPARISON BETWEEN COMPUTED AND EXPERIMENTAL DEFLECTIONS FOR ALUMINUM PLATE ON FOUR-POINT SUPPORT

Load: 40 lb in center

Program: DSLAB 21 (50 x 50 increments)

Test Series	Deflections at Points (inch) 1	2	3	4	5	6	8	Remarks
	-0.03956	-0.03519	-0.03134	-0.02272	-0.01772	-0.02840	+0.00840	DSLAB solution
286 Exptl	-0.04010	-0.03510	-0.03125	-0.02298	-0.01808	-0.02922	+0.00810	
% Error	1.34	-0.20	-0.20	0.65	0.89	2.05	0.75	
287 Exptl	-0.04018	-0.03533	-0.03185	-0.02290	-0.01810	-0.02910	+0.00810	
% Error	1.54	0.35	1.27	0.45	0.95	1.74	0.75	
288 Exptl	-0.04010	-0.03505	-0.03145	-0.02290	-0.01803	-0.02910	+0.00804	
% Error	1.34	-0.35	0.27	0.45	0.77	1.97	0.89	
286 Exptl	-0.03990	-0.03490	-0.03105	-0.02278	-0.47880	-0.02902	+0.00830	Deflections obtained at the supports, 0.0002 inch subtracted
% Error	0.85	-0.75	-0.75	0.15	0.40	1.58	0.25	
287 Exptl	-0.03998	-0.03513	-0.03165	-0.02270	-0.17900	-0.02890	+0.00830	Deflections obtained at the supports, 0.0002 inch subtracted
% Error	1.05	-0.15	0.78	-0.05	0.45	1.24	0.25	
288 Exptl	-0.03985	-0.03480	-0.03120	-0.02265	-0.01778	-0.02885	+0.00829	Deflections obtained at the supports, 0.0002 inch subtracted
% Error	0.72	-0.78	-0.35	-0.18	0.15	1.22	0.28	

Note: Plots along center line and diagonal are given in Figs 16 and 17.

TABLE 9. COMPARISON FOR PRINCIPAL STRESSES FOR ALUMINUM PLATE ON FOUR-POINT SUPPORT UNDER CENTER LOAD

Load: 40 lb in center

Program: DSLAB 21 (50 x 50 increments)

Test Series		Principal Stresses Rosette 1 σ_1	Rosette 1 σ_3	Rosette 2 σ_1	Rosette 2 σ_3	Rosette 3 σ_1	Rosette 3 σ_3	Rosette 4 σ_1	Rosette 4 σ_3	Remarks
	DSLAB	486.40	448.40	839.20	578.80	-448.40	-486.40	-578.80	-839.20	
287	Exptl	478.00	466.00	836.00	589.00	-460.00	-518.00	-581.00	-844.00	Percentage error computed as a function of the individual measured value
	% Error	-1.80	3.80	-0.40	1.70	2.50	6.10	0.30	0.60	
288	Exptl	461.00	450.00	795.00	597.00	-466.00	-478.00	-591.00	-850.00	
	% Error	-5.50	0.40	-5.60	3.00	1.80	3.80	2.00	1.30	
287	Exptl	478.00	466.00	852.00	605.00					With average strain values of top and bottom strain gages
	% Error	-1.80	3.80	1.50	4.33					
288	Exptl	499.00	462.00	828.00	597.00					With average strain values of top and bottom strain gages
	% Error	2.52	2.92	-1.35	3.05					

Note: Rosettes 1 and 2 at the bottom.
Rosettes 3 and 4 at the top.

individual strains of the top and bottom gages. This difference reduced to 4.3 percent when average strain values of these gages were used.

Aluminum Plate under Off-Center Load

To investigate unsymmetrical loading a second test was run with the load applied 6 inches from center on the center line (point 3 in Fig 15). The plots for deflections along the center line and diagonal are given in Figs 18 and 19, respectively, and percentage errors in Table 10. The agreement between measured and analytical deflections was within 1 percent. The comparison for principal stresses as given in Table 11 showed the maximum difference was 8.6 percent using individual strain values and 6.8 percent with average strain values.

Aluminum Plate with Slot under Center Load

A third test, of an aluminum plate with a discontinuity, was conducted. Figure 20 shows the positions of a 6 by 1/2-inch cut along the center line, dial gages (with more points included near the cut), and rosettes with load at point 1. The analytical solutions were obtained using both DSLAB 21 and VISAB 3 (Refs 28 and 30, respectively). Using VISAB 3, the increment lengths were made smaller near the positions of loading, support, and discontinuity, as shown in Fig 21. The plots for deflections along the entire center line and the diagonal are shown in Figs 22 and 23, respectively, and percentage errors in Table 12. Agreement was within 4.0 percent. The comparison of principal stresses as given in Table 13 showed the maximum difference was 9 percent using individual strains and 6 percent using average strains.

Plexiglas Plate under Center Load

To study the modeling of another plate material, a fourth test on Plexiglas plate was conducted. The test data and comparison with the analytical, DSLAB 21 (Ref 28), solutions are shown in Figs 24 and 25 and Table 14. Deflections agreed within 2.4 percent. Strains were not measured on the Plexiglas plate due to instability in strain readings.

Orthotropic Plexiglas Plate under Center Load

A 25 by 25 by 1/2-inch plate was stiffened, on one side only, by 25 by 1/2 by 1/4-inch-thick stiffeners running parallel to one of the edges and 1/2

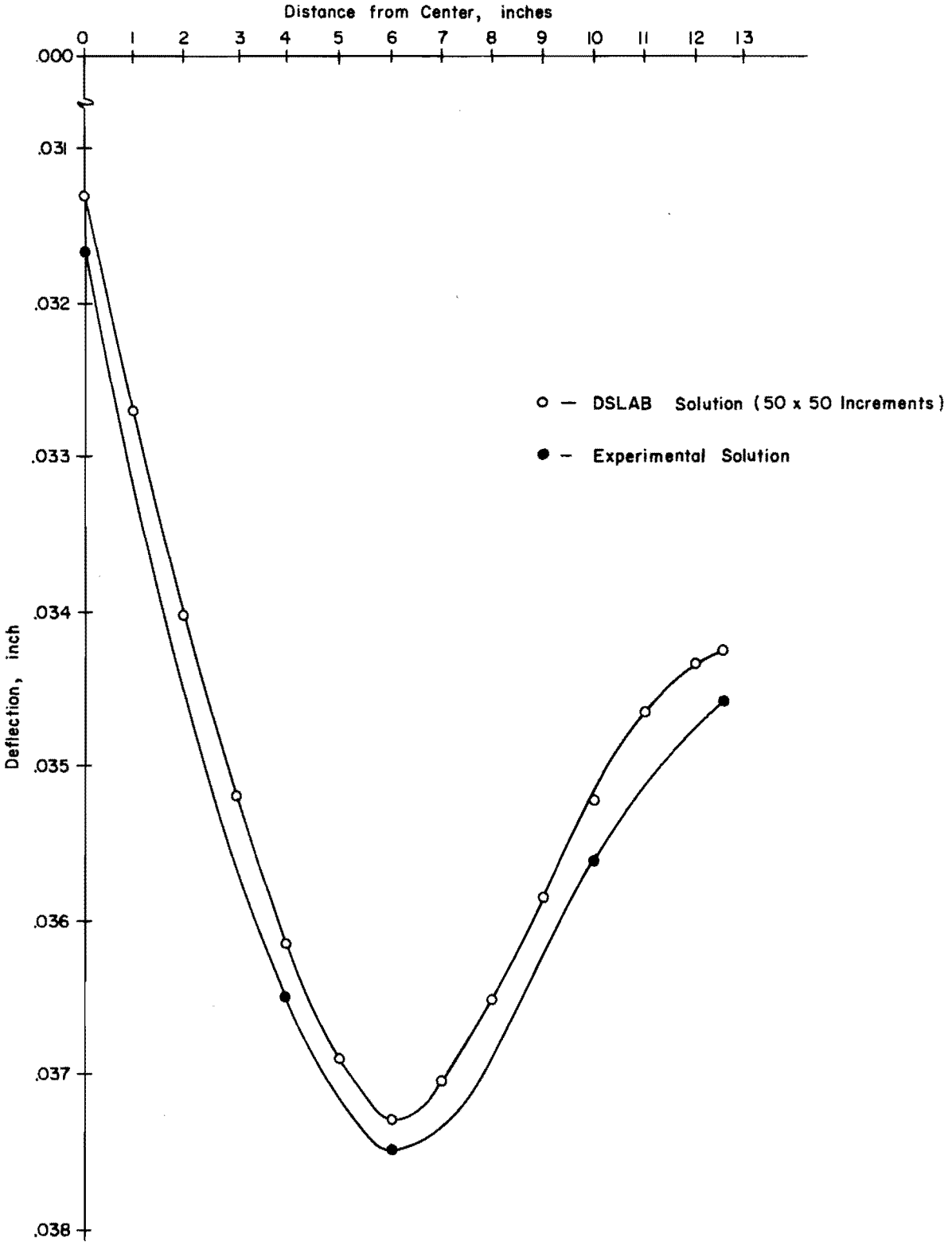

Fig 18. Experimental and analytical deflections on center line for aluminum plate under off-center load (see Table 10).

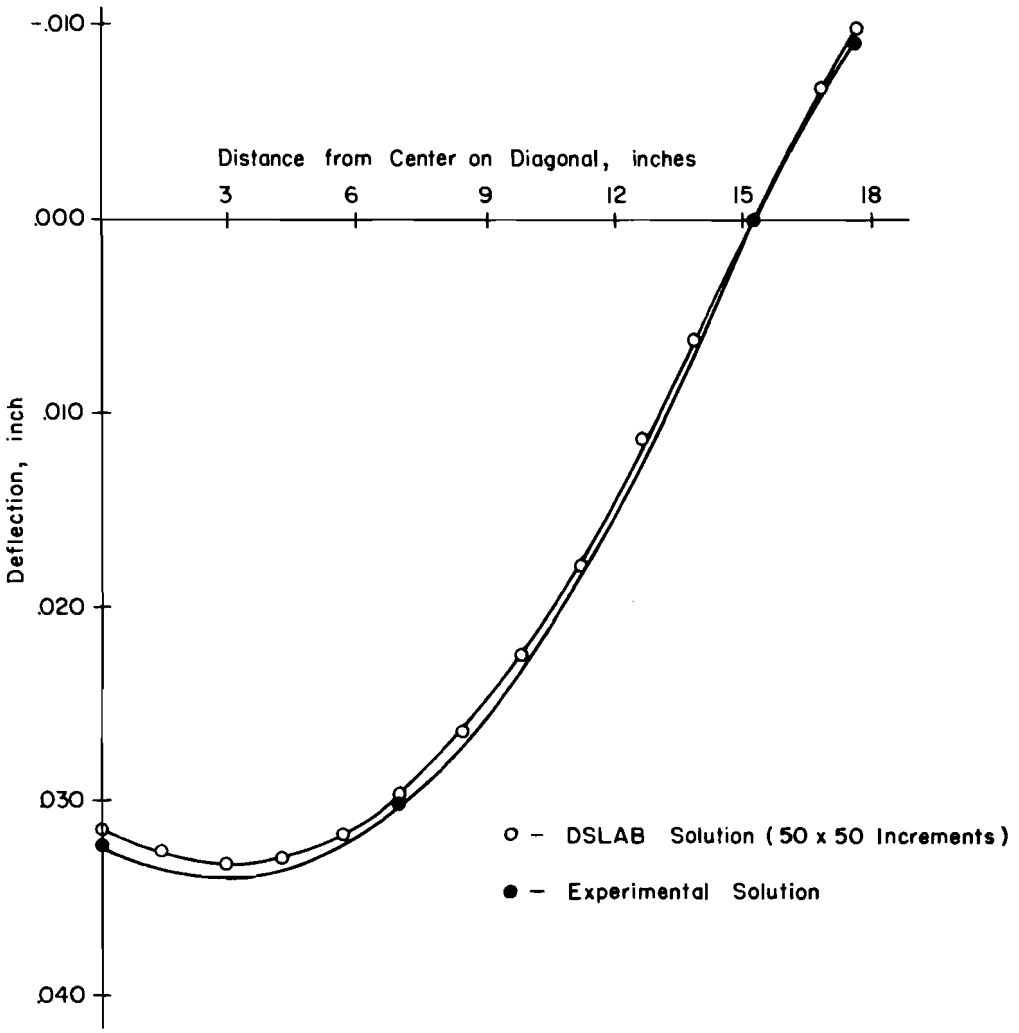

Fig 19. Experimental and analytical deflections on diagonal for aluminum plate under off-center load (see Table 10).

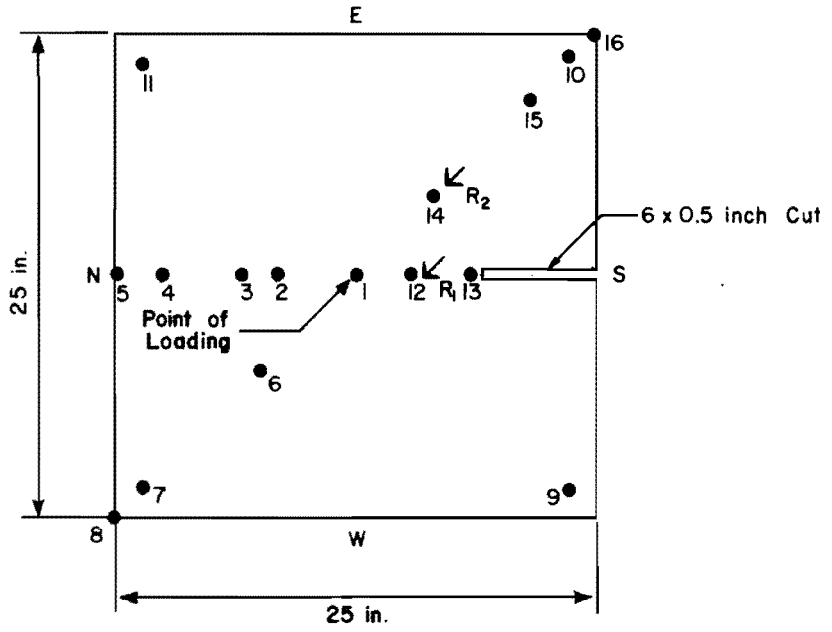

Dial Number	Distance from Center
1	at center
2	4 in. N on Center Line
3	6 in. N on Center Line
4	10 in. N on Center Line
5	12.5 in. N on Center Line
6	7.1 in. NW on Diagonal
7	15.6 in. NW on Diagonal - Support
8	17.7 in. NW on Diagonal
9	15.6 in. SW on Diagonal - Support
10	15.6 in. SE on Diagonal - Support
11	15.6 in. NE on Diagonal - Support
12	3 in. S on Center Line
13	6 in. S on Center Line
14	5.7 in. SE on Diagonal
15	12.7 in. SE on Diagonal
16	17.7 in. SE on Diagonal

Rosettes R_1, R_2, R_3, R_4 at the same locations as for plate without cut.

Fig 20. Positions of dial gages and rosettes for aluminum plate with cut.

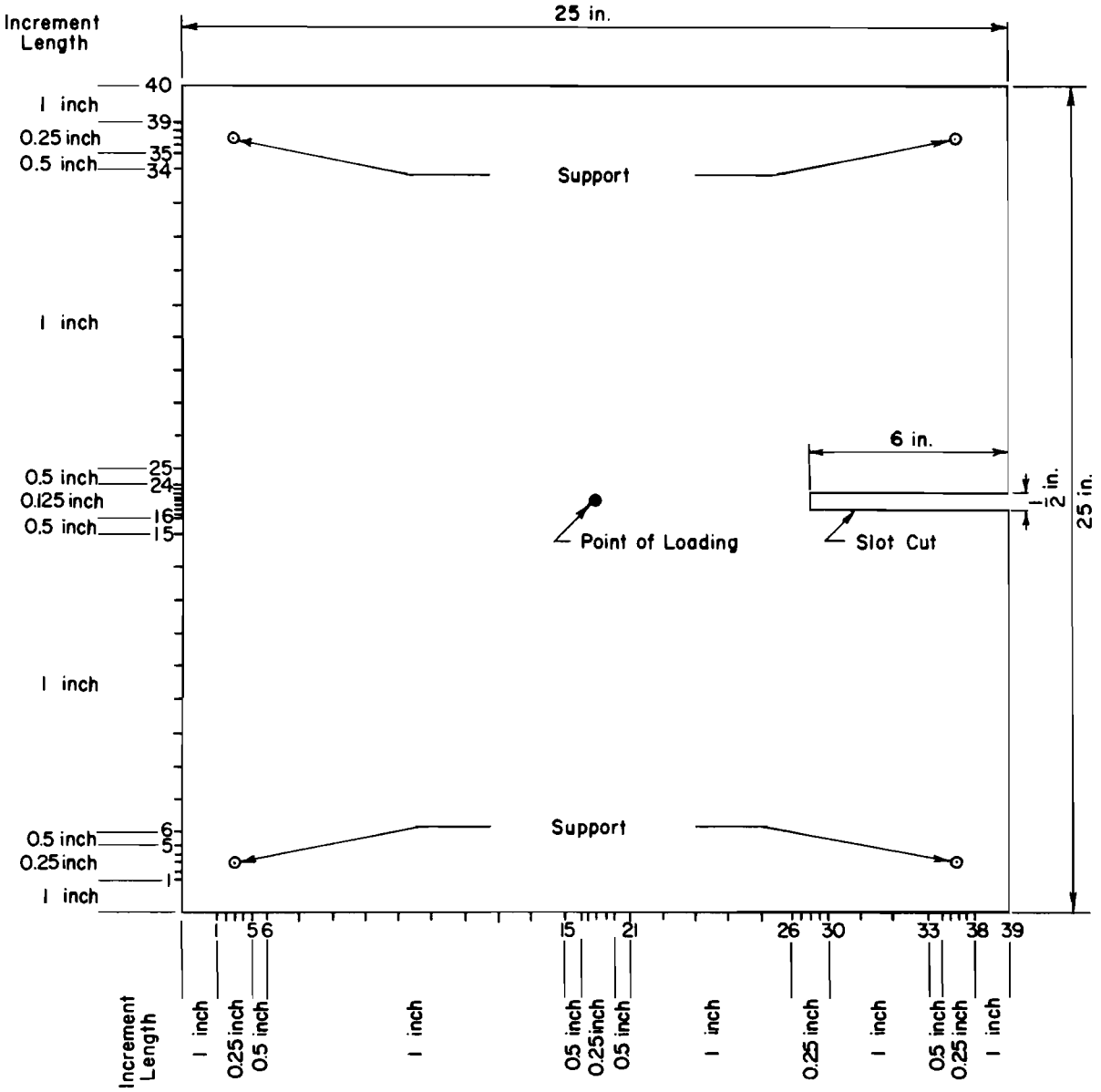

Fig 21. Increment lengths for aluminum plate with cut used in variable increment length program.

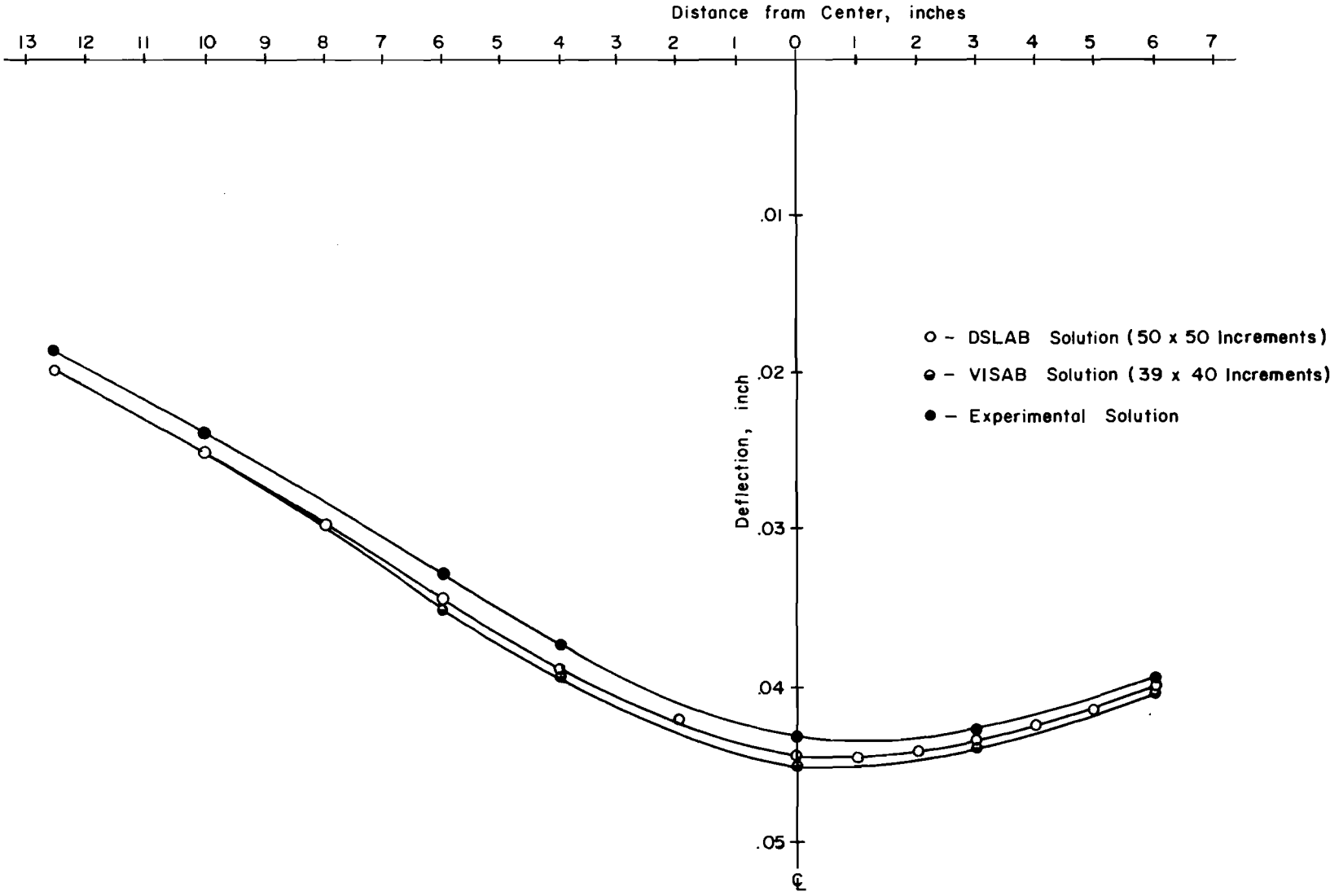

Fig 22. Experimental and analytical deflections on center line for aluminum plate with cut under center load (see Table 12).

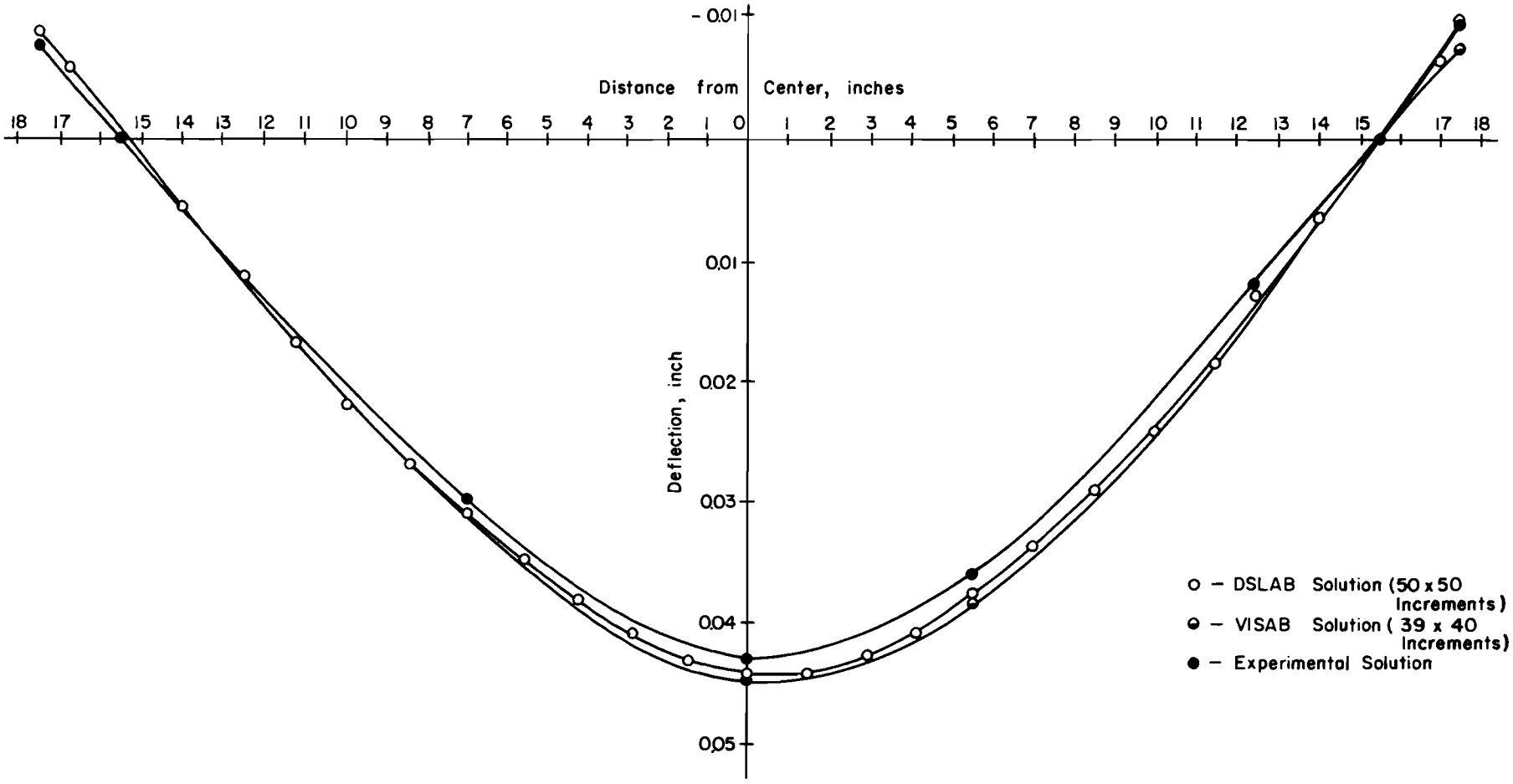

Fig 23. Experimental and analytical deflections on diagonal for aluminum plate with cut under center load (see Table 12).

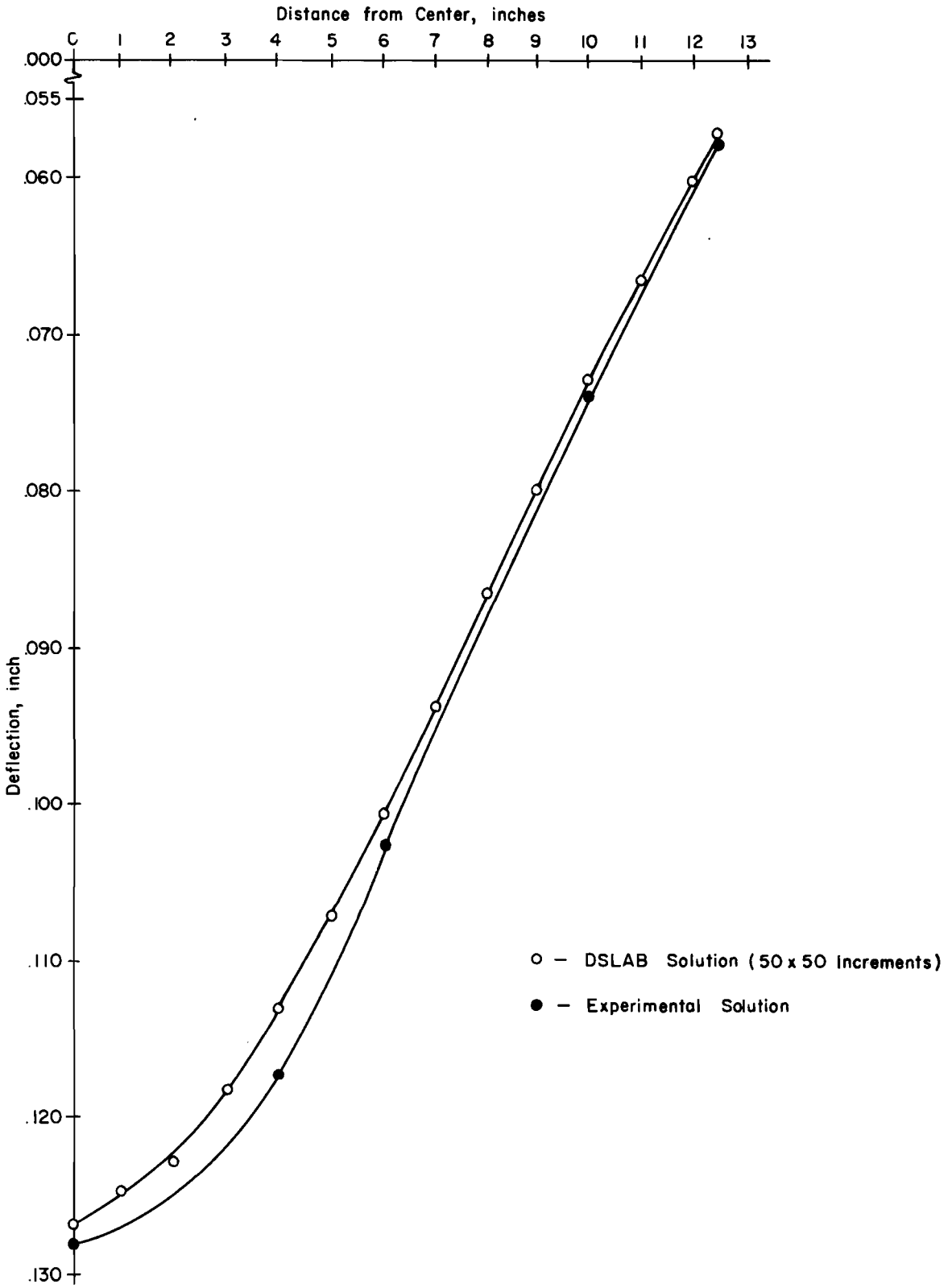

Fig 24. Experimental and analytical deflections on center line for Plexiglas plate under center load (see Table 14).

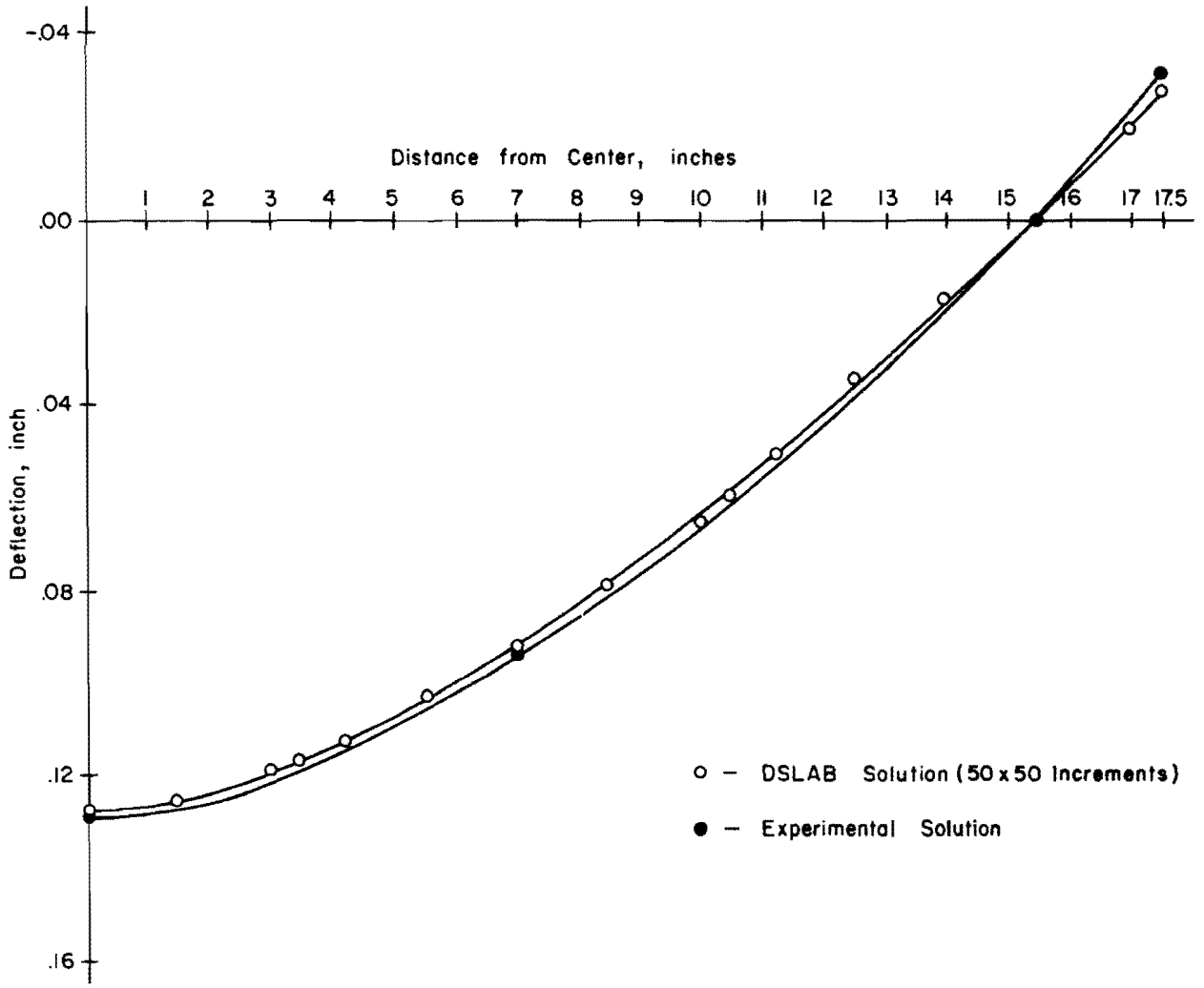

Fig 25. Experimental and analytical deflections on diagonal for Plexiglas plate under center load (see Table 14).

TABLE 10. COMPUTED AND EXPERIMENTAL DEFLECTIONS FOR ALUMINUM PLATE ON FOUR-POINT SUPPORT UNDER OFF-CENTER LOAD

Load: 40 lb at 6 inches from center on center line

Program: DSLAB 21 (50 x 50 increments)

Test Series	Deflections at Points (inch) 1	2	3	4	5	6	8	Remarks
	-0.03134	-0.03617	-0.03731	-0.03523	-0.03426	-0.02922	+0.09749	DSLAB solution
292 Exptl	-0.03165	-0.03650	-0.03750	-0.03560	-0.03465	-0.02975	+0.00850	
% Error	0.80	0.88	0.50	1.00	1.04	1.40	3.30	
293 Exptl	-0.03160	-0.03650	-0.03750	-0.03560	-0.03450	-0.02980	+0.00865	
% Error	0.70	0.88	0.50	1.00	0.60	1.54	2.93	
292 Exptl	-0.03145	-0.03630	-0.03730	-0.03540	-0.03440	-0.02960	+0.00870	Deflections obtained at the supports, 0.0002 inch subtracted
% Error	0.30	0.35	-0.02	0.45	0.37	1.01	2.82	
293 Exptl	-0.03140	-0.03630	-0.03730	-0.03540	-0.03430	-0.02960	+0.00885	Deflections obtained at the supports, 0.0002 inch subtracted
% Error	0.16	0.35	-0.02	0.45	0.11	1.01	2.41	

Note: Plots along center line and diagonal are given in Figs 18 and 19.

TABLE 11. COMPARISON FOR PRINCIPAL STRESSES FOR ALUMINUM PLATE ON FOUR-POINT SUPPORT UNDER OFF-CENTER LOADING

Load: 40 lb at 6 inches from center on center line

Program: DSLAB 21 (50 x 50 increments)

Test Series		Principal Stresses Rosette 1 σ_1	Rosette 1 σ_3	Rosette 2 σ_1	Rosette 2 σ_3	Rosette 3 σ_1	Rosette 3 σ_3	Rosette 4 σ_1	Rosette 4 σ_3	Remarks
	DSLAB	721.70	375.80	592.10	299.90	-375.80	-721.70	-299.90	-592.10	Percentage error computed as function of the individual measured value
291	Exptl	757.00	368.00	640.00	323.00	-346.00	-776.00	-309.00	-619.00	
	% Error	4.66	-2.12	7.50	7.67	-8.60	-7.00	-2.94	-4.35	
293	Exptl	782.00	394.00	630.00	298.00	-398.00	-762.00	-309.00	-619.00	
	% Error	7.71	4.62	6.02	0.60	-5.58	-5.29	-2.94	-4.35	
291	Exptl	761.00	358.00	629.00	315.00					Using average strain values of top and bottom gages
	% Error	5.16	-4.97	5.87	4.79					
293	Exptl	774.00	402.00	629.00	315.00					Using average strain values of top and bottom gages
	% Error	6.76	6.50	5.87	4.79					

Note: Rosettes 1 and 2 at the bottom.
Rosettes 3 and 4 at the top.

TABLE 12. COMPUTED AND EXPERIMENTAL DEFLECTIONS FOR AL PLATE WITH SLOT CUT UNDER CENTRAL LOADING

Load: 40 lb in center

Programs: DSLAB 21 (50 x 50 increments)
VISAB 3 (39 x 40 increments)

Series		Deflections at Points (inch) 1	2	3	4	5	6	8	12	13	14	15	16
	DSLAB Solution	-0.04404	-0.03841	-0.03410	-0.02481	-0.01953	-0.03069	+0.00894	-0.04305	-0.04048	-0.03698	-0.01270	+0.00983
	VISAB Solution	-0.04444	-0.03882	-0.03443	-0.02489	-0.01943	-0.03086	+0.00892	-0.04318	-0.04004	-0.03745	-0.01311	+0.00735
295	Exptl	-0.04320	-0.03697	-0.03285	-0.02365	-0.01860	-0.02980	+0.00750	-0.04240	-0.04020	-0.03580	-0.01200	+0.00970
	% Error (DSLAB)	-1.94	-3.33	-2.89	-2.68	-2.15	-2.06	+3.57	-1.50	-0.65	-2.70	-1.62	+0.30
	% Error (VISAB)	-2.87	-4.28	-3.66	-2.87	-1.92	-2.45	+3.27	-1.80	0.37	-3.82	-2.56	-5.45
296	Exptl	-0.04305	-0.03697	-0.03285	-0.02360	-0.01860	-0.02980	+0.00740	-0.04240	-0.03925	-0.03580	-0.01240	+0.01000
	% Error (DSLAB)	-2.29	-3.34	-2.90	-2.81	-2.16	-2.06	+3.56	-1.50	-2.85	-2.70	-0.70	-0.39
	% Error (VISAB)	-3.22	-4.30	-3.67	-3.00	-1.93	-2.45	+3.52	-1.80	-1.84	-3.82	-1.65	-6.17
295*	Exptl	-0.04300	-0.03677	-0.03265	-0.02345	-0.01840	-0.02960	+0.00770	-0.04220	-0.04000	-0.03560	-0.01180	+0.00990
	% Error (DSLAB)	-2.41	-3.81	-3.37	-3.16	-2.62	-2.53	+2.87	-1.98	-1.12	-3.21	-2.09	-0.16
	% Error (VISAB)	-3.35	-4.77	-4.14	-3.35	-2.39	-2.93	+2.83	-2.28	-0.10	-4.30	-3.05	-5.93
296*	Exptl	-0.04285	-0.03677	-0.03265	-0.02340	-0.01840	-0.02960	+0.00760	-0.04220	-0.03905	-0.03560	-0.01220	+0.01020
	% Error (DSLAB)	-2.78	-3.83	-3.38	-3.29	-2.64	-2.54	+3.12	-1.98	-3.34	-3.22	-1.17	-0.86
	% Error (VISAB)	-3.71	-4.78	-4.15	-3.48	-2.40	-2.94	+3.07	-2.29	-2.31	-4.32	-2.12	-6.65

*Deflections obtained at the supports, 0.0002 inch subtracted.
Note: Plots along center line and diagonal are given in Figs 22 and 23.

TABLE 13. COMPARISON FOR PRINCIPAL STRESSES FOR ALUMINUM PLATE WITH CUT ON FOUR-POINT SUPPORT UNDER CENTRAL LOAD

Load: 40 lb in center

Programs: DSLAB 21 (50 x 50 increments)
VISAB 3 (39 x 40 increments)

Test Series		Principal Stresses Rosette 1 σ_1	Rosette 1 σ_3	Rosette 2 σ_1	Rosette 2 σ_3	Rosette 3 σ_1	Rosette 3 σ_3	Rosette 4 σ_1	Rosette 4 σ_3	Remarks
	DSLAB	553.20	405.30	1241.00	488.70	-405.30	-553.20	-488.70	-1241.00	Percentage error computed as function of the individual measured value
	VISAB	567.20	408.80	1179.00	515.80	-408.80	-567.20	-515.80	-1179.00	
295	Exptl	569.00	375.00	1170.00	503.00	-422.00	-539.00	-503.00	-1170.00	
	% Error (DSLAB)	2.77	-8.08	6.07	2.78	4.03	2.59	2.78	6.07	
	% Error (VISAB)	0.30	9.01	0.77	2.54	3.30	5.23	2.54	0.77	
296	Exptl	578.00	400.00	1179.00	495.00	-433.00	-567.00	-511.00	-1162.00	
	% Error (DSLAB)	4.29	1.33	5.26	1.21	8.60	2.47	6.50	1.82	
	% Error (VISAB)	1.86	2.20	0.00	4.20	7.72	0.04	9.39	1.55	
295	Exptl	556.00	405.00	1170.00	503.00					Using average strain values of top and bottom gages
	% Error (DSLAB)	0.50	0.07	6.07	2.78					
	% Error (VISAB)	2.01	0.93	6.07	2.78					
296	Exptl	572.00	422.00	1170.00	503.00					
	% Error (DSLAB)	3.29	3.96	6.07	2.78					
	% Error (VISAB)	0.84	3.21	6.07	2.78					

Note: Rosettes 1 and 2 at the bottom.
Rosettes 3 and 4 at the top.

TABLE 14. COMPUTED AND EXPERIMENTAL DEFLECTIONS FOR PLEXIGLAS PLATE ON FOUR-POINT SUPPORT UNDER CENTRAL LOAD

Load: 40 lb in center

Program: DSLAB 21 (50 x 50 increments)

Test Series	Deflections at Points (inch) 1	2	3	4	5	6	8	Remarks
	-0.12670	-0.11528	-0.10050	-0.07332	-0.05780	-0.09103	+0.02720	DSLAB solution
282 Exptl	-0.12790	-0.11830	-0.10365	-0.07465	-0.05910	-0.09290	+0.03080	
% Error	0.93	2.35	2.50	1.03	1.01	1.50	-2.81	
283 Exptl	-0.12975	-0.11795	-0.10190	-0.07464	-0.05890	-0.09320	+0.03050	
% Error	2.35	2.06	1.07	1.01	0.85	1.67	-2.55	
282 Exptl	-0.12730	-0.11770	-0.10305	-0.07405	-0.05850	-0.09230	+0.03020	Average support deflection,
% Error	0.47	1.90	2.00	0.57	0.58	1.00	-2.35	0.0006 inch subtracted
283 Exptl	-0.12815	-0.11735	-0.10130	-0.07404	-0.05830	-0.09260	+0.02990	Average support deflection,
% Error	1.13	1.61	0.62	0.56	0.39	1.23	-2.10	0.0006 inch subtracted

Note: Plots along center line and diagonal are given in Figs 24 and 25.

inch apart. The stiffeners were chemically bonded to the plate with dichloromethane applied through hypodermic needles (Ref 34). The dimensions of the plate with stiffeners are shown in Fig 26 and the test arrangements in Fig 27.

Three different analytical solutions for orthotropic plates were obtained using

(1) experimentally obtained stiffness values, ν_{yx} obtained by testing the strap with longitudinal stiffners, and DSLAB 30;

(2) experimentally obtained stiffness values, ν of isotropic plate, and DSLAB 21; and

(3) experimentally obtained stiffness values, ν of isotropic plate, and DSLAB 30.

The test data for deflections and the comparison with the analytical solution for Case 1 are given in Figs 28 and 29 and Table 15.

From the three cases for orthotropic plates studied, the following observations were made:

(1) With Poisson's ratio for orthotropic plate (Table 15) and using DSLAB 30 (Case 1), the maximum discrepancy was within 5.1 percent.

(2) With Poisson's ratio for isotropic plate for the entire plate and using DSLAB 21 (Case 2), the discrepancy was within 6.8 percent (Ref 26).

(3) With Poisson's ratio for isotropic plates in one direction and using DSLAB 30 (Case 3), the discrepancy was within 6.2 percent (Ref 26).

This indicated a small difference between (1) and (3), and, therefore, for all practical purposes, if Poisson's ratio for isotropic plates in one direction is used with program DSLAB 30, which determines the corresponding Poisson's ratio for the other direction, the solution is acceptable.

Causes of Discrepancy

The discrepancy between the experimental and analytical solutions can possibly be due to the following:

(1) Plate thicknesses that were not constant throughout. The difference for aluminum plate was 0.005 inch; for Plexiglas plate, 0.006 inch; and for orthotropic Plexiglas plate, 0.05 inch.

(2) The possibility of a small error in the determination of elastic properties E and ν. When strain gages are used to determine the properties, the error is generally within a few percent.

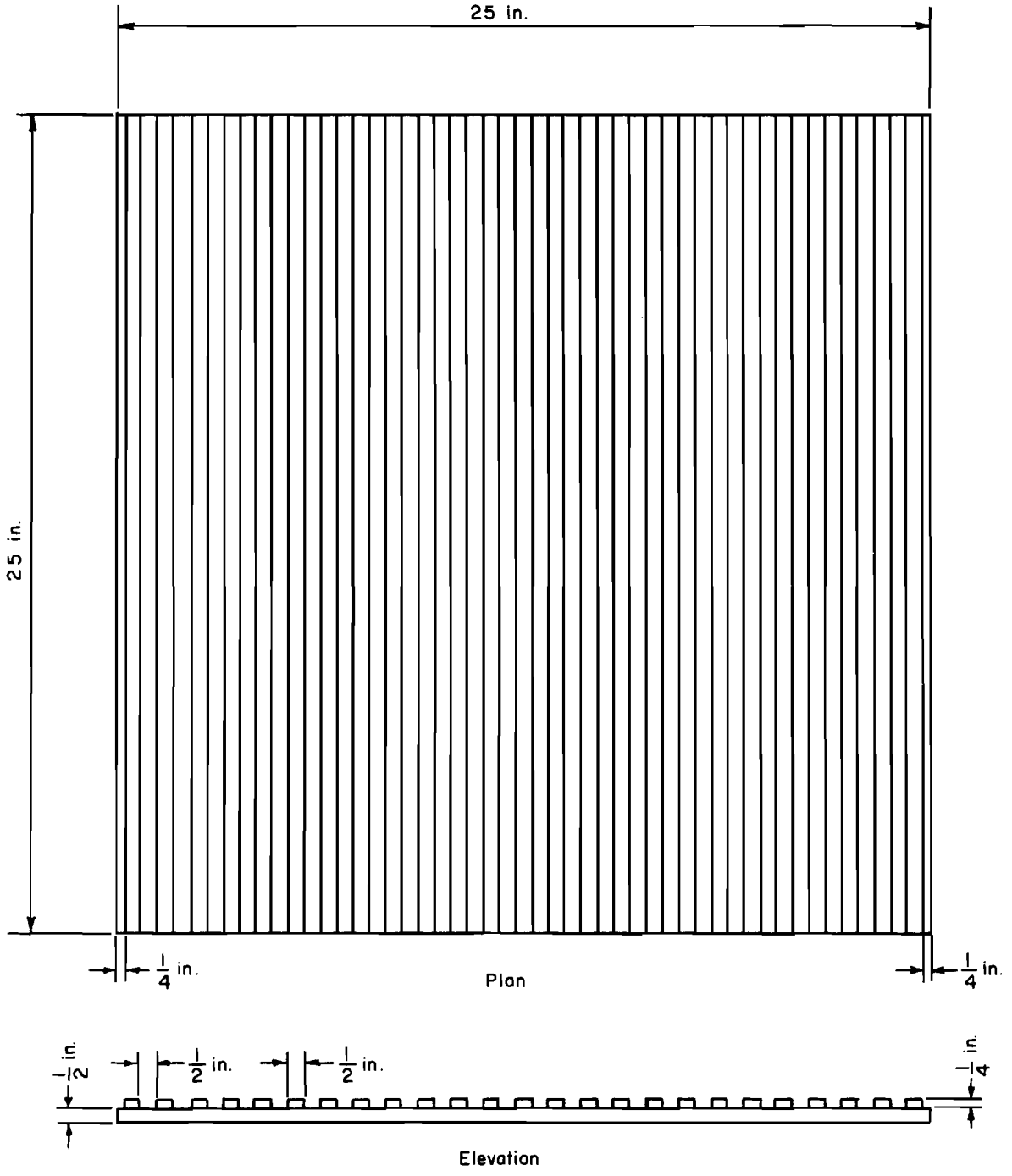

Fig 26. Plexiglas orthotropic plate (plate with stiffeners on one side).

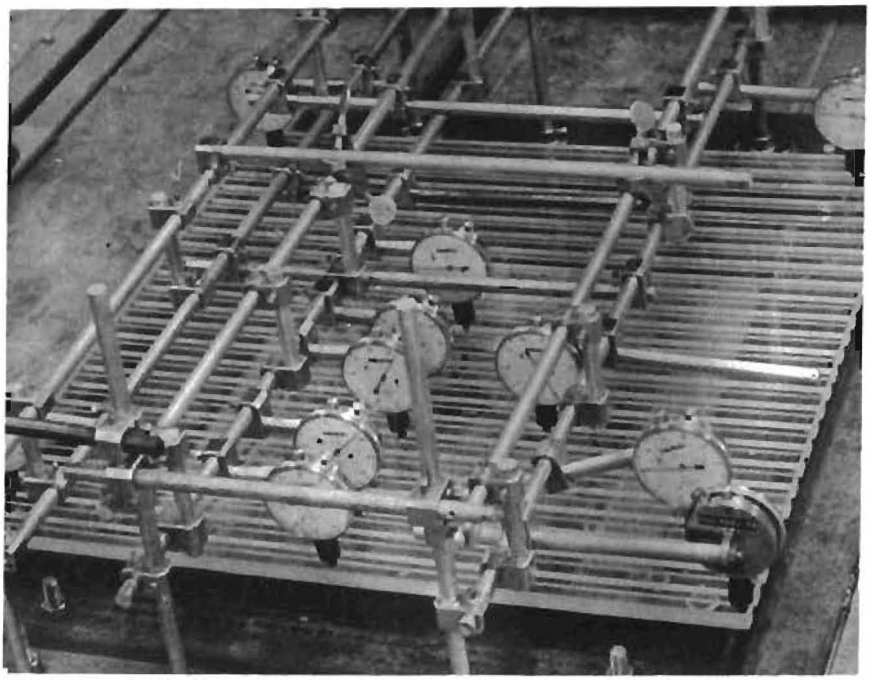

Fig 27. Test arrangements for Plexiglas orthotropic plate on four-point support.

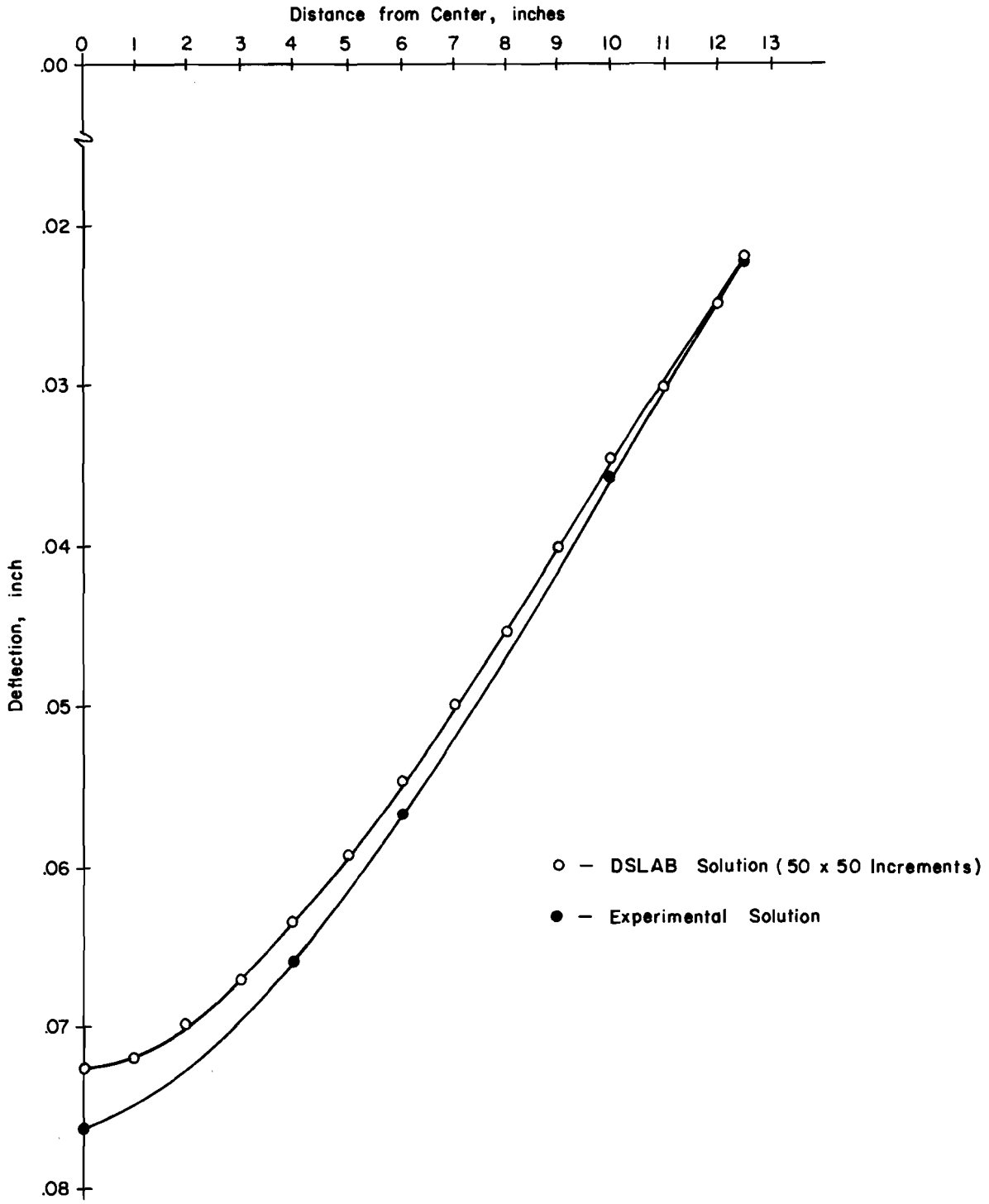

Fig 28. Experimental and analytical deflections on center line for Plexiglas orthotropic plate under center load (see Table 15).

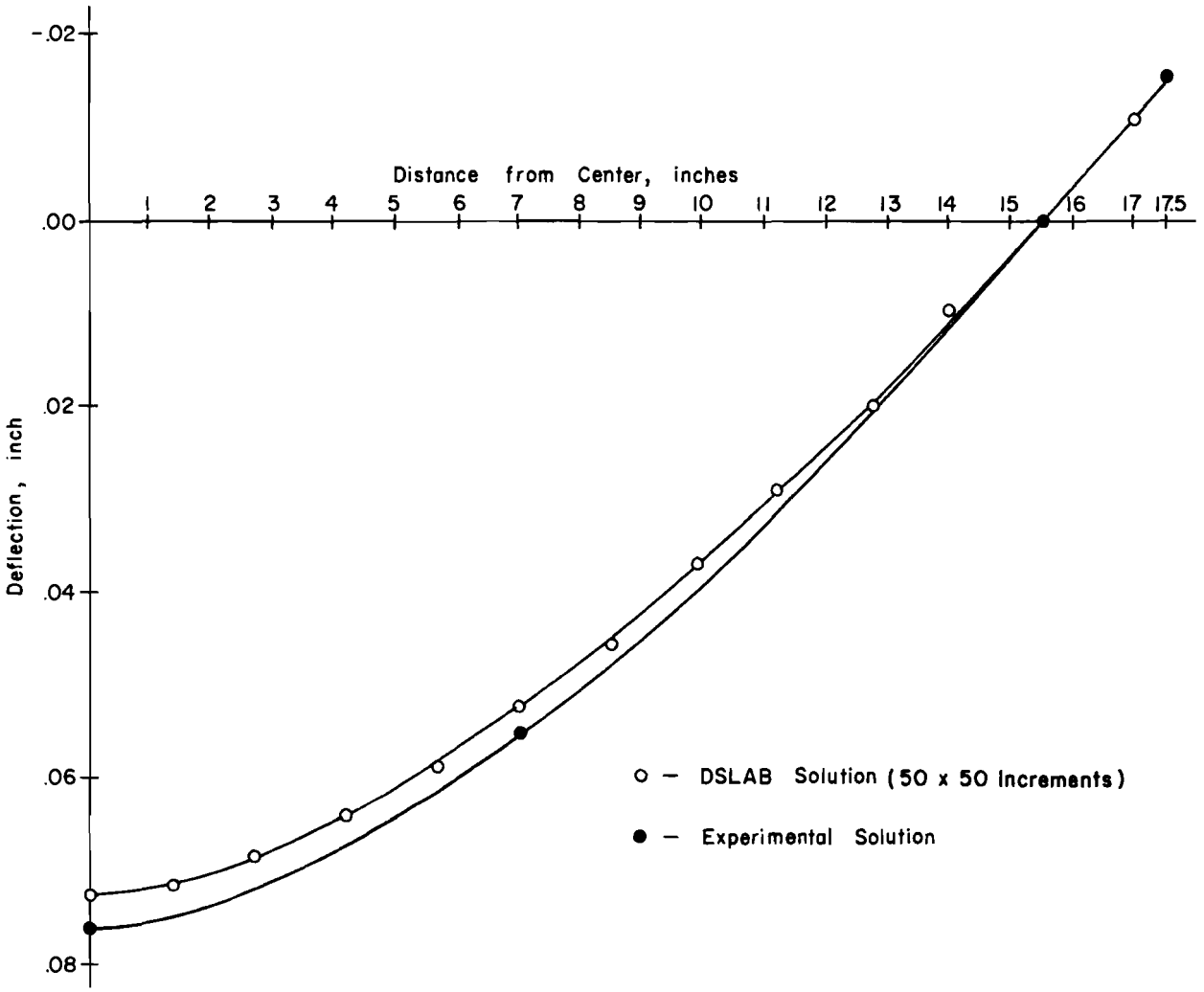

Fig 29. Experimental and analytical deflections on diagonal for Plexiglas orthotropic plate under center load (see Table 15).

TABLE 15. COMPUTED AND EXPERIMENTAL DEFLECTIONS FOR PLEXIGLAS ORTHOTROPIC PLATE UNDER CENTRAL LOADING

Load: 40 lb in center

Program: DSLAB 30 (50 x 50 increments)

Test Series	Deflections at Points (inch) 1	2	3	4	5	6	8	Remarks
DSLAB 30	-0.07250	-0.06326	-0.05475	-0.03484	-0.02247	-0.05212	+0.01529	With Poisson's ratio of orthotropic plate
298 (a) Exptl	-0.07670	-0.06520	-0.05685	-0.03670	-0.02310	-0.05500	+0.01450	
% Error	5.48	2.53	2.84	2.43	0.82	3.75	1.03	
298 (b) Exptl	-0.07700	-0.06665	-0.05675	-0.03600	-0.02335	-0.05625	+0.01485	
% Error	5.84	4.40	2.70	1.51	1.14	5.36	0.57	
298 (c) Exptl	-0.07645	-0.06520	-0.05610	-0.03540	-0.02290	-0.05580	+0.01450	
% Error	5.17	2.54	1.87	0.73	0.56	4.81	1.03	
298 (a) Exptl	-0.07610	-0.06460	-0.05625	-0.03610	-0.02250	-0.05440	+0.01510	Average support deflection, 0.0006 inch subtracted
% Error	4.73	1.76	2.08	1.66	0.04	3.00	0.25	
298 (b) Exptl	-0.07640	-0.06605	-0.05615	-0.03540	-0.02275	-0.05565	+0.01545	Average support deflection, 0.0006 inch subtracted
% Error	5.10	3.65	1.94	0.73	0.37	4.62	-0.21	
298 (c) Exptl	-0.07585	-0.06460	-0.05550	-0.03480	-0.02230	-0.05520	+0.01510	Average support deflection, 0.0006 inch subtracted
% Error	4.42	1.77	1.09	0.05	-0.22	4.06	0.25	

Note: Plots along center line and diagonal are given in Figs 28 and 29.

(3) Lack of measures to preclude creep effects for Plexiglas plates. The reason that the measured deflections are greater than the computed deflection may be partly due to creep effects.

(4) Experimentally determined stiffness properties that were slightly different from those obtained analytically for the orthotropic plates.

(5) The possibility that the rosettes were not fixed at identical positions on both sides of the plate.

(6) Failure to check the calibration of the strain-indicator before testing. A slight difference in the calibration could create an appreciable difference in the principal stresses.

Limitations of Analytical Solution

The analytical solution depends on accurately approximating the real plate with a model, particularly near the positions of supports, loads, and discontinuities; the closer the input data represent the real plate, the more precise the answers computed by this method will be; i.e., the greater the number of increments used to model a particular test set-up, the greater is the accuracy of the solution. In all the plate problems solved herein the number of increments was 50 in each direction, and the results can be expected to be within acceptable accuracy (Ref 19).

The algebraic solution is exact for the model within computer accuracy; small errors creep in due to round-off and truncation, but may not have any significant effect on the results. Small errors may also be introduced in approximating the differential equation of the fourth order to the finite difference equation.

The chief disadvantage of DSLAB is that it requires a large amount of computer storage, and thus the size of the problem which can be run depends on the storage capacity of a particular computer.

Observations from Plate Tests

A summary of percent error for deflections for all the tests is presented in Table 16 for points "under the load," "near the load," and "near the periphery." A similar summary of percentage errors for principal stresses is given in Table 17.

The experimental technique of the four-edge support test had many shortcomings which led to appreciable differences between the experimental solution

TABLE 16. SUMMARY OF PERCENTAGE ERROR FOR DEFLECTIONS

Support Condition	Plate Material and Load Condition	Percentage Error for Points Under the Load	Near the Load	Near the Periphery
Four-edge	AL plate under center load	5.60 to 9.80	3.84 to 11.57	1.34 to 7.75
Four-points	AL plate under center load	0.85 to 1.05	-0.78 to 1.24	0.15 to 0.45
Four-points	AL plate under off-center load	-0.02	0.16 to 1.01	0.11 to 2.82
Four-points	AL plate with cut under center load	-2.41 to -2.78	-1.12 to -3.81	-0.16 to 3.12
Four-points	Plexiglas plate under center load	0.47 to 1.13	0.56 to 2.00	0.39 to -2.35
Four-points	Plexiglas orthotropic plate under center load	4.42 to 5.10	0 to 3.65	-0.22 to 0.25

TABLE 17. SUMMARY OF PERCENTAGE ERROR FOR PRINCIPAL STRESSES

	Percentage Error			
	Rosette 1		Rosette 2	
	σ_1	σ_3	σ_1	σ_3
Al plate (central load)	-1.80 to 2.52	3.80 to 2.92	-1.35 to 1.5	3.05 to 4.33
Al plate (off-center load)	5.16 to 6.76	-4.97 to 6.50	5.87	4.79
Al plate with cut	0.50 to 0.84	0.07 to 3.21	6.07	2.78
	Agreement within 6 %			

and the analytical solution, while the experimental set-up with four-point support did not have any major technical discrepancy. From the experimental evidence based on tests conducted on plates with four-point support, the following observations can be made:

(1) For linearly elastic materials such as aluminum, the analytical solutions agreed with the experimental data within 4 percent for deflections and 6 percent for principal stresses, for continuous plates under center and off-center loadings and for plates with a discontinuity under central loading; the discrepancy may have been due to experimental error.

(2) For an approximate linearly elastic material like Plexiglas the discrepancy for deflections was within 2.0 percent for isotropic plates and 5.0 percent for orthotropic plates, possibly due partly to creep effects and experimental error in determining the elastic properties and bending and twisting stiffness.

(3) For material like Plexiglas, the elastic properties determined from the tension test (using strain gages) were higher than those from the bending test (Appendix 1). This may have been partly due to the local strengthening effect of the epoxy near the strain gages, and, therefore, the bending properties should be determined from the bending test, without using strain gages. There was no such result for aluminum.

(4) For orthotropic plates, the analytical solution gave reasonably good results if the bending and twisting stiffnesses and Poisson's ratio for both directions were determined accurately. However, if Poisson's ratio for isotropic plates were used with the program which considers Poisson's ratio in two directions (DSLAB 30), the results obtained for orthotropic plates would be reasonably acceptable from a practical point of view.

Based on the above, the validity of the analytical solution for plates of linearly elastic materials on rigid supports is proved. The small discrepancy may be due to experimental error. Having established the validity of the method of solution for linear materials on rigid supports, it is now possible to study the behavior of linear materials on nonlinear support such as soil subgrade.

CHAPTER 5. SLAB STUDY

After the method of solution based on the discrete-element model for linear materials on rigid supports was verified by actual tests, as described in Chapter 4, a study of the soil-structure interaction problem for a slab resting on soil subgrade having nonlinear characteristics was undertaken. This chapter describes the development of a test procedure, the different tests conducted, representation of the soil by linear and nonlinear characteristics, and comparison of analytical and experimental solutions for the tests under static loading.

Variables involved in the slab test and analysis, in addition to those for the plate problem, as enumerated in Chapter 4, are

(1) subgrade stress-strain characteristics and subgrade modulus and
(2) method of preparation of slab and subgrade.

The investigations were made on a small-dimension, thin aluminum slab resting on clay soil. The soil was prepared by extrusion and placed in a supporting box. The testing was done under increasing static load. The subgrade characteristics were determined by plate load test and the stress-strain characteristics of the soil.

A 9 by 9 by 1/8-inch aluminum slab was tested. Elastic properties, i.e., modulus of elasticity E and Poisson's ratio ν, were determined by testing a strap of the material in tension in the same way as for plates (Chapter 4). These data are given in Appendix 1. The slab properties determined are as follows:

$$D_x = D_y = 1.930 \times 10^3 \text{ lb-in}$$

$$C_x = C_y = 1.280 \times 10^3 \text{ lb-in}$$

Soil Selection, Its Preparation and Properties

Clay was used as the subgrade material. The several clays considered for use were Taylor Marl No. 1, Taylor Marl No. 2, Del Rio clay, Vicksburg silty clay, Eagle Ford, and Wilcox. Their index properties, classification, source of information, and availability in Austin are given in Table 18. Workability, ease of continuing to get consistent properties, and availability in Austin were considered in selecting the soil.

It was well known from previous work (Ref 42) that low plasticity clays have more uniform and consistent properties, and, on this basis, Taylor Marl No. 1 and Wilcox were the best choices. Taylor Marl No. 1 was selected and was brought from a natural deposit near the city of Manor, about 6 miles east of Austin.

After the clay was transported to the laboratory, it was thoroughly dried in the oven at about 130° F and crushed in a Chipmunk crusher. The crushed clay was redried in the oven and pulverized. It was then mixed with water in a mechanical mixer to get an approximate water content of 38 percent, and the mixed soil was placed in plastic bags and stored in a moisture-controlled room, to avoid evaporation. Storing of the prepared soil for a month helped to achieve uniform moisture content throughout the soil mass. After one test was performed, the soil was stored in a similar way until the next test.

The properties of Taylor Marl as determined in the laboratory were

Liquid limit = 53.8
Plastic limit = 24.5
Plasticity index = 29.3
Optimum moisture content = 17.5 percent
Maximum dry density = 106.5 lb/ft^3

The in situ properties of the clay in the test box were

Average density = 116 lb/ft^3
Moisture content = 38 percent
Average degree of saturation = 96 percent
Average shear strength from unconfined compression test = 177 lb/ft^2 (1.23 lb/in^2)
Modulus of subgrade reaction (tangent) k = 160 lb/in^3

Details of plate load tests, shear tests, and other soil property tests are given on pages 79 through 87.

TABLE 18. PROPERTIES OF CLAYS CONSIDERED

Soil Property	Taylor Marl No. 1	Taylor Marl No. 2	Del Rio Clay	Vicksburg Silty Clay	Eagle Ford	Wilcox
Liquid limit	49.0	73	53-65	34	38-90	59.0
Plastic limit	21.0	20	33-36	22	20	30.0
Plasticity index	28.0	53.1	20-29	12	20-70	29.0
Classification	CL	CH	CH	Inorganic silty clay	-	-
Plasticity	Medium	High	High	Low	High (highly variable)	Medium
Dry crushing strength	High	High	High	Medium	-	High
Availability in Austin	Available	Available	Available (contains nodules and grass roots)	Not available	Difficult to obtain (lies below residential area)	Available
Source of information	Ref 13	Ref 13	Ref 38	Ref 38	Personal Communication with Mr. Walter	Ref 9

Test Box and Slab Sizes

The size of the box was determined by the quantity of soil which could be handled in storing and the capacity of the crane to lift the box during its movements within the laboratory. A 2 by 2 by 2-foot box (inner dimensions), which could hold about 930 pounds of soil, was selected. The box was made of plywood 3/4-inch-thick, stiffened by 2 by 4-inch lumber. The box had detachable top and bottom covers which could be attached by means of bolts. The box had two handles.

The slab size was chosen considering the effects of the container walls and bottom and the relative stiffness between slab and soil. Lee (Ref 21) has discussed in detail the effect of the walls and bottom of the container on deflection of a rigid plate or average deflection of a slab. Using his Figs 2 and 7, the slab size was chosen to be 9 by 9 inches, so that there would be little restraining effect due to the container walls and bottom. This size also agreed with the rough criterion that the zone of influence extend to at least twice the width of the slab (Ref 45). The thickness of the aluminum slab was chosen so that increasing the horizontal dimensions of the slab would have negligible effect on the behavior of the slab under interior or corner loading.

Radius of relative stiffness ℓ is defined as

$$\ell = \sqrt[4]{\frac{Et^3}{12(1 - \nu^2)k}} \tag{5.1}$$

where

E = modulus of elasticity of slab,

t = thickness of slab,

ν = Poisson's ratio of slab,

k = modulus of subgrade reaction.

For the experimental slab

$$E = 10.5 \times 10^6 \text{ lb/in}^2$$

$$\nu = 0.338$$

$t = 0.125$ inch

$k = 160$ lb/in^3

$\ell = 1.87$ inches

The 9 by 9-inch slab had dimensions of $4.82\ell \times 4.82\ell$, agreeing with the minimum horizontal dimensions of $3.0\ell \times 3.0\ell$ observed by the Corps of Engineers (Ref 41), according to whom increasing these horizontal dimensions further did not significantly affect the slab behavior under center load.

Method of Placing Soil and Slab in the Test Box

Rosettes were fixed on the 9 by 9 by 1/8-inch aluminum slab at the selected locations, and the top and bottom covers of the test box were detached from it. To position the slab on the inside of the bottom cover, four plywood planks were fixed so that a 9 by 9-inch space was left in the center. This space was filled with plaster of paris, but the top 1/8-inch portion was left for the slab, which was positioned with the side having rosettes facing downward and the other side flush with the plywood planks, as shown in Fig 30. The lead wires of the rosettes were taken out through slots in the plywood planks. To reduce friction between soil and slab the top face of the slab, which was to be in contact with the soil was covered with a thin film of grease. A polyethylene sheet was spread on the planks, and the greased slab was left uncovered. The body of the test box was then fixed to this assembly by bolts (Fig 30).

The soil in the box was prepared by mixing and extrusion through an device available in a laboratory of The University of Texas. The soil was extruded in a 3 by 3-inch cross section in convenient lengths under a vacuum of about 20 psi, as shown in Fig 31. The method of extrusion provided a thorough mixing of the clay and removed any trapped air. The extruded soil was cut in different lengths and placed in the box as shown in Fig 32. The soil blocks were put together until one row was completed. Adjacent rows were laid, one after the other, until one layer was completed. To insure close contact between the adjacent blocks, several precautions were taken:

(1) In adjacent rows and layers the joints were staggered by use of blocks of different lengths.

(2) Adjacent layers were oriented at 90° to each other.

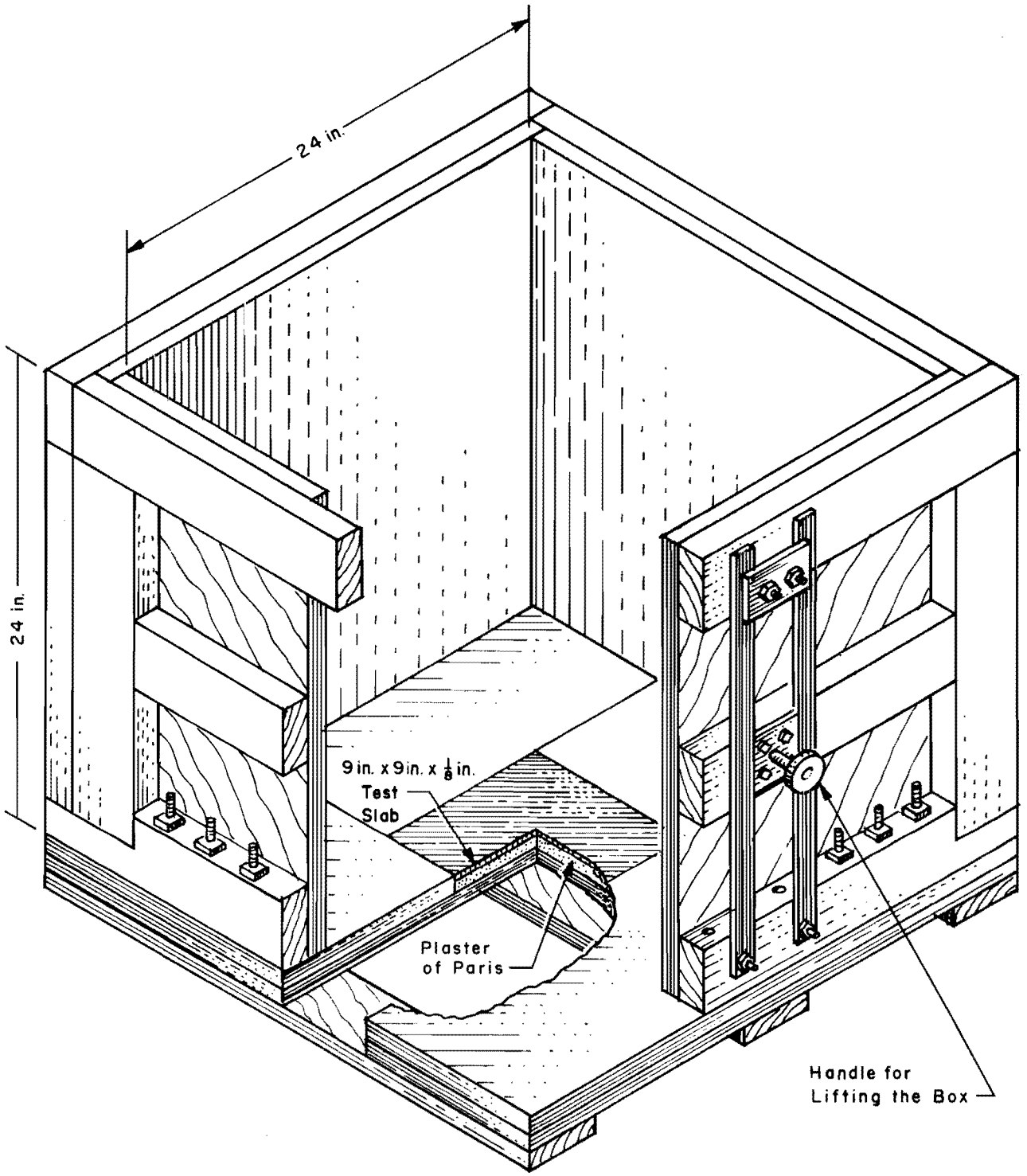

Fig 30. Details of supporting box with slab positioned upside down for filling.

Fig 31. Method of soil extrusion.

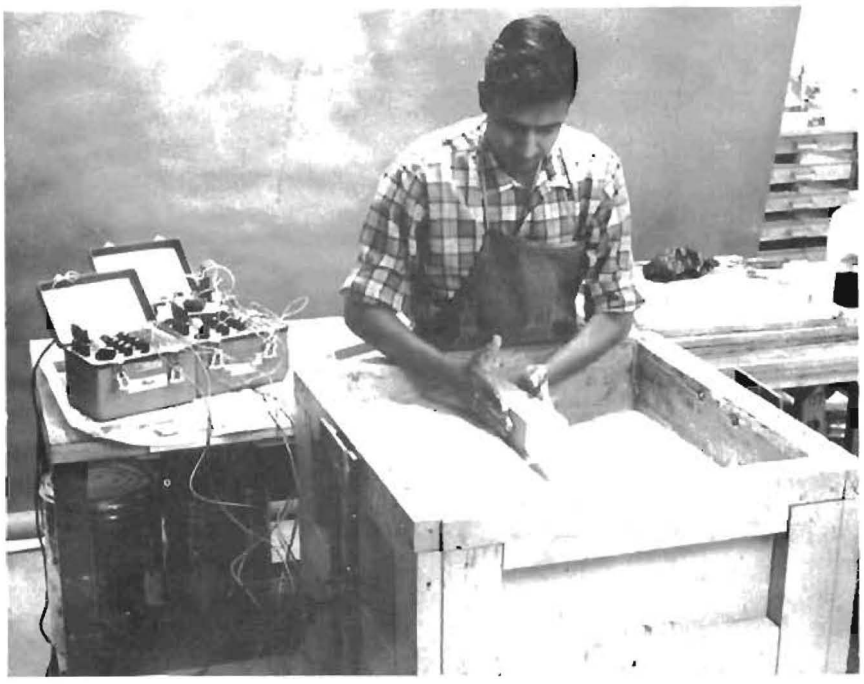

Fig 32. Method of placing extruded soil.

(3) Adjacent blocks were kneaded with the fingers.

(4) Each layer was compacted by a drop hammer with a compacting surface 6 by 6 inches with two blows at each position. Its weight was 10 pounds, and the height of fall was 18 inches. This procedure was continued until the whole box was filled. Then a polyethylene sheet was placed over it and the top cover was attached with bolts.

The box was taken to the testing bed, lifted by two small hoists, and supported from the ceiling (Fig 33). The box was turned over, bringing the slab to the top (Fig 34), and what was the top cover in the new position was removed. The plaster of paris block was also removed, leaving the slab and the rosettes directly exposed to the room temperature. The soil was covered by a polyethylene sheet and wooden planks until arrangements for loading and measuring were completed.

Loading

Load was applied by a mechanical screw jack, measured by a load cell, and recorded on a digital voltmeter. The output was read on the digital scanning system as well as on the digital voltmeter. The details and specifications of these devices are given in Chapter 3. Tests were performed under two loading positions: center load and corner loads.

Deflection and Strain Measurement

Deflections of slab were measured by 0.001-inch dial gages and LVDT's. An independent frame consisting of vertical, horizontal, and diagonal members and provided with stiffeners was made to support dial gages and LVDT's. The frame did not touch the box or the loading unit during the testing. All the LVDT's were calibrated before testing by inserting gage blocks of known thicknesses between the slab and the cores of the LVDT's. Strains were measured by four rosettes for center loading and three rosettes and two strain gages along one edge for corner loading. Output of LVDT, load cells, and strain gages was recorded on a 40-channel voltmeter by a digital scanning system.

Test Procedure

After the box was turned upside down, it was positioned under the loading frame, and the following precautionary measures were taken:

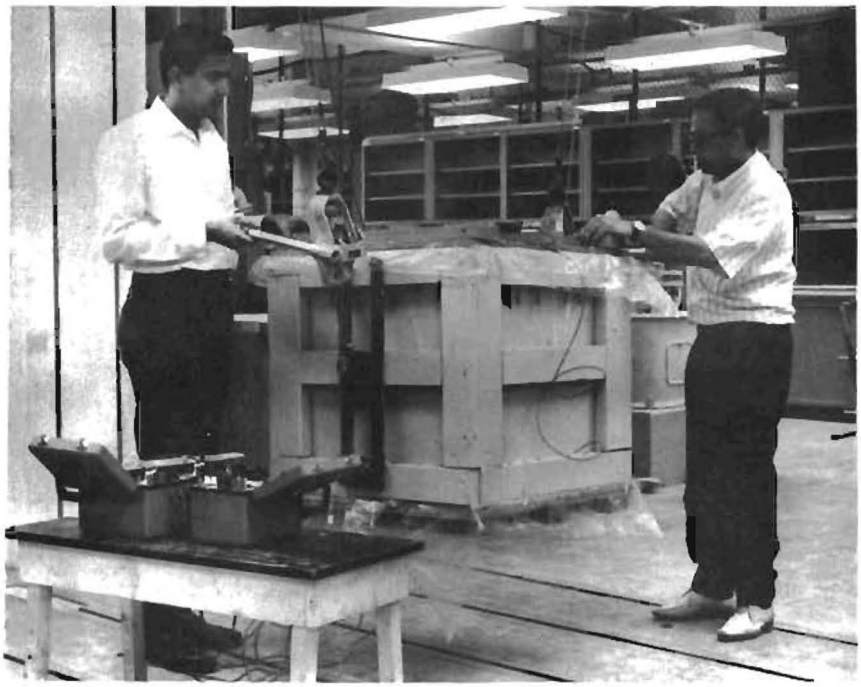

Fig 33. Method of lifting the box.

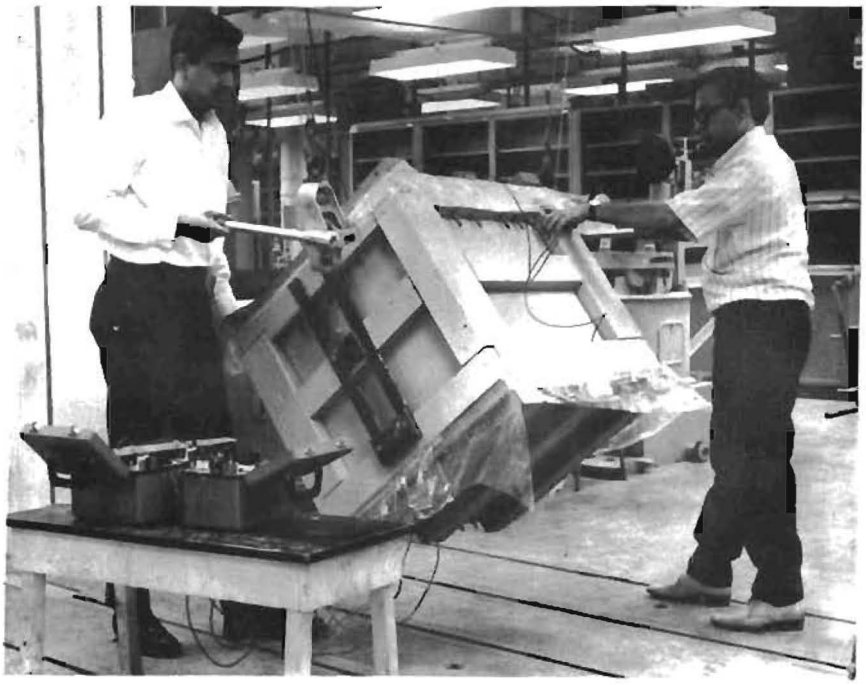

Fig 34. Method of overturning the box.

(1) The level of the top of the slab was checked along the center lines and the diagonals.

(2) The verticality of the applied load was ensured by checking the right angle between the loading rod and the slab.

The frame to support the dial gages and LVDT's was fixed to the testing bed, and the LVDT's and dial gages were fixed at their respective places. The connections of the LVDT's, strain gages, and load cells to the 40-channel voltmeter were completed. For each active gage, one compensating gage of similar type, mounted on an unstrained plate of the same material, provided temperature compensation. Alternate channels were used for load, to help in getting the output of the LVDT's and strain gages corresponding to exact loads separately, in case the load changed during the recording of all channels. Thus, 18 channels were used for load and 18 for LVDT's and strain gages. When all the test arrangements were completed, the LVDT's and strain gages were calibrated, prior to each test. To check the stability of each channel, several readings were taken before loading was started.

The screw jack was set at a convenient speed with the gear reduction 1/1,000 and the gear setting 90. This produced a movement of the loading rod of about 0.0124 inch/minute on the slab. Initial readings of all the dial gages and channels were taken with no load on the slab. Load was then applied continuously with the same movement of the loading rod, and output of all the channels and dial gages was obtained at regular intervals. The loading was continued until the maximum load was 255 pounds for center loading and 208 pounds for corner loading. The slab was then unloaded and readings were again taken at regular intervals. The load was cycled to a constant deflection for center loading and the maximum deflection for corner loading, as discussed in Chapter 6.

After the test, the slab was removed. The plate load test was conducted on a rigid plate 1/2-inch-thick and 9 inches in diameter. The testing of the rigid plate was done at the same speed as for the slab. The load was measured by a proving ring, and deflections by dial gages at four points. Tests on rigid plates of 1, 2, 4, and 6 inches in diameter were also conducted, as in the preliminary series (Appendix 2). Vane shear tests were done at eight locations and up to 5 inches from the surface, and torvane shear tests were also conducted. Samples were taken for moisture content, density, and degree of saturation and for unconfined compression tests during the soil placement and

after the test. The unconfined compression tests were performed at the same speed as for the slab testing and also at several moisture contents.

Tests Conducted

Tests were conducted in a three-phase program. Phase 1 was preliminary slab testing under center load to establish a suitable test procedure. Two preliminary slab series (series 300 and 320) were conducted, one on an uninstrumented slab and the other on an instrumented slab. Both series were conducted under small loads producing deflections within linear characteristics of the soil. Test data, analysis, and difficulties encountered in these preliminary series are reported in Appendix 2.

Phase 2 was the actual testing (series 330) on the instrumented slab under center load. The testing was done under loads producing deflections within linear and nonlinear soil characteristics, first under static and then under cyclic loads.

Phase 3 was the actual testing on the instrumented slab under two-point corner loads (series 340), producing deflections within linear and nonlinear soil characteristics, first under static and then under cyclic loads.

Slab series 330 and 340, the main test series, were analyzed for the static case and are reported here. The chief findings of the preliminary series are also included wherever helpful. Test data of series 330 and 340 under cyclic loading are discussed in Chapter 6.

Center Load Slab Test (Series 330)

Load was applied by the mechanical jack (Fig 35) through a 3/4-inch-diameter loading rod and transmitted to the slab by a ball so as to apply only a vertical component of load. The slab was loaded continuously until the load was 255 pounds and then unloaded. The test data were recorded at regular intervals during both loading and unloading.

Soil Properties

Soil subgrade was represented by the Winkler foundation, which was determined from the pressure versus deflection characteristics obtained from plate load tests. From the preliminary series, as reported in detail by Siddiqi (Ref 39), it was observed that these characteristics were influenced by the

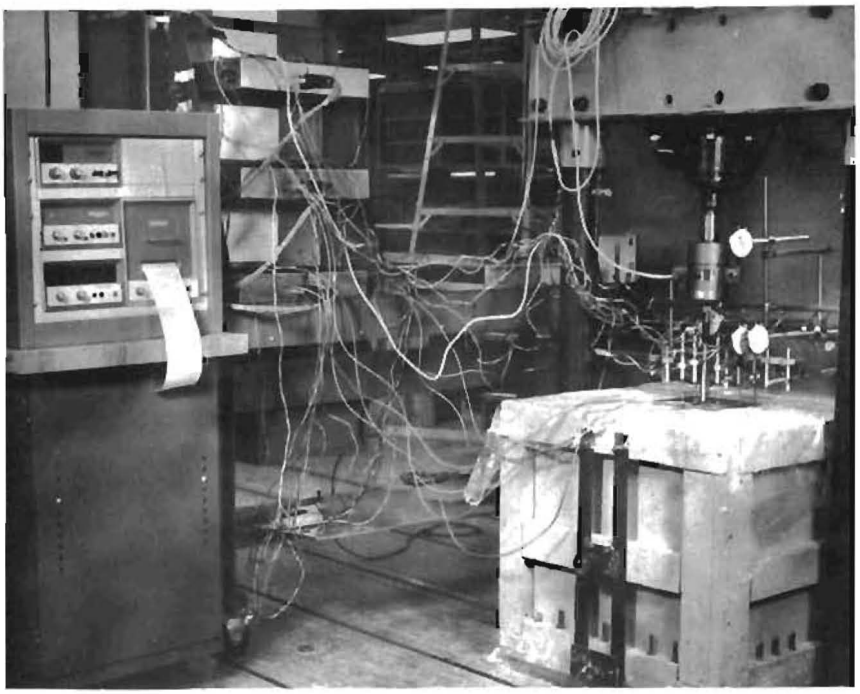

(a) Test set-up.

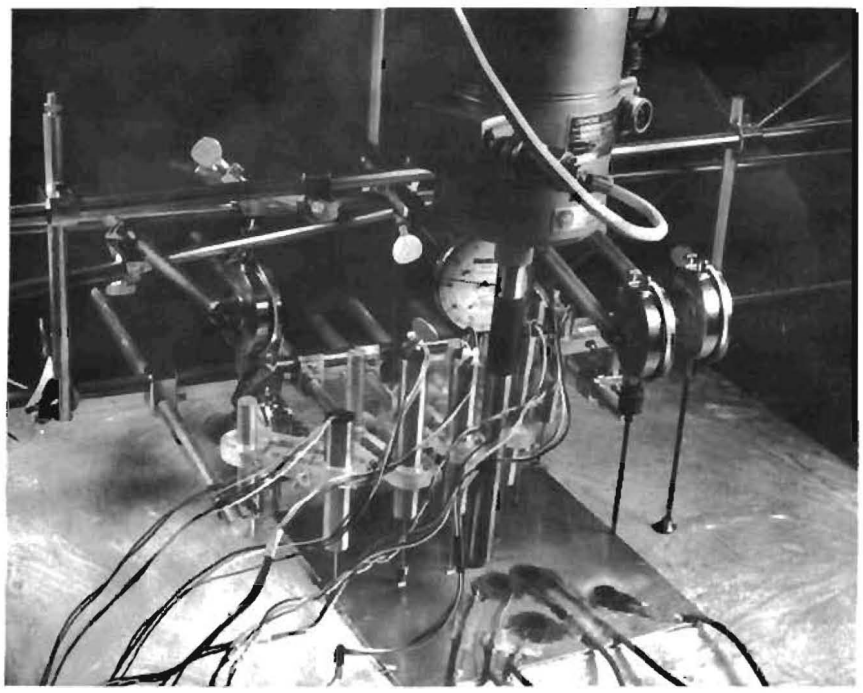

(b) Close-up of slab with loading and measurement devices.

Fig 35. Slab test arrangement for center load slab test (series 330).

plate size; therefore, it was decided to use the data of the 9-inch-diameter rigid plate in analysis of the 9 by 9-inch slab.

A plate load test on the 9-inch-diameter rigid plate was conducted according to modified ASTM specifications (Ref 3), as shown in Fig 36. After loading and unloading the plate with a small seating load, the plate was loaded at the same speed as that for testing of the slab. The plate was loaded continuously and deflections on the four dial gages were recorded at regular intervals. The plate was loaded continuously until deflections increased without any change in the load. Pressure versus average deflection data is shown in Fig 37 along with two more sets of test data, one for a preliminary series on an instrumented slab under center load (series 320) and the other for the corner load slab test (series 340). The curves for the material used in series 330 and 340 are almost identical, but the behavior in series 320 was significantly different. A piece-wise linear estimate was made for use in the DSLAB solutions. Curve I, joined by a solid line, for the main slab tests (series 330 and 340) and curve II, joined by a dotted line, for the preliminary series 320, were used in subsequent linear and nonlinear analyses.

Figure 38 shows the typical stress-strain characteristics of the clay at selected moisture contents. These characteristics were obtained from unconfined compression tests on samples 1.40 inches in diameter and 3 inches in height. The rate of loading in these tests was 0.0124 inch/minute, the same as that in the slab test. Shear strengths obtained from these unconfined compression tests are shown in Fig 39. Average shear strength was found to be 177 lb/ft^2 (1.23 psi). Shear strengths obtained using a vane apparatus are given in Table 19. The vanes used were 1/2 inch in depth. These tests were conducted at the surface and five different depths in the box, each at six locations in the box. The average values at each location ranged from 185 to 210 lb/ft^2 (1.28 to 1.46 psi) with an average constant value of 196 lb/ft^2 (1.36 psi). Shear strength at the surface using a torvane was found to be 215 lb/ft^2 (1.28 psi). The variation in water content, shown in Fig 40, had an average value of 38 percent. The wet density, as determined after obtaining the weights and volumes of the extruded samples varied from 112 to 120 lb/ft^3 with an average value of 116 lb/ft^3.

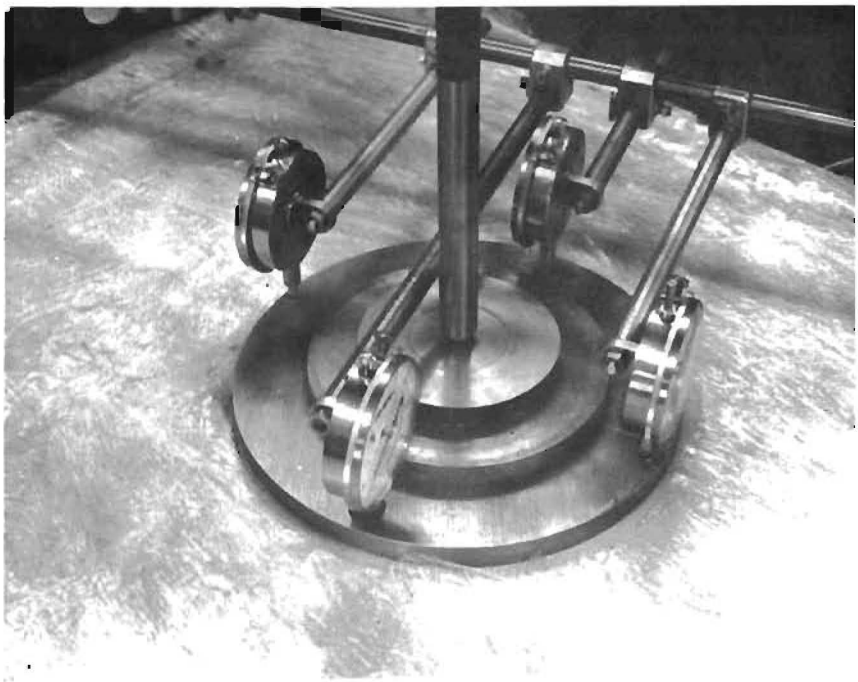

Fig 36. Plate load test of 9-inch-diameter plate.

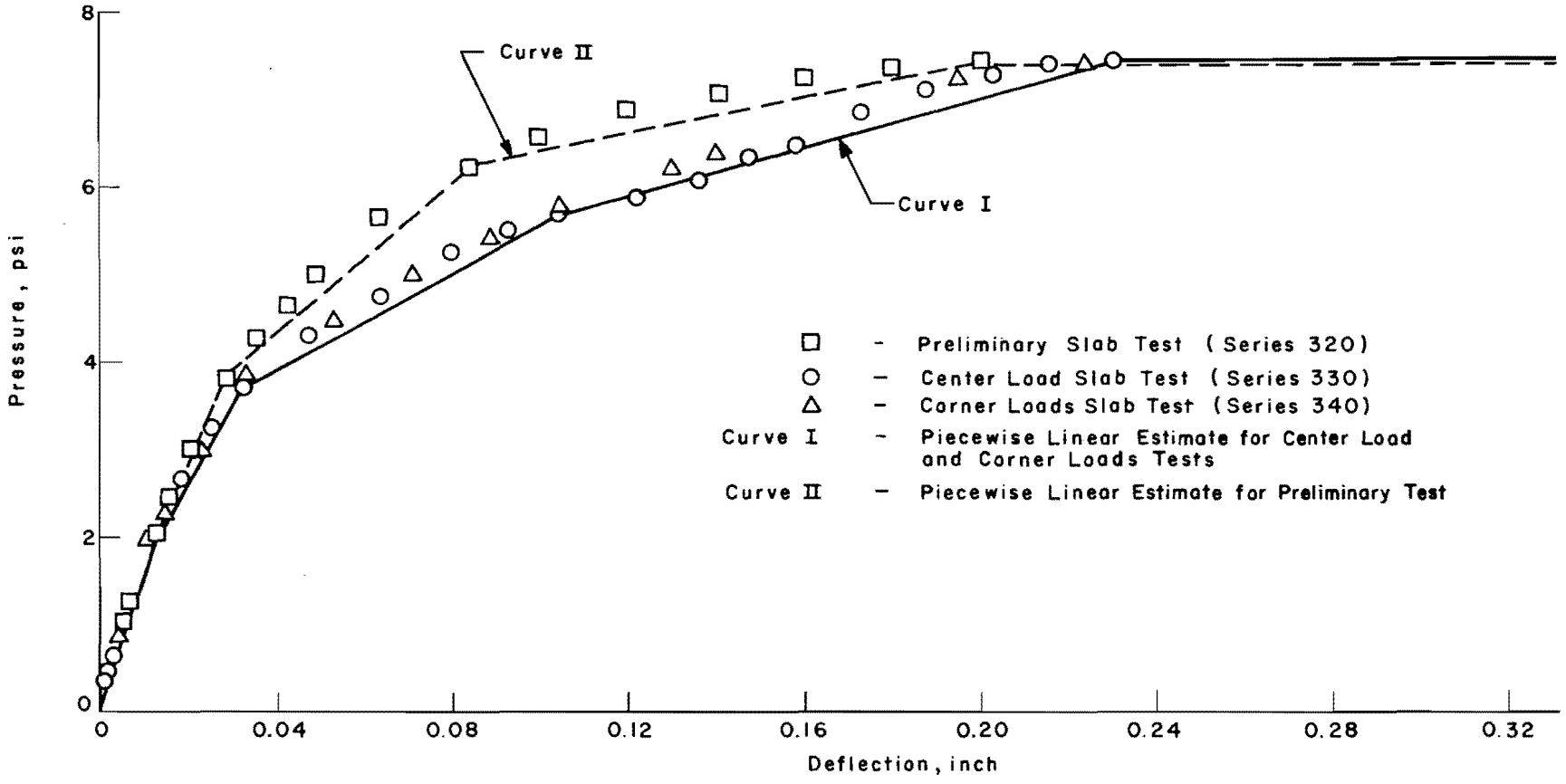

Fig 37. Pressure versus deflection data of 9-inch-diameter rigid plate.

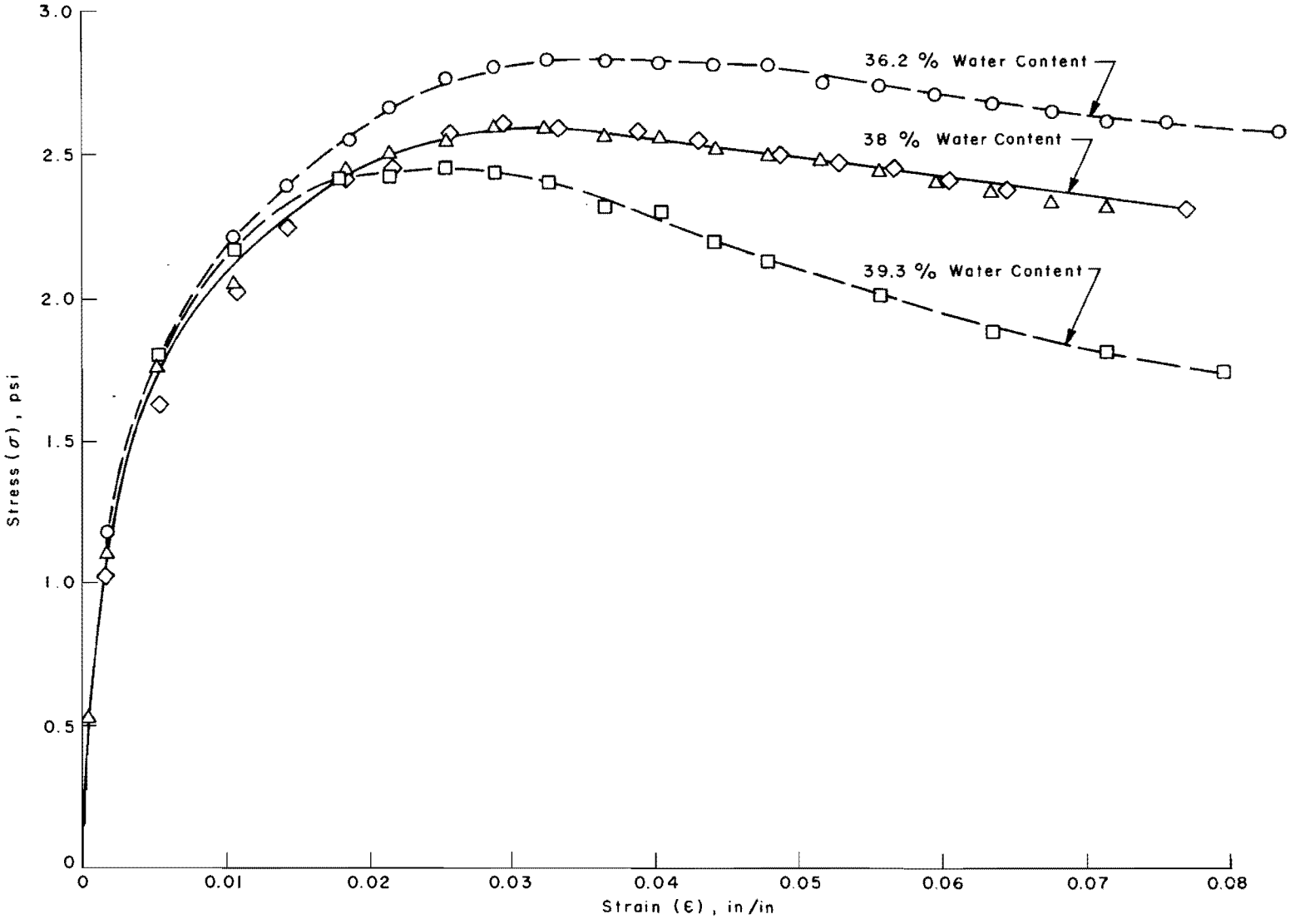

Fig 38. Stress-strain characteristics of soil under unconfined compression tests.

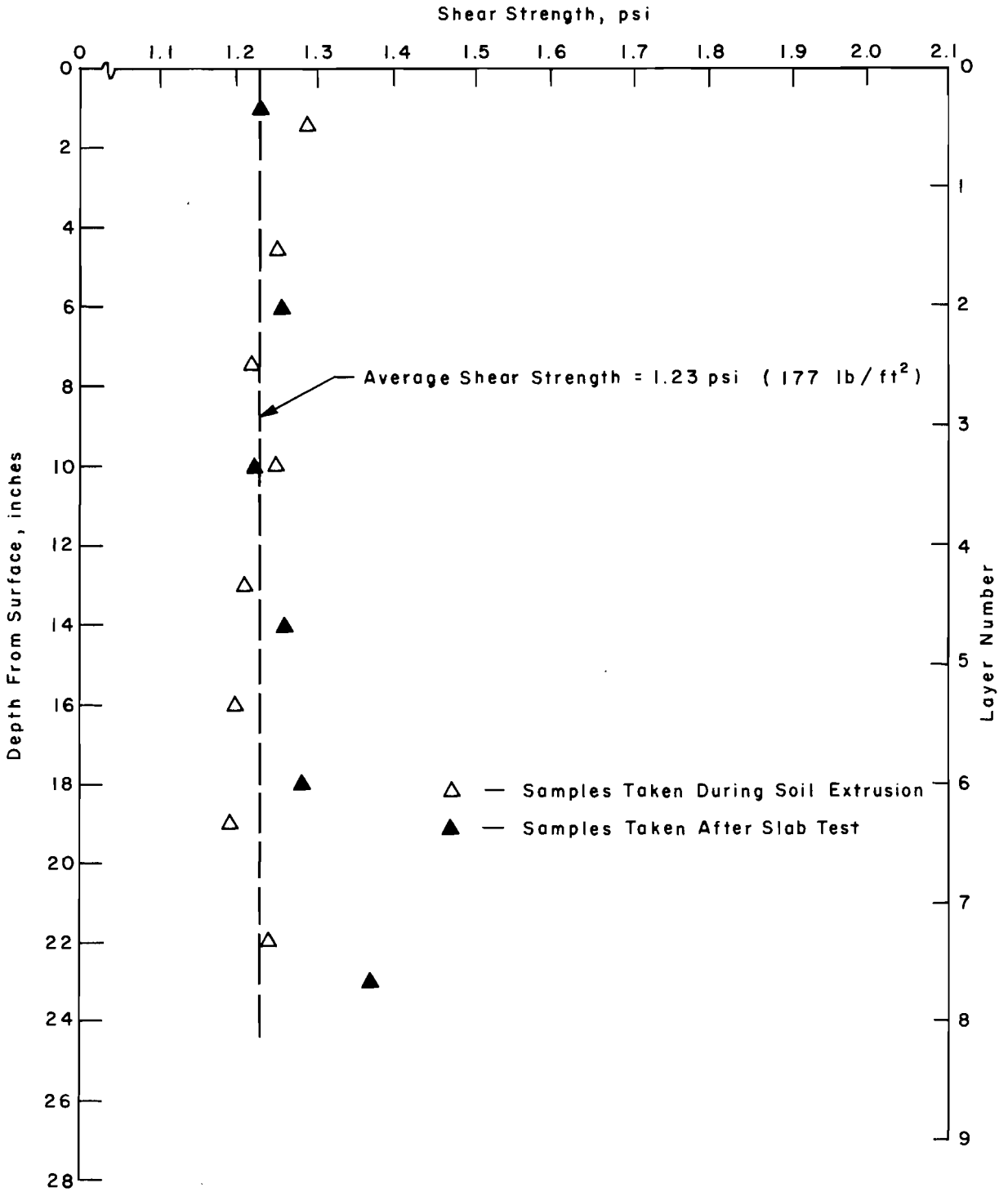

Fig 39. Shear strength variation of soil in center load slab test.

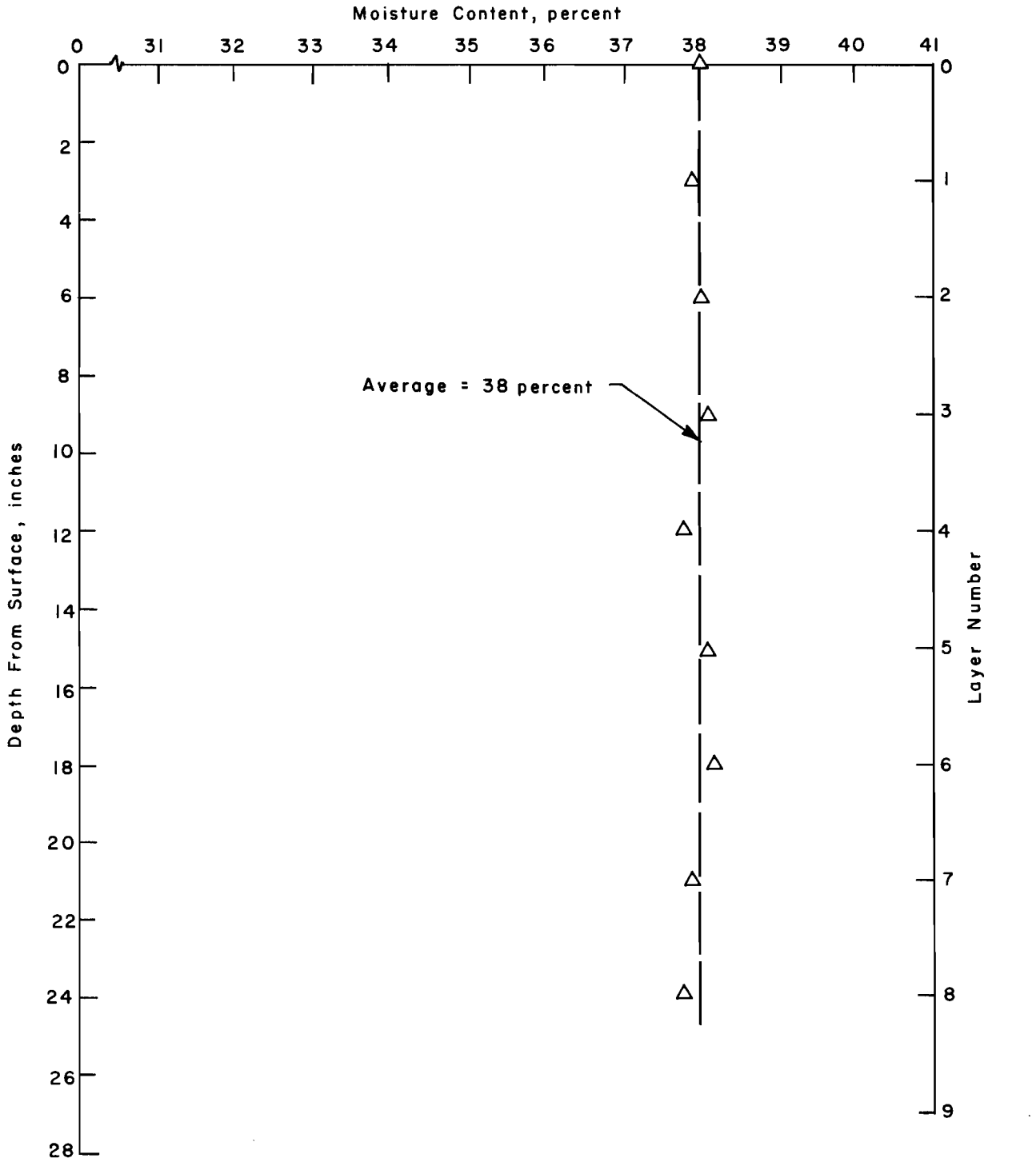

Fig 40. Water content variation in center load slab test.

TABLE 19. SHEAR STRENGTH USING VANE APPARATUS FOR CENTER LOAD SLAB TEST (SERIES 330)

Depth from Surface (inch)	Shear Strength at Locations (lb/ft^2)						Average Shear Strength
	1	2	3	4	5	6	
At surface	200	190	185	185	190	190	190
1	205	190	190	190	190	195	193
2	200	195	190	195	195	195	195
3	205	195	190	190	195	200	196
4	210	205	195	195	200	200	201
5	210	200	200	195	200	205	202

Variation: 185 to 210 lb/ft^2 (1.28 to 1.46 psi).

Average constant value: 196 lb/ft^2 (1.36 psi).

Test Results

Deflections and strains were calculated for different loads during loading and unloading. The method of data reduction is described in Appendix 3.

Figure 41 shows the positions of LVDT's, dial gages, rosettes, and load. Dial gages on the slab served as checks for LVDT's at identical positions. Two dial gages were placed on the soil near the slab periphery for deflection measurement. Figure 42 shows the load versus deflection curves for the 6 LVDT's. In the initial stages, as the load increased, the deflections increased almost linearly, but as the load increased further, the deflections increased with nonlinear variations. At all points, except the corner, deflections were downwards. At the corner the deflections (measured by LVDT 6) were downward up to 55 pound loads and then upward for the rest of the loading. During unloading, the curves did not follow the loading curves, having permanent sets of different magnitudes at the various points at zero load. It can also be seen that LVDT's 1 and 4 were out of range after a load of 220 pounds.

Figure 43 shows the load versus deflection curves for the three dial gages on the slab which served as checkpoints for three LVDT's at identical positions. It can be seen from these curves that nonlinear behavior, following different paths during loading and unloading and different permanent sets, was similar to that for LVDT's. At the corner, the deflections (measured by Dial 2), downward up to 60 pounds and then upward, were similar but less than those for LVDT 6.

Figure 44 shows the load versus deflection curves for two points on the soil near the slab periphery. Dial 5 (1.5 inches from the mid-edge) and Dial 3 (1.41 inches from the corner) showed downward and upward movements, respectively, with nonlinear behavior and large permanent sets on unloading, indicating that the adjoining soil was affected as the slab was loaded.

Figure 45 shows the load versus largest principal stresses and their directions at the four rosette locations. The method of getting largest principal stresses from the strain readings of the rosette is described in Appendix 3. It can be observed from these curves that the behavior of nonlinear variations, having different paths during loading and unloading, and different residual stresses at various locations on unloading, was similar to that for deflections.

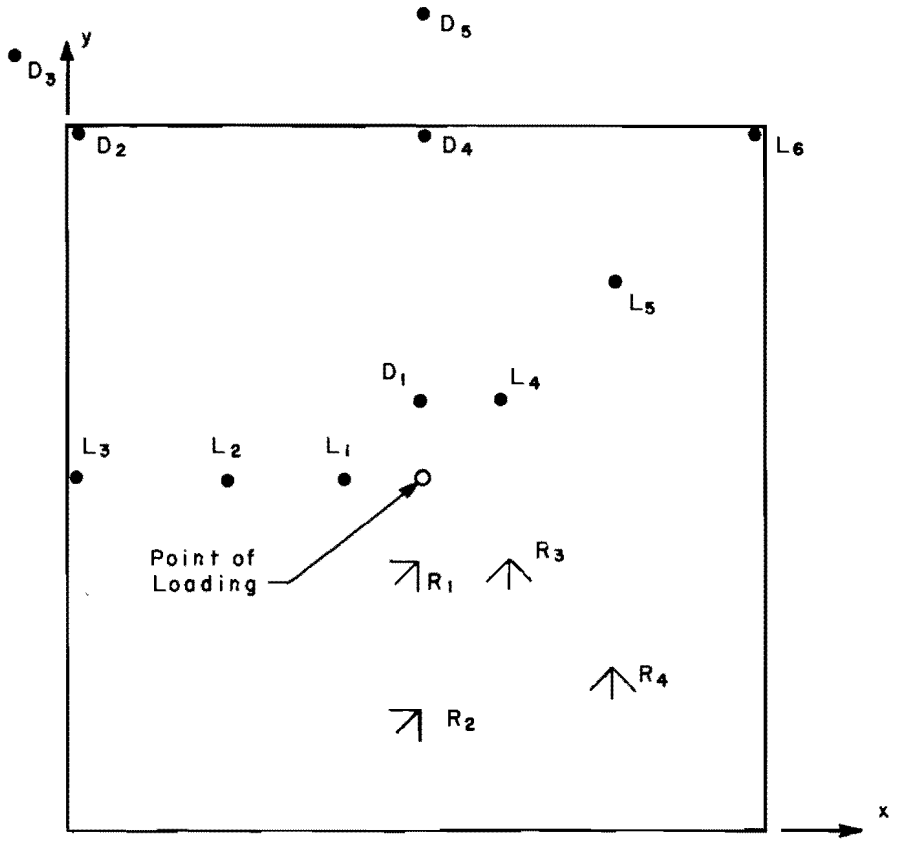

LVDT No	Distance	Dial No.
L_1	1 in. from Center on Center Line	D_1
L_2	2.5 " " " " " "	
L_3	4.5 " " " " " "	D_4
L_4	1.41 " " " " Diagonal	
L_5	3.53 " " " " "	
L_6	6.36 " " " " "	D_2
	1.5 in. from Mid-edge on Soil	D_5
	1.41 " " Corner " "	D_3
Rosettes		
R_1	1 in. from Center on Center Line	
R_2	3 " " " " " "	
R_3	1.41 " " " " Diagonal	
R_4	3.53 " " " " "	

Fig 41. Positions of LVDT's, dial gages, rosettes, and load for center load slab test.

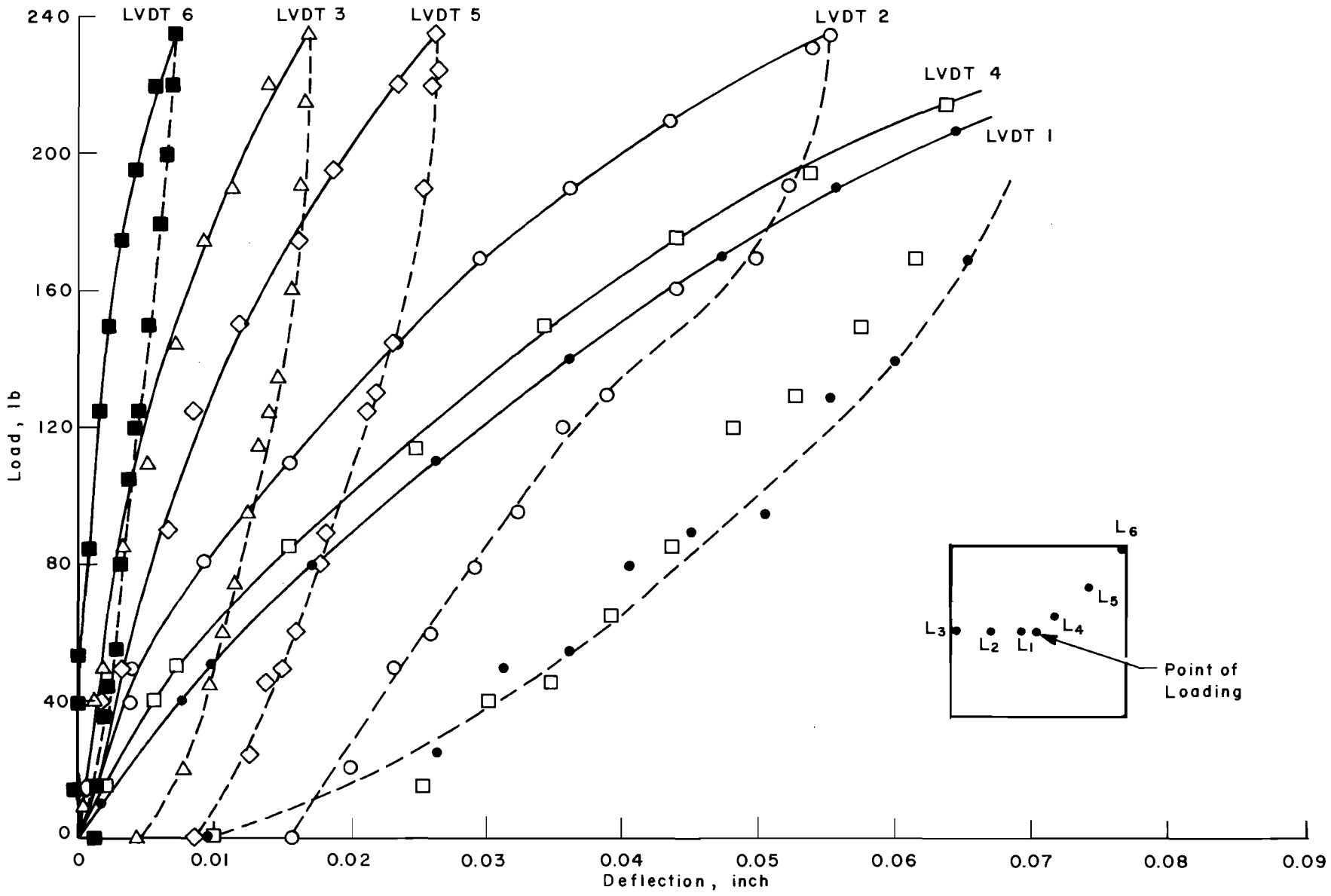

Fig 42. Load versus deflection curves for LVDT's for center load slab test (series 300).

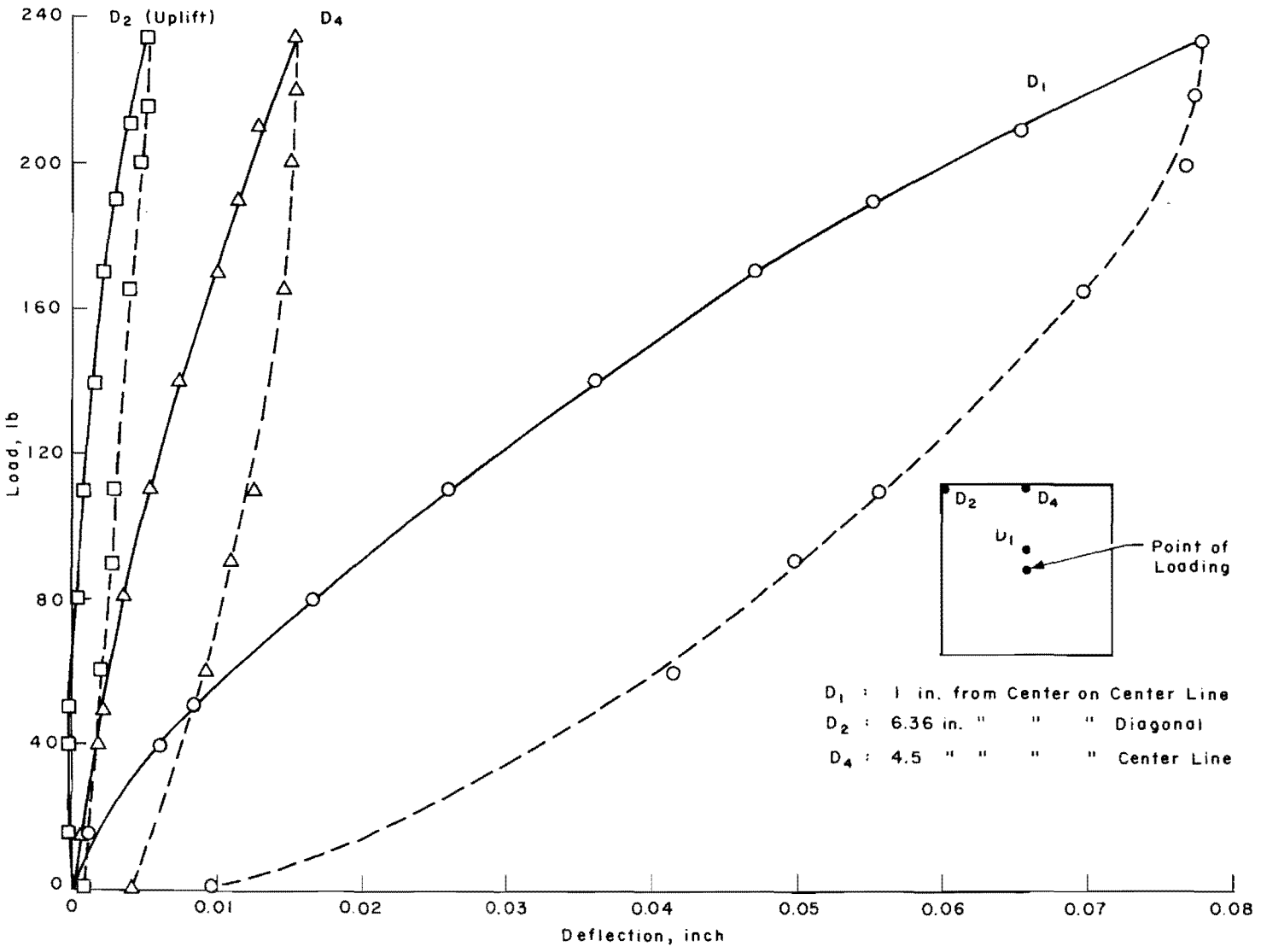

Fig 43. Load versus deflection curves for dial gages for center load slab test (series 330).

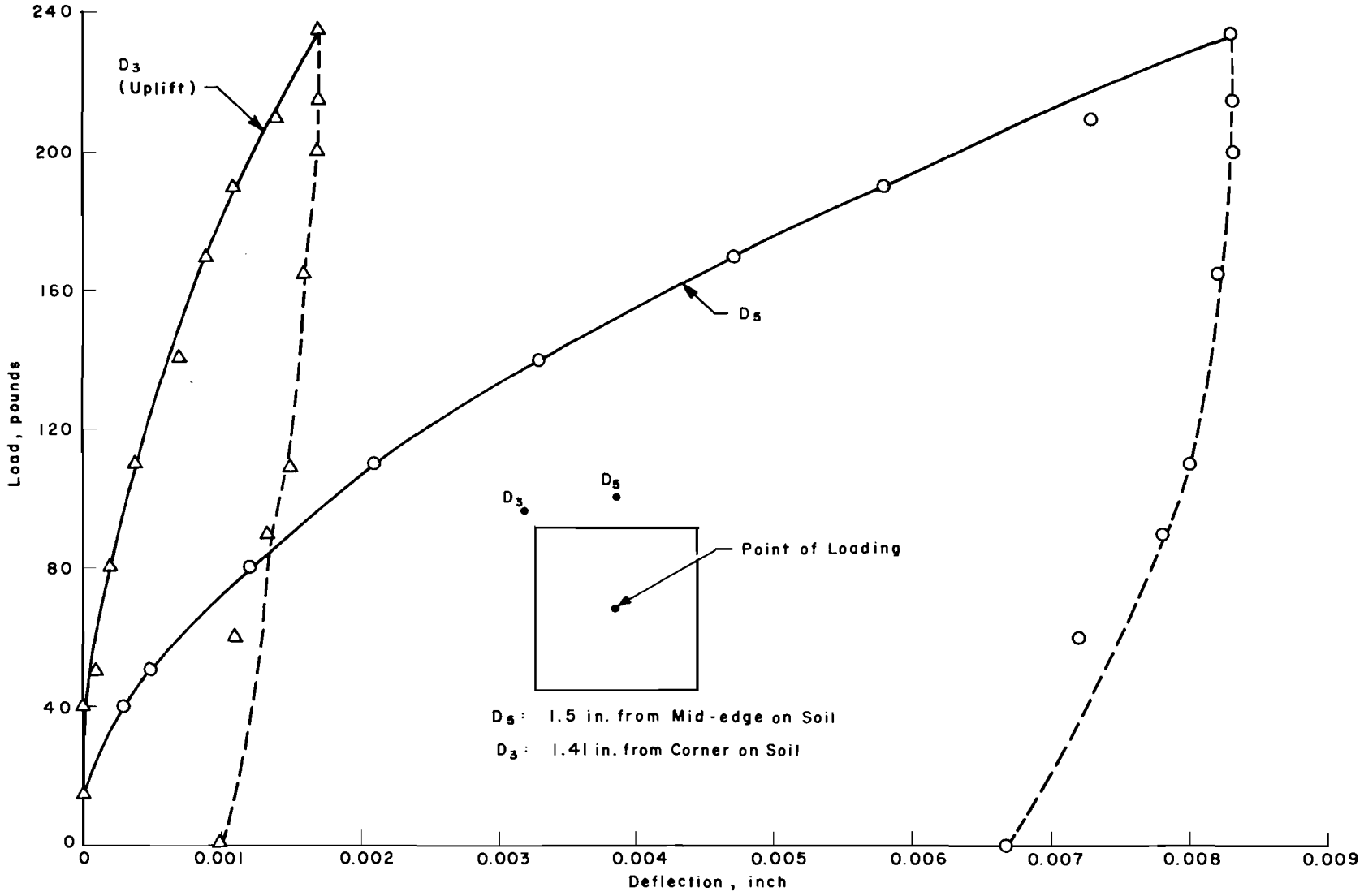

Fig 44. Load versus deflection curves for dial gages on soil for center load slab test (series 330).

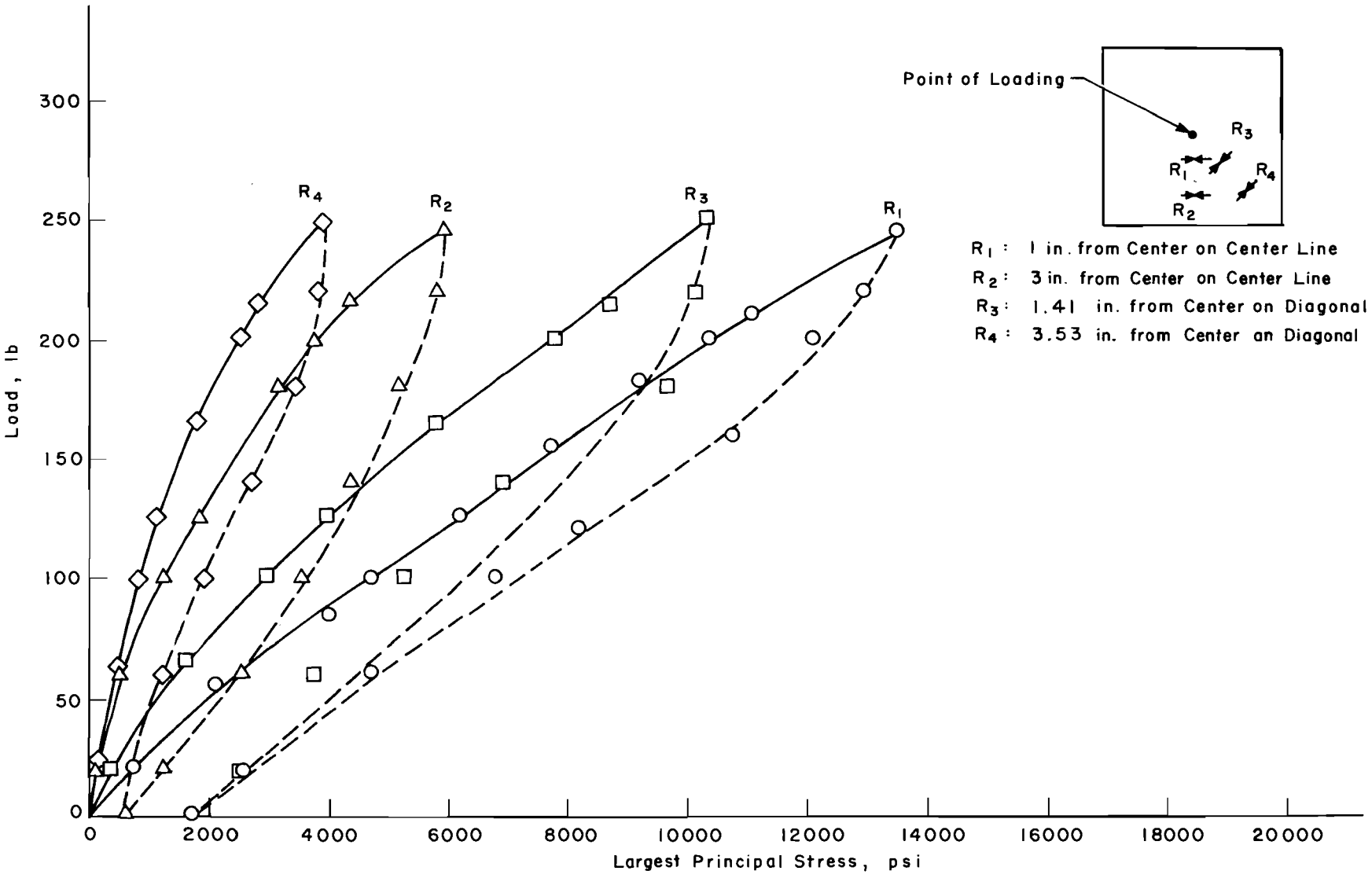

Fig 45. Load versus largest principal stress for rosettes for center load slab test (series 330).

Analytical Solutions

Analytical solutions based on the discrete-element model were found using DSLAB 30 (Ref 29), with soil represented by linear springs; and DSLAB 26 (Ref 20), with soil represented by nonlinear springs. The soil below the slab was represented by the Winkler foundation (Ref 55), i.e., closely spaced independent springs. Such springs, linear and nonlinear, were obtained by the following methods:

(A) linear springs from 9-inch-diameter rigid plate test data corresponding to $y = 0.01$ inch (tangent modulus). Soil modulus k thus obtained was 160 lb/in^3.

(B) linear springs from 9-inch-diameter rigid plate test data corresponding to 0.02-inch deflection (secant modulus). Modulus k thus obtained was 144 lb/in^3.

(C) nonlinear springs using the entire pressure versud deflection curve of the 9-inch-diameter plate test.

(D) nonlinear springs using Skempton's recommendation for unconfined compression test data (derivation given in Appendix 4).

The different soil representations outlined above are shown in Fig 46.

Linear modulus of subgrade reaction known as k, in lb/in^3, was converted to the units of S, lb/in, according to the DSLAB requirement, by multiplying it by the area occupied by the spring at each station, e.g.,

$$k = 160 \text{ lb/in}^3$$

$$h_x = h_y = 1/2 \text{ inch}$$

$$S = 160 \times 1/2 \times 1/2 = 40 \text{ lb/in}$$

These linear springs act in tension as well as compression.

Nonlinear soil modulus represented by the pressure p versus deflection y curve (Fig 37) was similarly converted to the load q versus deflection w characteristic as shown in Fig 47. Curves obtained by both the 9-inch-diameter plate load test and by Skempton's recommendation are shown in this figure. These nonlinear springs act in compression only. As clays can take small amounts of tension (Ref 49), these springs were made active in tension also, with the same slope as that in compression for the earlier portion of the curve, as shown in Fig 47.

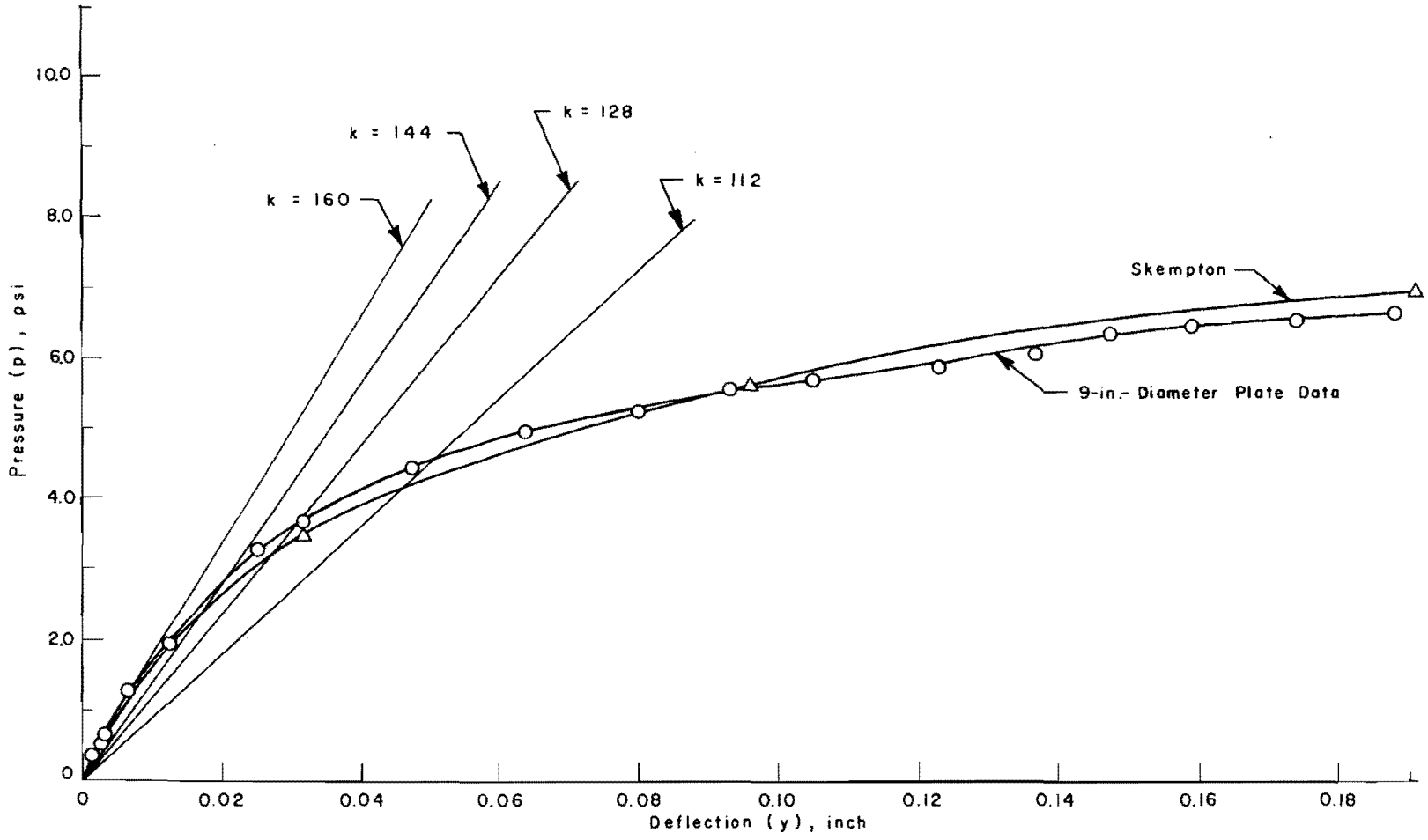

Fig 46. Linear and nonlinear soil representation.

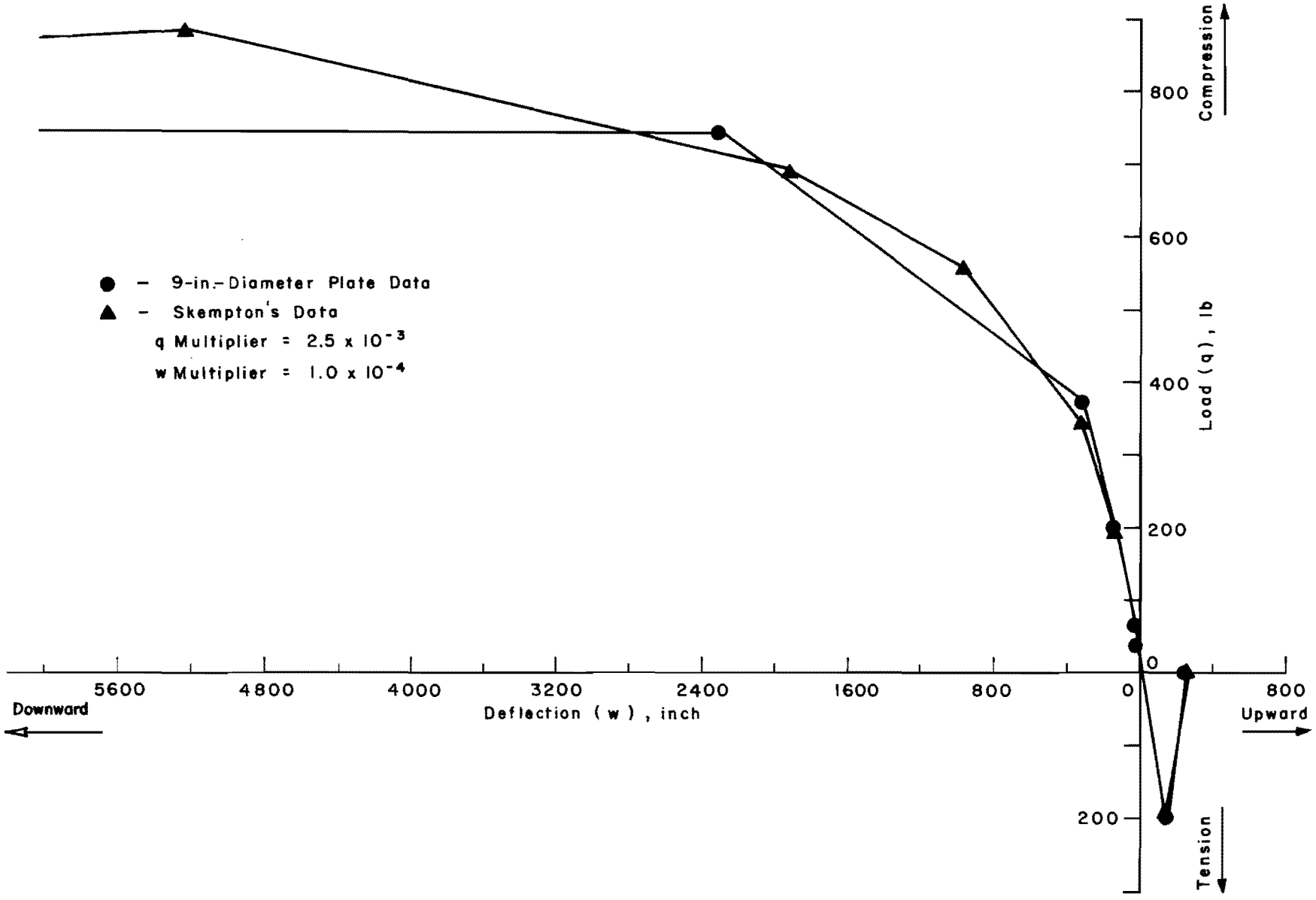

Fig 47. Nonlinear soil representation for DSLAB solution.

Comparison of Experimental and Analytical Deflections

The measured and computed deflections using linear and nonlinear springs for soil for a particular load on the slab were compared and the error was calculated as percentage of maximum measured deflection, in the same way as for plates, i.e.,

$$\text{Percentage error} = \frac{w_{mi} - w_{ci}}{(w_{max})_m} \times 100 \qquad (5.2)$$

where

w_{mi} = measured deflection at point i,

w_{ci} = computed deflection at point i,

$(w_{max})_m$ = maximum measured deflection for the load under consideration.

Plots of the measured and computed deflections were made along the center line and the diagonal. The plots were drawn and percentage errors calculated for loads of 100 and 200 pounds on the slab for all the four types of soil springs.

For a load of 100 pounds (categorized as small load), maximum measured deflection at point 1, i.e., at 1 inch from the center on the center line (Fig 48 and Table 20) was -0.0229 inch. The plots along center line and diagonal for measured and analytical deflections using different linear and nonlinear springs are shown in Figs 48 and 49, respectively, and the comparison and percentage errors are in Table 20. It is observed that, first, good correlation exists between the experimental and DSLAB solutions using springs B, C, and D. The error is within 5 percent near the loaded area, 7 percent near the mid-edge, and 22 percent near the corner. The difference in error at the corresponding checkpoints, using dial gages, is within 2 percent. Second, for a load of 100 pounds producing small deflections on the slab, results obtained using linear springs (secant modulus corresponding to maximum deflection) are almost the same as those using nonlinear springs. Similar comparisons in both preliminary slab tests (series 300 and 320) were observed, as reported in Appendix 2.

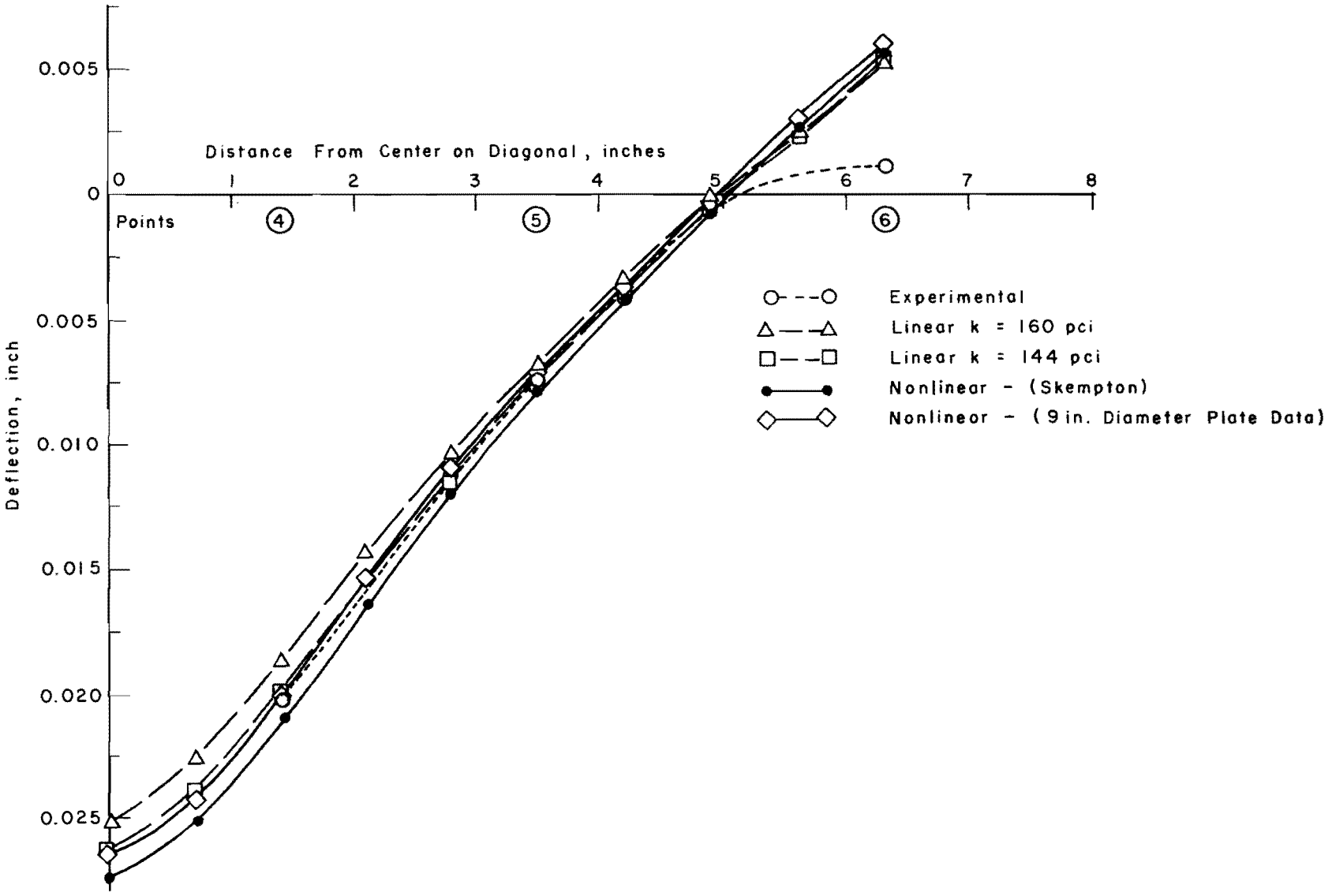

Fig 49. Experimental and analytical deflections on diagonal under center load of 100 pounds (series 330) - see Table 20.

TABLE 20. EXPERIMENTAL AND ANALYTICAL DEFLECTIONS FOR CENTER LOAD SLAB TEST (SERIES 330)

Load: 100 lb in the center

Programs: DSLAB 30 for linear springs (18 x 18 increments)
DSLAB 26 for nonlinear springs (18 x 18 increments)

Type of Solution	LVDT's						Dial Gages		
	1	2	3	4	5	6	1	4	2
Distance from Center	1 inch	2.5 inch	4.5 inch	1.41 inch	3.53 inch	6.36 inch	Check LVDT 1	Check LVDT 3	Check LVDT 6
Experimental	-0.02290	-0.01320	-0.00420	-0.01970	-0.00730	0.00117	-0.02290	-0.00490	0.00061
Linear springs k = 160 psi	-0.02112	-0.01231	-0.00271	-0.01862	-0.00671	0.00548	-0.02112	-0.00271	0.00548
% Error	7.77	3.89	6.52	4.72	2.59	-21.00	7.77	9.58	-21.27
Linear springs k = 144 psi	-0.02250	-0.01343	-0.00339	-0.01995	-0.00755	0.00548	-0.02250	-0.00339	0.00548
% Error	1.75	1.00	3.52	-1.09	-1.07	-18.82	1.75	6.58	-21.27
Nonlinear q - w curve (9-inch-diameter plate data)	-0.02248	-0.01312	-0.00272	-0.01986	-0.00706	0.00616	-0.02248	-0.00272	0.00616
% Error	1.83	0.35	6.48	-0.70	1.04	-21.81	1.83	9.54	-24.25
Nonlinear q - w curve (Skempton's)	-0.02359	-0.01411	-0.00353	-0.02094	-0.00792	0.00579	-0.02359	-0.00353	0.00579
% Error	-3.01	-3.97	2.92	-5.41	-2.69	-20.19	-3.01	5.98	-22.63

Note: Plots along center line and diagonal are given in Figs 48 and 49.

For a load of 200 pounds (categorized as high load), maximum measured deflection at point 1 (Fig 49 and Table 21) was -0.0607 inch. From the plots for measured and analytical deflections along the center line and diagonal (Figs 50 and 51, respectively), and percentage errors (Table 21), it can be observed that, first, good correlation exists using nonlinear springs only. Percentage error using C and D springs is within 8 percent near the load, 3 percent near the mid-edge, and 14 percent near the corner. The difference in error at the corresponding checkpoints, using dial gages, is within 2 percent. Second, solutions using linear springs (A and B) do not yield good agreement once the deflections on the slab are large and lie on the nonlinear part of the pressure versus deflection curve for the soil.

Comparison of Experimental and Analytical Principal Stresses

The largest principal stresses for loads of 100 and 200 pounds on the slab were calculated from the strains of the rectangular rosettes, as described in Appendix 3. The measured principal stresses thus obtained corresponded to the top of the slab whereas those obtained using DSLAB were with respect to the bottom. Keeping this difference in mind, a comparison of the measured and DSLAB largest principal stresses was made with the absolute values and percent errors calculated as a function of the maximum measured largest principal as stress, as shown below:

$$\text{Percentage Error} = \frac{\sigma_{im} - \sigma_{ic}}{(\sigma_{max})_m} \times 100 \qquad (5.3)$$

where

σ_{im} = measured largest principal stress at point i,

σ_{ic} = DSLAB largest principal stress at point i,

$(\sigma_{max})_m$ = maximum measured largest principal stress for the load under consideration.

For a 100-pound load on the slab, the comparison of measured largest principal stresses with the DSLAB solutions, using the linear and nonlinear springs, is given in Table 22. From this table it can be observed that the maximum percentage error is within 7 percent and that there is small difference

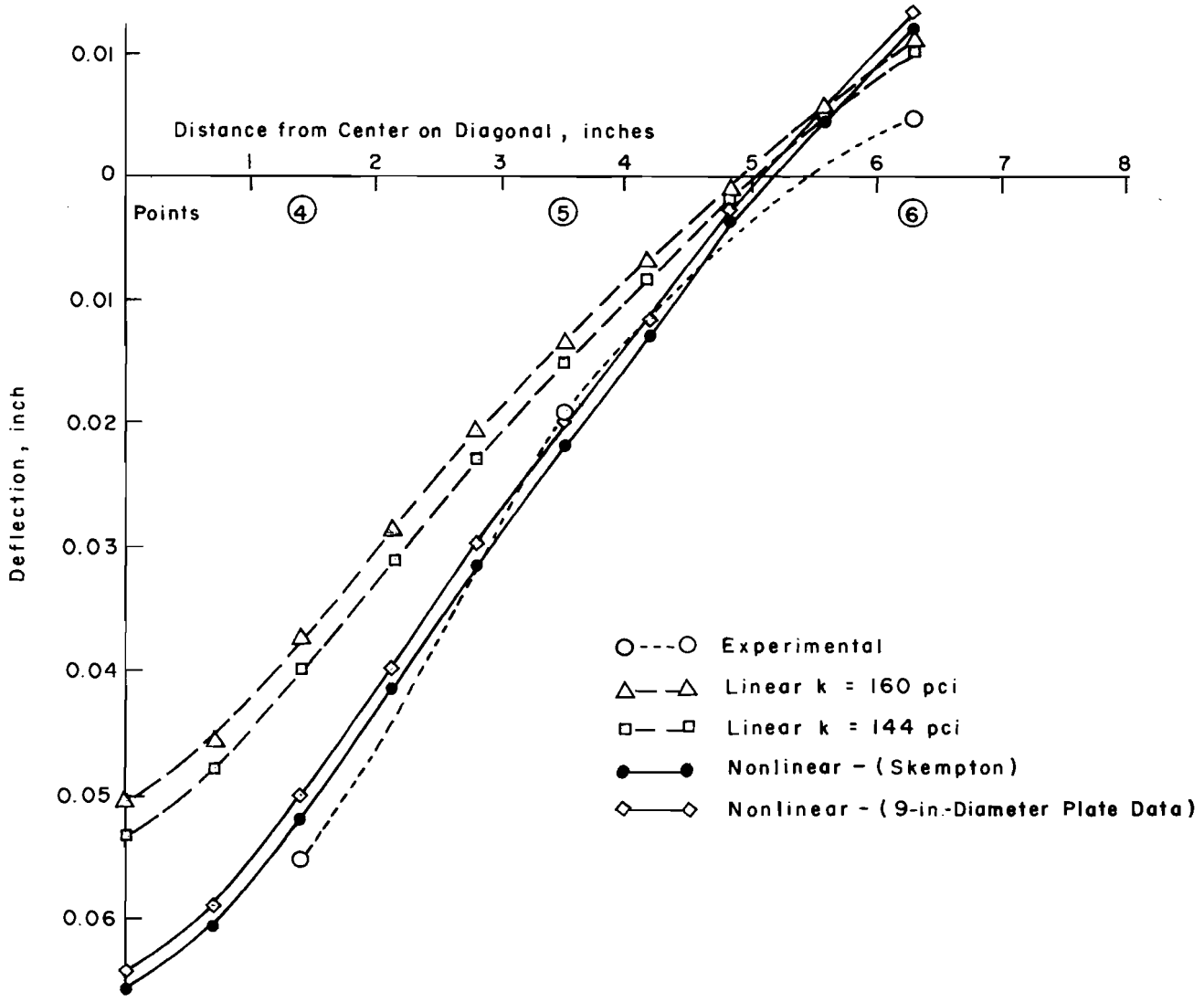

Fig 51. Experimental and analytical deflections on diagonal under center load of 200 pounds (series 330) - see Table 21.

TABLE 21. EXPERIMENTAL AND ANALYTICAL DEFLECTIONS FOR CENTER LOAD SLAB TEST (SERIES 330)

Load: 200 lb in the center

Programs: DSLAB 30 for linear springs (18 x 18 increments)
DSLAB 26 for nonlinear springs (18 x 18 increments)

Type of Solution	LVDT's						Dial Gages		
	1	2	3	4	5	6	1	4	2
Distance from Center	1 inch	2.5 inch	4.5 inch	1.41 inch	3.53 inch	6.36 inch	Check LVDT 1	Check LVDT 3	Check LVDT 6
Experimental	-0.06070	-0.03990	-0.01190	-0.05500	-0.01940	0.00460	-0.06050	-0.01250	0.00345
Linear springs k = 160 psi	-0.04223	-0.02462	-0.00541	-0.03724	-0.01341	0.01096	-0.04223	-0.00541	0.01096
% Error	30.43	25.17	10.69	29.26	9.87	-10.48	30.10	11.68	-12.37
Linear springs k = 144 psi	-0.04500	-0.02687	-0.00679	-0.03990	-0.01509	0.01096	-0.04500	-0.00679	0.01096
% Error	25.86	21.47	8.42	24.88	7.10	-10.48	25.54	9.41	-12.37
Nonlinear q - w curve (9-inch-diameter plate data)	-0.05583	-0.03467	-0.00992	-0.05006	-0.02012	0.01283	-0.05583	-0.00992	0.01283
% Error	8.02	8.62	3.27	8.14	-1.19	-13.56	7.69	4.26	-15.45
Nonlinear q - w curve (Skempton's)	-0.05754	-0.03629	-0.01128	-0.05175	-0.02154	0.01218	-0.05754	-0.01128	0.01218
% Error	5.12	5.95	1.02	5.35	-3.53	-12.49	4.88	2.01	-14.38

Note: Plots along center line and diagonal are given in Figs 50 and 51.

TABLE 22. EXPERIMENTAL AND ANALYTICAL LARGEST PRINCIPAL STRESSES FOR CENTER LOAD SLAB TEST (SERIES 330)

Load: 100 lb in the center

Programs: DSLAB 30 for linear springs (18 x 18 increments)
DSLAB 26 for nonlinear springs (18 x 18 increments)

Type of Solution	Rosette 1	Rosette 2	Rosette 3	Rosette 4
	Largest Stress	Largest Stress	Largest Stress	Largest Stress
Experimental	4788.00	1262.00	2973.00	876.00
Linear springs k = 160 psi	4656.00	1169.00	3063.00	747.80
% Error	2.76	1.94	-1.88	2.68
Linear springs k = 144 psi	4767.00	1245.00	3164.00	788.30
% Error	0.44	0.36	-3.99	1.81
Nonlinear q - w curve (9-inch-diameter plate data)	4900.0	1275.00	3280.00	817.00
% Error	-2.34	-0.27	-6.41	1.22
Nonlinear q - w curve (Skempton's)	4954.00	1313.00	3322.00	832.00
% Error	-3.47	-1.07	-7.29	0.91

in percentage errors for solutions using linear and nonlinear springs. Similar observations were made for the preliminary series (320) as reported in Appendix 2.

A similar comparison of largest principal stresses for 200 pounds (Table 23) shows agreement between measured and DSLAB solutions using nonlinear springs to be within 7 percent and that solutions using linear springs do not yield good agreement.

Corner Loads Slab Test (Series 340)

After testing the slab under center load, it was decided to study the problem further for another important loading condition, and testing was done under two-point corner loads. Load was transferred to the slab near the opposite corners through a loading beam, as shown in Figs 52 and 53. To get equal loads at the two ends, the beam was joined to the loading rod by a pin connection. As it was desired to measure deflections along the diagonal itself, 1/4-inch-diameter holes were made in the beam for the cores of the LVDT's to pass through. Identical holes were made on both sides of the center of the beam, so that equal loads were tansmitted at the two ends. The testing procedure was exactly the same as for center load slab test.

Plate load tests, shear tests, and other soil tests were conducted the same way as the center load test. The plate load test data for 9-inch-diameter plate were given in Fig 37. Shear strengths obtained from the unconfined compression tests are shown in Fig 54, with average value of 177 lb/ft^2 (1.23 psi). The average *in situ* shear strength using the vane apparatus was 201 lb/ft^2 (1.40 psi) as shown in Table 24. The variation in water content is shown in Fig 55. The average value was 38 percent. The average wet density was 116 lb/ft^3.

Test Results

Deflections and strains were calculated for different loads as described in Appendix 3. Figure 56 shows the positions of LVDT's, dial gages on the slab (checks for LVDT's) and on the soil, rosettes, and strain gages. Figure 57 shows the load versus deflection curves for all seven LVDT's. For all the LVDT's, except 6 and 7, the deflections increased with load nonlinearly. LVDT 6, placed at the unloaded corner, and LVDT 7, measuring the smallest deflections showed almost linear variation. The deflections at the unloaded

TABLE 23. EXPERIMENTAL AND ANALYTICAL LARGEST PRINCIPAL STRESSES FOR CENTER LOAD SLAB TEST (SERIES 330)

Load: 200 lb in the center

Programs: DSLAB 30 for linear springs (18 x 18 increments)
DSLAB 26 for nonlinear springs (18 x 18 increments)

Type of Solution	Rosette 1	Rosette 2	Rosette 3	Rosette 4
	Largest Stress	Largest Stress	Largest Stress	Largest Stress
Experimental	10421.00	3733.00	7854.00	2531.00
Linear springs k = 160 psi	9311.00	2337.00	6127.00	1496.00
% Error	10.65	13.40	16.57	9.93
Linear springs k = 144 psi	9534.00	2491.00	6327.00	1577.00
% Error	8.51	11.92	14.65	9.15
Nonlinear q - w curve (9-inch-diameter plate data)	10852.00	3176.00	7496.00	1989.00
% Error	-4.14	5.34	3.44	5.20
Nonlinear q - w curve (Skempton's)	10879.00	3242.00	7530.00	2017.00
% Error	-4.39	4.71	3.11	4.93

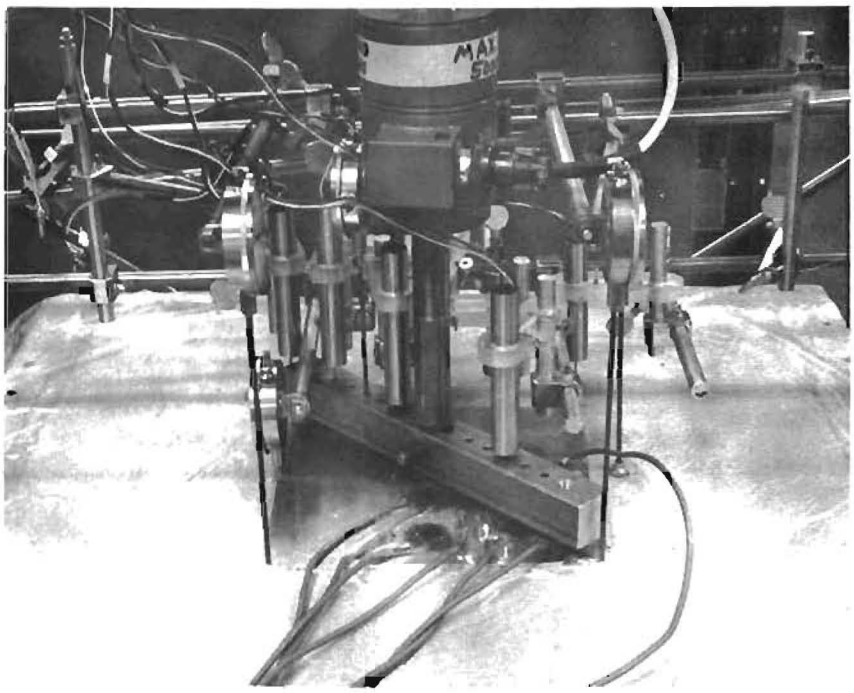

(a) Test set-up of slab with loading and measurement devices.

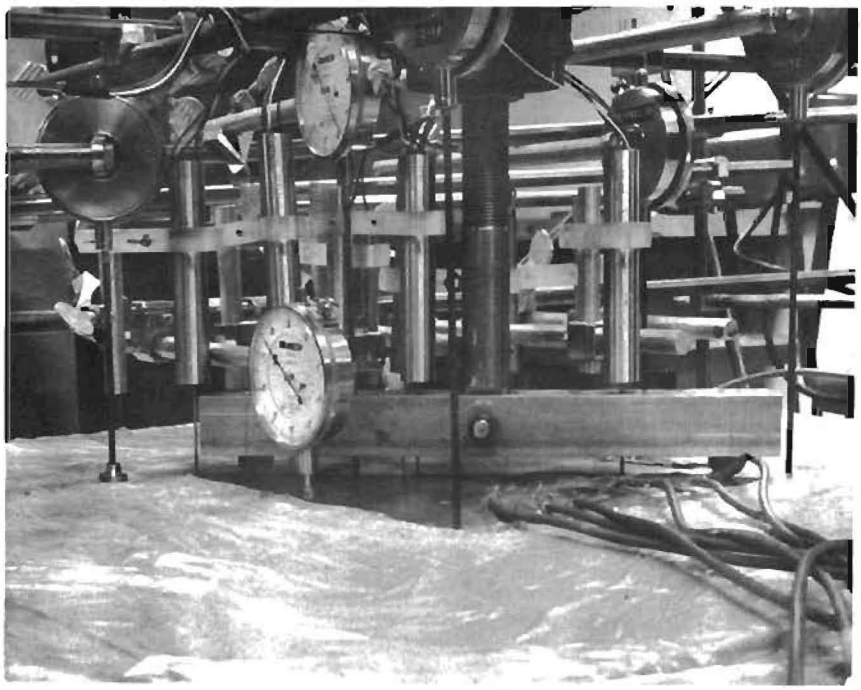

(b) Close-up of loading beam.

Fig 52. Slab test arrangement under corner loads slab test (series 340).

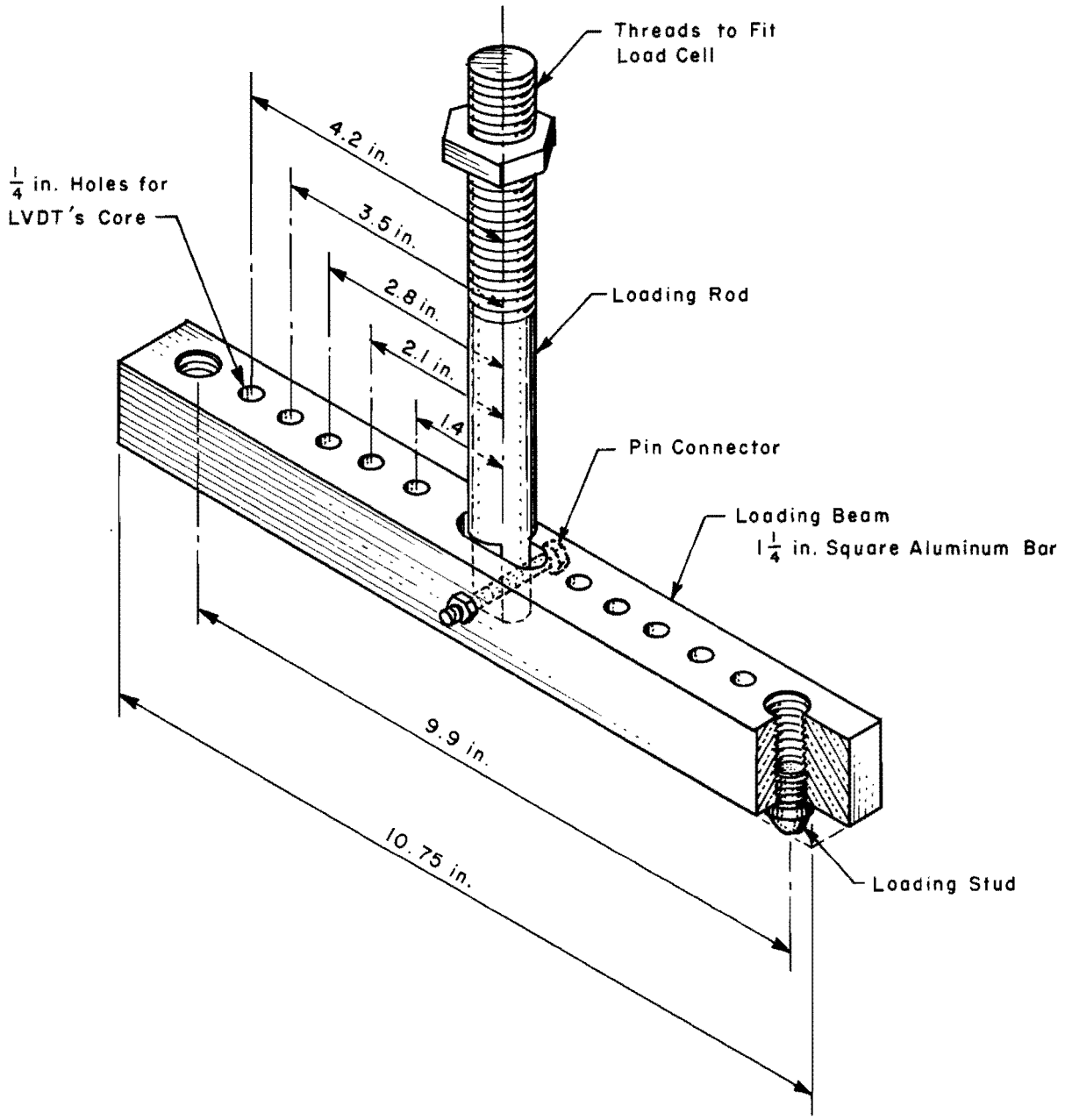

Fig 53. Details of loading beam for corner loads slab test (series 340).

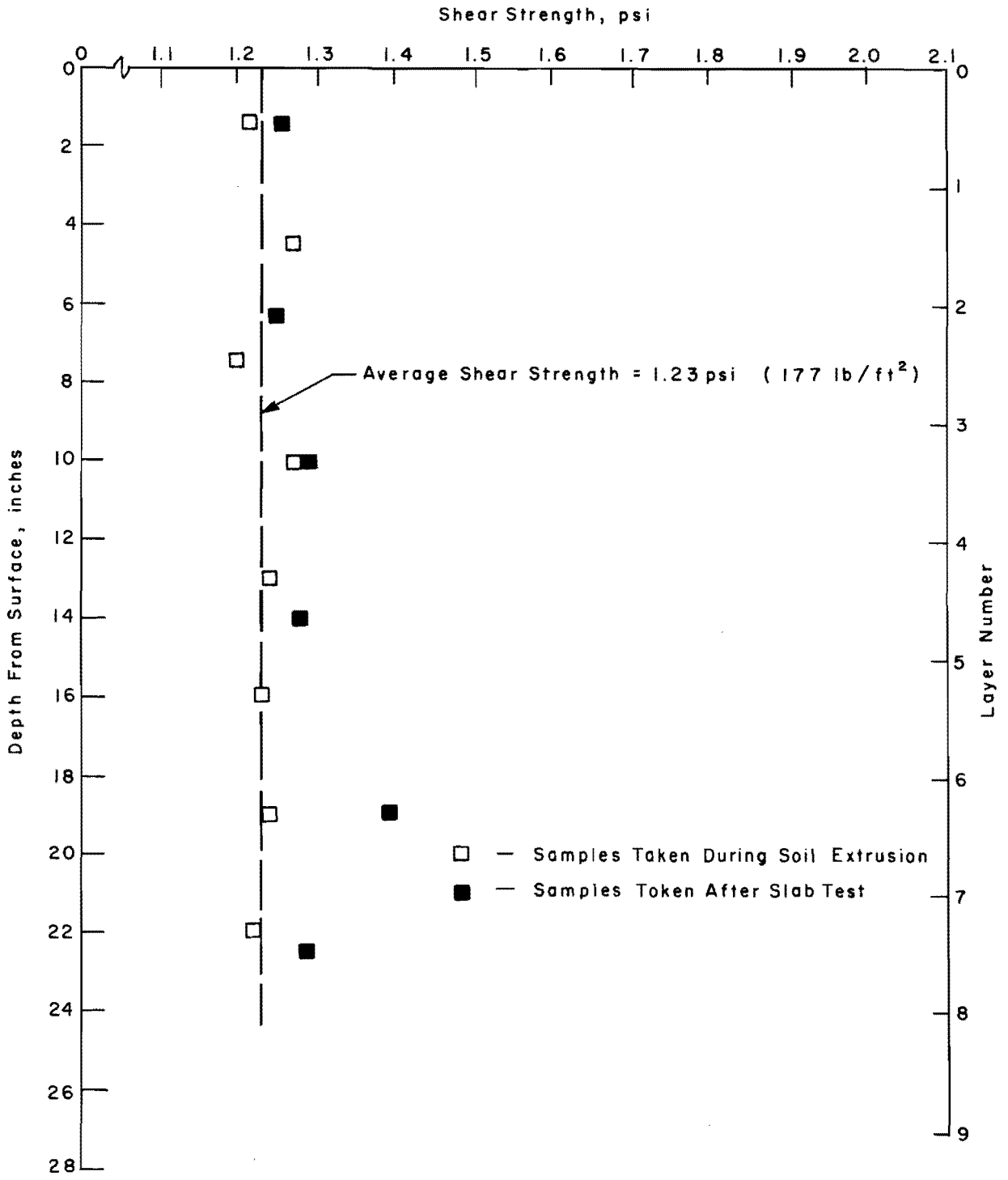

Fig 54. Shear strength variation of soil in corner loads slab test (series 340).

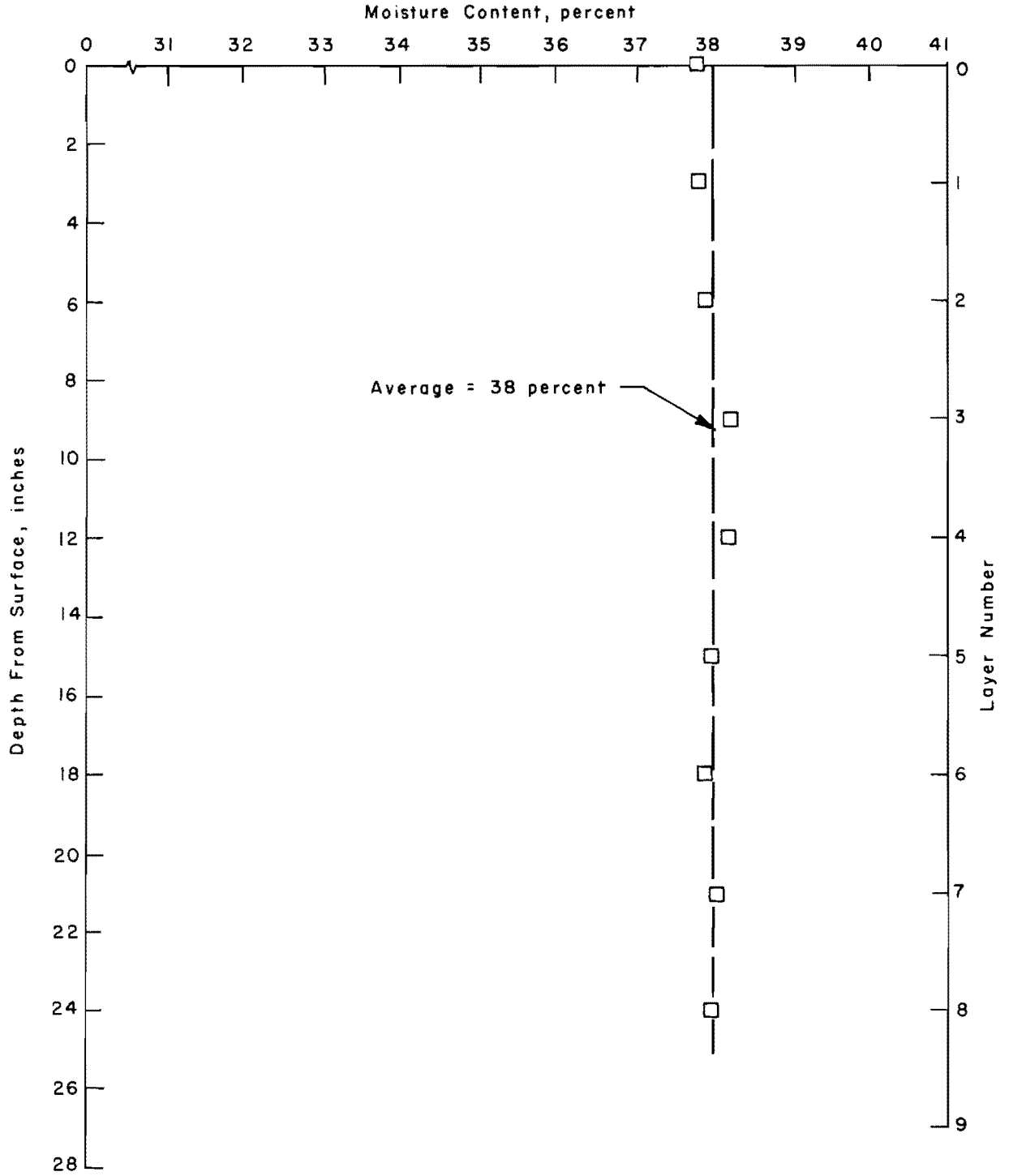

Fig 55. Water content variation in corner loads slab test (series 340).

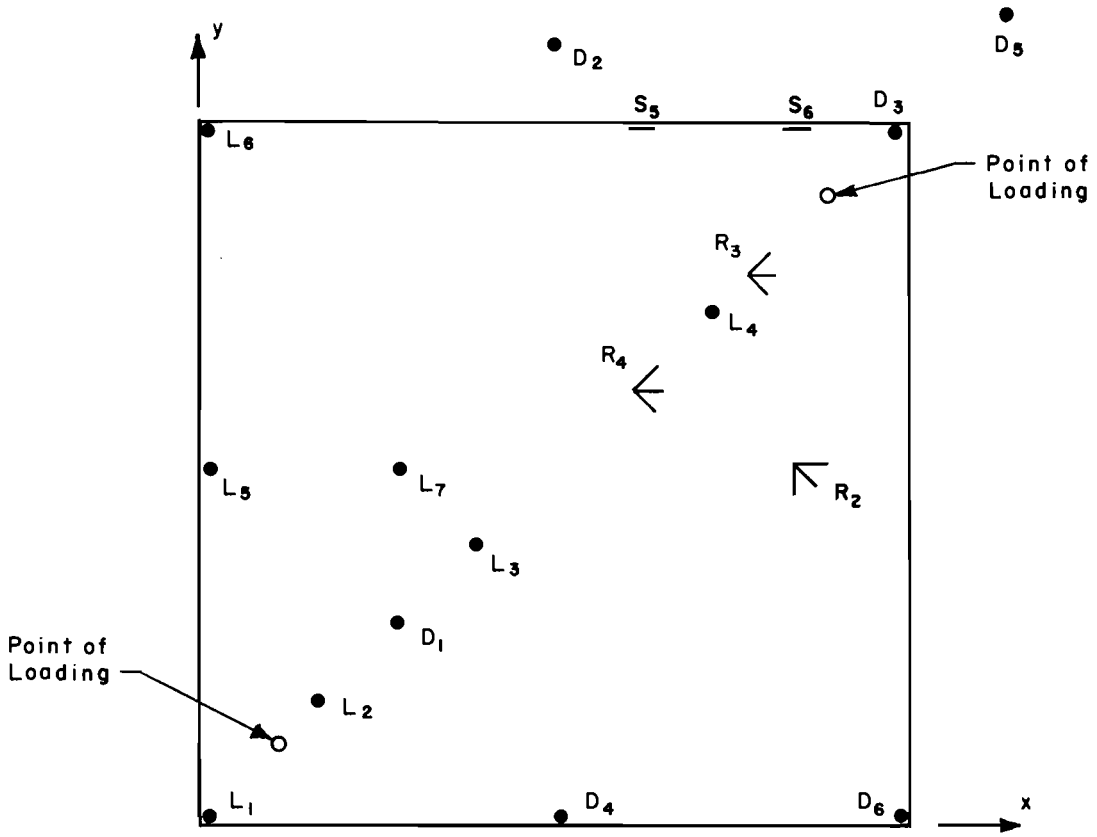

LVDT No.	Distance	Dial No.
L_1	6.36 in. from Center on Diagonal	D_3
L_2	4.23 in. " " " "	
L_3	1.41 " " " " "	
L_4	2.83 " " " " "	D_1
L_5	4.5 " " " " Center Line	D_4
L_6	6.36 " " " " Diagonal	D_6
L_7	2.0 " " " " Center Line	
	1.0 in. from Mid-edge on Soil	D_2
	2.12 " " Corner " "	D_5
Gages & Rosettes		
S_5	3.5 in. from Corner on Edge	
S_6	1.5 " " " " "	
R_2	3.0 " " Center on Center Line	
R_3	3.53 " " " " Diagonal	
R_4	1.41 " " " " "	

Fig 56. Positions of LVDT's, dial gages, rosettes, and loads for corner loads slab test (series 340).

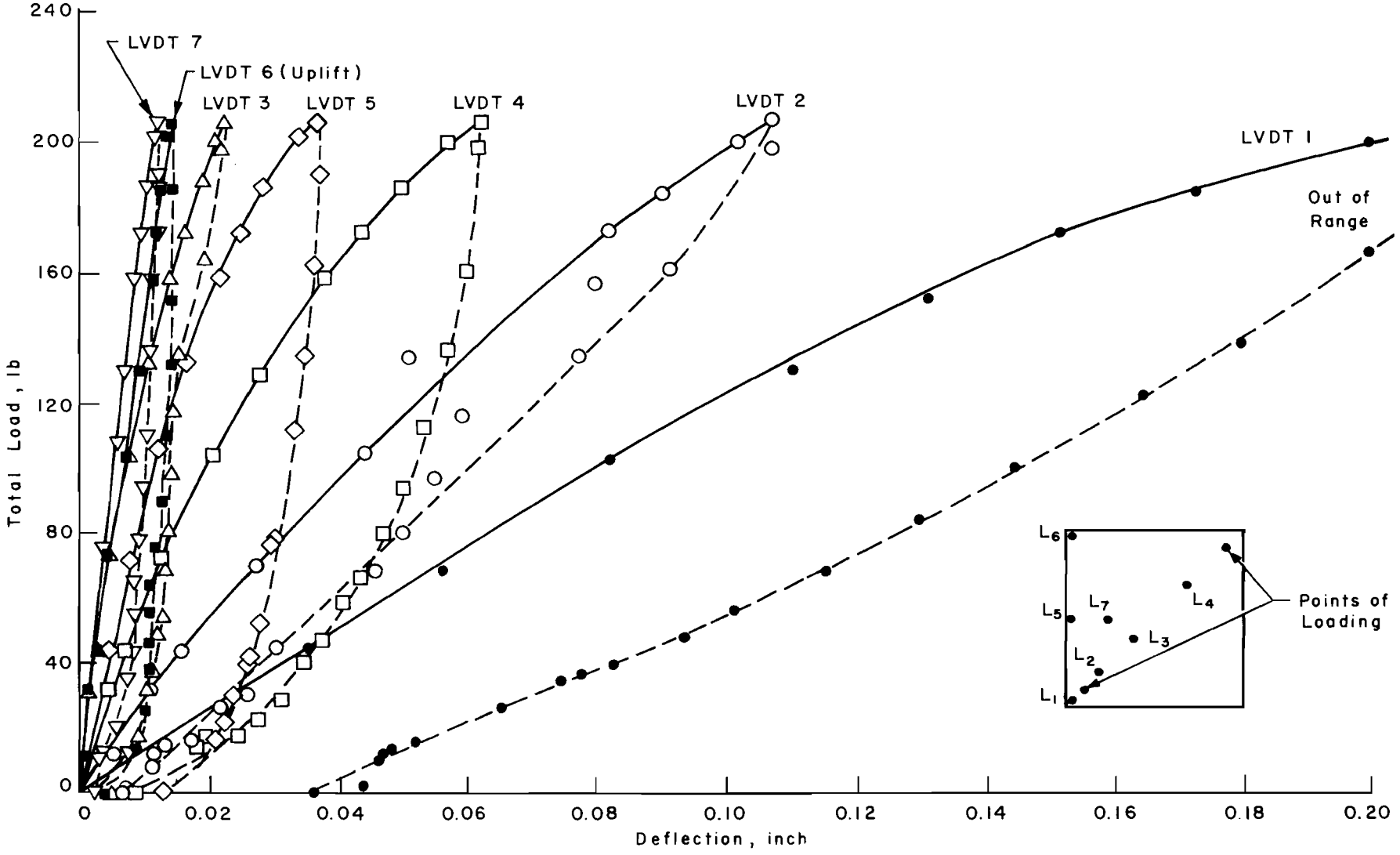

Fig 57. Load versus deflection curves for LVDT's for corner loads slab test (series 340).

TABLE 24. SHEAR STRENGTH USING VANE APPARATUS FOR CORNER LOADS SLAB TEST (SERIES 340)

Depth from Surface (inch)	Shear Strength at Locations (lb/ft^2)						Average Shear Strength
	1	2	3	4	5	6	
At surface	190	195	190	195	200	190	193
1	195	195	200	195	205	190	197
2	200	200	205	195	205	195	200
3	200	205	205	195	210	195	202
4	205	210	205	200	210	200	205
5	205	210	210	200	210	200	206

Variation: 190 to 210 lb/ft^2 (1.32 to 1.46 psi).

Average constant value: 201 lb/ft^2 (1.40 psi).

corner were upward, and for all the other points downward. The results, which showed different paths during unloading and permanent sets on no load, were similar to center load slab test results. It can also be observed that LVDT 1 was out of range after a load of 200 pounds.

Figure 58 shows the load versus deflection curves for the 4 dial gages on the slab which served as checkpoints for 4 LVDT's at identical positions. It can be seen from these curves that the nonlinear behavior during loading and unloading was similar to that of LVDT's. It can also be observed that deflections at all these checkpoints were greater using dial gages than using LVDT's.

Figure 59 shows the load versus deflection curves for two points on the soil near the slab periphery, one 1 inch from the mid-edge, and the other 2.12 inches from the corner. It can be seen from these curves that the deflections at both points were nonlinear and downwards, with large permanent sets on unloading. This indicates that the adjacent soil was affected as the slab was loaded.

Figure 60 shows load versus largest principal stresses and their directions at the three rosette locations. Figure 61 shows load versus stresses along the edge for the two strain gages. The methods of getting these stresses from strain readings are described in Appendix 3. It can be observed that the nonlinear behavior with permanent sets on unloading is similar to that for deflections.

Analytical Solutions

Analytical solutions were obtained using DSLAB 30 (Ref 29) for linear soil springs and DSLAB 26 (Ref 20) for nonlinear springs, for total loads of 100 and 200 pounds (50 and 100 pounds each point, respectively), and using the following soil springs:

(A) linear springs corresponding to tangent modulus from 9-inch-diameter rigid plate test data. Modulus k thus obtained was 160 lb/in^3.

(B) linear springs from 9-inch-diameter rigid plate test data for deflections of 0.02, 0.03, and 0.04 inch. Secant moduli thus obtained were 144, 128, and 112 lb/in^3, respectively. Obtaining a secant modulus beyond a deflection of 0.04 inch was not attempted.

(C) nonlinear springs using the entire pressure versus deflection curve of the 9-inch-diameter plate test.

(D) nonlinear springs using Skempton's recommendation from unconfined compression test data (derivation given in Appendix 4).

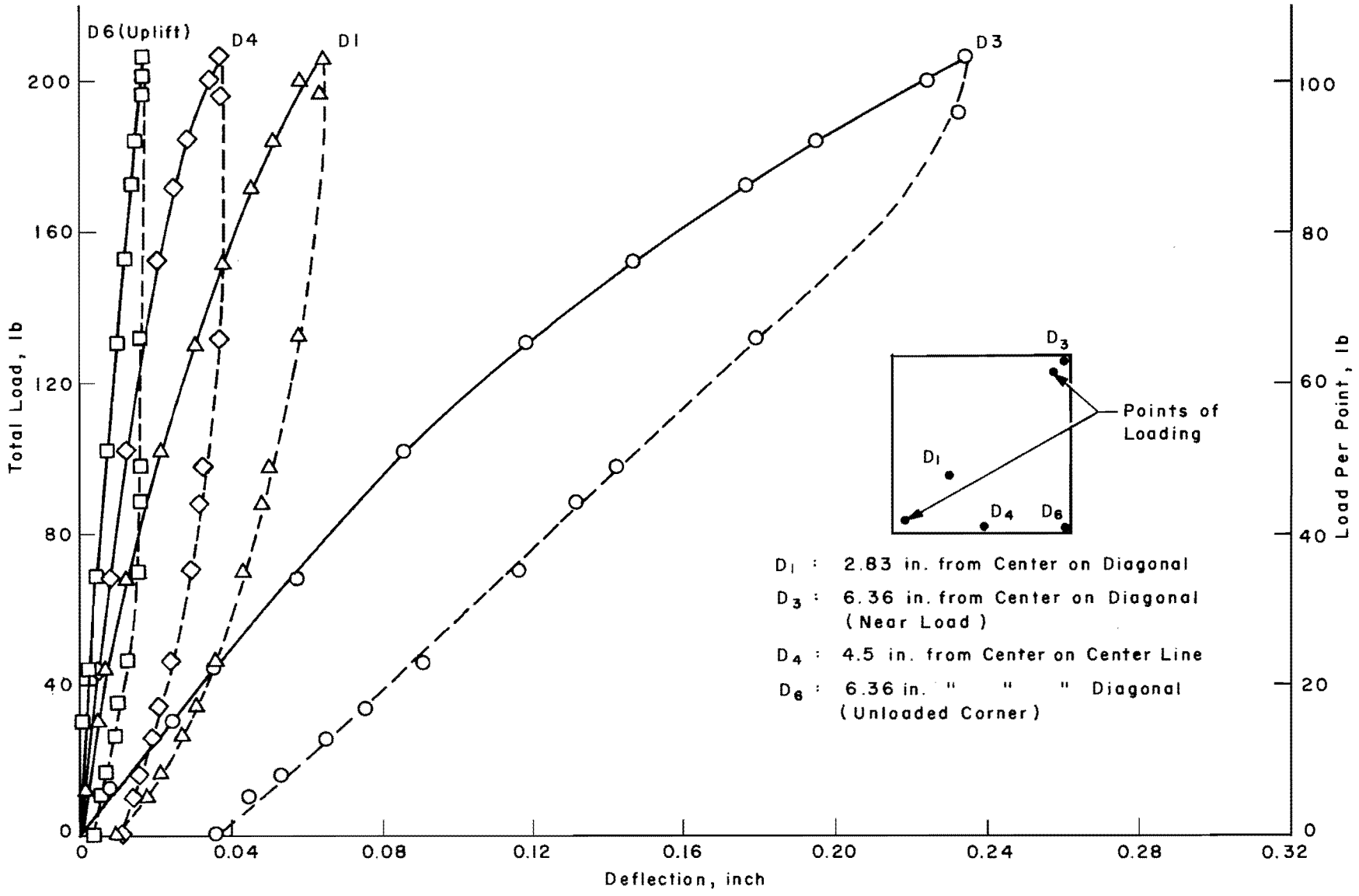

Fig 58. Load versus deflection curves for dial gages for corner loads slab test (series 340).

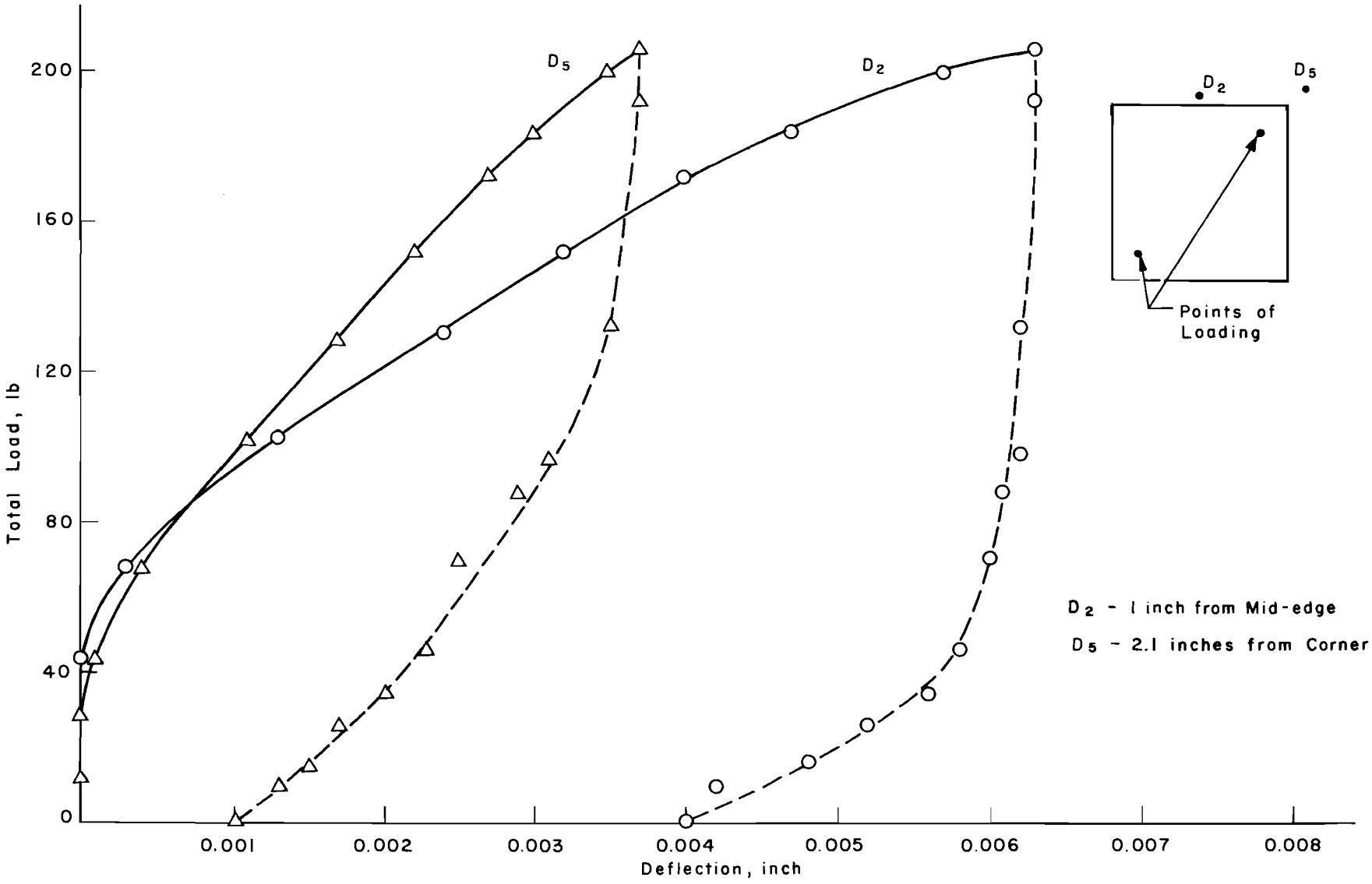

Fig 59. Load versus deflection curves for dial gages on soil for corner loads slab test (series 340).

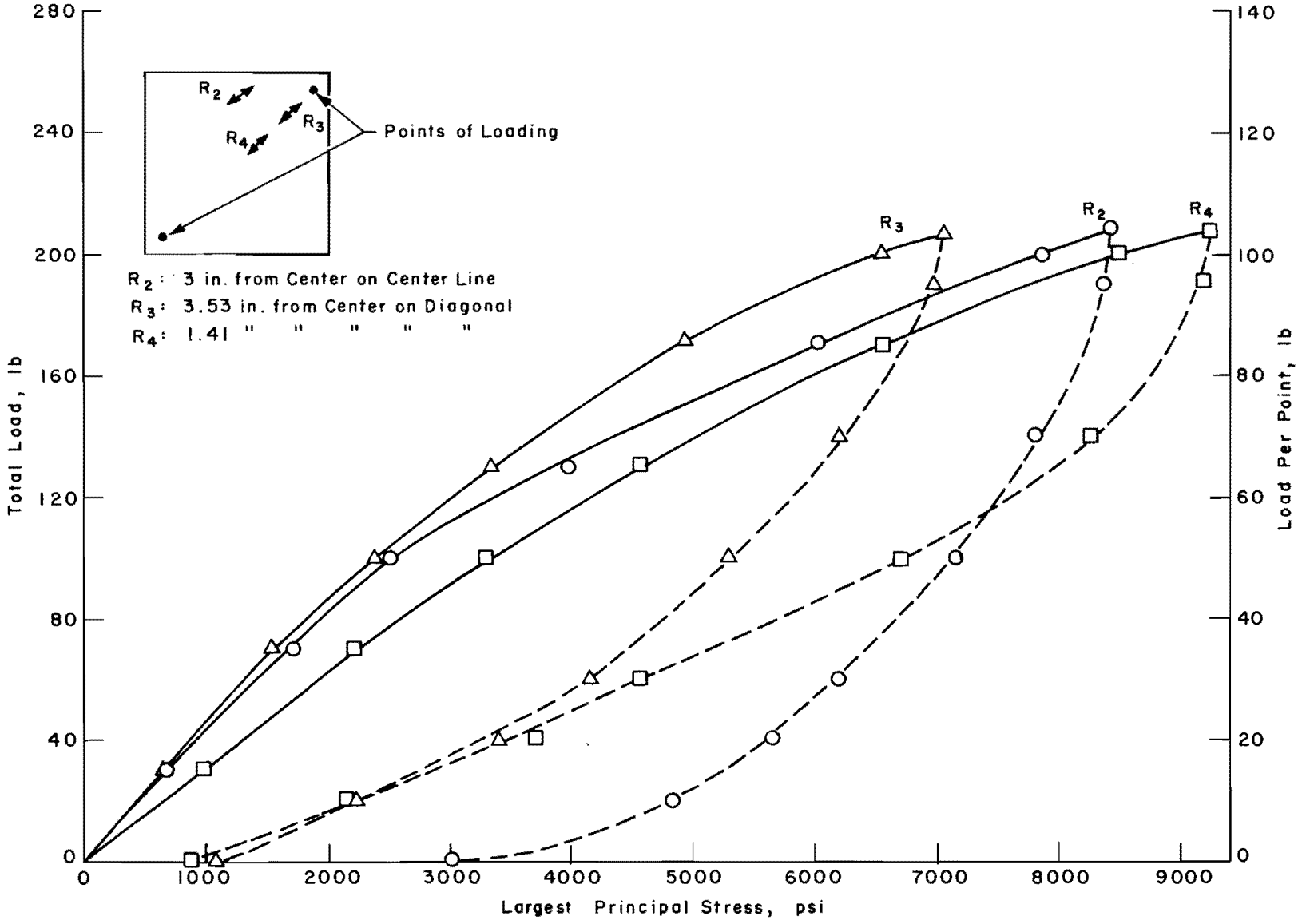

Fig 60. Load versus largest principal stresses for rosettes for corner loads slab test (series 340).

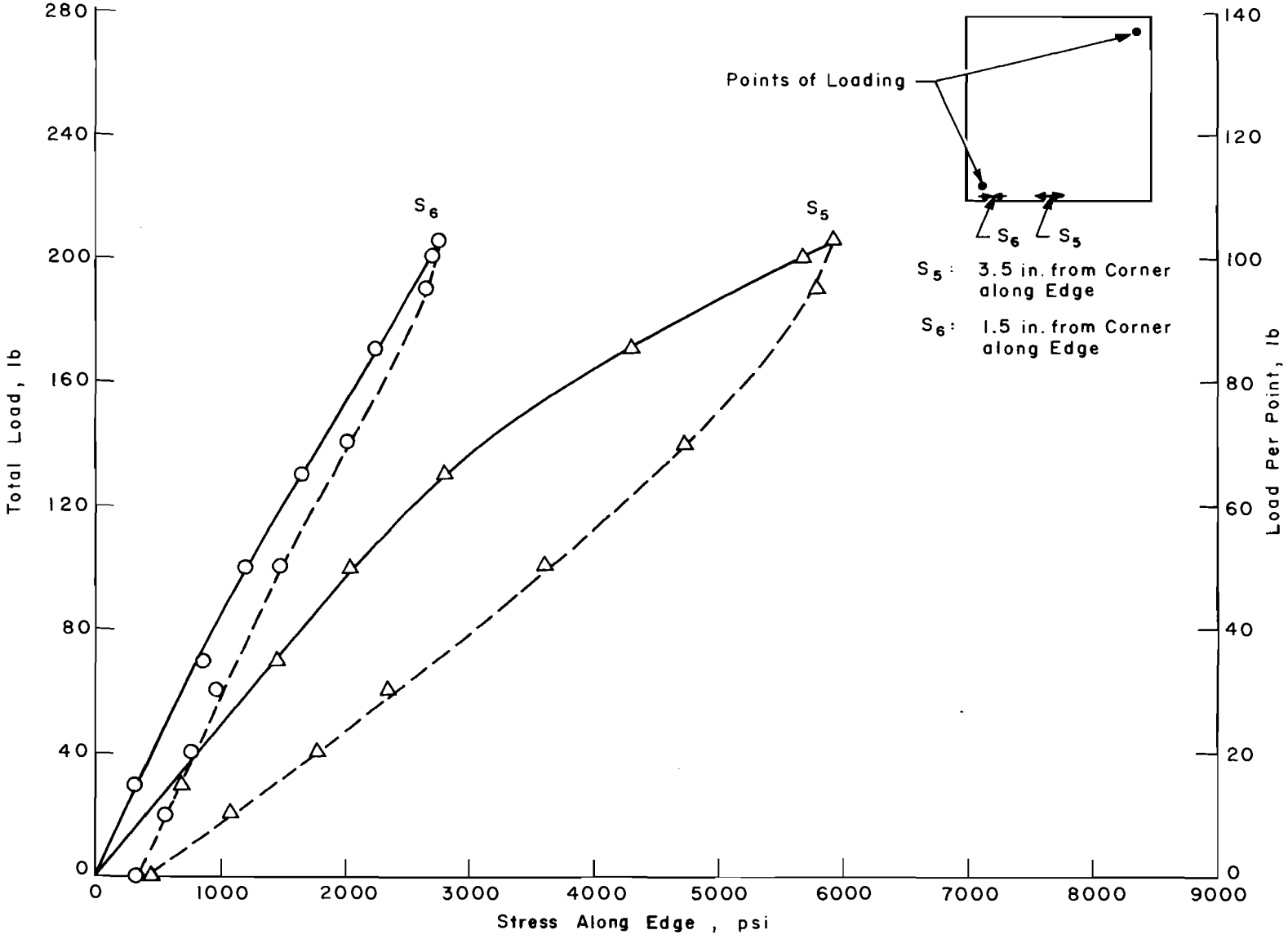

Fig 61. Load versus stresses along edge for corner loads slab test (series 340).

Comparison of Experimental and Analytical Solutions

Comparison of measured and analytical solutions for deflections, principal stresses, and stresses along the edge was made and percentage errors calculated as a function of the maximum measured value for the load under consideration. The measured and analytical deflections were plotted along the diagonal and the edge. As the loads were placed symmetrically on the diagonal, the measured values on both sides of the center were taken the same while plotting the deflections on the diagonal.

For a total load of 100 pounds (50 pounds each point), the maximum measured deflection at point 1, i.e., corner near load, was -0.081 inch. From the plots for measured and analytical deflections along the diagonal and the edge given in Figs 62 and 63 and the comparison in Table 25, it can be observed that, first, good correlation existed using nonlinear springs only. The percentage error using nonlinear springs (C and D) was within 6 percent on the entire slab. The difference in error at checkpoints using dial gages was within 1 percent. Second, solutions using linear springs (A and B) did not yield go good agreement, as the deflections on the slab were large and lay on the nonlinear part of pressure versus deflection characteristics of the soil.

Table 26 shows the comparison for largest principal stresses and stresses along the edge. It can be observed from this table that the maximum discrepancy using nonlinear springs (C and D) was within 14 percent and using linear springs (B) was 27 percent.

For a total load of 200 pounds (100 pounds each point), the maximum measured deflection at point 1 was -0.200 inch. From the plots along the diagonal and the edge shown in Figs 64 and 65, and the comparison in Table 27, it can be seen that, first, good correlation existed using nonlinear springs only. The percentage error using C and D springs was within 11 percent near the loaded area, 6 percent near the unloaded corner, and 3 percent on the rest of the slab. The percentage error for the corresponding checkpoints using dial gages was 5 percent for points near the load, 5 percent near the unloaded corner, and 5 percent near the mid-edge. Second, solutions using linear springs (A and B) did not yield good agreement, as the deflections lay on the nonlinear part of the pressure versus deflection characteristics of soil.

The comparison of largest principal stresses and stresses along the edge, as given in Table 28, shows maximum discrepancy between measured and analytical

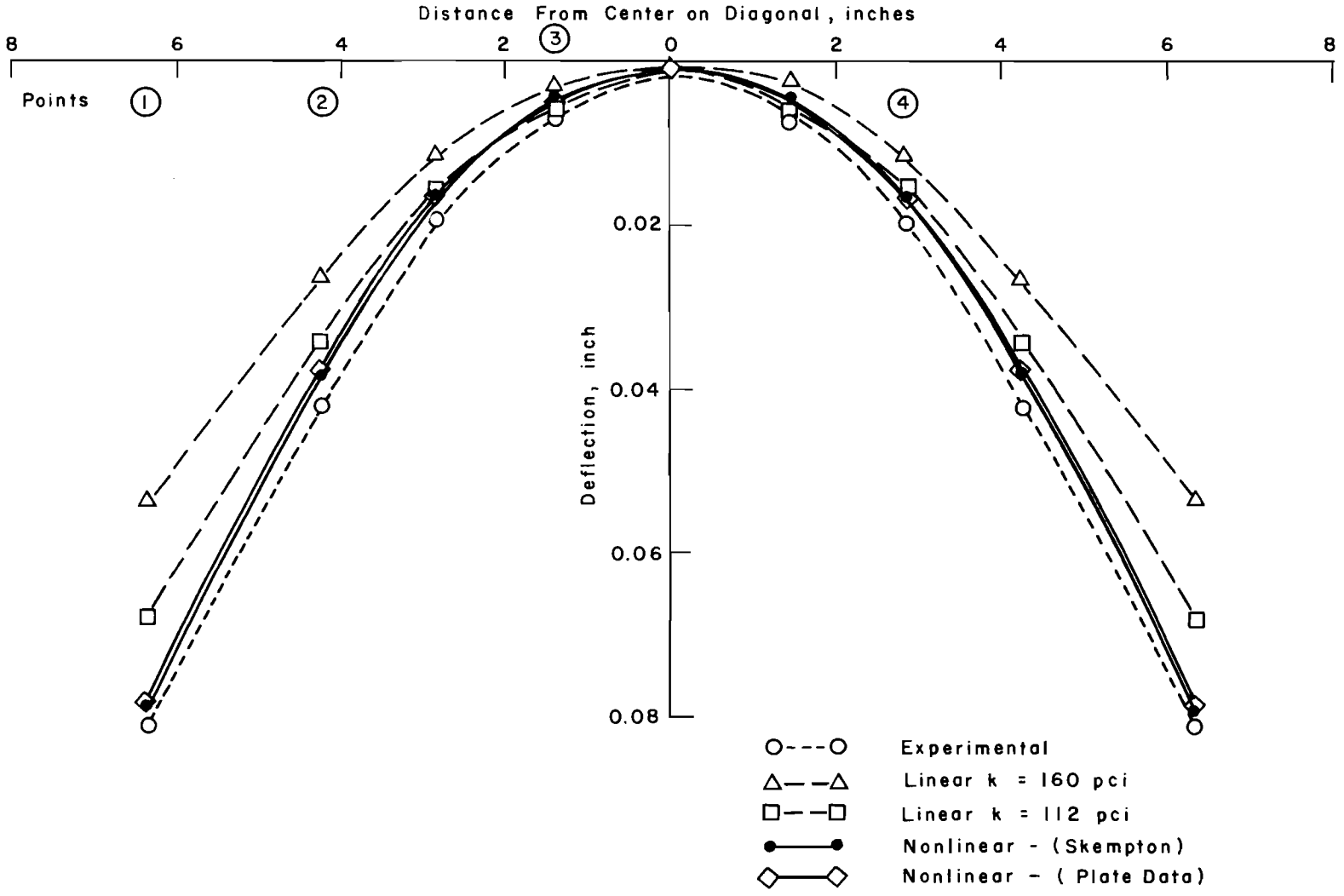

Fig 62. Experimental and analytical deflections on diagonal under corner loads of 100 pounds (50 pounds each point) - see Table 25.

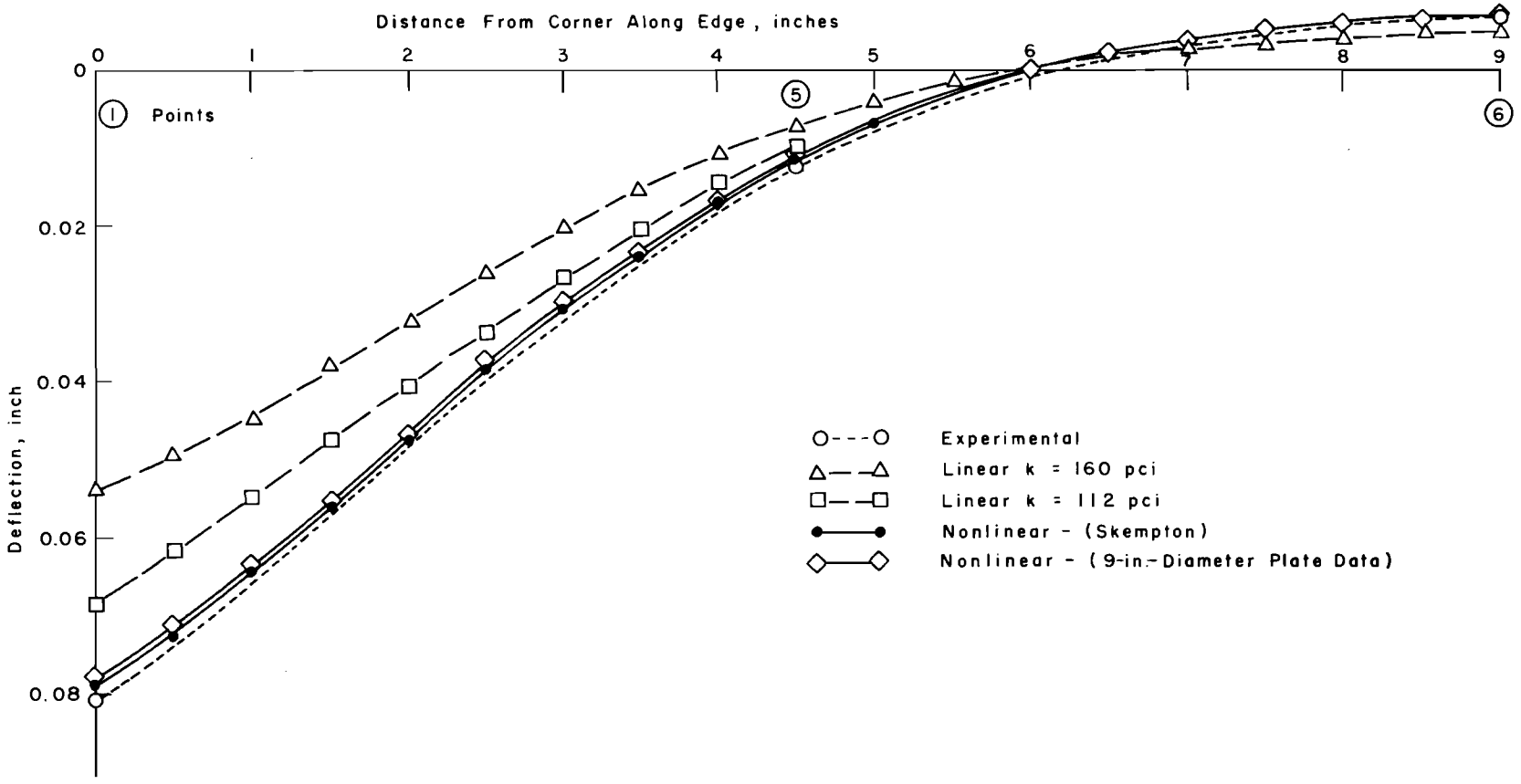

Fig 63. Experimental and analytical deflections on edge under corner loads of 100 pounds (50 pounds each point) - see Table 25.

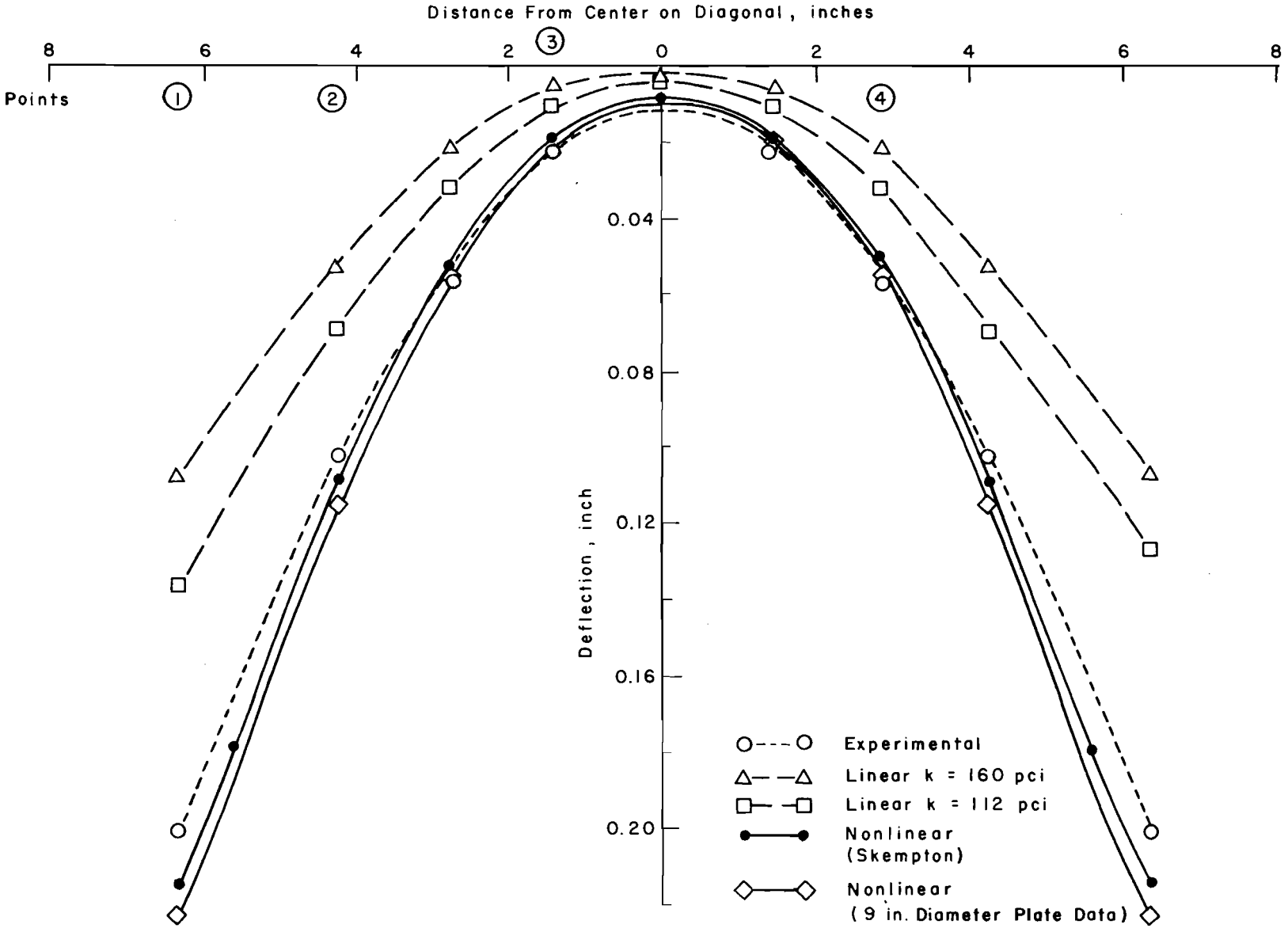

Fig 64. Experimental and analytical deflections on diagonal under corner loads of 200 pounds (100 pounds each point) - see Table 27.

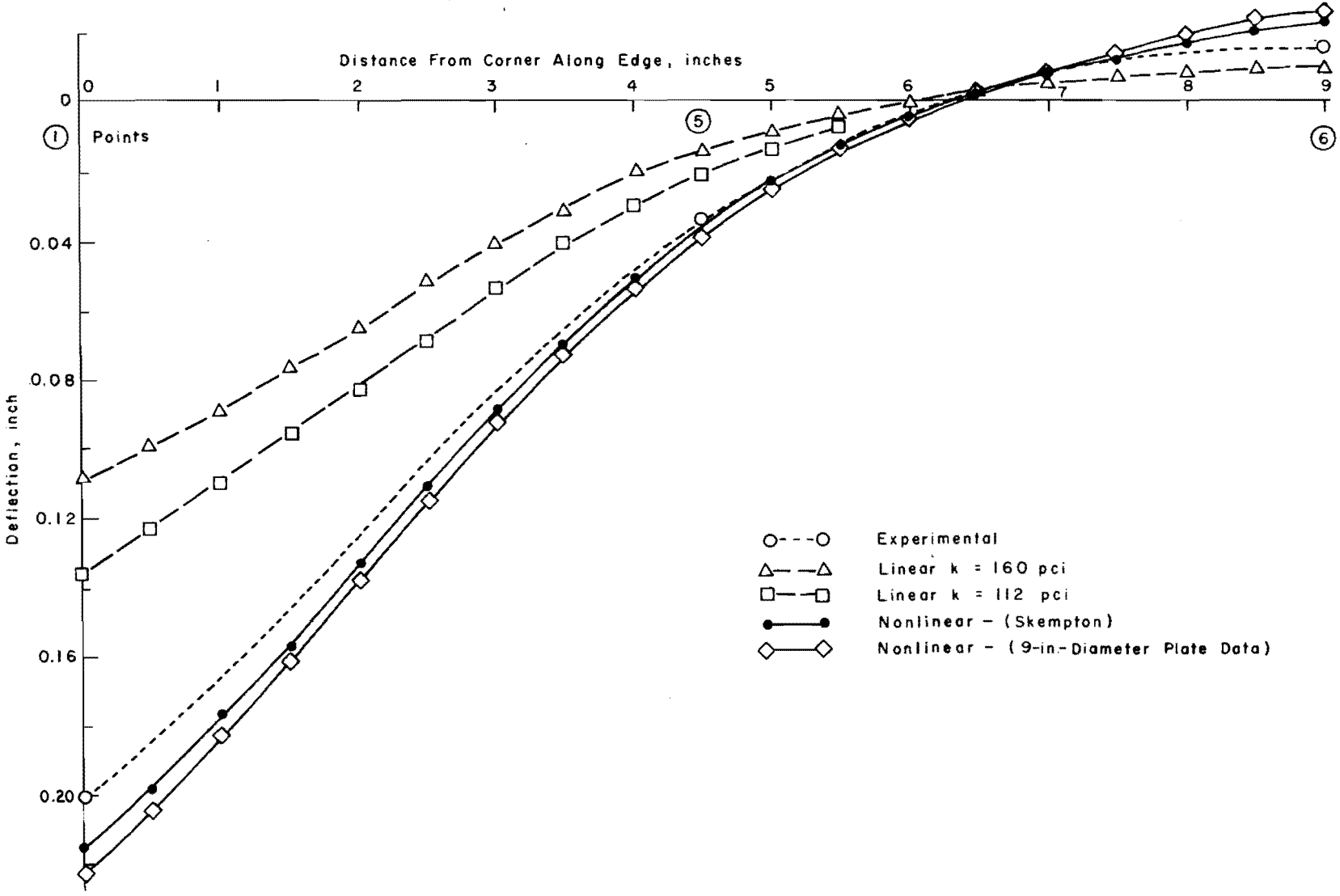

Fig 65. Experimental and analytical deflections on edge under corner loads of 200 pounds (100 pounds each point) - see Table 27.

TABLE 25. EXPERIMENTAL AND ANALYTICAL DEFLECTIONS FOR CORNER LOADS SLAB TEST (SERIES 340)

Load: 50 lb each point near opposite corners
(Total load = 100 lb)

Programs: DSLAB 30 for linear springs (18 x 18 increments)
DSLAB 26 for nonlinear springs (18 x 18 increments)

Type of Solution	LVDT's							Dial Gages			
	1	2	3	4	5	6	7	3	1	4	6
Distance from Center	6.36 inch	4.24 inch	1.41 inch	2.83 inch	4.5 inch	6.36 inch	2.0 inch	Check LVDT 1	Check LVDT 4	Check LVDT 5	Check LVDT 6
Experimental	-0.08100	-0.04240	-0.00732	-0.01970	-0.01220	0.00690	-0.00560	-0.08350	-0.02150	-0.01280	0.00730
Linear springs k = 160 psi	-0.05388	-0.02645	-0.00286	-0.01121	-0.00729	0.00495	-0.00227	-0.05388	-0.01121	-0.00729	0.00495
% Error	33.48	19.69	5.51	10.48	6.06	2.40	4.11	36.57	12.70	6.80	2.90
Linear springs k = 112 psi	-0.06823	-0.03462	-0.00548	-0.01604	-0.01085	0.00742	-0.00460	-0.06825	-0.01604	-0.01085	0.00742
% Error	15.77	9.60	2.27	4.52	1.67	-0.64	1.23	18.83	6.74	2.41	-0.14
Nonlinear q - w curve (9-inch-diameter plate data)	-0.07810	-0.03774	-0.00403	-0.01610	-0.0109	0.00712	-0.00324	-0.07810	-0.01610	-0.01090	0.00712
% Error	3.58	5.75	4.06	4.44	-1.60	-0.28	2.92	6.67	6.67	2.35	0.22
Nonlinear q - w curve (Skempton's)	-0.07903	-0.03874	-0.00484	-0.01703	-0.01160	0.00746	-0.00398	-0.07903	-0.01703	-0.01160	0.00746
% Error	2.43	4.52	3.06	3.30	0.74	-0.69	2.00	5.52	5.52	1.48	-0.20

Note: Plots along diagonal and edge are given in Figs 62 and 63.

TABLE 26. EXPERIMENTAL AND ANALYTICAL LARGEST PRINCIPAL STRESSES AND STRESSES ALONG EDGE FOR CORNER LOADS SLAB TEST (SERIES 340)

Load: 50 lb each point near opposite corners
(Total load = 100 lb)

Programs: DSLAB 30 for linear springs (18 x 18 increments)
DSLAB 26 for nonlinear springs (18 x 18 increments)

Type of Solution	Rosette	Rosette 4	Rosette 3	Gage 5	Gage 6
	Largest Stress	Largest Stress	Largest Stress	Stress Along Edge	Stress Along Edge
Experimental	2714.00	3313.00	2389.00	2074.00	1209.00
Linear springs k = 160 psi	1887.00	-1963.00	-1979.00	-1852.00	1002.00
% Error	24.96	40.75	12.38	6.70	6.25
Linear springs k = 112 psi	2281.00	-2424.00	-2221.00	-1984.00	1134.00
% Error	13.07	26.83	5.07	2.72	2.26
Nonlinear q - w curve (9-inch-diameter plate data)	2732.00	-2849.00	-2753.00	-2514.00	1126.00
% Error	-0.54	14.01	-10.99	-13.28	2.51
Nonlinear q - w curve (Skempton's)	2728.00	-2856.00	-2706.00	-2454.00	1156.00
% Error	-0.42	13.79	-9.57	-11.47	1.60

TABLE 27. EXPERIMENTAL AND ANALYTICAL DEFLECTIONS FOR CORNER LOADS SLAB TEST (SERIES 340)

Load: 100 lb each point near opposite corners
(Total load = 200 lb)

Programs: DSLAB 30 for linear springs (18 x 18 increments)
DSLAB 26 for nonlinear springs (18 x 18 increments)

Type of Solution	LVDT's							Dial Gages			
	1	2	3	4	5	6	7	3	1	4	6
Distance from Center	6.36 inch	4.24 inch	1.41 inch	2.83 inch	4.5 inch	6.36 inch	2.0 inch	Check LVDT 1	Check LVDT 4	Check LVDT 5	Check LVDT 6
Experimental	-0.20000	-0.10300	-0.02160	-0.05800	-0.03400	0.01430	-0.01180	-0.22400	-0.05900	-0.03470	0.01650
Linear springs k = 160 psi	-0.10780	-0.05290	-0.00571	-0.02242	-0.01458	0.00991	-0.00454	-0.10780	-0.02242	-0.01458	0.00991
% Error	46.26	16.83	7.92	17.74	9.68	2.19	3.62	57.93	18.24	10.03	3.29
Linear springs k = 112 psi	-0.13650	-0.06924	-0.01097	-0.03208	-0.02169	0.01483	-0.00920	-0.13650	-0.03208	-0.02169	0.01483
% Error	31.95	16.83	5.30	12.92	6.14	-0.26	1.29	43.62	13.42	6.49	0.83
Nonlinear q - w curve (9-inch-diameter plate data)	-0.22340	-0.11440	-0.01982	-0.05506	-0.03878	-0.02631	-0.01689	-0.22340	-0.05506	-0.03878	0.02631
% Error	-11.37	-5.68	0.89	1.47	-2.38	-5.99	-2.54	0.30	1.96	-2.03	-4.89
Nonlinear q - w curve (Skempton's)	-0.21470	-0.10970	-0.01909	-0.05270	-0.03720	-0.02394	-0.01632	-0.21270	-0.05270	-0.02393	0.02393
% Error	-7.03	-3.34	1.25	2.64	-1.59	-4.8	-2.24	4.64	3.14	5.37	-3.70

Note: Plots along diagonal and edge are given in Figs 64 and 65.

TABLE 28. EXPERIMENTAL AND ANALYTICAL LARGEST PRINCIPAL STRESSES AND STRESSES ALONG EDGE FOR CORNER LOADS SLAB TEST (SERIES 340)

Load: 100 lb each point near opposite corners
(Total load = 200 lb)

Programs: DSLAB 30 for linear springs (18 x 18 increments)
DSLAB 26 for nonlinear springs (18 x 18 increments)

Type of Solution	Rosette 2	Rosette 4	Rosette 3	Gage 5	Gage 6
	Largest Stress	Largest Stress	Largest Stress	Stress Along Edge	Stress Along Edge
Experimental	7886.00	8489.00	6542.00	5690.00	2714.00
Linear springs k = 160 psi	3773.00	3927.00	3957.00	3704.00	2004.00
% Error	48.45	53.74	30.45	23.39	8.36
Linear springs k = 112 psi	4562.00	4848.00	4442.00	3966.00	2270.00
% Error	39.16	42.89	24.74	20.31	5.23
Nonlinear q - w curve (9-inch-diameter plate data)	7473.00	8064.00	6348.00	5458.00	2980.00
% Error	4.87	5.01	2.29	2.73	-3.13
Nonlinear q - w curve (Skempton's)	7154.00	7703.00	6248.00	5384.00	2858.00
% Error	8.62	9.26	3.46	3.60	-1.70

solutions of 9 percent using nonlinear springs (C and D) and 43 percent using linear springs (B).

Causes of Discrepancy

In the slab tests discussed in this chapter, the slab was resting on soil, whereas plates in Chapter 4 were resting on rigid supports. From the study on plates under a variety of stiffness, load and support conditions, the method of solution where the rigid supports could be represented adequately in the input data has already been verified. This means that the closer the input data represent the real problem, the better the agreement is between the analytical and experimental solutions. Therefore, the major cause of discrepancy in the slab tests may be in the representation of soil.

From the comparison for deflections, largest principal stresses, and stresses along the edge under the two loading conditions it has been observed that soil can be represented satisfactorily by the Winkler foundation provided:

(1) Linear or nonlinear springs are input for loads producing small deflections.

(2) Only nonlinear springs are used for loads producing large deflections.

It has also been observed that the maximum discrepancy is near the corners or near the edge, i.e., along the periphery, and to a smaller degree in the interior of the slab. The following factors may be some of the causes of the discrepancy:

(1) According to the Winkler foundation, the soil springs act only under the slab and the adjoining soil is not affected at all. This is in contradiction to the observed deflections of the soil surface during the tests. Deflections were observed at two points on the soil as shown in Figs 41 and 56 for center load and corner loads slab tests, respectively. Load (on the slab) versus deflection (on the soil) data for both points are given in Figs 44 and 59. From these observations, it seems that the effect of the outside the perimeter of the slab may also be included while representing the soil.

(2) According to the DSLAB input, the properties of the slab and soil are lumped in joints and bars, in proportion to the area occupied by each station. This necessitates full values at the interior stations, half values at the edge, and quarter values at the corners. This applies to the slab as well as to the soil, and may be true only if the slab (9 by 9 inch) is resting on 9 by 9-inch soil. If the soil is not represented beyond the dimensions of the slab, the soil springs acting along the periphery may need to be modified. The possible ways to carry out such modification should be thoroughly investigated.

(3) The interaction between the slab and the soil has not been taken into account. The effect of the frictional forces developed due to such interaction should be thoroughly investigated. The present DSLAB solutions neglect these frictional forces. The bottom of the slab was, therefore, lubricated with a thin film of grease before the soil placement. Whether the frictional forces during the testing were completely reduced is not known.

(4) The soil is represented by linear and nonlinear independent springs in the DSLAB solutions. The interaction between these springs, in both vertical and horizontal directions, is neglected. Such interaction between the soil springs in the horizontal direction may be incorporated by introducing coupled springs. A thorough investigation regarding coupled-spring foundation for both linear and nonlinear solutions and the method of representing this parameter needs to be made to understand the phenomenon.

(5) Only one nonlinear pressure versus deflection curve or uniform linear k was input for the entire soil surface below the slab. Different curves or nonuniform k for different areas below the slab may be necessary, as pointed out by Lewis and Harr (Ref 22). An experimental investigation with pressure measurements to determine such curves or k variation needs to be made.

(6) Experimental Errors. Although great care was taken during the entire test procedure, the following factors may be some of the experimental errors, at various stages of testing:

   (a) The soil placed by extrusion may not have been perfectly homogeneous in moisture content and density. In placing adjacent blocks, rows, and layers, perfect jointing may not have been achieved at all the places in the box.

   (b) The method adopted for a good contact between slab and soil may not have been perfect enough to ensure such a contact at all places.

   (c) A time lag in loading and recording the data may have produced a small error.

   (d) With LVDT's of 1 and 1/2-inch range used for deflections of ±0.2 inch or less, a good resolution could not be obtained. LVDT's of smaller range with greater resolution should have been used.

   (e) Slight imperfection in fixing gages and rosettes may have led to a small error.

   (f) The discrepancies in determining slab properties may have caused a small error, in the same way as for plates in Chapter 4.

CHAPTER 6. STUDY ON SLABS UNDER CYCLIC LOADING

Pavements are subjected to numerous repetitive loads (in some cases millions) during their useful life. Lee (Ref 21) has presented a comprehensive review of the factors influencing pavement behavior under repeated load applications. Besides temperature, environmental, and other factors, pavement behavior is a function of rate, frequency, duration, and stress level of the repetitive loads. The problem of soil-pavement systems under repetitive loads is thus quite a complex problem. However, qualitative information from testing slab sections under a constant rate of loading and cycling for either load or deflection for a few cycles may be useful in getting some idea of the phenomenon.

After the slab was tested under static center loads, it was decided to continue testing it under cyclic loads, and both the center load test (series 330) and the corner loads test (series 340) were made under deflection repetition. This chapter presents some of the cyclic test data, their interpretation, and an attempt to modify the soil representation for cyclic loading. The experimental results are compared with the preliminary analytical solutions thus obtained, to give some idea of the phenomenon.

Center Load Slab Test (Series 330)

Test Procedure

The set-up for testing and recording the data for load, deflections, and strains for this series is described in Chapter 5. After the slab was loaded to 255 pounds in the first cycle, it was observed that two LVDT's had gone out of range and the others were close to the maximum limit. To keep the LVDT's within the range of their travel, the load was cycled to a constant deflection of about 15 percent less than the maximum deflection for the instrument nearest the load (dial 1, see Fig 66). For the analysis presented here, the data were recorded at regular intervals during loading and unloading in the fifth and seventh cycles.

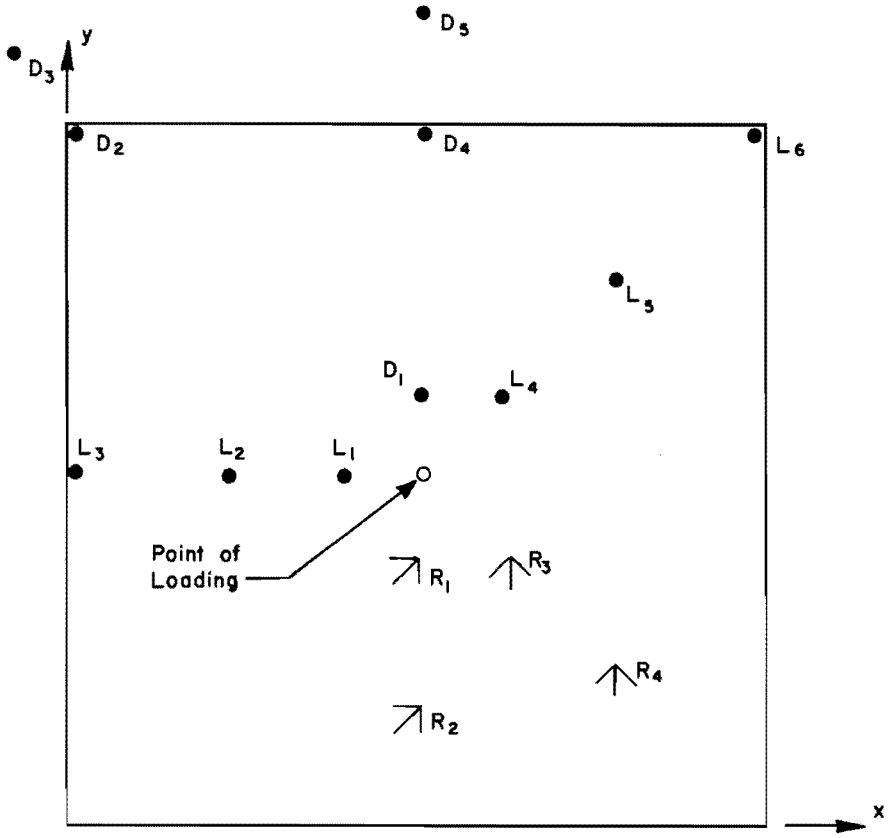

LVDT No	Distance	Dial No
L_1	1 in. from Center on Center Line	D_1
L_2	2.5 " " " " " "	
L_3	4.5 " " " " " "	D_4
L_4	1.41 " " " " Diagonal	
L_5	3.53 " " " " "	
L_6	6.36 " " " " "	D_2
	1.5 in from Mid-edge on Soil	D_5
	1.41 " " Corner " "	D_3
Rosettes		
R_1	1 in. from Center on Center Line	
R_2	3 " " " " " "	
R_3	1.41 " " " " Diagonal	
R_4	3.53 " " " " "	

Fig 66. Positions of load, LVDT's, and dial gages for center cyclic load slab test (series 330).

Test Results

The data were reduced, as described in Appendix 3 for the first cycle. As mentioned on the preceding page, the slab was loaded to 255 pounds and then cycled to a constant deflection about 15 percent less than the maximum deflection obtained during the first cycle. Under such a condition of cycling, the behavior of the slab may not be interpreted correctly if the cycling is not done for either maximum deflection or maximum load. The deflection data will be discussed in the following paragraphs to give an idea of the phenomenon involved. Analysis of test data for strains for cycling loading was not attempted.

Figure 67 shows the load versus deflection curve obtained during the first, fifth, and seventh cycles for the dial gage nearest the load (1 inch from center on the center line) which was used to govern deflection for cycling. From this plot it can be seen that the curves for the fifth and seventh cycles have the same general shape and slope as the first cycle curve. The effect of cycling to a constant deflection of -0.0655 inch was to reduce the required load from 210 pounds for the first cycle to 190 pounds for the fifth cycle and 185 pounds for the sixth and seventh cycles. This indicates that there may be a tendency for most of the reduction in load to take place during the first few cycles, which is followed by a stage of stabilization. However, this was probably accelerated by reducing the deflection level below the maximum for cycling.

During the first load application, the deflections increased and there was a permanent set on unloading. In the next cycle the deflections increased, starting from the permanent set left after the first cycle, with a different permanent set on unloading. This process of soil-slab adjustment continued, exhibited by different permanent sets after every cycle. It was also observed that after the first cycle the permanent set was large, followed by small increases in the total permanent set in the next four cycles and approximately the same in the sixth and seventh cycles.

At the start of any cycle, it is easier to measure the net deflections for that cycle than to measure the cummulative deflections starting from the first cycle. The cummulative deflections can, however, be measured if the permanent set before the cycle is determined, which may be difficult to do in most cases. Keeping this in mind, the net deflections of the first, fifth, and seventh cycles were compared. The net deflections obtained for loads of

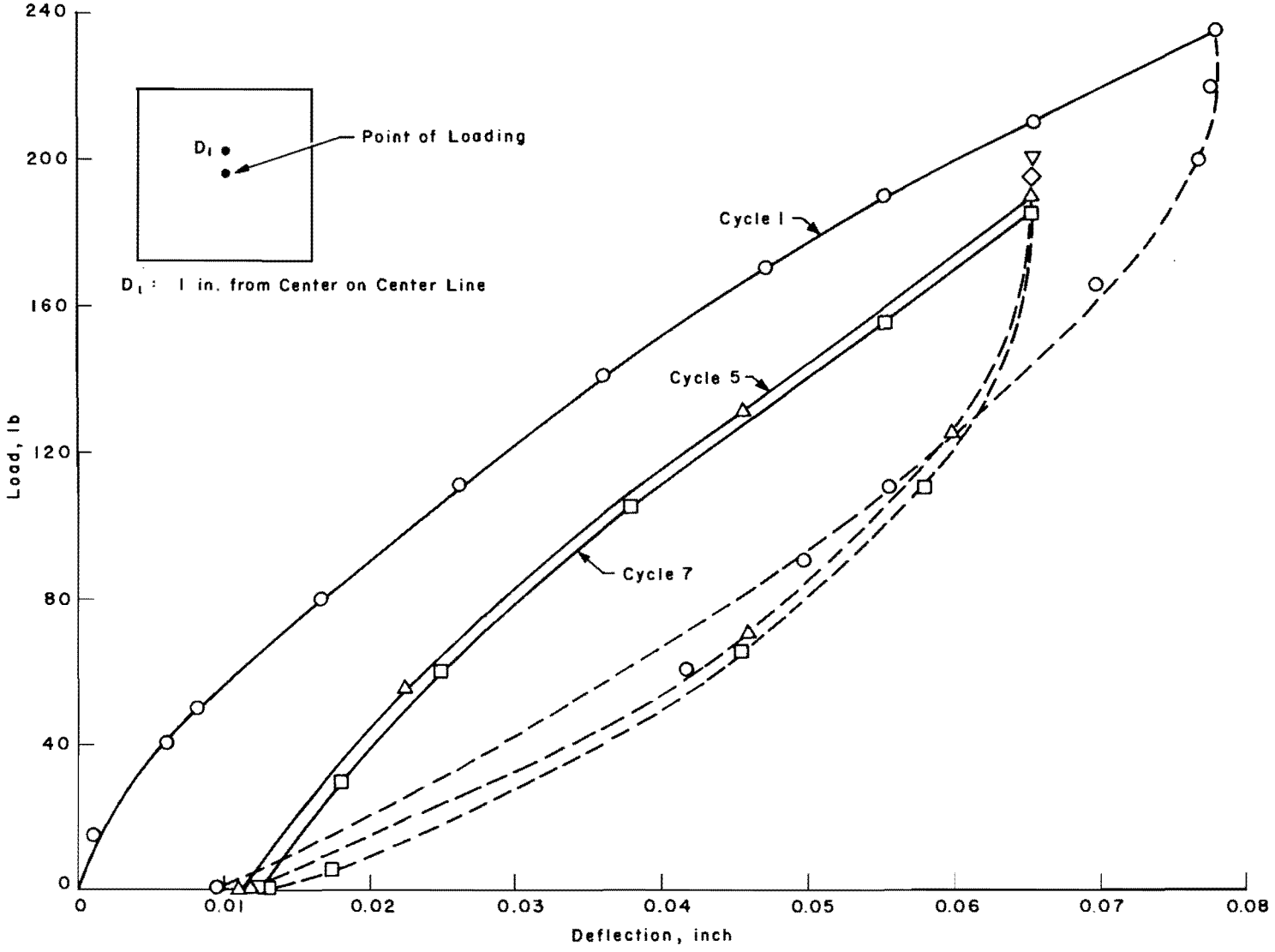

Fig 67. Load versus deflection for dial 1 under center cyclic load slab test (series 330).

100 and 185 pounds for the first, fifth, and seventh cycles were compared (Tables 28 and 29, respectively). The deflections were -0.0229, -0.0240, and -0.0241 inch for 100 pounds and -0.0528, -0.0531, and -0.0532 inch for 185 pounds. This shows that the effect of cycling loading is to increase the deflections within the first few cycles, which are followed by a stage of stabilization.

It is also desirable to evaluate the cyclic loading on other points within the slab. Consider three general areas, "points in the anterior of the slab," "points on mid-edge," and "points on corner."

Points in the Interior of the Slab

Data for this area were processed for LVDT 1 (1 inch from the slab center on the center line), and LVDT's 4 and 5 (1.41 and 3.53 inches from the center on the diagonal, respectively. Output of LVDT 2 (2.5 inches from center) could not be used, as an error message was indicated. Load versus deflection curves for LVDT 4 are shown in Fig 68. It can be observed from these curves and Tables 28 and 29 that the cycling effects of load stabilization, the curves for various cycles following in shape and slope, and the net deflections for the fifth and seventh cycles being greater than that for the first cycle were similar to that of dial gage 1. LVDT 1 served as a check for dial gage 1. The load versus deflection curves are given in Appendix 5 and net deflections for 100 and 185 pounds in Tables 28 and 29. It can be seen that the observations were almost similar to dial gage 1. The data of LVDT 5, as given in Tables 28 and 29 and Appendix 5, showed similar effects of cycling loading, except that the total deflection for 185 pounds for cycles 5 and 7 exceeded the total deflection obtained in the first cycle. This may be due to the effect of soil remolding.

Points on Mid-Edge

LVDT 3 and dial gage 4 were on the mid-edge so that one served as a check on the other. Load versus deflection curves for dial 4 are shown in Fig 69 and for LVDT 3 in Appendix 5. It can be observed from these curves that (1) the curves of the fifth and seventh cycles followed each other closely, although the slope was steeper than that of the first cycle curve; (2) the load stabilized after a few cycles, in general, as at points in the interior of the slab; (3) the net deflections for loads of 100 and 185 pounds (Tables 28 and 29) for the fifth and seventh cycles were less than those for the first cycle;

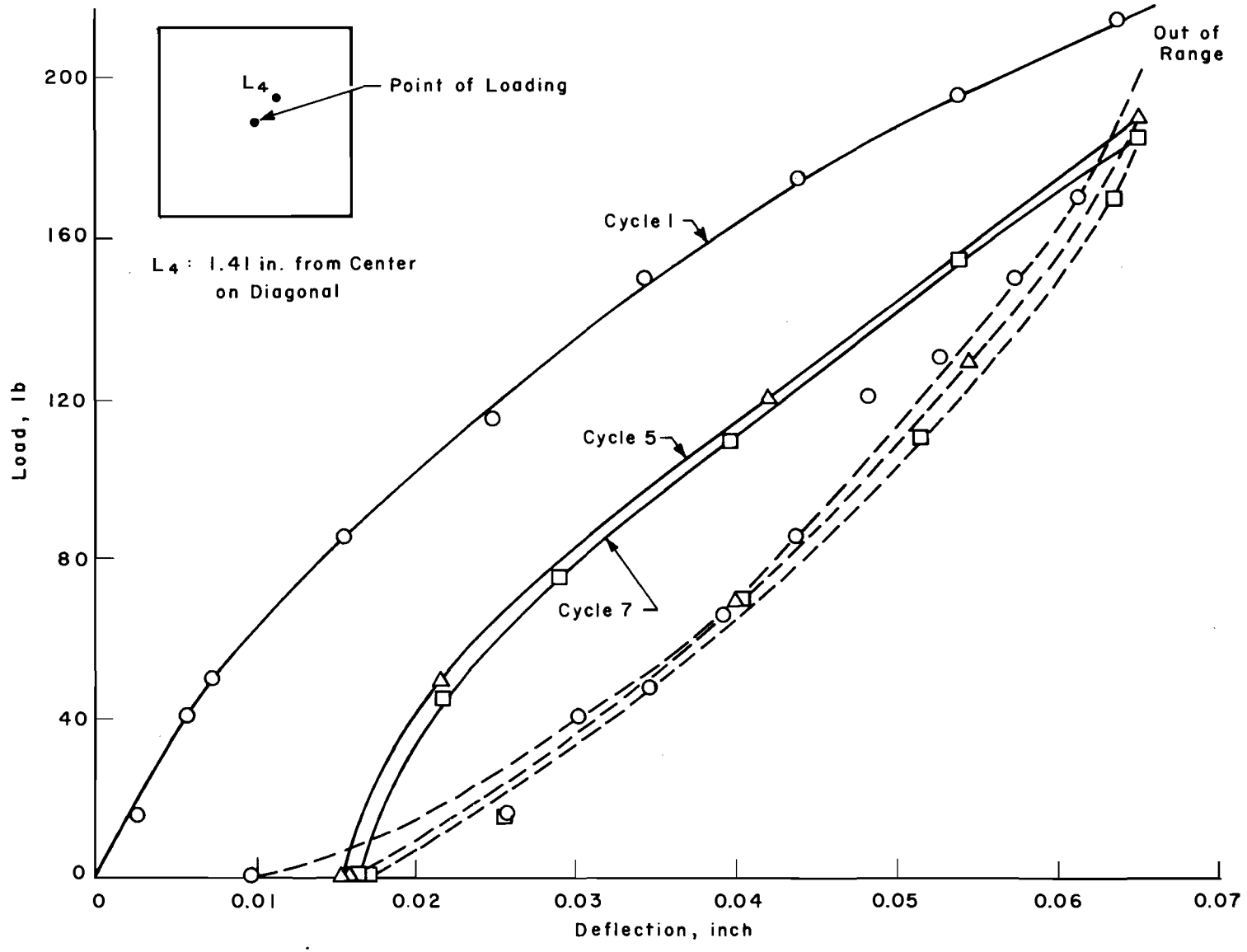

Fig 68. Load versus deflection for LVDT 4 under center cyclic load slab test (series 330).

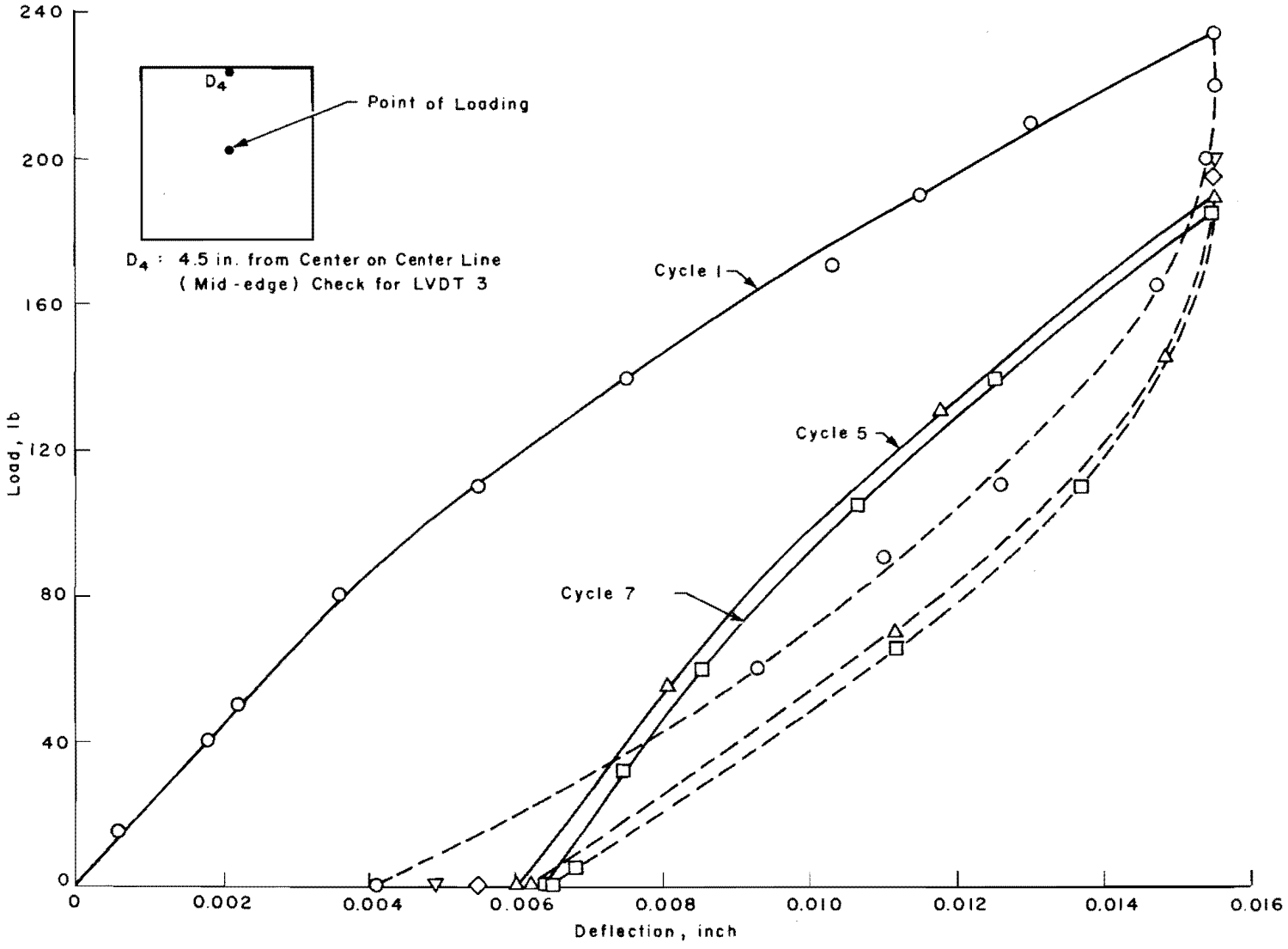

Fig 69. Load versus deflection for dial 4 under center cyclic load slab test (series 330).

TABLE 28. EXPERIMENTAL AND ANALYTICAL DEFLECTIONS FOR CENTER CYCLIC LOAD SLAB TEST (SERIES 330)

Load: 100 lb in the center

Program: DSLAB 26 (18 x 18 increments)

Type of Solution	LVDT's						Dial Gages		
	1	2*	3	4	5	6	1	4	2
Experimental — First cycle	-0.02290		-0.00420	-0.01970	-0.00730	0.00117	-0.02290	-0.00490	0.00061
Experimental — Fifth cycle	-0.02300		-0.00404	-0.02000	-0.00720	0.00173	-0.02400	-0.00410	0.00140
Experimental — Seventh cycle	-0.02300		-0.00410	-0.01990	-0.00720	0.00175	-0.02410	-0.00400	0.00143
Nonlinear q - w curve (q not reduced)	-0.02248		-0.00272	-0.01986	-0.00706	0.00616	-0.02248	-0.00272	0.00616
% Error (comparison with first cycle)	1.83		6.48	-0.70	1.04	-21.81	1.83	9.54	-24.25
Nonlinear q - w curve (q reduced 25 %)	-0.02250		-0.00270	-0.01988	-0.00705	0.00636	-0.02250	-0.00270	0.00636
% Error (comparison with seventh cycle)	2.17		6.07	0.09	0.66	-20.02	6.96	5.64	-21.41

*Test data not available.

Note: Experimental values are the net deflections for the fifth and seventh cycles.

TABLE 29. EXPERIMENTAL AND ANALYTICAL DEFLECTIONS FOR CENTER CYCLIC LOAD SLAB TEST (SERIES 330)

Load: 185 lb in the center

Program: DSLAB 26 (18 x 18 increments)

Type of Solution		LVDT's						Dial Gages		
		1	2*	3	4	5	6	1	4	2
Experimental	First cycle	-0.05240		-0.01030	-0.04850	-0.01680	0.00370	-0.05280	-0.01100	0.00314
	Fifth cycle	-0.05250		-0.00964	-0.04780	-0.01700	0.00483	-0.05310	-0.00880	0.00390
	Seventh cycle	-0.05280		-0.00980	-0.04850	-0.01730	0.00543	-0.05320	-0.00910	0.00400
Nonlinear q - w curve (q not reduced)		-0.04976		-0.00834	-0.04450	-0.01754	0.01182	-0.04976	-0.00834	0.01182
% Error (comparison with first cycle)		5.04		3.73	7.63	-1.41	15.50	5.80	5.07	16.56
Nonlinear q - w curve (q reduced 25 %)		-0.04950		-0.00788	-0.04423	-0.01702	0.01349	-0.04976	-0.00788	0.01349
% Error (comparison with tenth cycle)		6.25		3.63	8.09	0.53	15.27	6.52	2.31	17.97

*Test data not available.

Note: Experimental values are the net deflections for the fifth and seventh cycles.

and (4) the total deflection for 185 pounds in cycle 7 was approximately the same as that for 240 pounds in the first cycle.

Points on Corner

LVDT 6 and dial gage 2 were both on corners (one serving as a check on the other). Load versus deflection curves for dial 2 are shown in Fig 70 and for LVDT 6 in Appendix 5. It can be observed from these curves that (1) load stabilization was similar to that for other points; (2) curves for the fifth and seventh cycles followed each other very closely, with approximately the same slope as that of the first cycle curve; (3) in the first cycle, the corners moved down in the initial stages of loading and then started moving up, but during the fifth and seventh cycles, upward movement started from the beginning of the load; and (4) the net deflections for loads for 100 and 185 pounds (Tables 28 and 29) for the fifth and seventh cycles were greater than those for the first cycle.

Corner Loads Slab Test (Series 340)

To study the effect of cyclic loading for another important loading condition, the corner loads slab test was also continued. The load was applied at two points on the diagonal near opposite corners. The test procedure was the same as that for the center load test except that the load was cycled for 10 cycles for the maximum deflection obtained during the first cycle on dial gage 3 (corner near load). During the fifth and tenth cycles, data for load, deflection, and strain were recorded during both loading and unloading.

Deflections

Figure 71 shows the position of LVDT's, dial gages, and loads. Figure 72 shows the load deflection characteristics for dial 3 (corner near load), which was the governing point to control the maximum deflection. It can be seen that (1) slopes and shape of curves for cycles 1, 5, and 10 were approximately the same; (2) a stage of load stabilization seemed to be beginning after about 9 or 10 cycles, as the load reduced from 205 pounds in the first cycle to 178 pounds during the fifth cycle and 170 pounds during the eighth, ninth, and tenth cycles; and (3) the net deflections for 100 pounds and 170 pounds for the fifth and tenth cycles were greater than those for the first cycle (Tables 30 and 31). Note that LVDT 1 (the check for dial 3) was out of range, and, therefore, its data were not included.

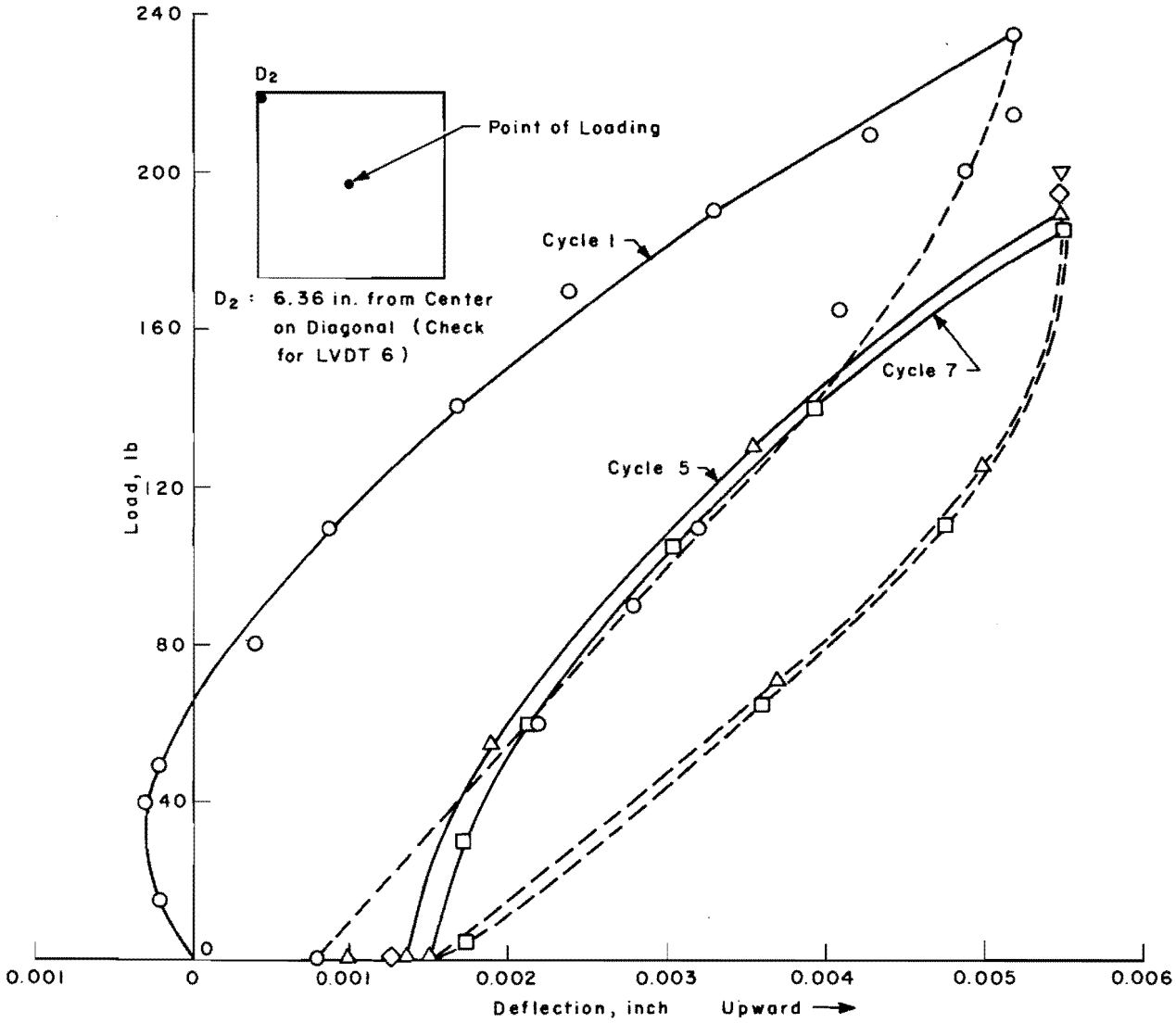

Fig 70. Load versus deflection for dial 2 under center cyclic load slab test (series 330).

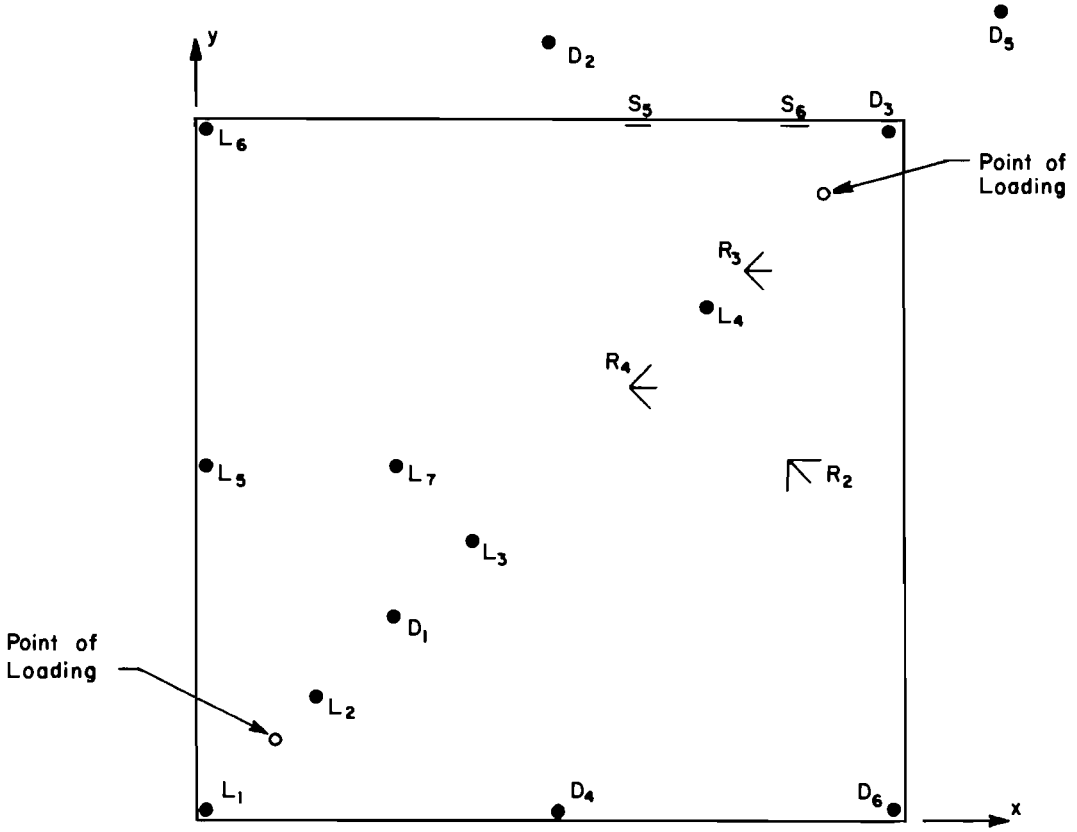

LVDT No	Distance	Dial No
L_1	6.36 in. from Center on Diagonal	D_3
L_2	4.23 " " " " "	
L_3	1.41 " " " " "	
L_4	2.83 " " " " "	D_1
L_5	4.5 " " " " Center Line	D_4
L_6	6.36 " " " " Diagonal	D_6
L_7	2.0 " " " " Center Line	
	1.0 in from Mid-edge on Soil	D_2
	2.12 " " Corner " "	D_5
Gages & Rosettes		
S_5	3.5 in. from Corner on Edge	
S_6	1.5 " " " " "	
R_2	3.0 " " Center on Center Line	
R_3	3.53 " " " " Diagonal	
R_4	1.41 " " " " "	

Fig 71. Position of loads, LVDT's, and dial gages for corner cyclic loads slab test (series 340).

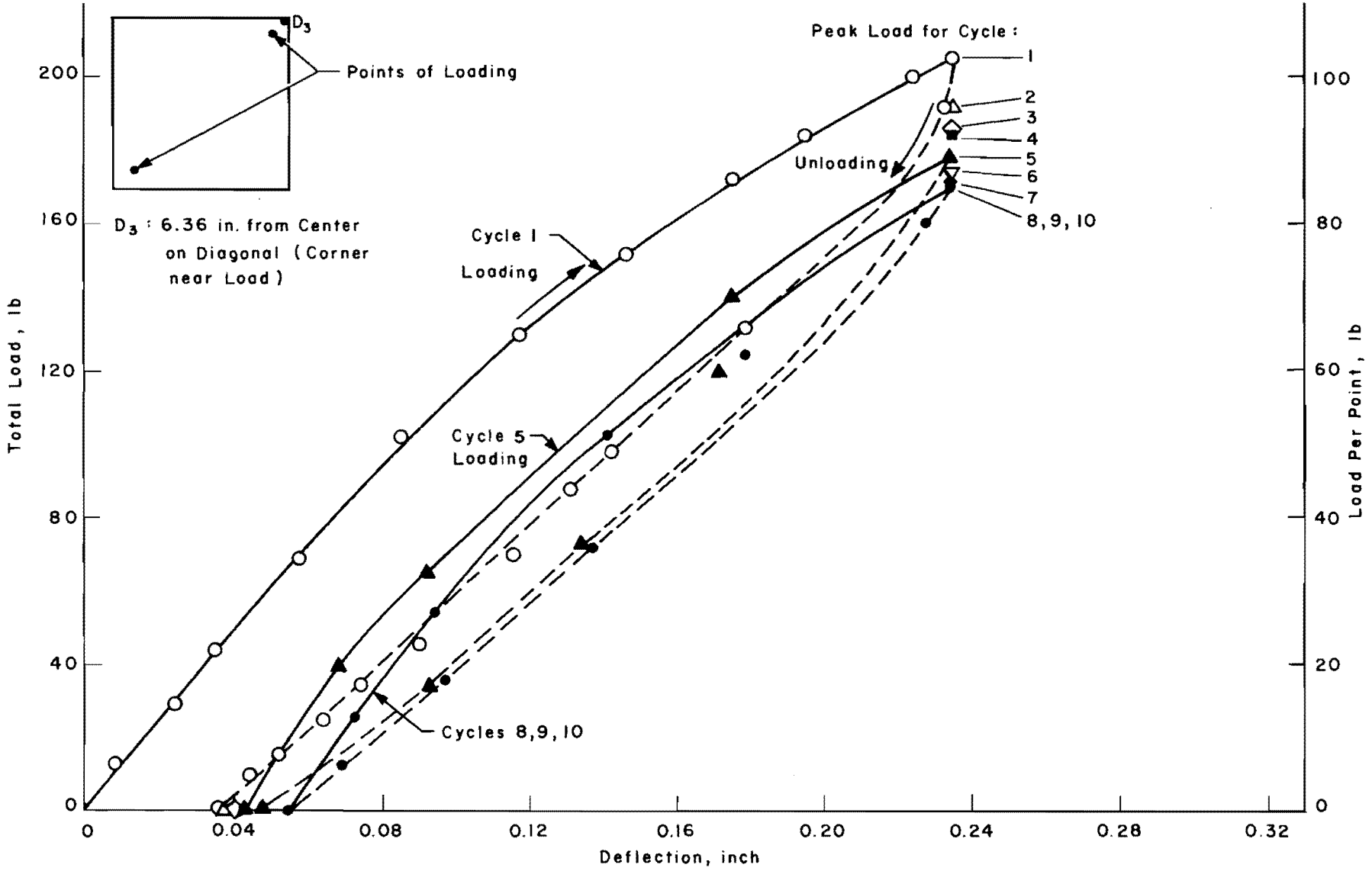

Fig 72. Load versus deflection for dial 3 under corner cyclic loads slab test (series 340).

TABLE 30. EXPERIMENTAL AND ANALYTICAL DEFLECTIONS FOR CORNER CYCLIC LOADS SLAB TEST (SERIES 340)

Load: 50 lb each point near opposite corners
(Total load = 100 lb)

Program: DSLAB 26 (18 x 18 increments)

Type of Solution	LVDT's							Dial Gages			
	1*	2	3	4	5	6	7	3	1	4	6
Experimental — First cycle		-0.04240	-0.00732	-0.01970	-0.01220	0.00690	-0.00560	-0.08350	-0.02150	-0.01280	0.00730
Experimental — Fifth cycle		-0.04300	-0.00720	-0.02640	-0.01220	0.00785	-0.00560	-0.08600	-0.02460	-0.01300	0.00730
Experimental — Tenth cycle		-0.04320	-0.00700	-0.02650	-0.01220	0.00833	-0.00600	-0.08600	-0.02460	-0.01300	0.00730
Nonlinear q - w curve (q not reduced)		-0.03774	-0.00403	-0.01610	-0.01090	0.00712	-0.00324	-0.07810	-0.01610	-0.01090	0.00712
% Error (Comparison with first cycle)		5.58	0.39	4.31	1.56	0.27	2.83	6.47	6.47	2.28	0.20
Nonlinear q - w curve (q reduced 25 %)		-0.03844	-0.00417	-0.01646	-0.00990	0.01544	-0.00302	-0.07950	-0.01646	-0.00990	0.01544
% Error (Comparison with tenth cycle)		5.53	3.29	11.67	2.67	8.27	3.46	7.56	9.81	3.60	9.47

*Out of range.

Note: Experimental values are the net deflections for the fifth and tenth cycles.

TABLE 31. EXPERIMENTAL AND ANALYTICAL DEFLECTIONS FOR CORNER CYCLIC LOADS SLAB TEST (SERIES 340)

Load: 85 lb each point near opposite corner
(Total load = 170 lb)

Program: DSLAB 26 (18 x 18 increments

Type of Solution		LVDT's							Dial Gages			
		1*	2	3	4	5	6	7	3	1	4	6
Experimental	First cycle		-0.08150	-0.01620	-0.04320	-0.02500	0.01200	-0.00965	-0.17400	-0.04550	-0.02480	0.01370
	Fifth cycle		-0.08950	-0.01600	-0.05170	-0.02420	0.01325	-0.00975	-0.17700	-0.05050	-0.02500	0.01370
	Tenth cycle		-0.09330	-0.01640	-0.05400	-0.02460	0.01400	-0.01015	-0.18100	-0.05400	-0.02600	0.01420
Nonlinear q - w curve (q not reduced)			-0.08880	-0.01358	-0.04133	-0.02913	0.01748	-0.01149	-0.17630	-0.04133	-0.02913	0.01748
% Error (Comparison with first cycle)			-4.19	1.57	1.07	2.37	3.15	1.06	1.32	2.40	2.49	2.17
Nonlinear q - w curve (q reduced 25 %)			-0.09052	-0.01319	-0.04173	-0.02581	0.03873	-0.01011	-0.18100	-0.04173	-0.02581	0.03873
% Error (Comparison with tenth cycle)			1.54	1.77	9.54	0.67	13.66	0.02	0.00	6.78	0.10	13.55

*Out of range.

Note: Experimental values are the net deflections for the fifth and tenth cycles.

The effect of cycling to control deflection on dial gage 3 was studied for three areas, "interior of the slab," "mid-edge," and "unloaded corner."

Points in the Interior of the Slab. Points covered in this area were LVDT's 2, 4 (with dial gage 1 as a check), and 3, which were 4.23, 2.83, and 1.41 inches, respectively, from the center on the diagonal, and LVDT 7, which was 2 inches from the center on the center line. Figure 73 shows load deflection curves for LVDT 2. It can be seen from this plot that

(1) A stage of load stabilization seemed to begin after 9 or 10 cycles, which was similar to that for dial 3.

(2) Shapes and slopes of curves for cycles 1, 5, and 10 were identical.

(3) The net deflections obtained during the fifth and tenth cycles for 100 and 170 pounds were greater than those for the first cycle (Tables 30 and 31).

Similar observations could be made from plots for LVDT 4, dial 1, LVDT 3, and LVDT 7, which are given in Appendix 5.

Points on the Mid-Edge. Figure 74 shows the load deflection data for LVDT 5. The tendency for load to stabilize after 9 or 10 cycles; for slopes and shapes of first, fifth, and tenth cycles to be identical; and for the net deflections for fifth and tenth cycles to be greater than those for the first cycle (Tables 30 and 31) was similar to that for points in the interior of the slab. These observations could also be made from load deflection data of dial gage 4 (the check for LVDT 5), from the plot, as given in Appendix 5 and Tables 30 and 31.

Points on the Unloaded Corner. Figure 75 shows the load deflection curves for LVDT 6. It can be seen from this plot that the deflections were upwards and quite small and the curves during loading for cycles 1, 5, and 10 were approximately linear. The observations of a tendency for the load to stabilize and the net deflections for fifth and tenth cycles to be greater than those for the first cycle (Tables 30 and 31), were similar to those for other points. Dial gage 6 served as a check for LVDT 6, and these observations could also be made from the plot as given in Appendix 5 and Tables 30 and 31.

Stresses

Principal stresses were calculated from strains of the rosettes during loading and unloading for the fifth and tenth cycles, as was done in Chapter 5

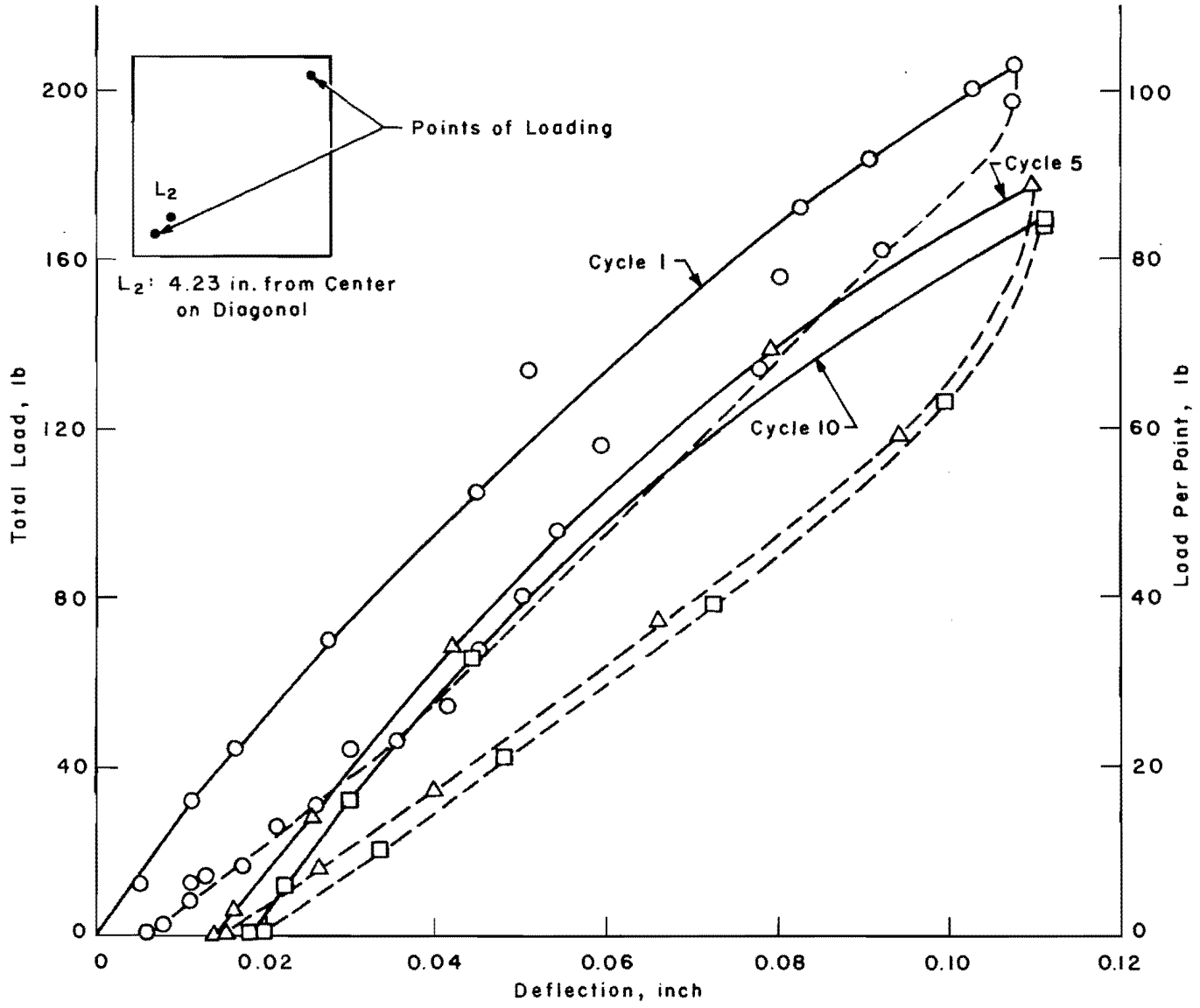

Fig 73. Load versus deflection for LVDT 2 under corner cyclic loads slab test (series 340).

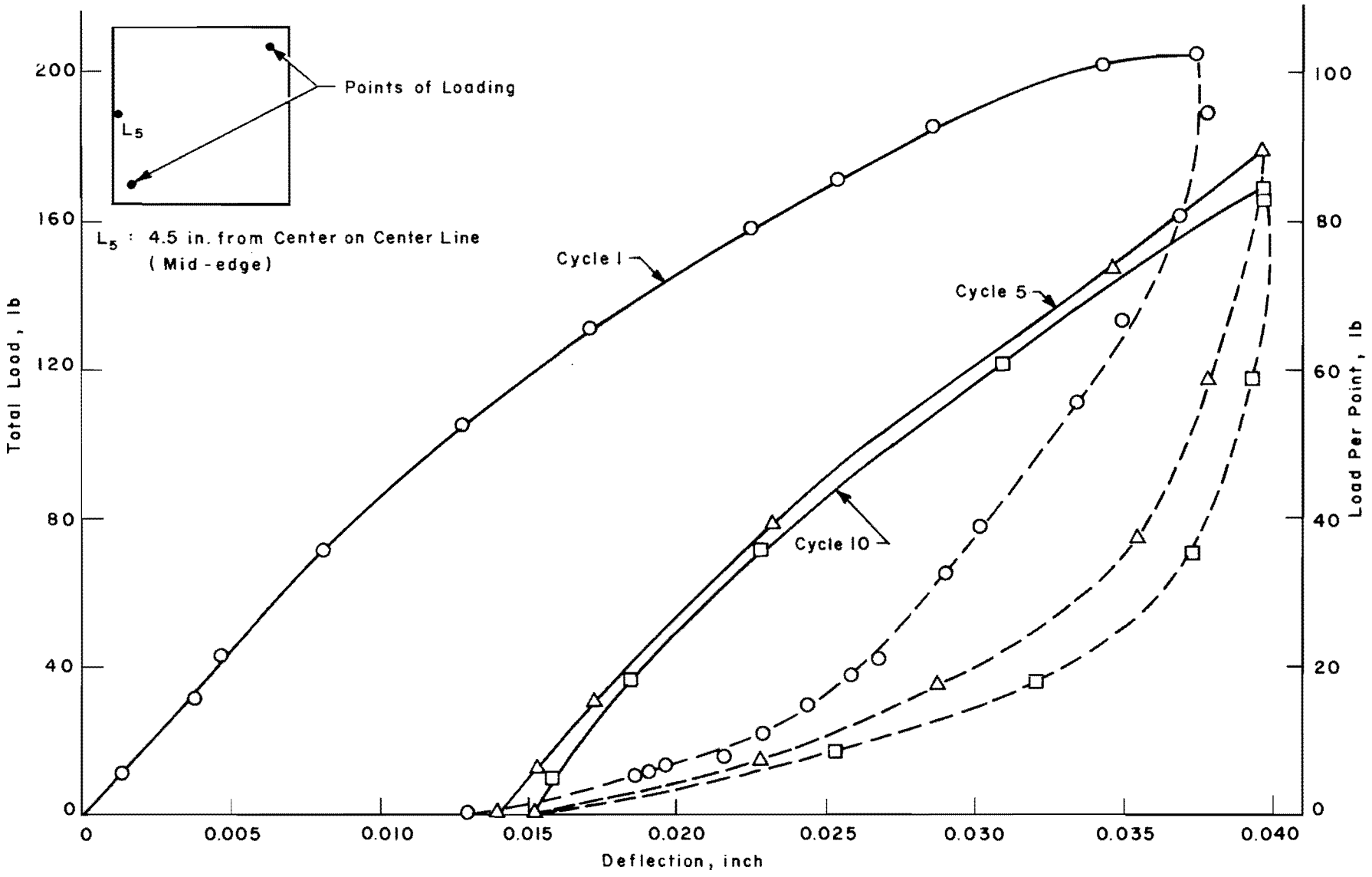

Fig 74. Load versus deflection for LVDT 5 under corner cyclic loads slab test (series 340).

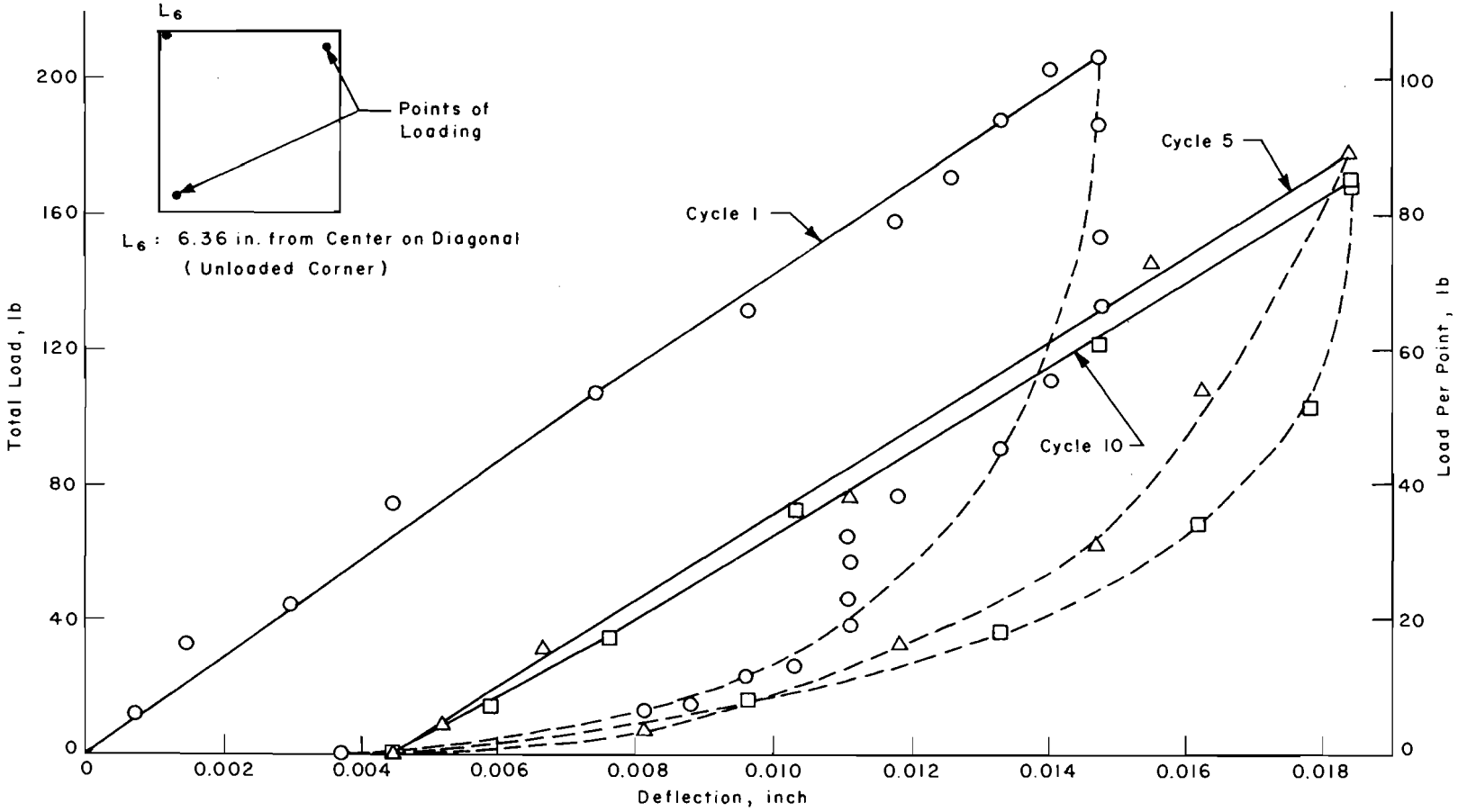

Fig 75. Load versus deflection for LVDT 6 under corner cyclic loads slab test (series 340).

for the first cycle. The method of these computations is described in Appendix 3. Figure 76 shows the load versus principal stress curves for rosette 3 and the net principal stresses for total loads of 100 and 170 pounds for cycles 1, 5, and 10 are given in Tables 32 and 33. From Fig 76 and Tables 32 and 33 it can be seen that the observations that the slopes and shapes for the fifth and tenth cycles were approximately the same as those for the first cycle, that there was a tendency for the load to stabilize after 9 or 10 cycles, and that the net principal stresses for the fifth and tenth cycles tended to be greater than those for the first cycle were similar to observations for deflections. The plots for rosettes 2 and 4 as given in Appendix 5, and the net principal stresses in Tables 32 and 33, indicated the same effects of cyclic loading as for rosette 3.

Stresses along the edge were calculated from strains of strain gages 5 and 6, fixed along the edge for the fifth and tenth cycles, as described in Appendix 3. Figure 77 shows load versus edge stresses for gage 6, and the net stresses for total loads of 100 and 170 pounds for cycles 1, 5, and 10 are given in Tables 32 and 33. The tendency of curves of the fifth and tenth cycles to follow those of the first cycle, for the load to stabilize, and for the net stresses for fifth and tenth cycles to be greater than those for the first cycle was similar to that for principal stresses. The data for strain gage 5, as given in Appendix 5 and Tables 32 and 33, also indicated these effects of cycling loading.

Comparison of Analytical and Experimental Solutions for Cyclic Data

Lee (Ref 21) discussed two methods to represent soil for repetitive loading: (1) converting the stress-strain characteristics of the soil obtained by testing the soil samples under repetitive loads to the pressure-deflection relations using a method similar to Skempton's criteria and (2) performing plate load tests under repetitive loads. Both methods can be useful if testing of soil samples or rigid plates can be done under repetitive loads by elaborate equipment. In the absence of such tests, a preliminary attempt can be made to model the soil for cycling loading on the basis of slab tests results.

From the test data discussed previously, the effects of cyclic loading can be summarized. First, a stage of stabilization takes place after a few cycles. Second, the net deflections and stresses for a particular load in

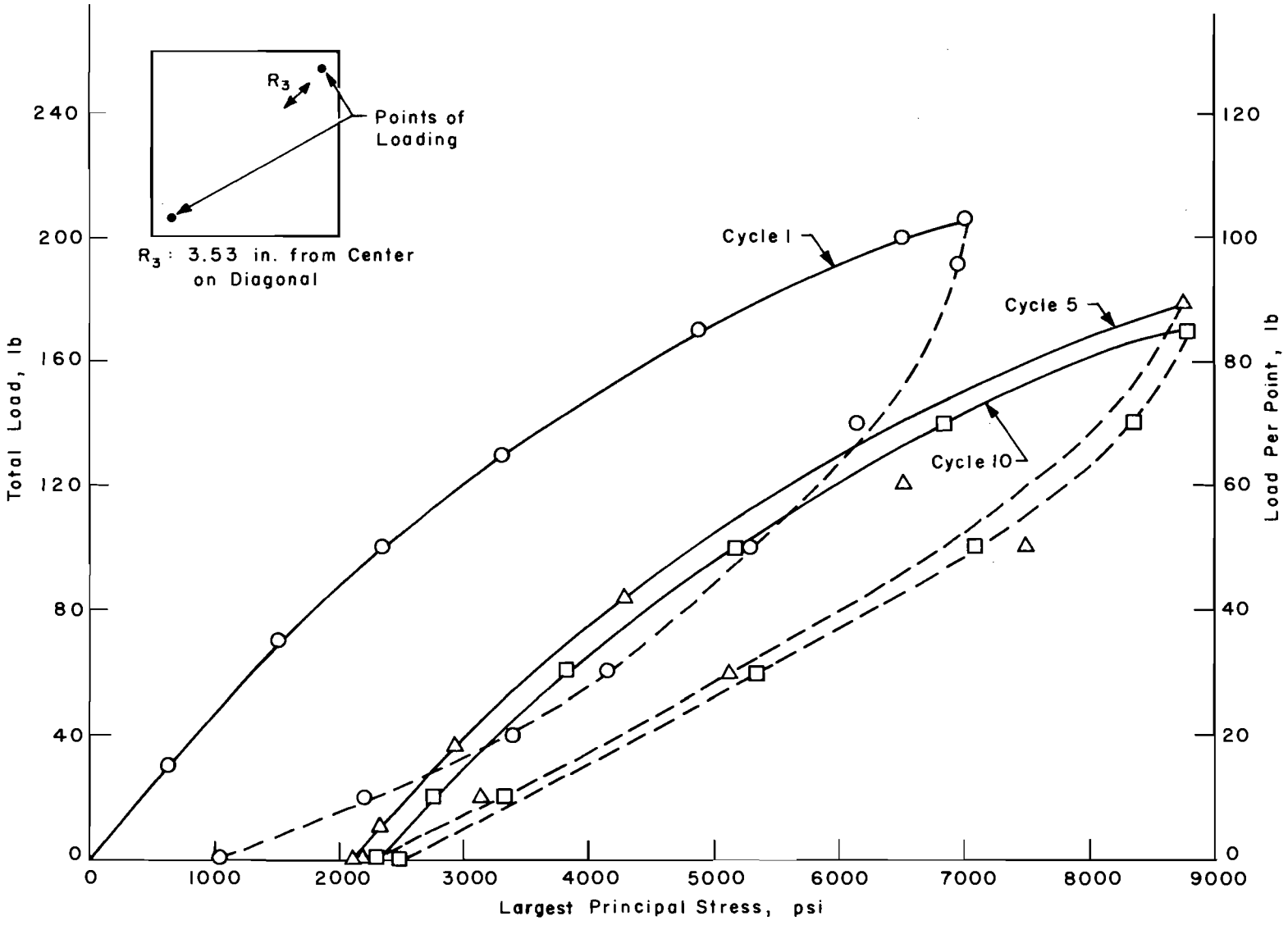

Fig 76. Load versus largest principal stresses for rosette 3 under corner cyclic loads slab test (series 340).

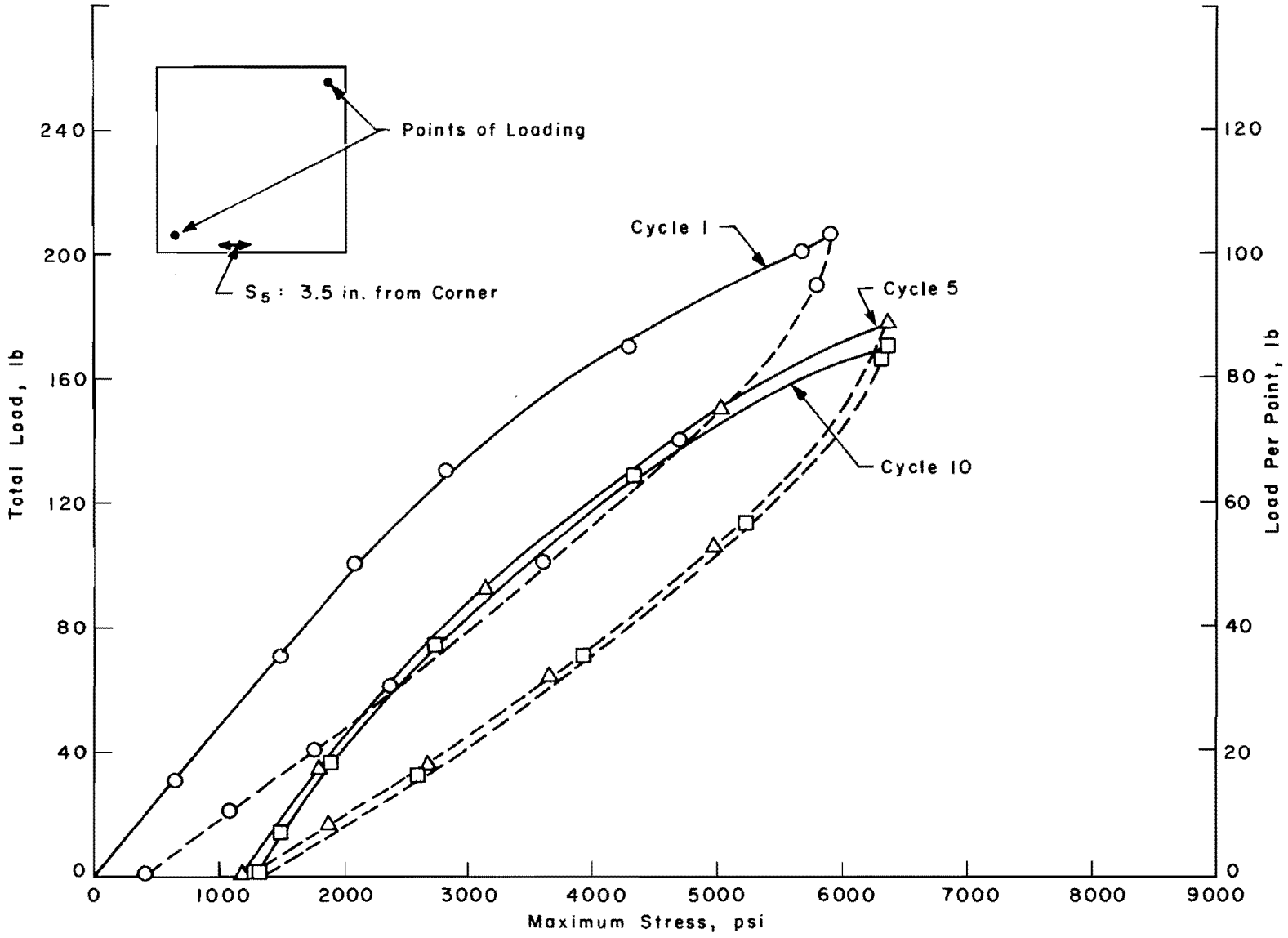

Fig 77. Load versus stresses along edge for strain gage 6 under corner cyclic loads slab test (series 340).

TABLE 32. EXPERIMENTAL AND ANALYTICAL LARGEST PRINCIPAL STRESSES AND EDGE STRESSES FOR CORNER CYCLIC LOADS SLAB TEST (SERIES 340)

Load: 50 lb each point (total load = 100 lb)

Program: DSLAB 26 (18 x 18 increments)

Type of Solution		Rosette 2	Rosette 4	Rosette 3	Strain 5	Strain 6
		Largest Stress	Largest Stress	Largest Stress	Stress Along Edge	Stress Along Edge
Experimental	First cycle	2714.00	3313.00	2389.00	2074.00	1209.00
	Fifth cycle	2893.00	3328.00	2662.00	2205.00	1233.00
	Tenth cycle	2914.00	3386.00	2667.00	2228.00	1245.00
Nonlinear q - w curve (q not reduced)		2732.00	2849.00	2753.00	2514.00	1126.00
% Error (Comparison with first cycle)		-0.54	14.01	-10.99	-13.28	2.51
Nonlinear q - w curve (q reduced 25 %)		2670.00	2816.00	2743.00	2330.00	1208.00
% Error (Comparison with tenth cycle)		7.21	16.83	-2.24	3.01	1.09

Note: Experimental values are the net stresses for the fifth and tenth cycles.

TABLE 33. EXPERIMENTAL AND ANALYTICAL LARGEST PRINCIPAL STRESSES AND EDGE STRESSES FOR CORNER CYCLIC LOADS SLAB TEST (SERIES 340)

Load: 85 lb each point (total load = 170 lb)

Program: DSLAB 26 (18 x 18 increments)

Type of Solution		Rosette 2	Rosette 4	Rosette 3	Strain 5	Strain 6
		Largest Stress	Largest Stress	Largest Stress	Stress Along Edge	Stress Along Edge
Experimental	First cycle	4930.00	6542.00	6001.00	4327.00	2252.00
	Fifth cycle	6111.00	7119.00	5618.00	4682.00	2477.00
	Tenth cycle	6515.00	7539.00	6116.00	5121.00	2596.00
Nonlinear q - w curve (q not reduced)		6025.00	6432.00	5307.00	4704.00	2370.00
% Error (Comparison with first cycle)		16.74	16.81	10.61	5.76	1.80
Nonlinear q - w curve (q reduced 25 %)		5940.00	6386.00	5322.00	4278.00	2580.00
% Error (Comparison with tenth cycle)		7.63	15.29	10.53	11.18	0.21

Note: Experimental values are the net stresses for the fifth and tenth cycles.

stabilized stage are greater, in general, than those in the first cycle. Based on these observations, an attempt was made to obtain the analytical solution by modifying the nonlinear representation of the soil from 9-inch-diameter-plate load test data by the following methods:

(1) Adjust the nonlinear $q - w$ curve by reducing $q_{ultimate}$ by a certain amount so that analytical solutions thus obtained agree favorably with the experimental results.

(2) From the test data for various LVDT's and dial gages, the permanent set after a particular cycle is known. If the entire slab area is observed by a sufficient number of such deflection gages, areas of similar behavior can be chosen. Areas of such nature for center load slab test (series 330) can be divided as shown in Fig 78(a). An initial offset can be given on the $q - w$ curves, depending on the particular area, as shown in Fig 78(b). Solutions can then be obtained by inputting the $q - w$ curves with different offsets for the various areas. Reductions in $q_{ultimate}$ as suggested in method 1 can be introduced further until a better agreement exists between the analytical and experimental solutions.

The second method was tried for center load slab test (series 330) with different offsets on the $q - w$ curves of areas as shown in Fig 78 without reducing $q_{ultimate}$. With the input of curves of such highly nonlinear nature, with a different offset at every station, the results obtained were not symmetric. This approach was not tried any further. A thorough study to solve such highly nonlinear problems is greatly needed.

Method 1 was tried with the input of the $q - w$ curve, as shown in Fig 79 with an arbitrary reduction of 25 percent in $q_{ultimate}$. Because the tension was considered to be fully effective up to ten cycles, no modification was done on the tension side. Solutions were obtained for loads of 100 and 185 pounds for center load slab test (series 330) and 100 and 170 pounds (50 and 85 pounds at each point) for corner loads slab test (series 340).

Comparison

A comparison of net deflections and stresses was made the same way as for cycle 1, described in Chapter 5. For the static case, i.e., for cycle 1, percentage errors were calculated using analytical solutions obtained using the $q - w$ curve for the 9-inch-diameter plate load test data without any reduction in $q_{ultimate}$. For cyclic loading, percentage errors were calculated for the last cycle, using the modified $q - w$ curve.

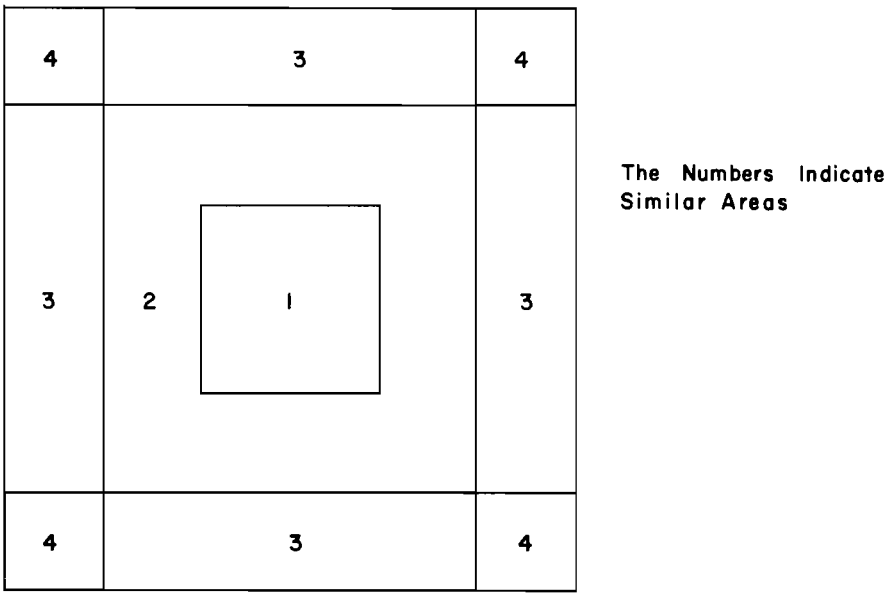

(a) Division of areas for soil representation to be modified for center load slab test.

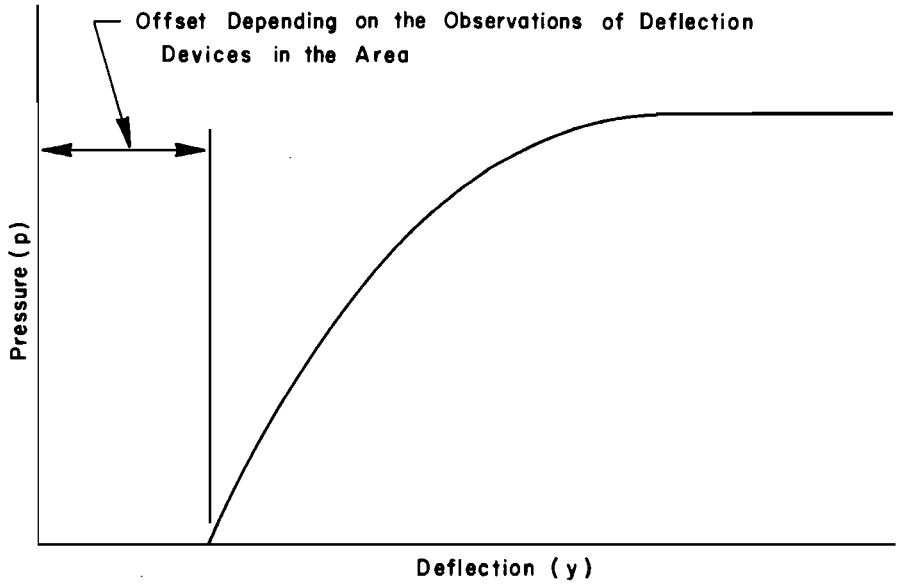

(b) Method of offsetting the nonlinear curves.

Fig 78. Method of modifying soil representation for cyclic loads.

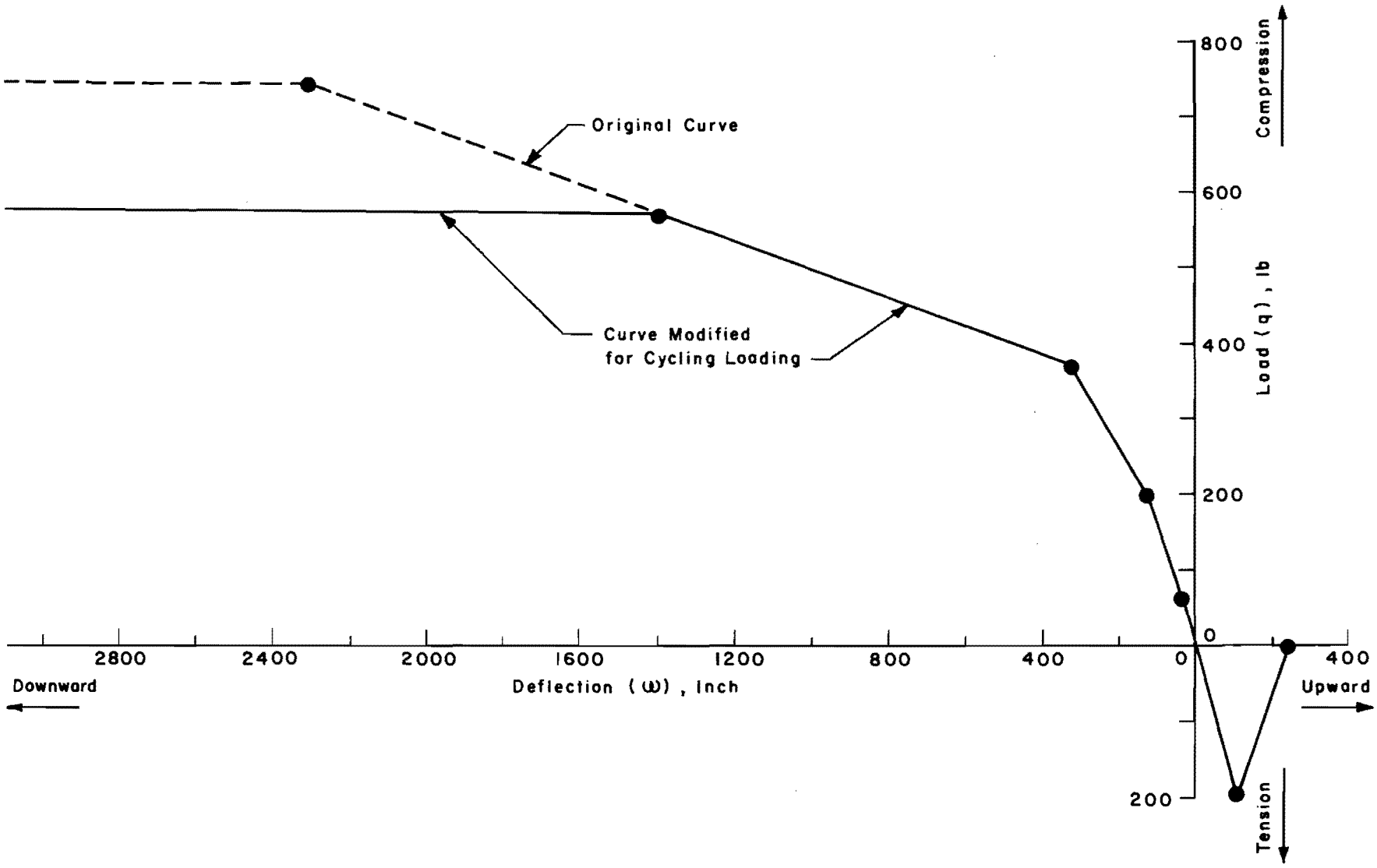

Fig 79. Nonlinear soil representation modified for cyclic loading.

For center load slab test (series 330), a comparison of net deflections for center loads of 100 and 185 pounds for cycles 1 and 7 is given in Tables 28 and 29. It is observed that percentage errors for cycle 7 compared well with those of cycle 1 at most points.

For corner loads slab test (series 340) a comparison of net deflections for loads of 100 and 170 pounds (50 and 85 pounds at each point) for cycles 1 and 10 is given in Tables 30 and 31. The percentage errors for cycles 1 and 10 are quite comparable at most points; at a few points the comparison for cycle 10 showed greater discrepancy. A comparison of net principal stresses and net stresses along the edge, as given in Tables 32 and 33, shows that the percentage errors obtained for cycles 1 and 10 were quite comparable.

Observations on the Cycling Behavior

From the cycling test data and their comparison with the analytical solution obtained by modifying the nonlinear support representation, the following observations can be made:

(1) The effect of cyclic loading the slab for the maximum deflection or a constant deflection was that, first, a stage of load stabilization seemed to begin after a few cycles, and such load stabilization took place earlier if the load were cycled for a deflection less than the maximum obtained during the first cycle. Second, the slopes and shapes of curves for deflections and stresses for cycle 1 and for those obtained in the stabilized stage after cycling were approximately the same. Third, the net deflections and stresses after cycling were, in general, greater than those for the first cycle.

(2) By modifying the nonlinear support representation based on a lower bounds equilibrium response, it is possible to obtain an analytical solution for the slab under cyclic loads comparable to the experimental results. This solution is a tool by which various soil representations can be investigated and fitted to the data and points out how even crude representations of a very complex phenomenon can produce useful engineering answers. It is possible that other methods can be used to obtain the nonlinear support characteristics, for example, plate load tests or triaxial tests under cyclic loads.

CHAPTER 7. SUMMARY

Conclusions

The experimental evidence in this report shows that discrete-element solution techniques provide extremely good results in predicting plate and slab stresses and deflections and can be useful tools in the analysis of bridge slabs and pavements. The following specific conclusions can be drawn regarding the results.

For linearly elastic plates on rigid supports under two different loading conditions with or without discontinuities, the analytical solutions agree with the experimental data within 4 percent of the maximum measured value for deflections and within 6 percent for principal stresses. For linearly elastic plates the discrepancy for deflections is within 2 percent for the isotropic plate and within 5 percent for the orthotropic plate.

For a slab-on-foundation problem, the soil support can be satisfactorily represented as a Winkler foundation, by linear and nonlinear springs as determined by plate load tests or from stress-strain data for the soil. Using such soil representation for a linearly elastic slab resting on clay soil and tested under two different loading configurations good correlation exists for small loads between experimental and analytical results for deflections and stresses using linear springs for the soil. However, for loads producing larger deflections on the slab, nonlinear springs are required. The maximum discrepancy is near the periphery of the slab, possibly because the effect of the soil outside the perimeter of the slab is ignored.

Cyclic loading on the slab for the maximum or a constant deflection seems to begin to stabilize the load after a few cycles. Then the shapes and slopes of curves for deflections and stresses follow approximately those for the first cycle, and the net deflections and stresses are greater than those for the first cycle. It was also observed that by modifying the support representation, it was possible to model the soil for cyclic loading based on a lower bound equilibrium response and obtain analytical solutions comparable to the experimental results.

Suggestions for Future Work

From the analysis of the slab test, it was observed that the maximum discrepancy between the measured and DSLAB solutions was at points on the periphery of the slab. DSLAB solutions using both linear and nonlinear soil springs should, therefore, be modified by coupled spring model or other methods to consider the effect of the soil outside the perimeter of the slab.

The discrete-element solutions investigated herein do not take into account the friction between the slab and the soil, temperature and environmental effects, and nonlinear slab properties. The completion of current work to include these effects will help to model the actual pavements, and a study of full-scale prototypes would then be desirable to check the analytical solutions.

Development of methods to represent soil for cyclic loading is needed and more tests are required to evaluate such representation. The inclusion of the repetitive and dynamic behavior of soil will also be useful in further understanding of actual pavement behavior.

Application of Results

This report provides more confidence in the use of the discrete-element solution for plates, isotropic or orthotropic, with or without discontinuities, and under different load and support conditions, if the plate properties are determined accurately and the deflections are small.

For the slab-on-foundation problem, the tests confirm that the discrete-element solutions can be used with confidence, provided linear springs, based on the Winkler foundation, are limited to small loads. The finding that nonlinear springs are required for larger loads and deflections is significant. These linear and nonlinear soil springs can be determined by plate load tests or from stress-strain data for the soil. A plate load test may not always be feasible in practice, and laboratory testing of the saturated clay sample under triaxial compression test is sometimes recommended.

The important application of this work will involve the future use of nonlinear support springs in the analysis of slabs-on-foundation. Further application will be the continuation of the preliminary cyclic loading tests reported herein.

REFERENCES

1. Barkan, D. D., Dynamics of Bases and Foundations, McGraw-Hill, New York, 1962.

2. Biot, M. A., "Bending of an Infinite Beam on an Elastic Foundation," Journal of Applied Mechanics, Vol 4, 1937, pp A1-A7.

3. "Bituminous Materials, Soils, Skid Resistance," American Society for Testing Materials Standards, Part 11, 1968.

4. Budd Instrument Company, Catalog (general information section).

5. Cheung, Y. K., and D. K. Nag, "Plates and Beams on Elastic Foundations - Linear and Non-Linear Behavior," Geotechnique, Vol 18, 1968, pp 250-260.

6. Chopane, B. B., "Evaluation of Soil Modulus in Horizontal and Vertical Directions for Cohesionless Soils," Master's Thesis, The University of Roorkee, Roorkee, India, 1965.

7. Clough, Ray, "The Finite-Element Method in Plane Stress Analysis," Proceedings of the Second Conference on Electronic Computation, American Society of Civil Engineers, Pittsburgh, Pennsylvania, 1960.

8. "Data Logging System Instruction Manual for Model DAS-1," Honeywell, Inc., San Diego, California.

9. Desai, C. S., "Solution of Stress-Deformation Problems in Soil and Rock Mechanics using Finite Element Method," Ph.D. Dissertation, The University of Texas at Austin, August 1968.

10. "Electronics for Measurement, Analysis, and Computation," Hewlett-Packard, Inc., Palo Alto, California, 1968.

11. Endres, Frank L., "DSLAB 19 - Improved Version of DSLAB 5," unpublished development at Center for Highway Research, The University of Texas, Austin, November 1967.

12. Foil Strain Gage Specification, Bulletin 101-3, BLH Electronics, Inc., December 1966.

13. Gazzaly, Osman I., and Raymond F. Dawson, "Laboratory Stress-Deformation Characteristics of Soils under Static Loading," a report to National Aeronautics and Space Administration prepared by the Department of Civil Engineering, The University of Texas, Austin, January 1966.

14. Herrmann, Leonard R., "Finite-Element Bending Analysis for Plates," Journal of the Engineering Mechanics Division, Vol 93, No. EM5, Proceedings of the American Society of Civil Engineers, 1967.

15. Hogg, A. H. A., "Equilibrium of a Thin Plate, Symmetrically Loaded Resting on Air Elastic Foundation of Infinite Depth," Philosophical Magazine, Series 7, Vol 25, 1938, pp 576-582.

16. Holl, D. L., "Thin Plates on Elastic Foundations," Proceedings, Fifth International Congress for Applied Mechanics, Cambridge, Massachusetts, 1938, John Wiley & Sons, New York, 1939, pp 71-74.

17. Hopmann, N. R., II, N. J. Huffington, Jr., and L. S. Magness, "A Study of Orthogonally Stiffened Plates," Journal of Applied Mechanics, ASME Transactions, September 1956.

18. Huffington, N. J., Jr., and V. A. Blacksburg, "Theoretical Determination of Rigidity Properties of Orthogonally Stiffened Plates," Journal of Applied Mechanics, ASME Transactions, March 1956.

19. Hudson, W. Ronald, and Hudson Matlock, "Discontinuous Orthotropic Plates and Slabs," Research Report No. 56-6, Center for Highway Research, The University of Texas, Austin, May 1966.

20. Kelly, Allan E., "Dynamic Analysis of Discrete-Element Plates on Nonlinear Foundation," (DSLAB 26), Ph.D. Dissertation, The University of Texas at Austin, January 1970.

21. Lee, Clyde E., "The Determination of Pavement Deflections under Repeated Load Applications," Ph.D. Dissertation, The University of California, Berkley, California, 1961.

22. Lewis, K. H., and M. E. Harr, "Analysis of Concrete Slabs on Ground and Subjected to Warping and Moving Loads," Proceedings, Forty-Eighth Annual Meeting of the Highway Research Board, January 1969.

23. Matlock, Hudson, and T. A. Haliburton, "A Finite-Element Method of Solution for Linearly Elastic Beam-Columns," Research Report No. 56-1, Center for Highway Research, The University of Texas, Austin, 1965.

24. Matlock, Hudson, "Soil-Structure Interaction," C.E.394.2 class notes, The University of Texas, Austin, Spring 1967.

25. "Micro-Measurements Catalog 91," Micro-Measurements, Romulus, Michigan, August 1968.

26. "Model Plate and Slab Tests Data," Center for Highway Research, The University of Texas at Austin, author's working files.

27. Pahl, P. J., and K. Soosaar, "Structural Models for Architectural and Engineering Education," R64-3, Department of Civil Engineering, Massachusetts Institute of Technology, Cambridge, February 1964, pp 239-250.

28. Panak, John, "DSLAB 21 - Preliminary Version of DSLAB 30," unpublished development at Center for Highway Research, The University of Texas at Austin, March 1968.

29. Panak, John J., and Hudson Matlock, "A Discrete-Element Method of Multiple-Loading Analysis for Two-Way Bridge Floor Slabs," (DSLAB 30), Research Report No. 56-13, Center for Highway Research, The University of Texas at Austin, August 1968.

30. Pearre, Charles M. III, and W. Ronald Hudson, "A Discrete-Element Solution of Plates and Pavement Slabs Using a Variable-Increment-Length Model," Research Report No. 56-11, Center for Highway Research, The University of Texas at Austin, July 1968.

31. Perry, C. C., and H. R. Lissner, The Strain Gage Primer, McGraw-Hill, New York, 1962.

32. Pickett, G., and G. H. Nay, "Influence Charts for Concrete Pavements," Transactions, Vol 116, American Society of Civil Engineers, 1951, pp 49-73.

33. Pickett, G., M. E. Raville, W. C. Janes, and F. J. MacCormick, "Deflections Moments and Reactive Pressures for Concrete Pavements," Bulletin No. 65, Kansas State College, October 15, 1951.

34. Porter, D. T., "Load Test of a Model Reinforced Concrete Cylindrical Shell Designed by Ultimate Strength," Master's Thesis, The University of Texas, Austin, 1968.

35. Radhakrishnan, Narayanaswamy, "Solution of Some Plane Strain Problems in Soil Mechanics Using the Method of Finite Elements," Ph.D. Dissertation, The University of Texas at Austin, May 1969.

36. Reese, Lymon C., Discussion on paper "Soil Modulus for Laterally Loaded Piles by B. McClelland and J. A. Focht, Transactions, Vol 123, Proceedings of the American Society of Civil Engineers, 1958.

37. Reese, Lymon C., "Soil-Structure Interaction," C.E.394.1 class notes, The University of Texas, Austin, Fall 1966.

38. Reichmuth, Donald R., Robin P. Stagg, David P. Womack, and William R. Cox, "A Study of Soil-Spacecraft Interaction During Impact," a report to National Aeronautics and Space Administration prepared by the Department of Civil Engineering, The University of Texas, Austin, December 1966.

39. Siddiqi, Qaiser S., "Experimental Evaluation of Subgrade Modulus and its Application for Model Slab Studies," M.S. Thesis, The University of Texas at Austin, January 1970.

40. Skempton, A. W., "The Bearing Capacity of Clays," Building Research Congress, 1951.

41. "Small Scale Model Study to Determine Minimum Horizontal Dimensions for Infinite Slab Behavior," Technical Report No. 4-32, Ohio River Division Laboratories, U. S. Army Corps of Engineers, Cincinnati, Ohio, July 1964.

42. Spangler, M. G., Soil Engineering, Internal Textbook, Co., Scranton, Pennsylvania, 1951.

43. Stelzer, C. Fred, Jr., and W. Ronald Hudson, "A Direct Computer Solution for Plates and Pavement Slabs," (DSLAB 5), Research Report No. 56-9, Center for Highway Research, The University of Texas, Austin, 1967.

44. Terzaghi, K., Theoretical Soil Mechanics, John Wiley and Sons, New York, 1943.

45. Terzaghi, K., "Evaluation of Coefficients of Subgrade Reaction," Geotechnique, Vol 5, 1955, pp 297-326.

46. Timoshenko, S., Theory of Elasticity, McGraw-Hill, New York, 1934.

47. Timoshenko, S., and S. Woinowsky-Krieger, Theory of Plates and Shells, 2nd Edition, McGraw-Hill, New York, 1959.

48. Troitsky, M. S., Orthotropic Bridges Theory and Design, The James F. Lincoln Arc Welding Foundation, Cleveland, 1967.

49. Tshebotarioff, G. P., E. R. Ward, and A. A. DePhillippe, "The Tensile Strength of Disturbed and Recompacted Soils," Proceedings, Third International Conference on Soil Mechanics and Foundations Engineering, Switzerland, Vol I, 1953, pp 207-212.

50. Vesic, A. S., and S. K. Saxena, "Analysis of Structural Behavior of Road Test Rigid Pavements," Project Report 1-4(1), National Cooperative Highway Research Programs, School of Engineering, Duke University, 1968.

51. Westergaard, H. M., "Analytical Tools for Judging Results of Structural Tests of Concrete Pavements," Public Roads, Vol 14, No. 10, 1933.

52. Westergaard, H. M., "Computation of Stresses in Concrete Roads," Proceedings, Fifth Annual Meeting of the Highway Research Board, 1926.

53. Westergaard, H. M., "New Formulas for Stresses in Concrete Pavements of Airfields," Proceedings, Vol 73, No. 5, American Society of Civil Engineers, May 1947.

54. Westergaard, H. M., "Stresses in Concrete Pavements Computed by Theoretical Analysis," Public Roads, Vol 7, No. 2, April 1926.

55. Winkler, E., "Die Lehre von Elastegatat und Festigkeit" (On Elasticity and Fixity), Prague, 1867, pp 182-184.

56. Zienkiewicz, O. C., and Y. K. Cheung, The Finite-Element Method in Structural and Continuum Mechanics, McGraw-Hill, New York, 1967.

APPENDICES

APPENDIX 1

DETERMINATION OF PLATE AND SLAB PROPERTIES

APPENDIX 1. DETERMINATION OF PLATE AND SLAB PROPERTIES

Aluminum Plate

Tension Test

A 2 by 18 by 1/4-inch-thick strap was tested under tension. Longitudinal and transverse strains were measured by using foil strain gages oriented at 90 degrees. The strain gages were used on both sides of the strap at identical positions. The load was measured by a load cell. The test data are given in Fig A1.1, where it can be observed that the load versus strain relation is linear. For a load of 2000 pounds

$$\text{Average longitudinal strain} = \frac{725 + 720 + 728}{3 \times 2} = \frac{2173}{6} \times 10^{-6} \text{ in/in}$$

$$\text{Average transverse strain} = \frac{240 + 242 + 245}{3 \times 2} = \frac{727}{6} \times 10^{-6} \text{ in/in}$$

$$\text{Stress} = \frac{2000}{2 \times 0.25} = 4000 \text{ lb/in}^2$$

$$E = \frac{4000 \times 6}{2173} \times 10^6 = 11 \times 10^6 \text{ lb/in}^2$$

$$\nu = \frac{727}{6} \times \frac{6}{2173} = 0.336$$

Bending Test

The strap tested under tension was also tested under bending as a cantilever. The load was applied 4 inches from the free end, where deflection was measured. The test data are given in Fig A1.2. From Fig A1.2

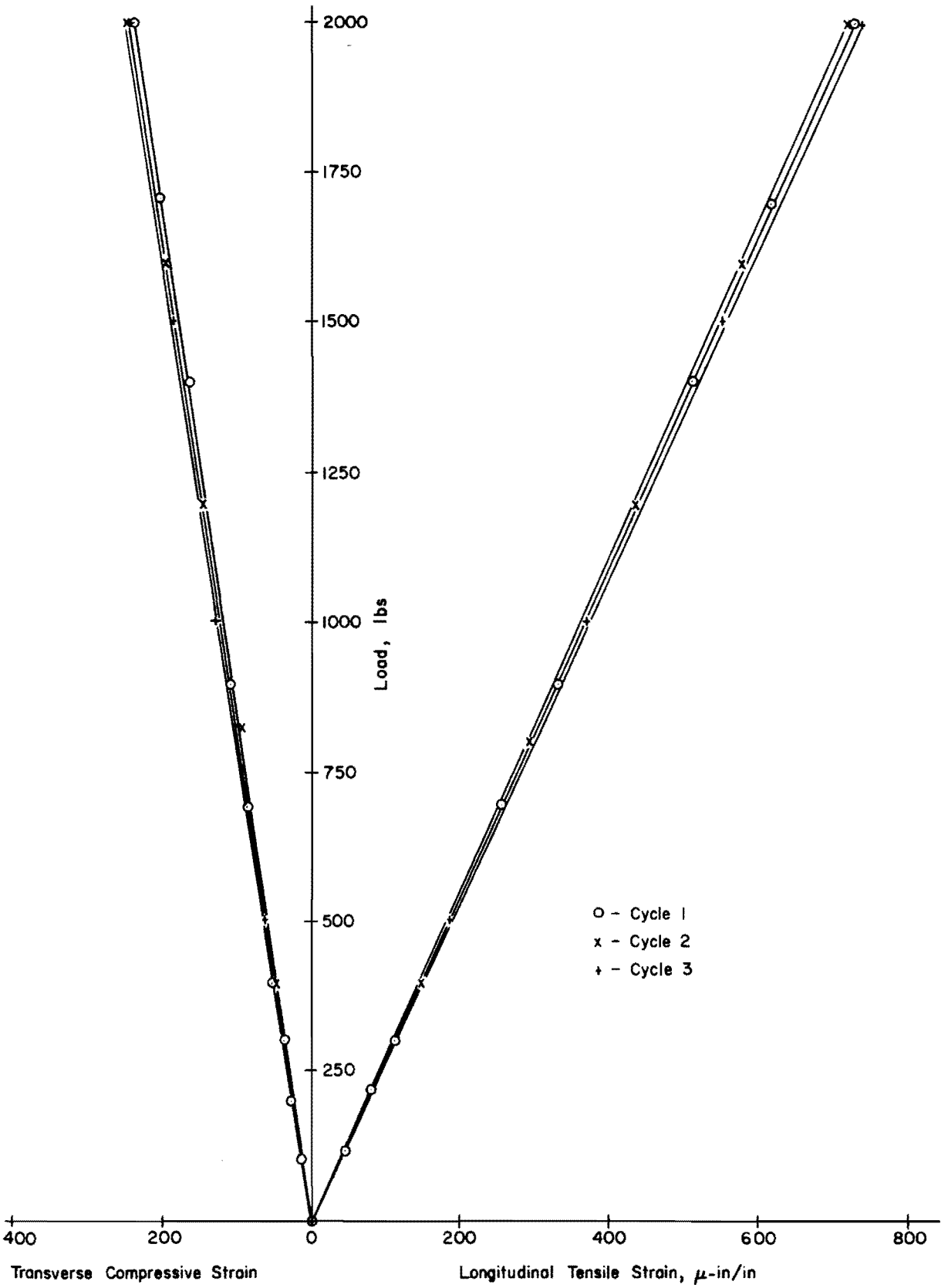

Fig A1.1. Tension test data for aluminum strap of plate material.

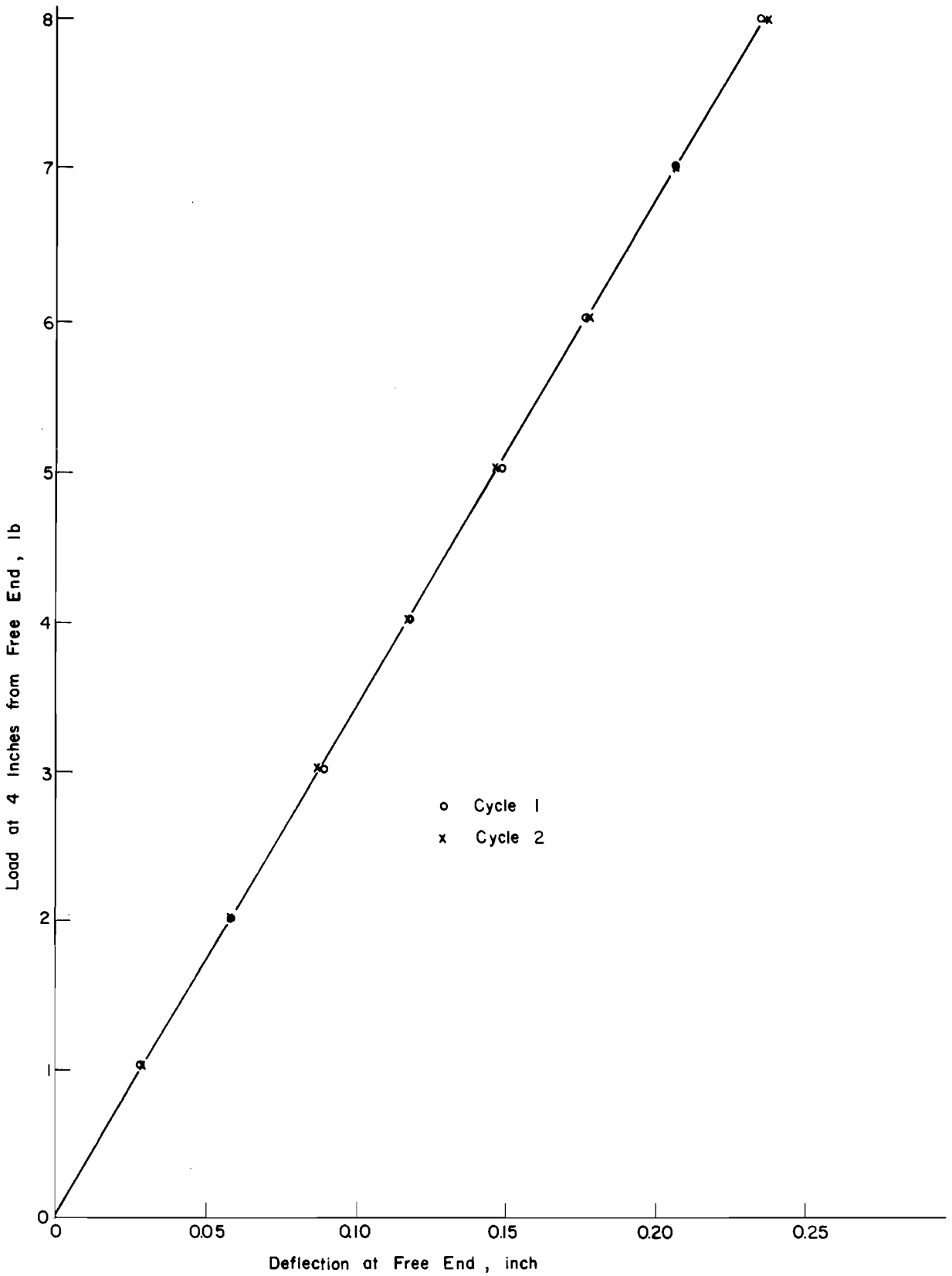

Fig A1.2. Bending test data for aluminum strap of plate material.

Load = 8 lb

Deflection at the free end = 0.2385 inch

Using the deflection equation for a cantilever

$$EI = 28950 \text{ lb-in}^2$$

$$E = 11.1 \times 10^6 \text{ lb/in}^2$$

Practically there is no difference in the values of E obtained by tension tests and by bending tests. The value obtained by the bending test was used to compute the stiffness properties of the plate:

$$D_x = D_y = \frac{Et^3}{12(1 - \nu^2)} = 1.6 \times 10^4 \text{ lb-in}$$

$$C_x = C_y = \frac{Et^3}{12(1 + \nu)} = 1.061 \times 10^4 \text{ lb-in}$$

Plexiglas Isotropic Plate

Tension Test

A 2 by 18 by 1/2-inch-thick strap was tested in tension, and strain was recorded in the same manner as for the aluminum strap. The test data are given in Fig A1.3. The average values of E and ν obtained are

$$E = 0.44 \times 10^6 \text{ lb/in}^2$$

$$\nu = 0.375$$

Bending Test

The data from testing a 2 by 18 by 1/2-inch strap under bending as a cantilever are given in Fig A1.4. For a load of 3 pounds

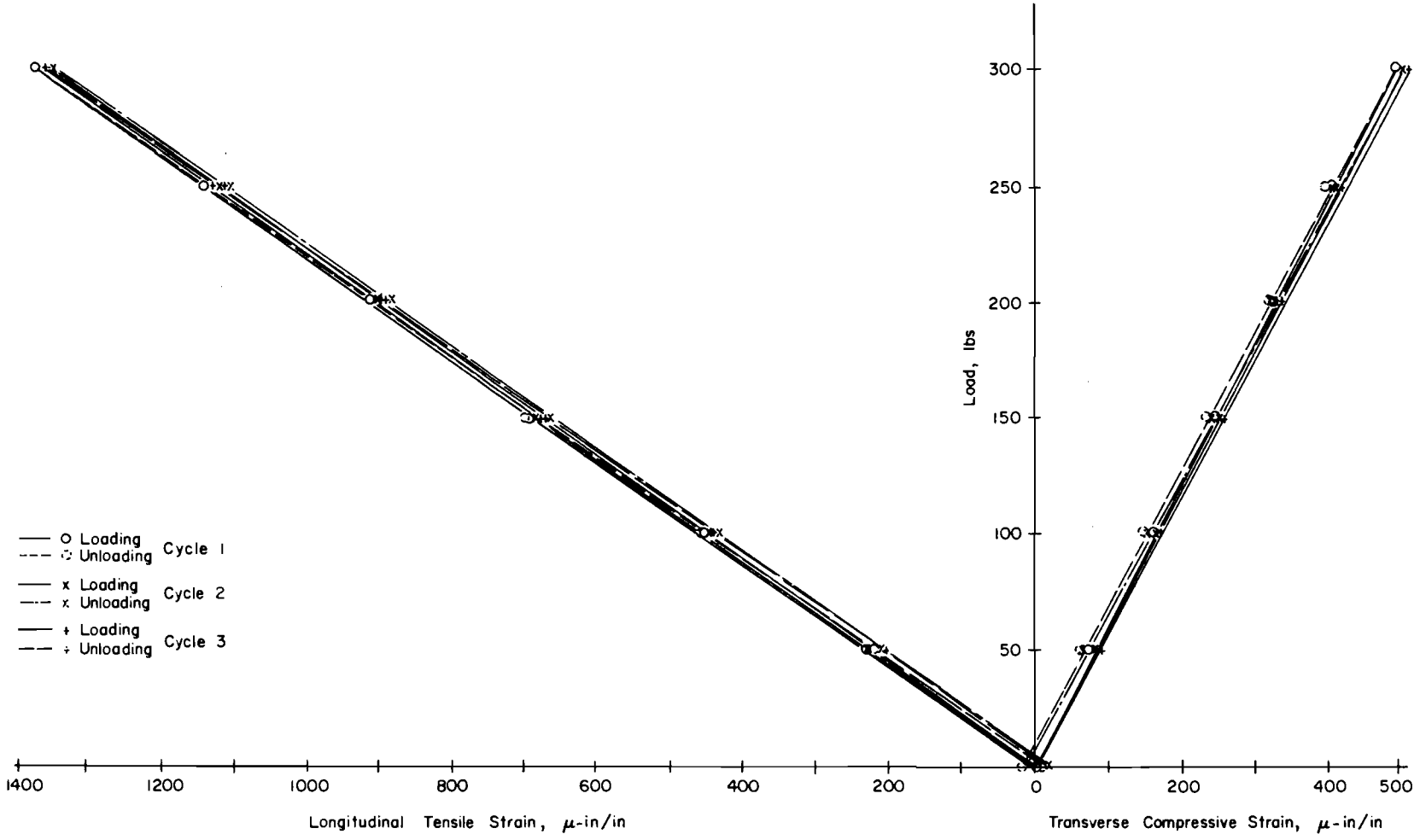

Fig A1.3. Tension test data for Plexiglas strap.

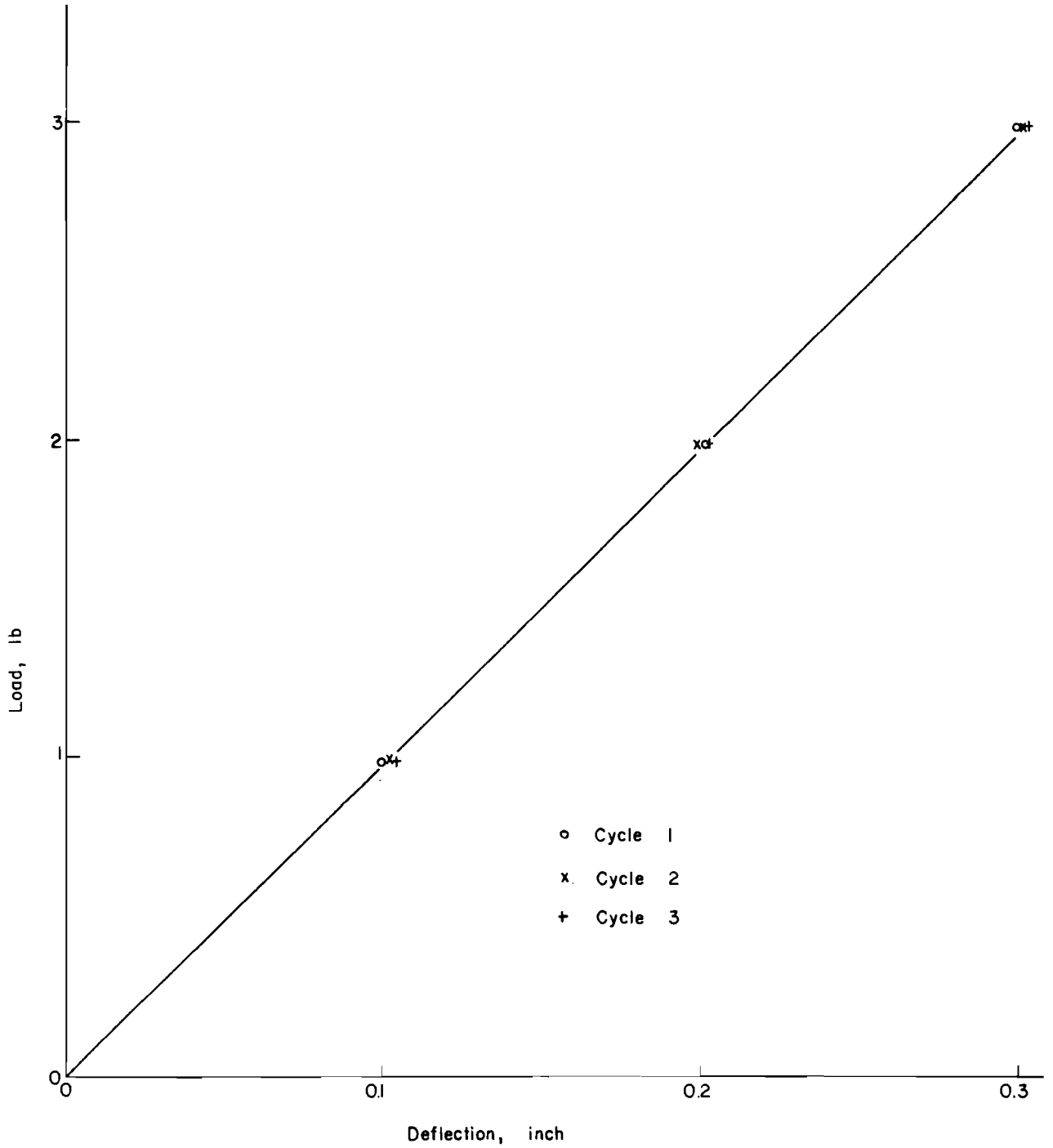

Fig A1.4. Bending test data for Plexiglas strap.

Deflection of free end = 0.30310 inch

$EI = 8550 \text{ lb-in}^2$

$E = 0.41 \times 10^6 \text{ lb/in}^2$

The value of E obtained from the bending test is less than that obtained from the tension test, which used strain gages. This may be due to the local strengthening effect of epoxy near the strain gages. The value obtained by the bending test was used to compute stiffness properties of the plate:

$$D_x = D_y = \frac{Et^3}{12(1 - \nu^2)} = 4950 \text{ lb-in}$$

$$C_x = C_y = \frac{Et^3}{12(1 + \nu)} = 3.12 \times 10^3 \text{ lb-in}$$

Plexiglas Orthotropic Plate

Tension Test

Testing was done under tension on

(1) a 2 by 18 by 1/2-inch Plexiglas unstiffened strap,
(2) a 2 by 18 by 1/2-inch Plexiglas strap with transverse stiffeners, and
(3) a 2 by 18 by 1/2-inch Plexiglas strap with longitudinal stiffeners.

The stiffeners were bonded chemically to the strap in the same manner and at identical positions as those on the orthotropic plate. The longitudinal deflection was measured by dial gage, whereas transverse deflection was measured by screw gages at different points along the specimens. Longitudinal versus transverse strains are plotted in Fig A1.5 for all cases. The Poisson's ratios ν obtained are 0.375 for plain strap (same as obtained earlier), 0.329 with longitudinal stiffeners, and 0.29 with transverse stiffeners (average of values obtained at the locations with and without stiffeners).

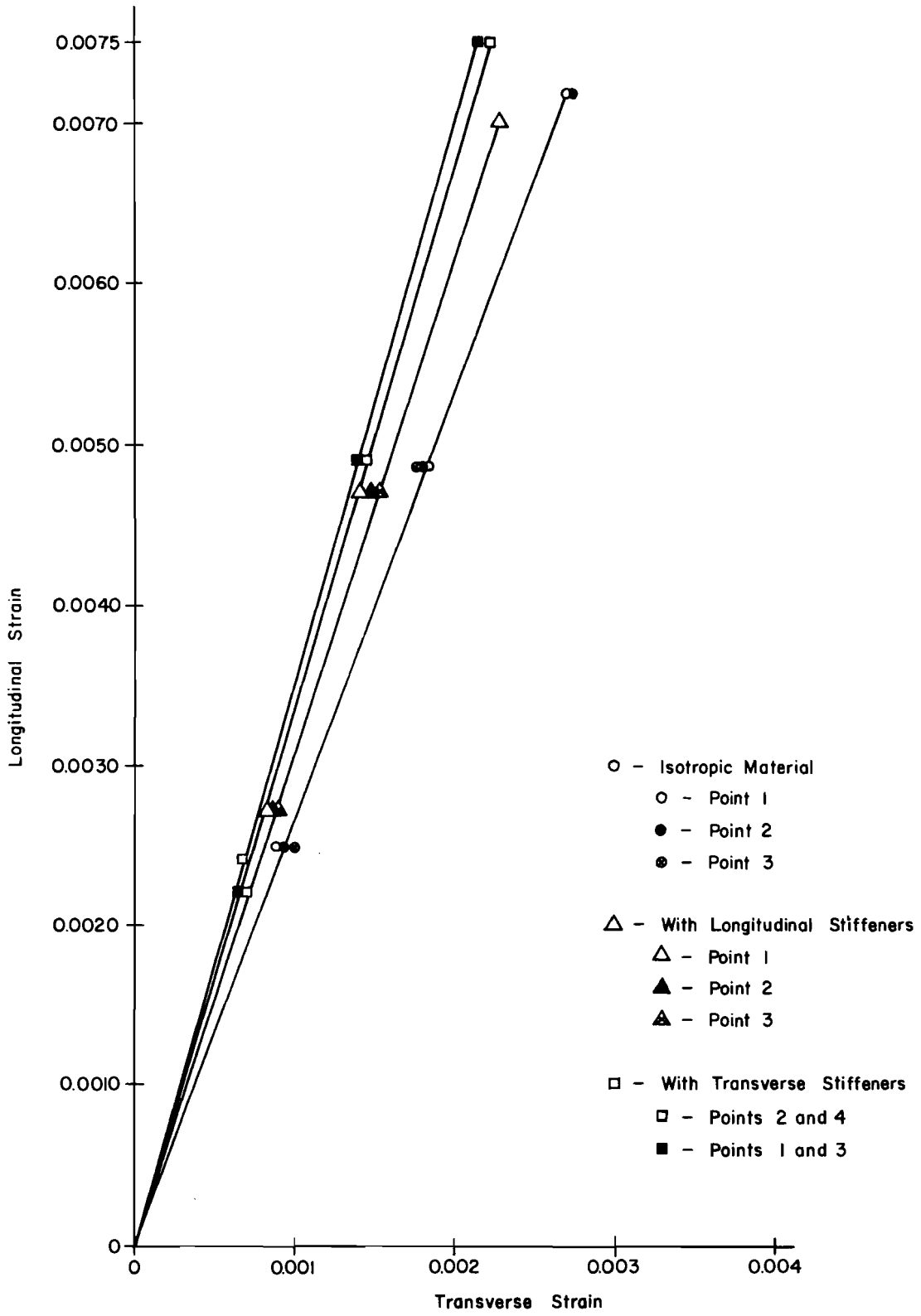

Fig A1.5. Tension test data for Plexiglas straps with and without stiffness.

Bending Test

The straps with longitudinal and transverse stiffeners were tested in bending as a cantilever. The test data for straps with transverse and longitudinal stiffeners are shown in Figs A1.6 and A1.7, respectively. EI values obtained for both cases are

$$(EI)_y \text{ (with transverse stiffeners)} = 6524 \text{ lb-in}$$

$$(EI)_x \text{ (with longitudinal stiffeners)} = 9340 \text{ lb-in}$$

From these values D_x and D_y were obtained using the Poisson's ratio of the original material:

$$D_x = \frac{(EI)_x}{1 - \nu^2} = \frac{9340}{1 - 0.375^2} = 10825 \text{ lb-in}$$

$$D_y = \frac{(EI)_y}{1 - \nu^2} = \frac{6524}{1 - 0.375^2} = 7560 \text{ lb-in}$$

D_x and D_y were also calculated analytically as suggested by Huffington and Blacksburg (Refs 17 and 18):

$$D_x = 11178 \text{ lb-in}$$

$$D_y = 7640 \text{ lb-in}$$

As the plate and the straps were stiffened by the same method, the stiffness values obtained experimentally were used for the analytical solutions.

Twisting Stiffness

Twisting stiffness of the orthotropic plate was determined experimentally as suggested by Hudson (Ref 19). The plate was tested under a corner load, as shown in Fig A1.8. Test data are given in Fig A1.9. The twisting stiffness obtained is

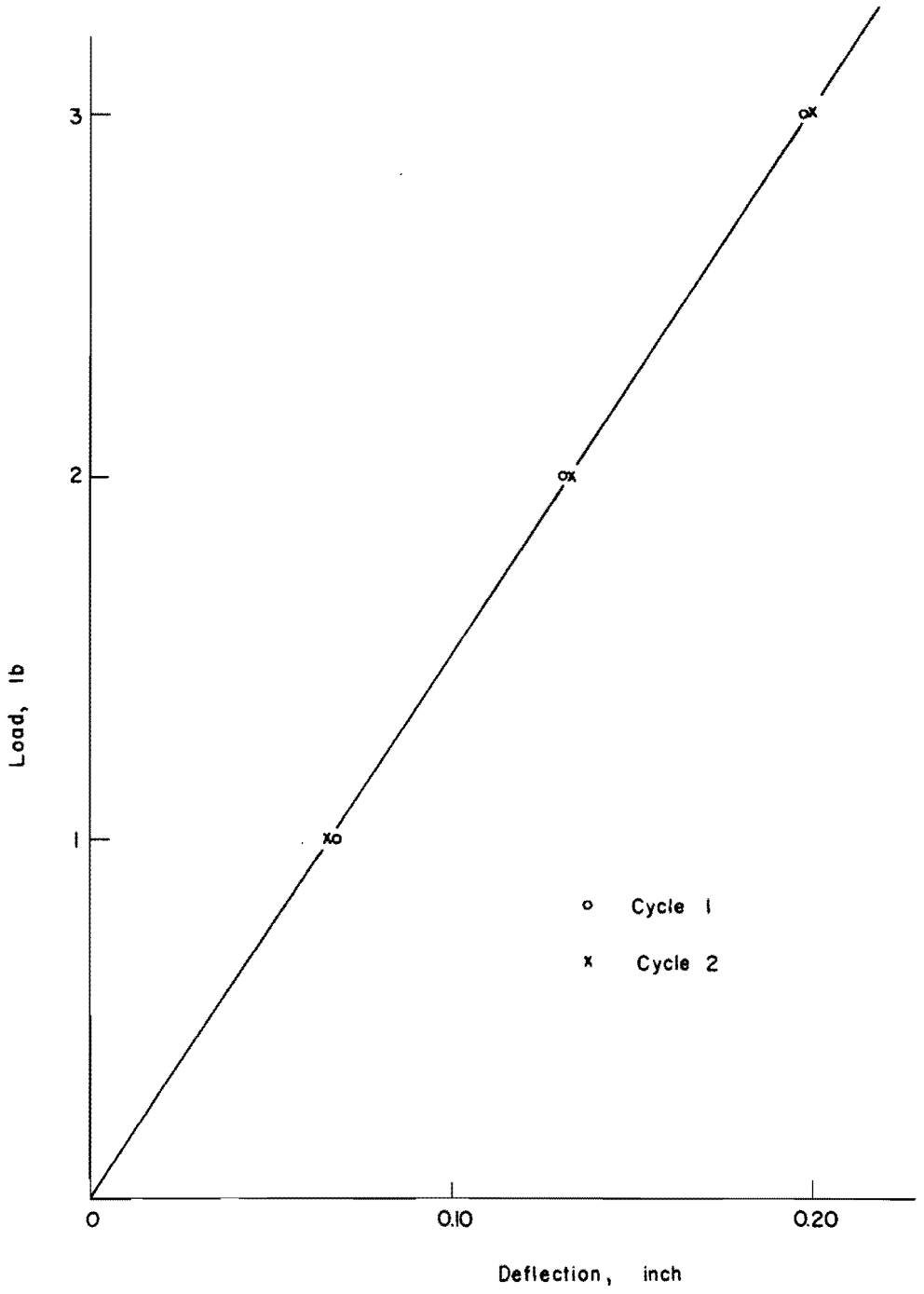

Fig A1.6. Bending test data for Plexiglas strap with transverse stiffness.

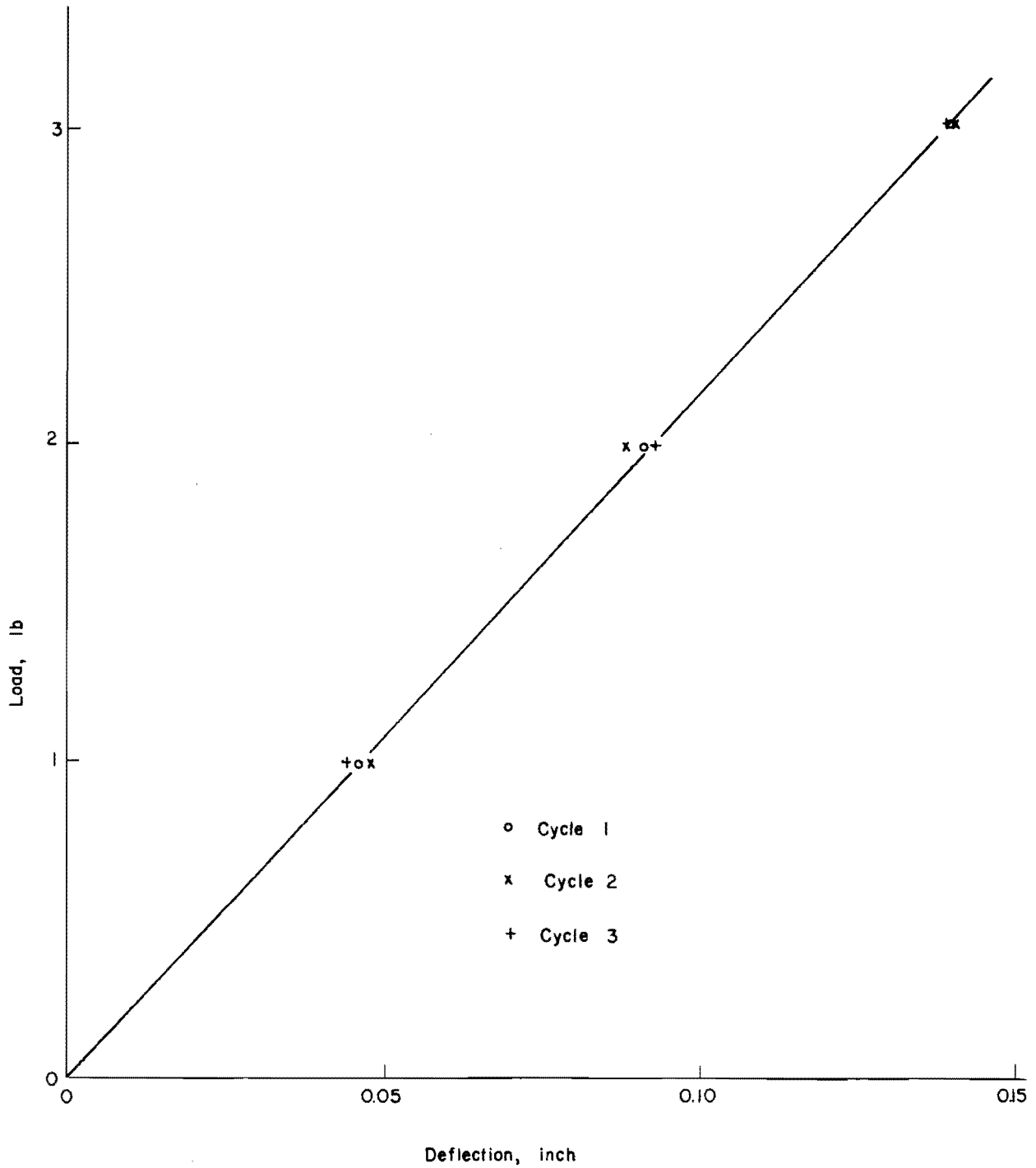

Fig A1.7. Bending test data for Plexiglas strap with longitudinal stiffness.

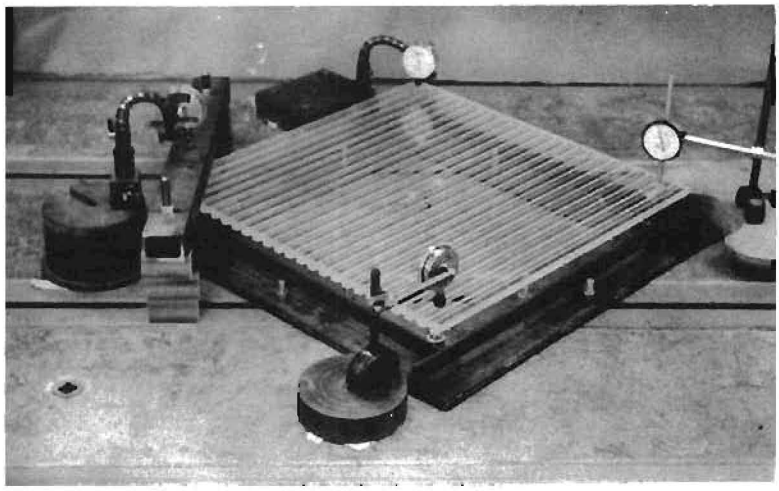

(a) Test set-up.

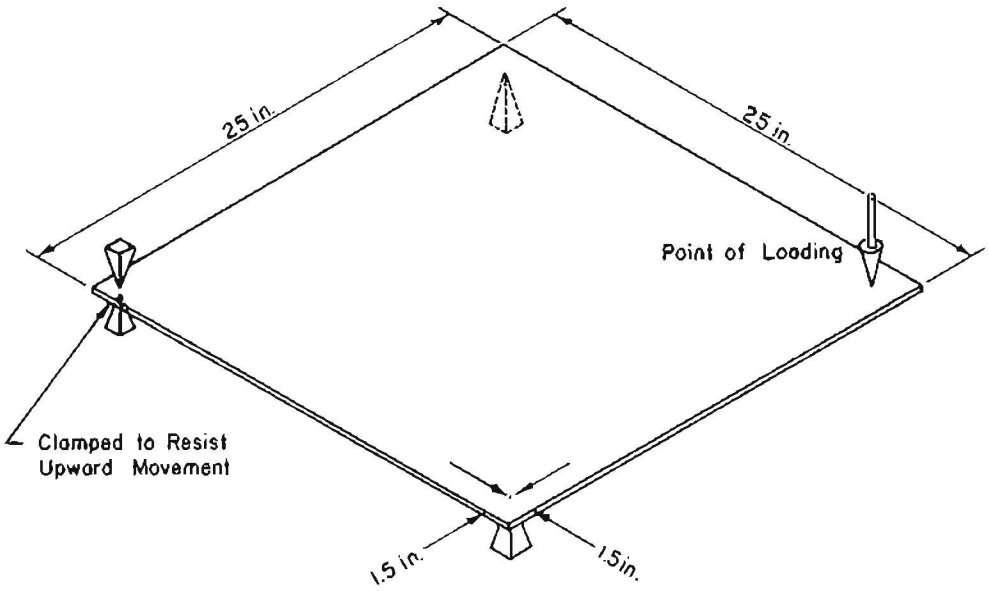

(b) Dimensions.

Fig A1.8. Test arrangements for determination of twisting stiffness of orthotropic plate under corner loading.

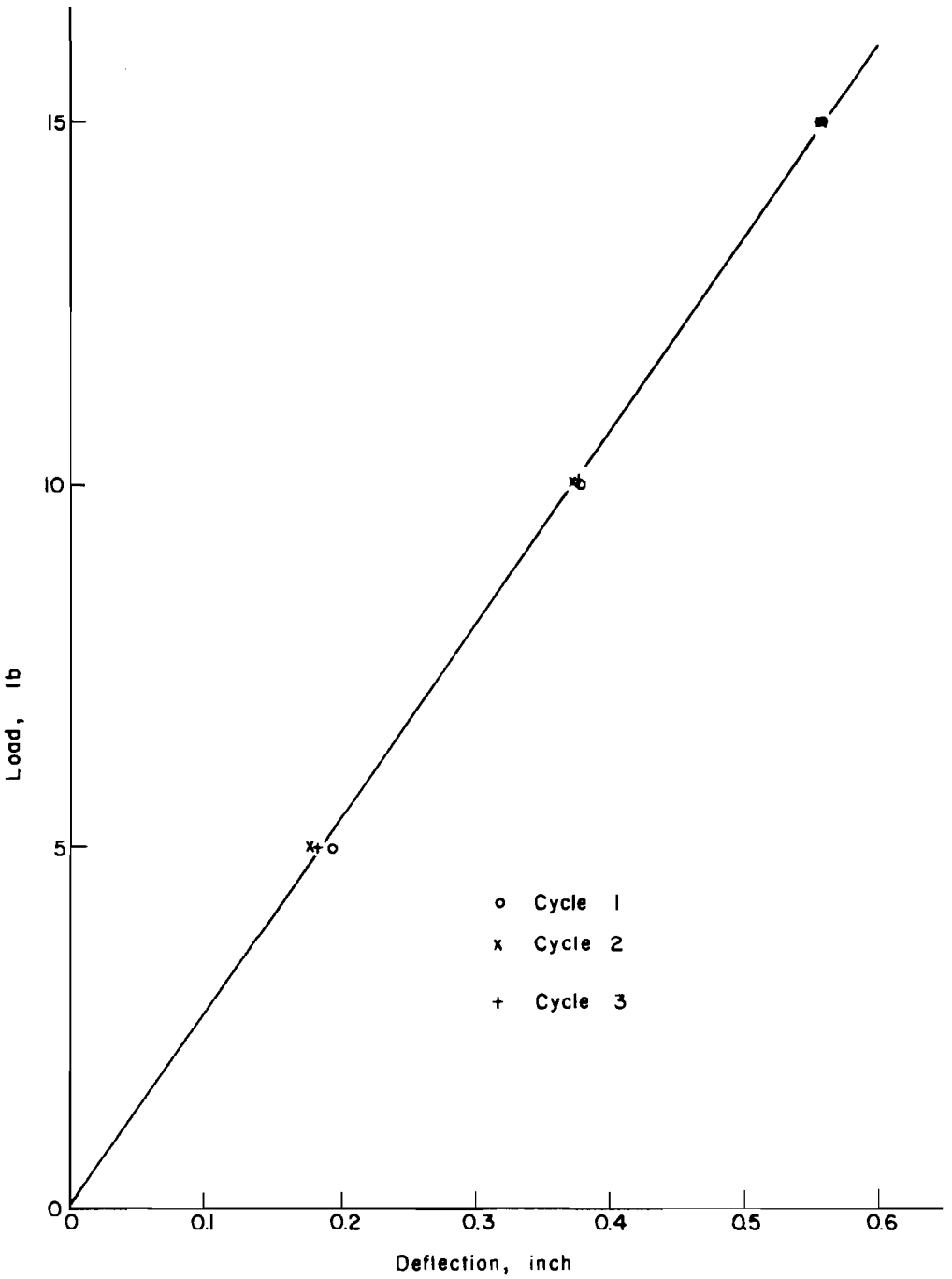

Fig A1.9. Test data for orthotropic plate under corner load.

$$C_x = C_y = 6440 \text{ lb-in}$$

Aluminum Slab

A 1-1/2 by 18 by 1/8-inch strap was tested in both tension and bending in the same way as for plates. The test data for tension test are shown in Fig A1.10. The elastic and stiffness properties thus obtained were

$$E = 10.5 \times 10^6 \text{ lb/in}^2$$

$$\nu = 0.338$$

$$D_x = D_y = 1.930 \times 10^3 \text{ lb-in}$$

$$C_x = C_y = 1.280 \times 10^3 \text{ lb-in}$$

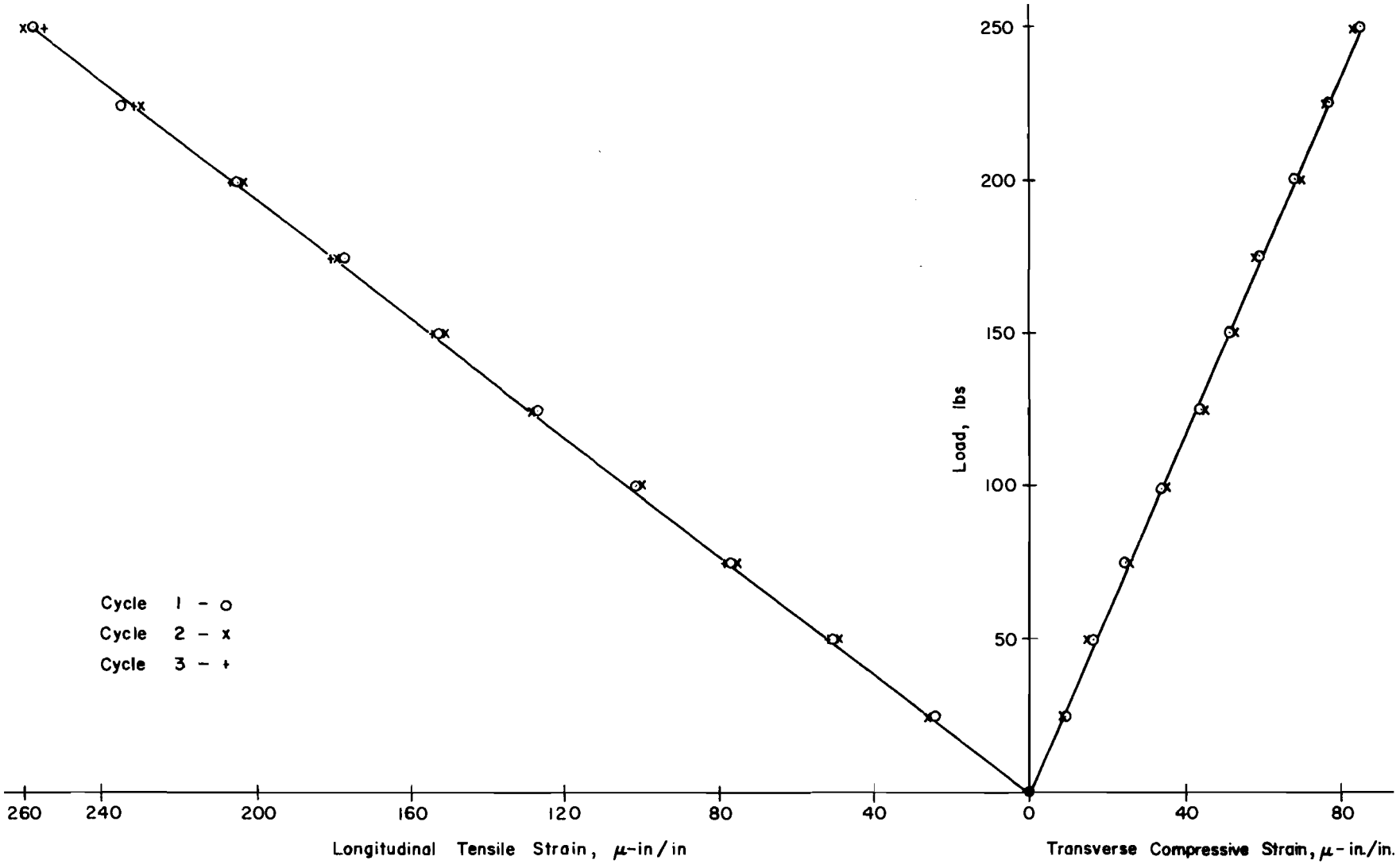

Fig A1.10. Tension test data for aluminum strap of slab material.

APPENDIX 2

PRELIMINARY SLAB TESTS UNDER CENTER LOAD

APPENDIX 2. PRELIMINARY SLAB TESTS UNDER CENTER LOAD

Before the final slab testing under the center load, two preliminary slab series were conducted to establish a suitable test procedure. The methods of soil placement and load application in these series were the same as those described in Chapter 5. The main difference in the two preliminary series was in the recording and measurement of load and deflection.

Test on Uninstrumented Slab (Series 300)

The first preliminary test series was conducted on an uninstrumented slab. The test arrangements are shown in Fig A2.1(a) and (b). The load was measured by a proving ring, and deflections by 0.0001-inch dial gages. Initial readings of all dial gages were taken with no load on the slab. Loading was then started and increased to 25 pounds. After recording the gage readings, the slab was unloaded completely. The load was then cycled for the maximum deflection at the point nearest the load until it became constant in two successive cycles. The load was increased to 50 pounds and cycled until the deflection at Point 1 was constant in two successive cycles. Testing was also done under loads of 75 and 100 pounds with deflection cycled at 75 pounds and load cycled at 100 pounds.

After the test, the slab was removed. In order to represent the soil subgrade by linear and nonlinear springs, i.e., Winkler foundation, plate load tests were conducted according to ASTM specifications (Ref 3) on plates of 1, 2, 4, and 6-inch diameters. The plates were positioned at different locations, keeping the center of the plate at a distance from the side of the box at least 3 times the radius of the plate. Shear strength and other soil properties were determined as for main center load slab test (series 330), as described in Chapter 5.

Soil Properties

Pressure versus average deflection characteristics of the plate load tests are shown in Fig A2.2. From the plots it can be seen that these characteristics

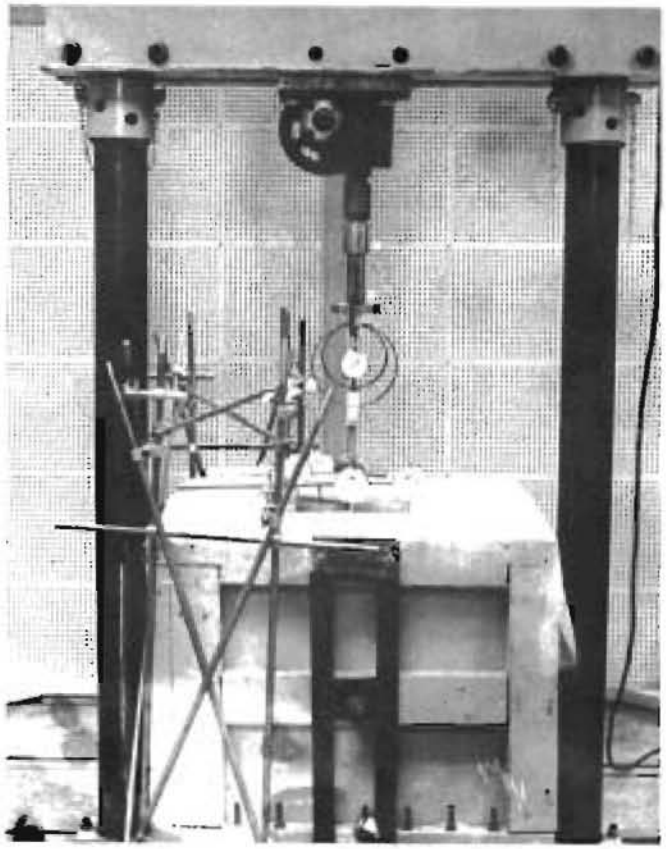

(a) Test set-up.

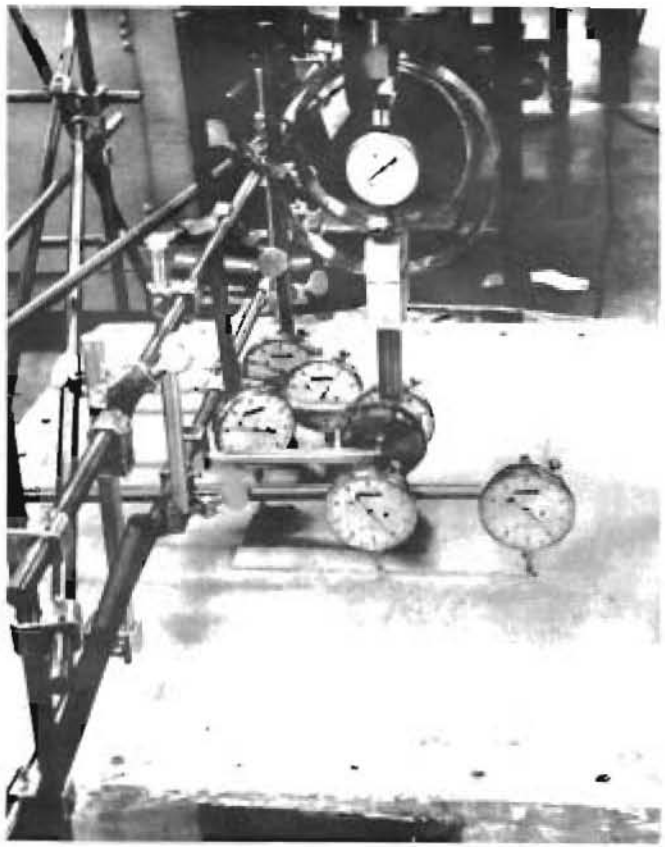

(b) Close-up of slab with loading and measurement devices.

Fig A2.1. Preliminary slab testing under center load.

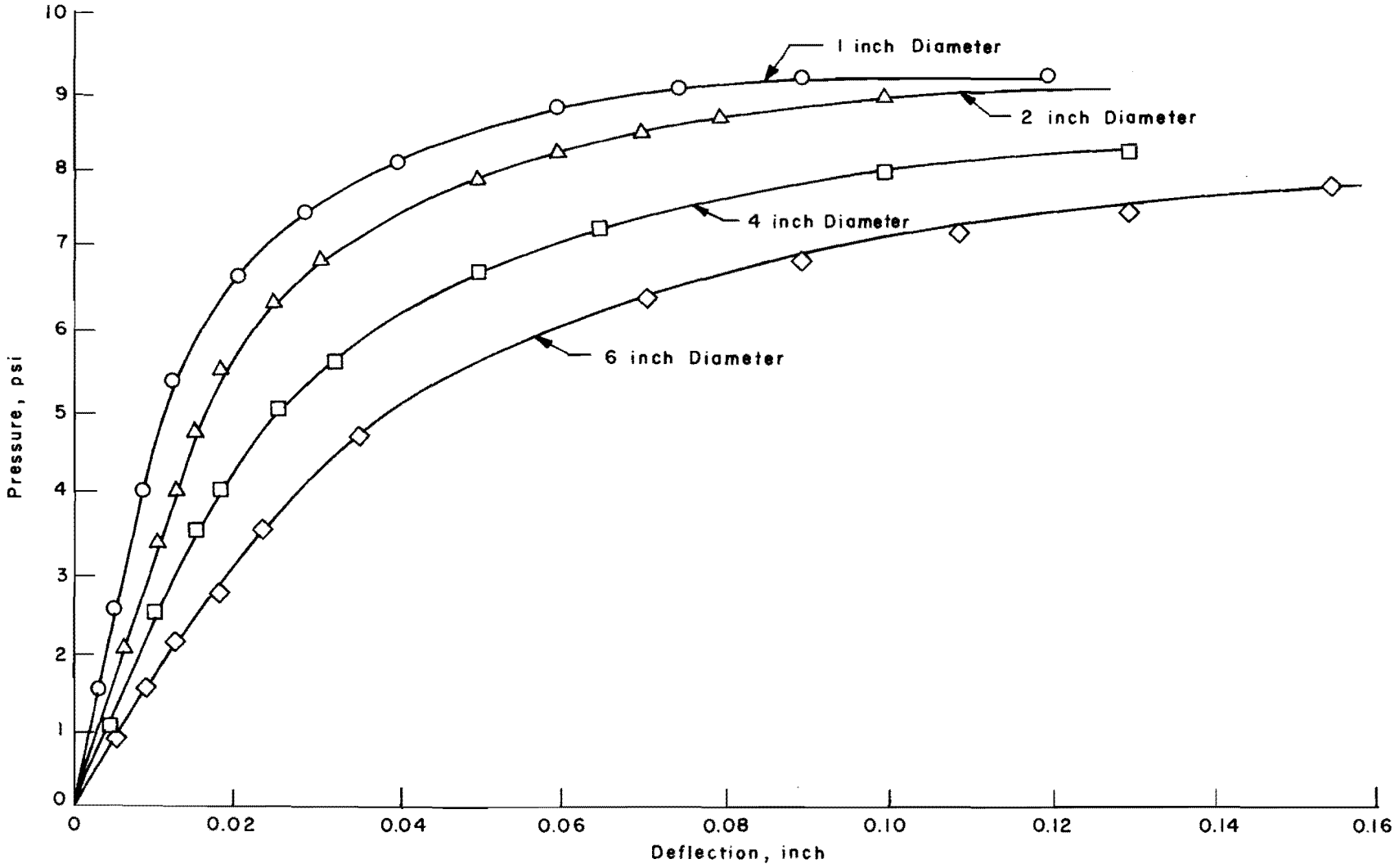

Fig A2.2. Pressure versus deflection data of plate load tests for preliminary slab test (series 300).

are influenced by the size of the loaded area. Shear strengths obtained from the unconfined compression tests are shown in Fig A2.3. Average shear strength was found to be 180 lb/ft^2 (1.25 psi). Shear strengths using the vane apparatus are given in Table A2.1. The average values at each location ranged from 195 to 255 lb/ft^2 (1.36 to 1.77 psi), with average constant value of 210 lb/ft^2 (1.46 psi). Shear strength at the surface using the torvane was found to be 260 lb/ft^2 (1.80 psi). The variation in water content is shown in Fig A2.4. The average value was 38.1 percent. The wet density, as determined from the weight and volume of the extruded samples, varied from 112 to 120 lb/ft^3 with the average 116 lb/ft^3.

Test Data

Figure A2.5 shows the positions of dial gages and point of loading on the slab. Figure A2.6 shows the load versus deflection curve for Point 1 (point controlling the deflections during various cycles), 1 inch from the center on the center line. The points on the curve correspond to those obtained during loading for loads of 25, 50, 75, and 100 pounds for various cycles and for zero load during unloading in each cycle. From this plot, the following can be observed. During cycling, a deflection of -0.0034 inch obtained for 25 pounds in the first cycle, was obtained for 23.4 pounds during the second cycle, and 22.8 pounds during the third and fourth cycles; during cycling for a load of 50 pounds, the deflections obtained were -0.0070 and -0.0072 inch in the first and second cycles and -0.0074 inch in the third and fourth cycles. This indicates that there might be a tendency for load to stabilize during deflection cycling and for deflection to stabilize during load cycling after a few cycles. A similar stage of stabilization seems to take place during deflection cycling after 4 cycles at 75 pounds and during load cycling after 5 cycles at 100 pounds. The deflections obtained for each step of load during the first and last cycles are plotted in Fig A2.7. It can be observed from this figure that the deflections obtained during the last cycle (representing the effect of cyclic load) are greater than those for the first cycle (representing approximately the static case).

It was also observed that deflections of all points except corners were downward. At corners the deflection was upward.

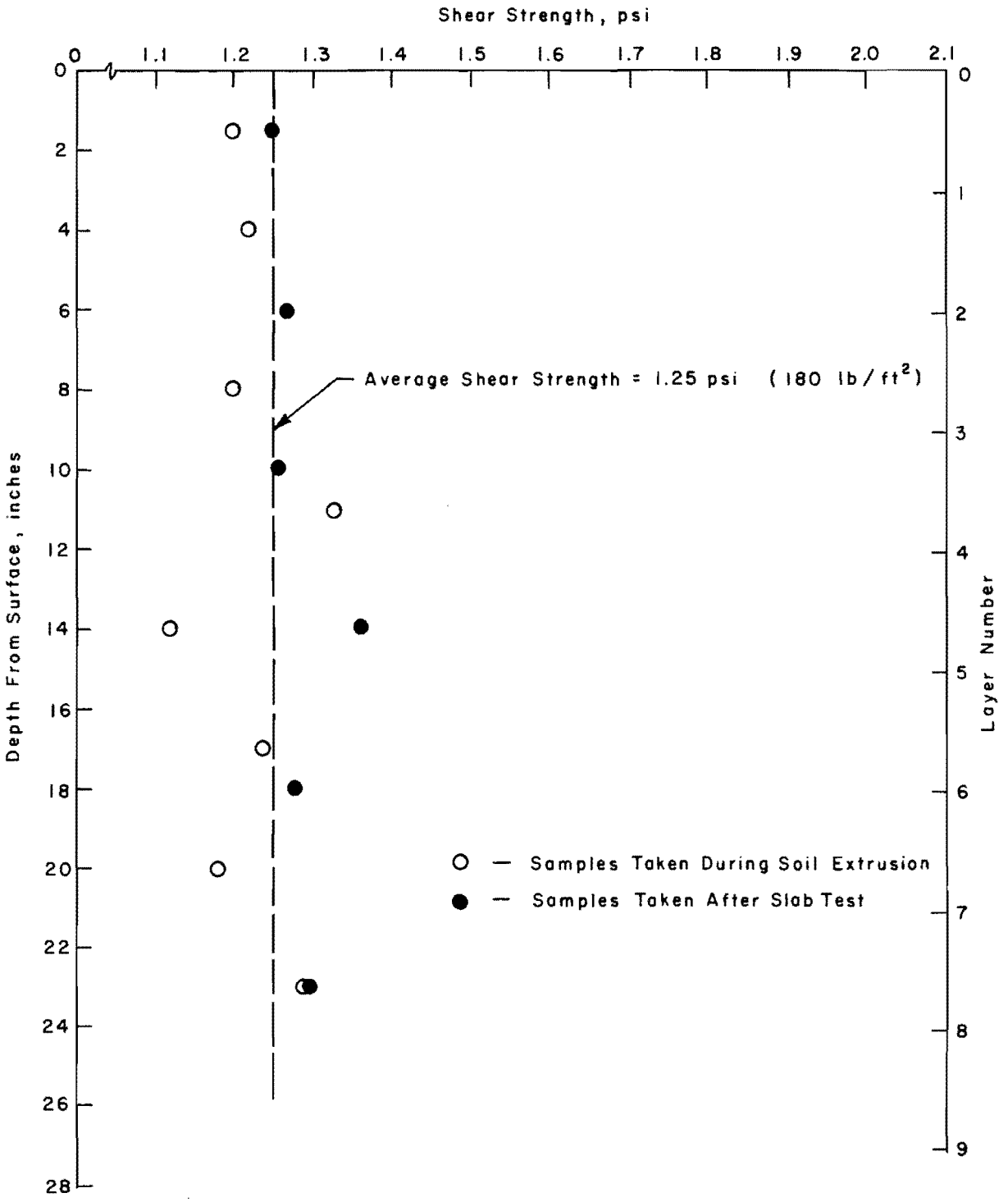

Fig A2.3. Shear strength variation of soil for preliminary slab test (series 300).

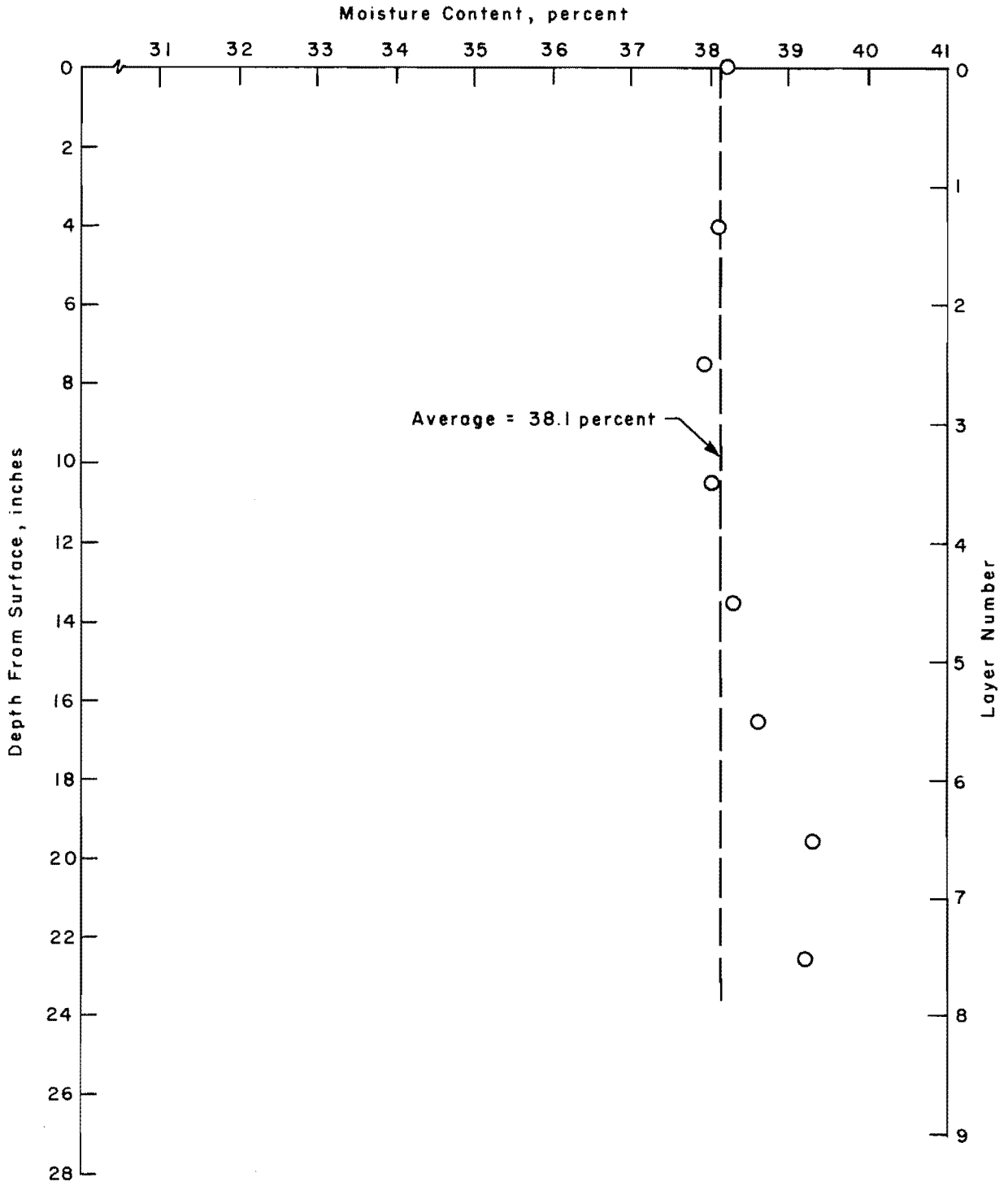

Fig A2.4. Water content variation in preliminary slab test (series 300).

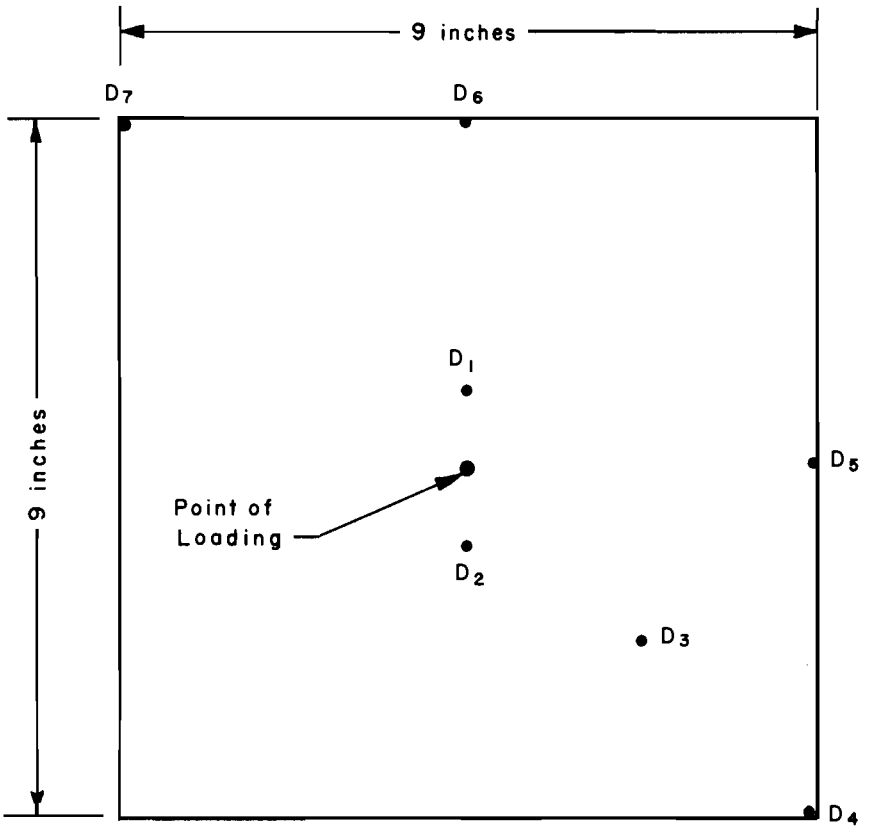

Dial Gage Number	Distance
D_1	1 in. from Center on Center Line
D_2	1 in. from Center on Center Line (Check 1)
D_3	3.53 in. from Center on Diagonal
D_4	6.36 in. from Center on Diagonal
D_5	4.5 in. from Center on Center Line
D_6	4.5 in. from Center on Center Line (Check 5)
D_7	6.36 in. from Center on Diagonal (Check 4)

Fig A2.5. Positions of load and dial gages for preliminary slab test (series 300).

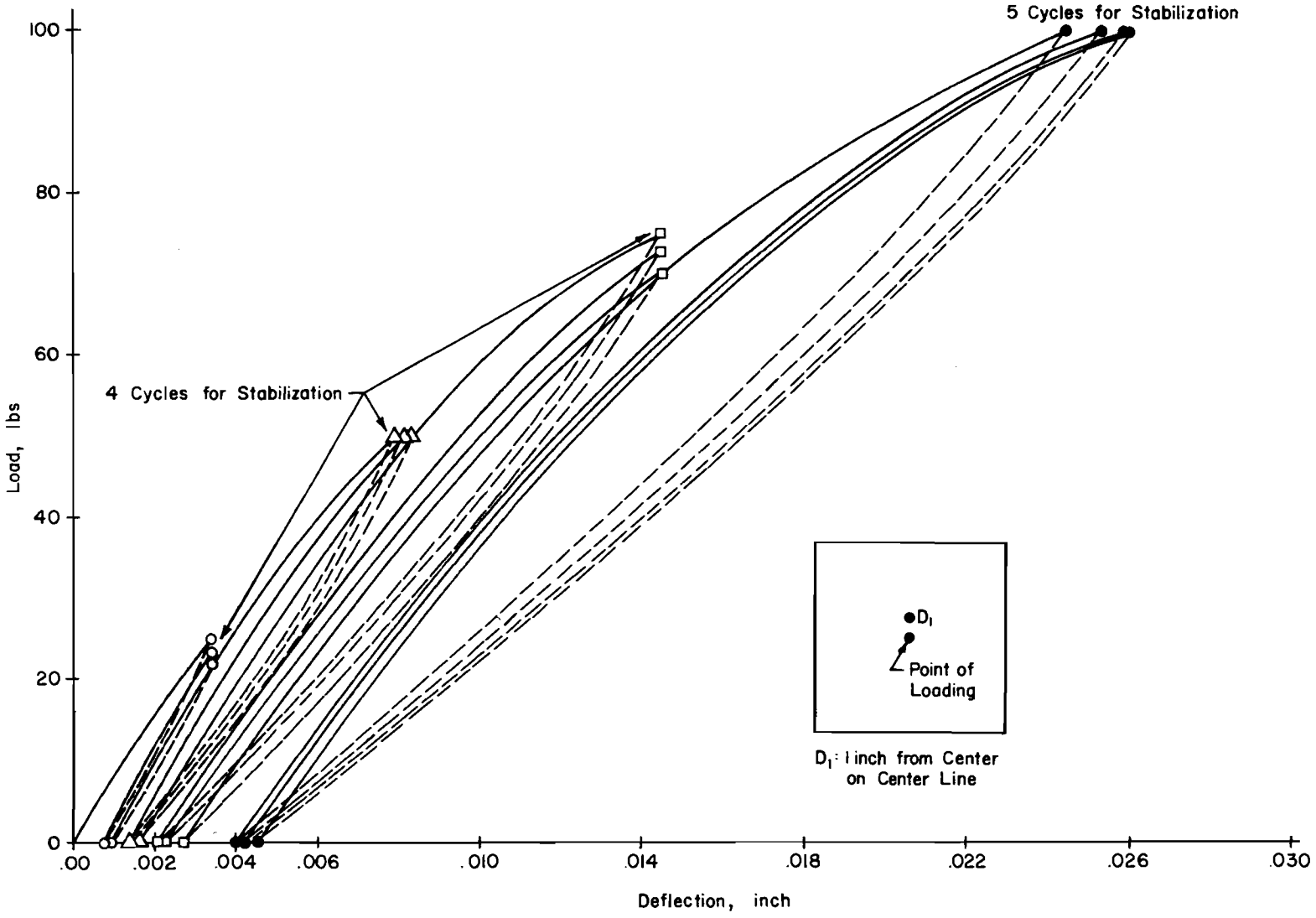

Fig A2.6. Load versus deflection characteristic for dial gage 1 for preliminary slab test under center load (series 300).

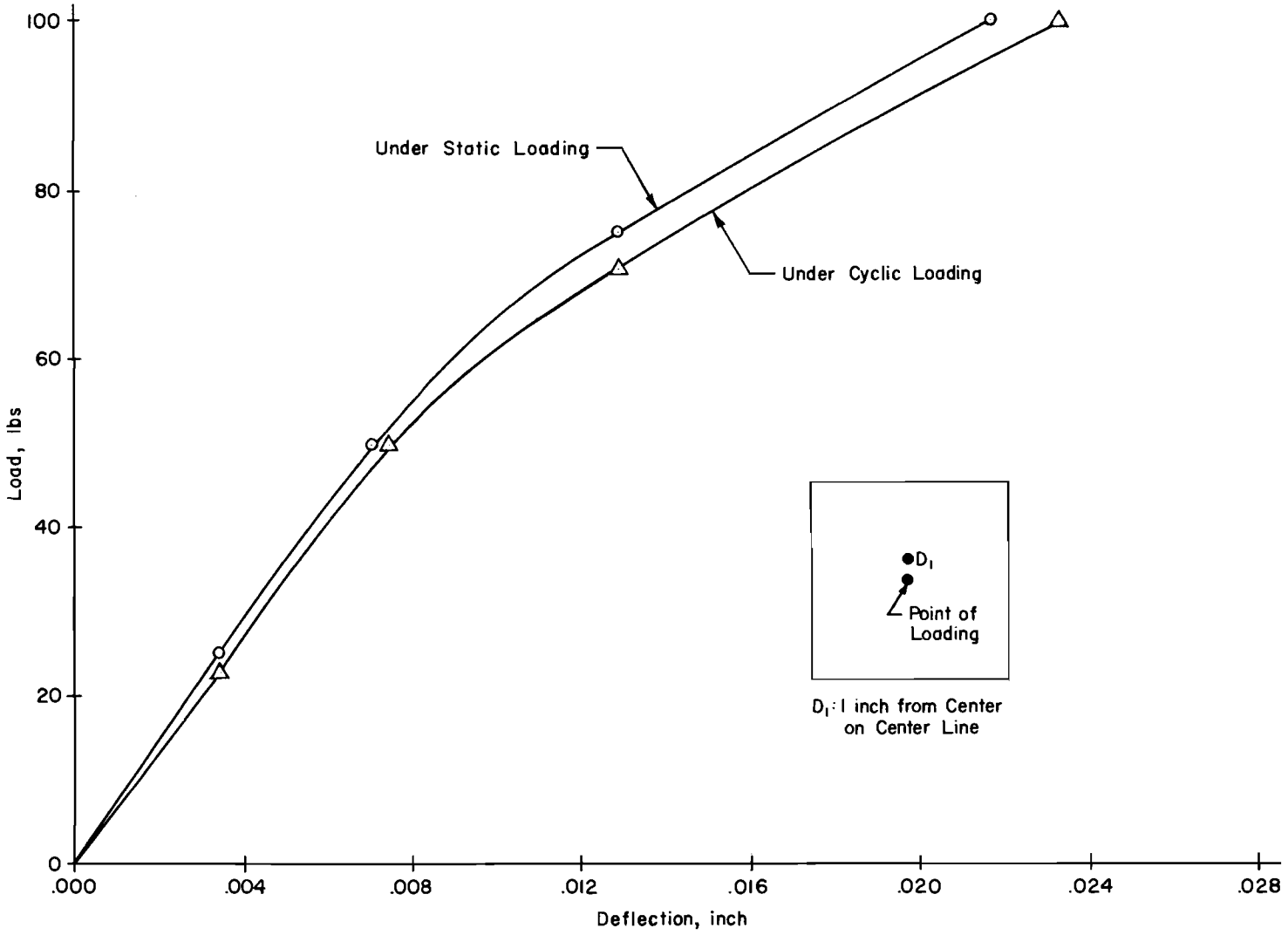

Fig A2.7. Static and cyclic deflections for dial gage 1 for preliminary slab test under center load (series 300).

TABLE A2.1. SHEAR STRENGTH USING VANE APPARATUS FOR PRELIMINARY SLAB SERIES (SERIES 300)

Depth from Surface (inch)	Shear Strength at Location (lb/ft^2)						Average Shear Strength
	1	2	3	4	5	6	
0	248	225	255	225	225	232	235
1	210	195	195	203	203	218	204
2	195	210	210	210	210	210	207
3	203	203	195	195	210	203	202
4	214	203	203	210	203	218	208
5	225	225	210	210	210	218	216

Variation in shear strength: 195 to 255 lb/ft^2 (1.36 to 1.77 psi).

Average constant value: 210 lb/ft^2 (1.46 psi).

Analytical Solutions

Plate load test data were plotted using various parameters and scales to try to get a normalized curve so that data for any other size could be extrapolated. Partial success was obtained in getting such a curve (Ref 39). Linear springs were first used to get DSLAB 30 (Ref 29) solutions. These springs were found from the plate load data by two methods:

(1) linear springs predicted for 9-inch-diameter plate for 0.01-inch deflection (tangent modulus). The k (soil modulus) thus obtained = 170 lb/in^3.

(2) linear springs predicted for 9-inch-diameter plate for 0.02-inch deflection (secant modulus). The k thus obtained = 144 lb/in^3.

The deflections obtained using DSLAB 30 were compared with the observed deflections in the first cycle (static case) and percentage error computed as a function of the maximum measured deflection. The comparison, as presented in Table A2.2, shows that good correlation exists between the experimental and DSLAB solutions using linear springs corresponding to $k = 144\ lb/in^3$. It is also observed that the maximum discrepancy is on the periphery of the slab.

To improve the analytical solutions, the following were used:

(1) nonlinear springs using 6-inch-diameter plate test data,

(2) nonlinear springs predicted for 9-inch-diameter plate, and

(3) nonlinear springs using Skempton's recommendations from unconfined compression test data.

The use of these nonlinear springs for DSLAB 26 (Ref 20) was similar to that reported in Chapter 5. Comparison of the analytical deflections thus obtained with the observed deflections as given in Table A2.2 shows that the percentage errors at all points including those of the periphery were almost of the same magnitude as those using linear springs.

The following shortcomings of the test method were revealed:

(1) The calibration of the proving ring was affected if the load applied was not perfectly vertical. As the connections between the screw jack, proving ring, and loading rod could not be adjusted much vertically, the load measurement might have been in error.

(2) The spring of the dial gage prevented the corner of the slab from lifting by 0.00065 inch.

(3) The friction developed between the slab and the soil was not reduced, but its effect was not considered in the analytical solutions.

TABLE A2.2. EXPERIMENTAL AND ANALYTICAL DEFLECTIONS FOR PRELIMINARY TEST ON UNINSTRUMENTED SLAB (SERIES 300)

Load: 100 lb in the center

Programs: DSLAB 30 and DSLAB 26

Type of Solution	Dial Gages						
	1	2	3	4	5	6	7
Experimental	-0.02170	-0.02120	-0.00650	0.00090	-0.00410	-0.00460	0.00100
Linear springs k = 170 psi	-0.02035	-0.02035	-0.00626	0.00544	-0.00235	-0.00235	0.00544
% Error	-6.22	-3.92	-1.11	20.92	-8.07	-10.37	20.46
Linear springs k = 144 psi	-0.02250	-0.02250	-0.00755	0.00548	-0.00339	-0.00339	0.00548
% Error	3.69	5.99	4.82	21.11	-3.25	-5.56	20.65
Nonlinear q - w curve (6-inch plate data)	-0.02072	-0.02072	-0.00634	0.00558	-0.00238	-0.00234	0.00558
% Error	-4.52	-2.21	-0.73	21.55	-8.12	-10.43	21.09
Nonlinear q - w curve (predicted for 9-inch plate data)	-0.02305	-0.02305	-0.00747	0.00594	-0.00308	-0.00308	0.00594
% Error	6.22	8.52	4.45	23.21	-4.72	-7.02	22.75
Nonlinear q - w curve (Skempton's recommendation)	-0.02359	-0.02359	-0.00792	0.00579	-0.00353	-0.00353	0.00579
% Error	8.71	11.01	6.52	22.55	-2.62	-4.93	22.09

(4) As the soil modulus was affected by the size of the loaded area, the values extrapolated for the 9-inch-square slab from test data for rigid plates of 1, 2, 4, and 6-inch diameters might be in error.

(5) Due to space limitations, only two dial gages could be placed, either on the diagonal or on the center line; this was not sufficient for plotting deflections.

Test on Instrumented Slab (Series 320)

Another preliminary series, on an instrumented slab, was conducted under center loading with the following improvements:

(1) Load was measured by a load cell.

(2) Load was applied through a ball so that only the vertical component of the load was transmitted to the slab.

(3) Deflections were measured by LVDT's, three along both the diagonal and the center line. The cores of the LVDT's did not exert enough pressure on the slab to have an affect, which the spring of the dial gage did.

(4) A thin film of grease was applied on the bottom of the slab.

(5) Plate load test on a 9-inch-diameter plate was also included.

The slab was loaded continuously and data for load, deflection, and strain measured by load cell, LVDT's, and rosettes were recorded by the scanning process on a 40-channel digital logging system. The details of recording the data are given in Chapter 3. The slab was tested for load up to 200 pounds and then unloaded. The data were obtained at regular intervals during loading and unloading.

Plate load tests, shear tests, and other soil tests were conducted the same way as for the preliminary series 300. The plate load test data for a 9-inch-diameter plate were given in Fig 37. Shear strengths obtained from the unconfined compression tests are shown in Fig A2.8 with an average value of 177 lb/ft^2 (1.23 psi). The *in situ* shear strength, as given in Table A2.3, varied from 185 to 205 lb/ft^2 (1.28 to 1.42 psi) with an average of 198 lb/ft^2 (1.38 psi). The variation in water, as shown in Fig A2.9, showed an average of 38 percent. The average wet density was 116 lb/ft^3.

The data reduction was done exactly as described in Appendix 3. It was then determined that one LVDT was out of range just after starting the load, and the others got out of range at different loads higher than 100 pounds. The data analysis was therefore done for 100 pounds only. It was also revealed that one gage of a rosette was disconnected.

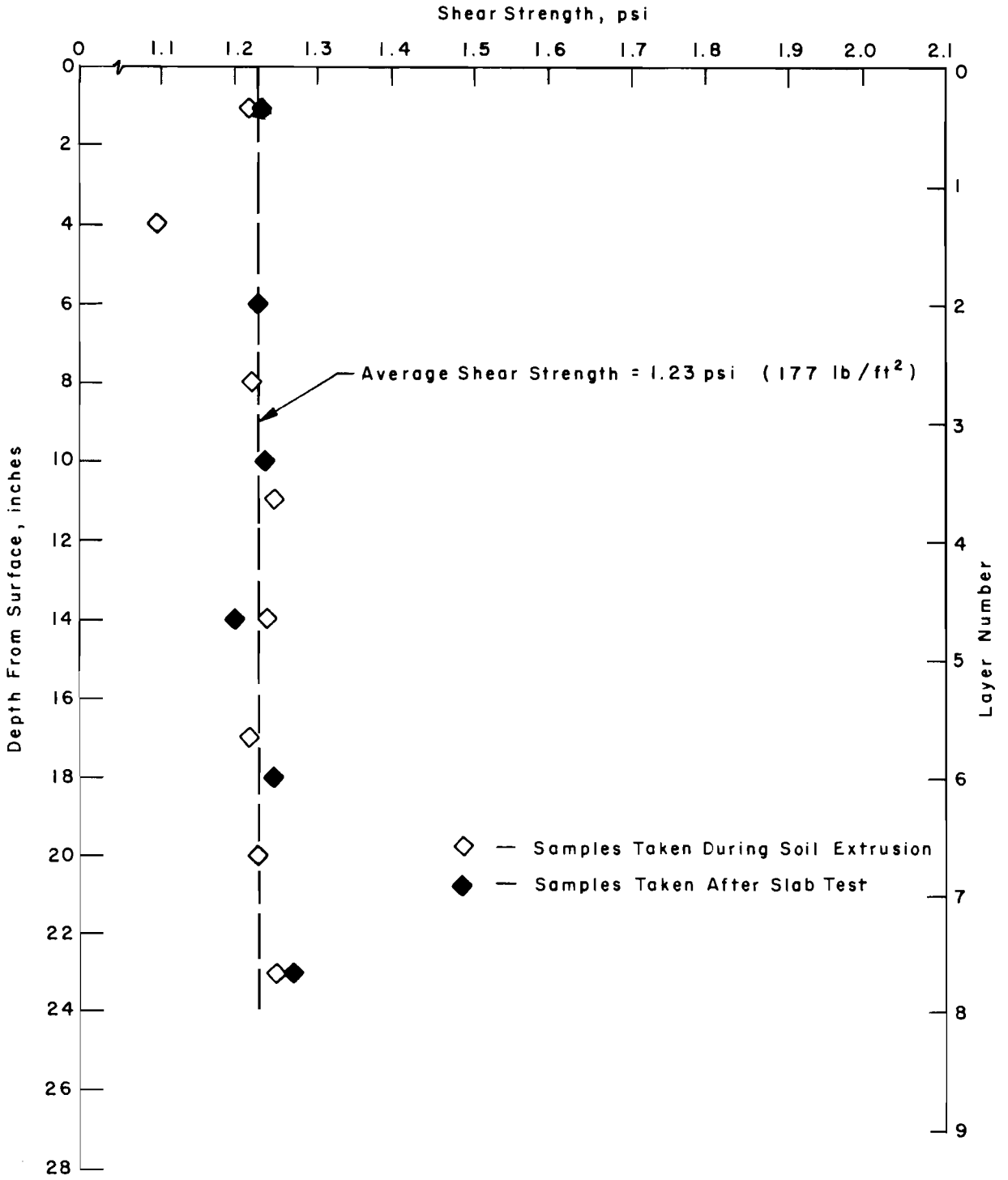

Fig A2.8. Shear strength variation for soil for the preliminary slab test (series 320).

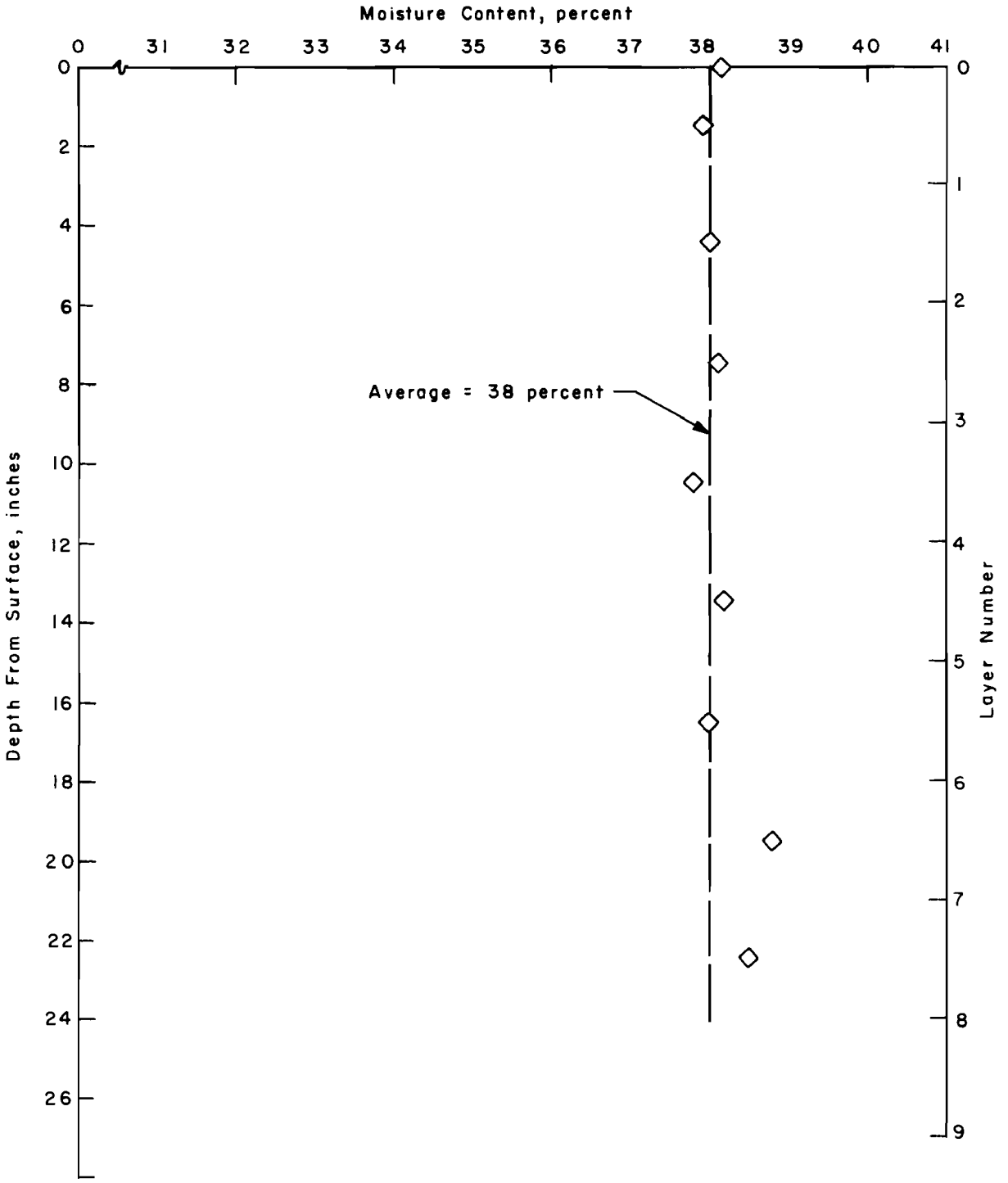

Fig A2.9. Water content variation for the preliminary slab test (series 320).

TABLE A2.3. SHEAR STRENGTH USING VANE APPARATUS FOR PRELIMINARY SLAB TEST (SERIES 320)

Depth from Surface (inch)	Shear Strength at Locations (lb/ft^2)						Average Shear Strength
	1	2	3	4	5	6	
0	185	190	185	185	190	195	188
1	190	190	195	195	195	200	194
2	190	195	195	195	195	200	195
3	200	200	200	205	205	205	203
4	205	200	205	200	205	205	203
5	205	205	205	205	205	205	205

Variation: 185 to 205 lb/ft^2 (1.28 to 1.42 psi).

Average constant value: 198 lb/ft^2 (1.38 psi).

As observed from the preliminary series 300, the soil modulus was dependent on the size of the plate, as reported by Siddiqi (Ref 39); the data of the 9-inch-diameter plate test (Fig 37) were used to determine linear and nonlinear springs. The soil was represented by the following springs:

(1) linear springs corresponding to tangent modulus for .01-inch deflection,

(2) linear springs corresponding to secant modulus for .02-inch deflection,

(3) nonlinear springs using the entire 9-inch-diameter plate data, and

(4) nonlinear springs using Skempton's recommendation.

DSLAB solutions using the different soil springs were compared with the observed deflections and principal stresses and the percentage error calculated in the same way as for the preliminary series 300 and for the center load slab test (series 320), discussed in Chapter 5. The comparison for deflection is given in Fig A2.10 and Table A2.4 and for principal stresses in Table A2.5. The comparison shows that good correlation exists between experimental and DSLAB solutions for deflections and principal stresses using linear or nonlinear soil springs.

The following shortcomings of the preliminary series 320 were found:

(1) The LVDT's were calibrated by moving the core upwards, whereas the deflections measured on the slab during testing were mostly downwards. The scale in the recording system was not properly adjusted for such movement.

(2) LVDT's of 1 and 1/2-inch range were used to measure deflection for ±0.200 inch or less.

(3) The lead wires from the rosettes were attached to the slab by a thick layer of epoxy, which may have had the effect of increasing the stiffness of the slab.

The center load slab test (series 330) and corner loads slab test (series 340) were conducted with the following improvements:

(1) The LVDT's were calibrated by moving the core downward so that deflections were recorded in the same range during testing and calibration.

(2) Calibration was done for the entire range of deflections expected. However, this resulted in reducing the resolution.

(3) The epoxy connecting the lead wires of the rosettes and the slab was scratched, except for a short distance near the gage.

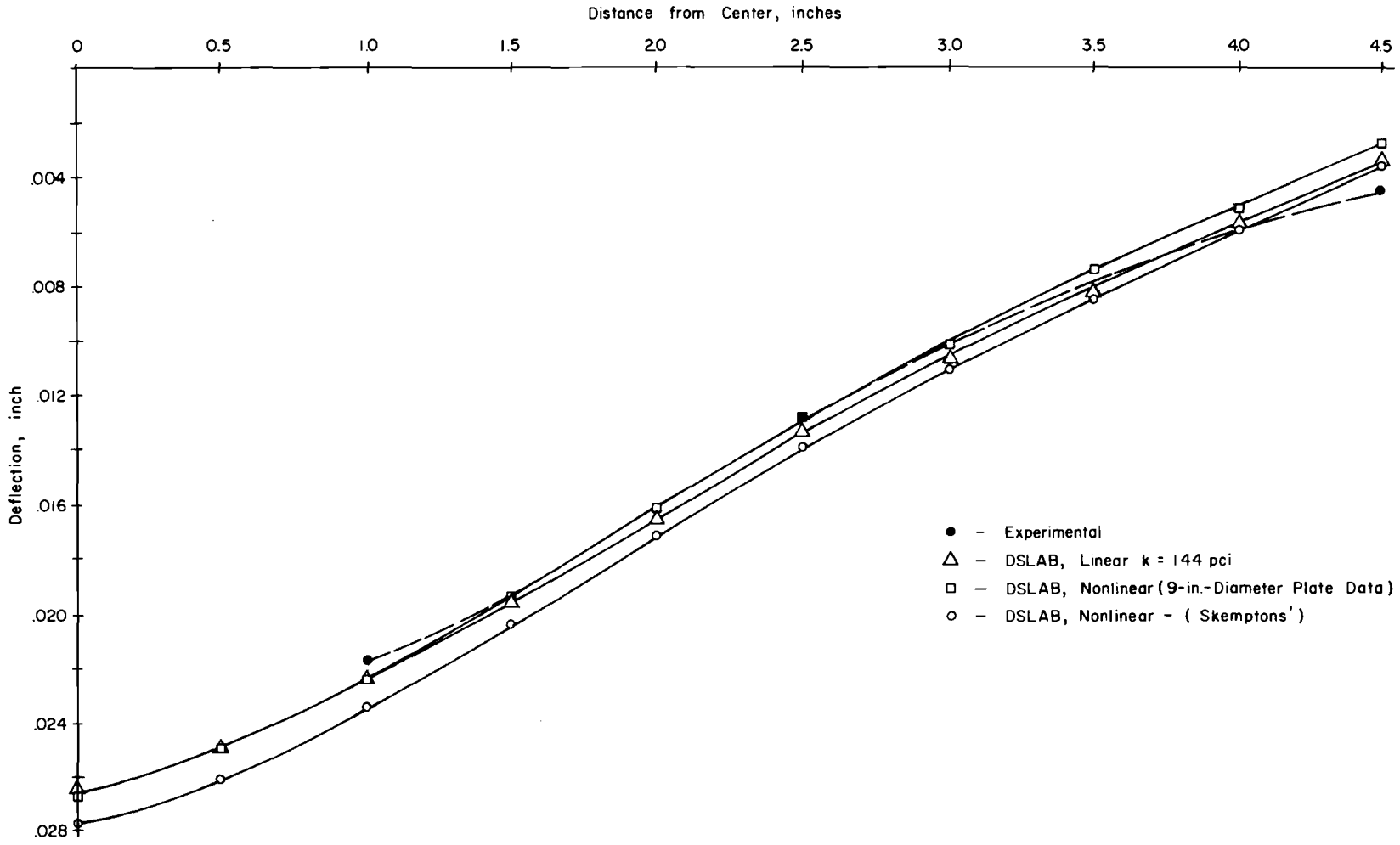

Fig A2.10. Experimental and analytical deflections on the center line for 100 pounds for preliminary center load test (series 320) - see Table A2.4.

TABLE A2.4. EXPERIMENTAL AND ANALYTICAL DEFLECTIONS FOR PRELIMINARY TEST ON INSTRUMENTED SLAB (SERIES 320)

Load: 100 lb in the center

Programs: DSLAB 30 and DSLAB 26 (18 x 18 increments)

Type of Solution	LVDT's					
	1	2	3	4	5	6
Distance from Center	1 inch	2.5 inch	4.5 inch	1.41 inch	3.53 inch	6.36 inch
Experimental	-0.02190	-0.01310	-0.00440	-0.01920	-0.00700	*
Linear springs k = 160 lbs/in^3	-0.02093	-0.01221	-0.00272	-0.01846	-0.00686	0.00385
% Error	-4.50	-4.06	-7.65	-3.38	-0.64	
Linear springs k = 144 lbs/in^3	-0.02231	-0.01330	-0.00332	-0.01978	-0.00765	0.00400
% Error	1.87	0.91	-4.92	2.65	2.97	
Nonlinear q - w curve (9-inch-diameter plate data)	-0.02241	-0.01311	-0.00271	-0.01980	-0.00706	0.00616
% Error	2.33	0.05	-7.71	2.74	0.27	
Nonlinear q - w curve (Skempton's)	-0.02359	-0.01411	-0.00353	-0.02094	-0.00792	0.00580
% Error	7.72	4.61	-3.97	7.94	4.18	

*Did not work.
Note: Plot along center line as shown in Fig A2.10.

TABLE A2.5. EXPERIMENTAL AND ANALYTICAL PRINCIPAL STRESSES FOR PRELIMINARY TEST ON INSTRUMENTED SLAB (SERIES 320)

Load: 100 lb in the center

Programs: DSLAB 30 and DSLAB 26 (18 x 18 increments)

Type of Solution	Rosette 1	Rosette 2	Rosette 3	Rosette 4
	Largest Stress	Largest Stress	Largest Stress	Largest Stress
Experimental	4820.00	1696.00	3264.00	*
Linear springs k = 160 psi	4614.00	1089.00	2543.00	658.00
% Error	-4.27	-12.60	-15.00	
Linear springs k = 144 psi	4738.00	1173.00	2639.00	694.70
% Error	-1.80	-10.85	-13.00	
Nonlinear springs (q - w curve) (9-inch-diameter plate data)	4892.00	1269.00	3272.00	815.00
% Error	1.49	-8.86	0.16	
Nonlinear springs (q - w curve) (Skempton's data)	4950.00	1310.00	3320.00	832.00
% Error	2.70	-8.01	1.16	

*Data not available.

APPENDIX 3

METHOD OF DATA REDUCTION FOR SLAB TESTS

APPENDIX 3. METHOD OF DATA REDUCTION FOR SLAB TESTS

Calibration Constants

Deflection

Deflections were measured by LVDT's which were calibrated before the slab testing. Calibration was accomplished by inserting locally machined gage blocks of known thickness and recording the output in millivolts (mv) on the digital voltmeter. Each calibration was repeated to check the reproducibility (details are given in Chapter 3). A plot between the deflection and related voltage was drawn. The slope of the linear curve drawn through most of the points established the calibration constant. Such curves along with the calibration constants are given in Figs A3.1, A3.2, and A3.3 for preliminary, center load, and corner loads slab tests (series 320, 330, and 340, respectively). The calibration constant of LVDT 1 for the center load slab test (series 330), for example, was 3.17 mv/0.001 inch (Fig A3.2).

Strain

Each gage was calibrated by shunting a known resistance in the gage circuit and recording the output, first on the digital voltmeter and then on the strain indicator. The calibration was also accomplished by using Eq 3.1. A calibration constant of 0.325 $\mu\epsilon/\mu v$ was established to get strain in μ-in/in.

Load

The calibration constants for load for the various test series were

(1) preliminary test (series 320) - 100 lb/mv,
(2) center load slab test (series 330) - 500 lb/mv, and
(3) corner loads slab test (series 340) - 200 lb/mv.

Sample Data Reduction

The output of loads, deflections (measured by LVDT's), and strains of the various channels were recorded on a digital voltmeter (DVM) by the

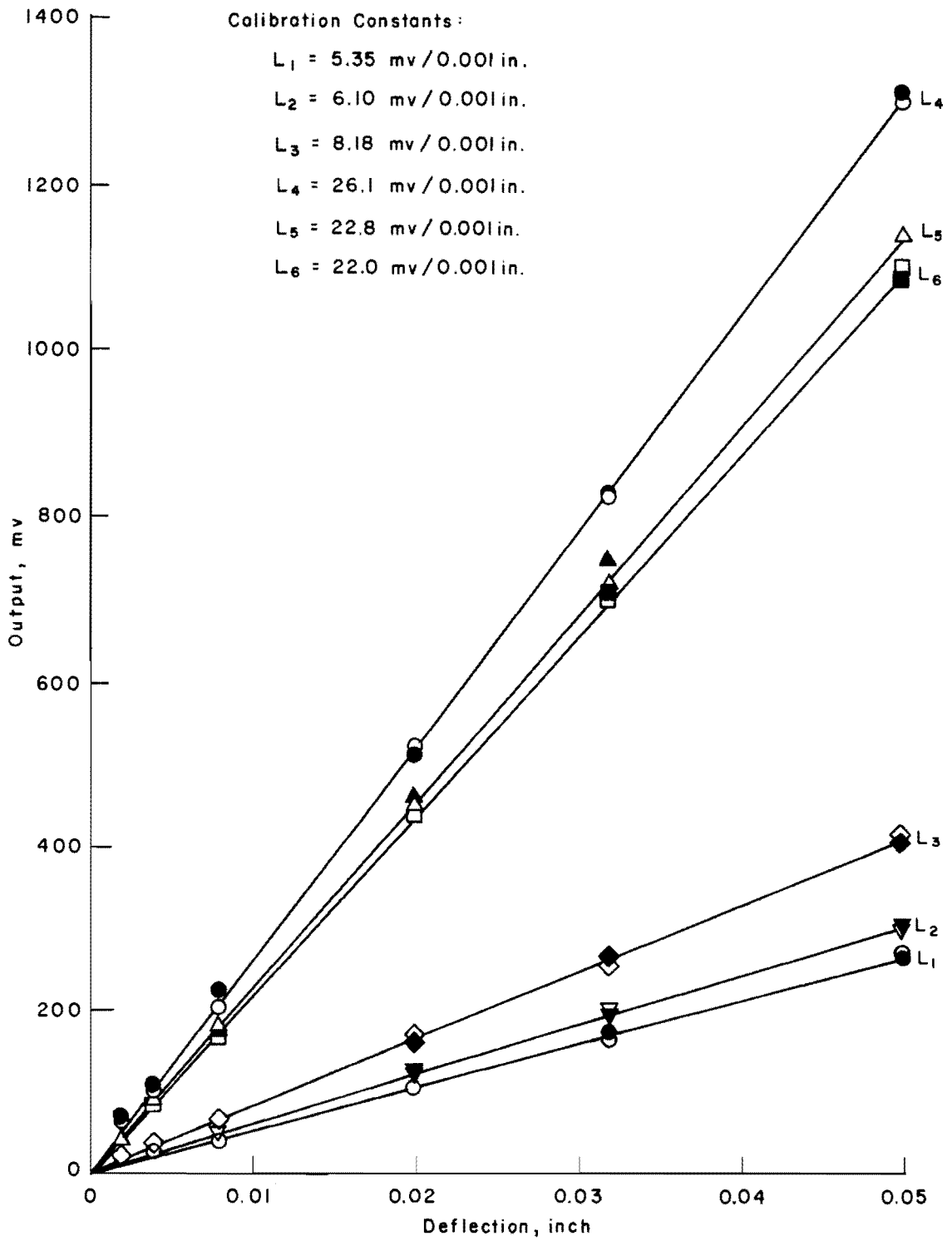

Fig A3.1. Calibration data for LVDT's for preliminary center load slab test (series 320).

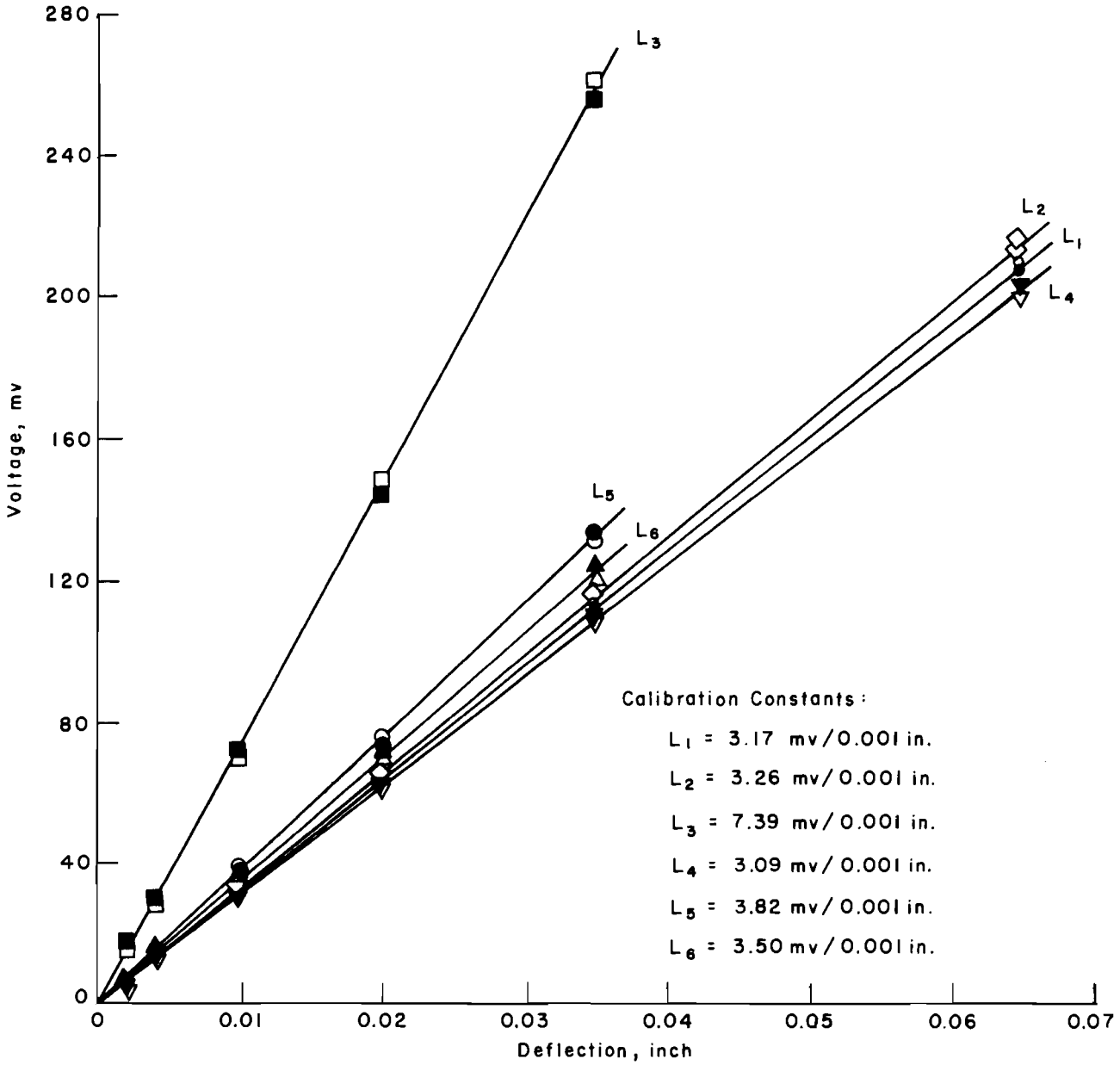

Fig A3.2. Calibration data for LVDT's for center load slab test (series 330).

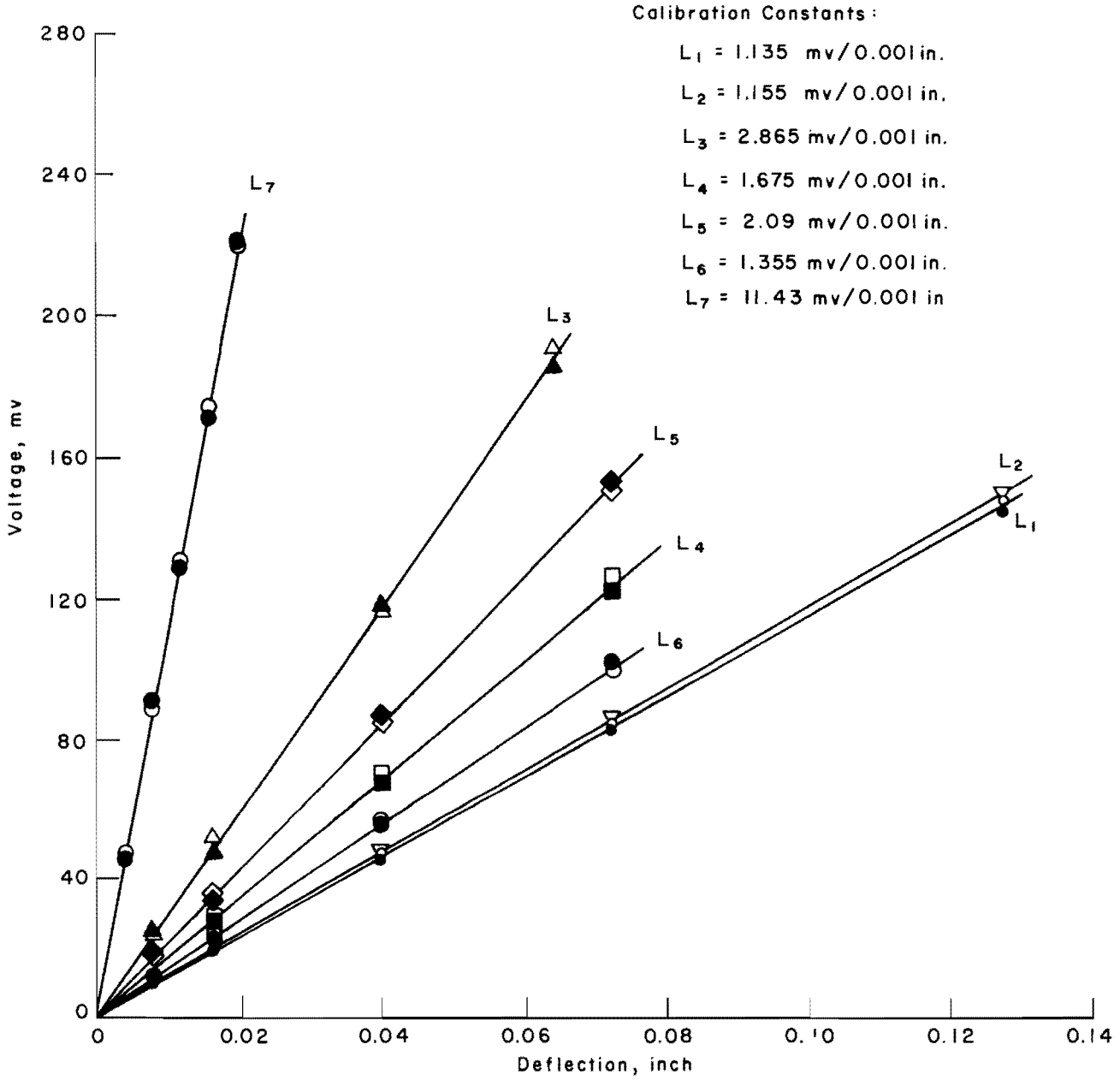

Fig A3.3. Calibration data for LVDT's for corner loads slab test (series 340).

scanning system. Table A3.1 shows the system connections for center load slab tests (series 320 and 330), and Table A3.2 for corner loads slab test (series 340).

Sample output as printed by the digital voltmeter is shown in Fig A3.4. This corresponds to channels 1 through 14 for center load slab test (series 330) taken during loading in the first cycle, five minutes after the load application. Sample calculations for load and corresponding deflection or strain are as follows:

Channel 1 (load):

Output = 28×10^{-5} v = 28×10^{-2} mv

Difference from initial reading = $(28 - 0)10^{-2}$ mv = 28×10^{-2} mv

Calibration constant = 500 lb/mv

Load = $28 \times 10^{-2} \times 500$ = 140 lb

Channel 2 (LVDT 1):

Output = -9 mv (rounded to full number)

Difference from initial reading = -9 - 106 = -115 mv

Calibration constant = 3.17 mv/0.001 inch

Deflection = $\frac{115}{3.17}$ = -0.0363 inch

Channel 13 (load):

Output = 31×10^{-2} mv

Difference from zero = $(31 - 0)10^{-2}$ = 31×10^{-2} mv

Load = 31×5 = 155 lb

Channel 14 (rosette 1(a)):

Output = -2080 μv

Difference from initial reading = -2080 - (-220) = -1860 μv

Calibration constant = 0.325 $\mu\varepsilon/\mu$v

Strain = -1860×0.325 = -605 μ-in/in

Similar computations for load, deflection, and strain were made for all the channels for all the tests during both loading and unloading. Sample calculations for the center load slab test during loading are given in Table A3.3 for loads and deflections for LVDT's 1, 2, and 3, and in Table A3.4 for loads and strains for rosette 1. Other calculations for all the tests are given in Ref 26.

Channel 14	1	4	−	·	0	0	2	0	8	5
Channel 13	1	3	+	·	0	0	0	3	1	5
	1	2	+	·	0	2	1	9	0	5
	1	1	+	·	0	0	0	3	2	5
	1	0	+	·	0	4	6	8	7	5
	0	9	+	·	0	0	0	3	1	5
	0	8	−	·	0	0	7	1	0	5
	0	7	+	·	0	0	0	3	0	5
	0	6	+	·	0	3	9	3	4	5
	0	5	+	·	0	0	0	2	9	5
	0	4	+	·	0	3	3	4	1	5
	0	3	+	·	0	0	0	2	9	5
Channel 2	0	2	−	·	0	0	8	6	8	5
Channel 1	0	1	+	·	0	0	0	2	8	5
	0	0	−	·	0	0	0	0	0	5

After Five Minutes During Loading

Fig A3.4. Sample output for center load slab test (series 330).

TABLE A3.1. SYSTEM CONNECTIONS FOR CENTER LOAD SLAB TEST (SERIES 320 AND 330)

DVM Channel	Function	Location
00	Shorted input	System zero
01	Load cell	
02	LVDT No. 1 (7v)	1 inch from center on center line
03	Load cell	
04	LVDT No. 2 (7v)	2.5 inches from center on center line
05	Load cell	
06	LVDT No. 3 (24v)	4.5 inches from center on center line (mid-edge)
07	Load cell	
08	LVDT No. 4 (7v)	1.41 inches from center on diagonal
09	Load cell	
10	LVDT No. 5 (24v)	3.53 inches from center on diagonal
11	Load cell	
12	LVDT No. 6 (24v)	6.36 inches from center on diagonal (corner)
13	Load cell	
14	Rosette No. 1(a)	1 inch from center on center line
15	Load cell	
16	Rosette No. 1(b)	1 inch from center on center line
17	Load cell	
18	Rosette No. 1(c)	1 inch from center on center line
19	Load cell	
20	Rosette No. 2(a)	3 inches from center on center line
21	Load cell	
22	Rosette No. 2(b)	3 inches from center on center line
23	Load cell	
24	Rosette No. 2(c)	3 inches from center on center line
25	Load cell	
26	Rosette No. 3(a)	1.41 inches from center on diagonal
24	Load cell	

(continued)

TABLE A3.1. (continued)

DVM Channel	Function	Location
28	Rosette No. 3(b)	1.41 inches from center on diagonal
29	Load cell	
30	Rosette No. 3(c)	1.41 inches from center on diagonal
31	Load cell	
32	Rosette No. 4(a)	3.53 inches from center on diagonal
33	Load cell	
34	Rosette No. 4(b)	3.53 inches from center on diagonal
35	Load cell	
36	Rosette No. 4(c)	3.53 inches from center on diagonal
37	Strain gage applied voltage	
38	LVDT power supply	
39	LVDT power supply	

TABLE A3.2. SYSTEM CONNECTIONS FOR CORNER LOADS SLAB TEST (SERIES 340)

DVM Channel	Function	Location
00	Shorted input	System zero
01	Load cell	
02	LVDT No. 1	6.36 inch from center on diagonal (corner near load)
03	Load cell	
04	LVDT No. 2	4.24 inch from center on diagonal
05	Load cell	
06	LVDT No. 3	1.41 inch from center on diagonal
07	Load cell	
08	LVDT No. 4	2.82 inch from center on diagonal (other side)
09	Load cell	
10	LVDT No. 5	4.5 inch from center on center line (mid-edge)
11	Load cell	
12	LVDT No. 7	2.5 inch from center on center line
13	Load cell	
14	LVDT No. 6	6.36 inch from center on diagonal (unloaded corner)
15	Load cell	
16	Strain gage No. 6	1.5 from corner along edge (near load)
17	Load cell	
18	Strain gage No. 5	3.5 from corner along edge
19	Load cell	
20	Rosette No. 3(a)	3.53 inch from center on diagonal
21	Load cell	
22	Rosette No. 3(b)	3.53 inch from center on diagonal
23	Load cell	
24	Rosette No. 3(c)	3.53 inch from center on diagonal
25	Load cell	

(continued)

TABLE A3.2. (continued)

DVM Channel	Function	Location
26	Rosette No. 2(a)	3.0 inch from center on center line
27	Load cell	
28	Rosette No. 2(c)	3.0 inch from center on center line
29	Load cell	
30	Rosette No. 2(b)	3.0 inch from center on center line
31	Load cell	
32	Rosette No. 4(b)	1.41 inch from center on diagonal (near load)
33	Load cell	
34	Rosette No. 4(a)	1.41 inch from center on diagonal
35	Load cell	
36	Rosette No. 4(c)	1.41 inch from center on diagonal
37	Strain gage applied voltage	
38	LVDT power supply	
39	LVDT power supply	

TABLE A3.3. TEST DATA FOR DEFLECTIONS FOR CENTER LOAD SLAB TEST (SERIES 330)

Time	LVDT No. 1					LVDT No. 2					LVDT No. 3				
Channel	1		2			3		4			5		6		
	Load		Deflection			Load		Deflection			Load		Deflection		
	Reading	Load lbs	Output μv	Difference from Zero μv	Deflection inch	Reading	Load lbs	Output μv	Difference from Zero μv	Deflection inch	Reading	Load lbs	Output μv	Difference from Zero μv	Deflection inch
0	0	0	106	0	.00000	0	0	109	0	.00000	0	0	91	0	.00000
20 sec	2	10	100	-6	-.00189	2	10	105	-4	-.00123	2	10	88	-3	-.00041
1 min	8	40	82	-24	-.00757	8	40	98	-11	-.00337	8	40	81	-10	-.00136
2 min	10	50	75	-31	-.00980	10	50	95	-14	-.00430	10	50	78	-13	-.00176
3 min	16	80	52	-54	-.01710	16	80	78	-31	-.00950	17	85	66	-25	-.00339
4 min	22	110	23	-83	-.02620	22	110	58	-51	-.01565	23	115	53	-38	-.00515
5 min	28	140	-9	-115	-.03630	29	145	33	-76	-.02330	29	145	39	-52	-.00705
6 min	34	170	-44	-150	-.00473	34	170	14	-95	-.02910	35	175	24	-67	-.00906
7 min	38	190	-70	-176	-.05550	38	190	-9	-118	-.03620	38	190	7	-84	-.01140
8 min	41	205	-98	-204	-.06440	42	210	-33	-142	-.04360	44	220	-12	-103	-.01395
9 min	47	235	-103*	-209	-.06600	47	235	-70	-179	-.05500	47	235	-32	-123	-.01665

*Out of range.

TABLE A3.4. TEST DATA FOR STRAINS FOR ROSETTE 1 FOR CENTER LOAD SLAB TEST SERIES (SERIES 330)

Time	Strain No. 1A					Strain No. 1B					Strain No. 1C				
Channel	13		14			15		16			17		18		
	Load		Strain			Load		Strain			Load		Strain		
	Output	Load lbs	Output μv	Difference from Zero μv	Strain με	Output	Load lbs	Output μv	Difference from Zero μv	Strain με	Output	Load lbs	Output μv	Difference from Zero μv	Strain με
0	-0	0	-220	0	0	1-0	0	-10	0	0	-0	0	-60	0	0
20 sec	3	15	-340	120	39	5-4	20	-70	60	19	4	20	-100	40	13
1 min	9	45	-600	380	124	10-9	45	-210	200	65	9	45	-140	80	26
2 min	11	55	-720	500	163	12-11	55	-260	250	81	12	60	-200	140	45
3 min	17	85	-1170	950	309	18-17	85	-470	460	150	17	85	-280	220	72
4 min	25	125	-1690	1470	480	26-25	125	-830	820	267	25	125	-450	390	127
5 min	31	155	-2080	1860	605	32-31	155	-1120	1110	361	31	155	-570	510	166
6 min	36	180	-2380	2160	704	37-36	180	-1350	1340	436	36	180	-740	680	221
7 min	40	200	-2650	2430	790	41-40	200	-1600	1590	517	40	200	-870	810	264
8 min	42	210	-2800	2580	840	43-42	210	-1700	1690	550	43	215	-950	890	290
9 min	49	245	-3340	3120	1020	50-49	245	-2120	2110	685	49	245	-1160	1100	358

Determination of Largest Principal Stress

Measured

From the strains of the rectangular rosettes for a particular load, the principal stresses were calculated, using the following equations (Ref 31):

$$\sigma_{max} = \frac{E}{2}\left[\frac{\epsilon_a - \epsilon_c}{1 - \nu} + \frac{1}{1 + \nu}\sqrt{(\epsilon_a + \epsilon_3)^2 + \left(2\epsilon_b - (\epsilon_a + \epsilon_3)\right)^2}\right] \quad \text{(A3.1)}$$

$$\sigma_{min} = \frac{E}{2}\left[\frac{\epsilon_a - \epsilon_c}{1 - \nu} - \frac{1}{1 + \nu}\sqrt{(\epsilon_a + \epsilon_3)^2 + \left(2\epsilon_b - (\epsilon_a + \epsilon_3)\right)^2}\right] \quad \text{(A3.2)}$$

where

σ_{max} = maximum principal stress,

σ_{min} = minimum principal stress,

E = modulus of elasticity of material,

ν = Poisson's ratio of material,

ϵ_a, ϵ_b, ϵ_c = strain readings of the rosette.

The largest principal stress corresponded to the larger absolute value of σ_{max} and σ_{min}. The direction of the largest principal stress was then calculated using

$$\alpha = \frac{1}{2} \tan^{-1} \left[\frac{2\epsilon_b - (\epsilon_a + \epsilon_c)}{\epsilon_a - \epsilon_c} \right] \quad \text{(A3.3)}$$

where

α = angle made by the largest principal with the ϵ_a direction.

For example, Fig A3.5 shows the load versus strain for the three gages of rosette 1 for the center load slab test.

For a load of 200 pounds

ϵ_a = -790 μ-in/in

ϵ_b = -517 μ-in/in

ϵ_c = -264 μ-in/in

Using Eq A3.1 and A3.2, the largest principal stress is 10,421 lb/in^2 (compressive). Its angle in relation with the direction of ϵ_a equals 1^o.

Similar calculations were done for different loads during both loading and unloading. Load versus largest principal stress curves thus obtained are given in Fig 45. For the other rosettes in the center load and corner loads slab tests, the largest principal stresses and their directions were obtained the same way and are given in Ref 26.

DSLAB Solutions

The DSLAB 30 solution prints out the largest principal stresses directly whereas DSLAB 26 gives the largest principal moments. The principal moments thus obtained were converted into principal stresses using

$$\sigma = \frac{My}{I} \quad \text{(A3.4)}$$

where

σ = largest principal stress,

M = largest principal moment,

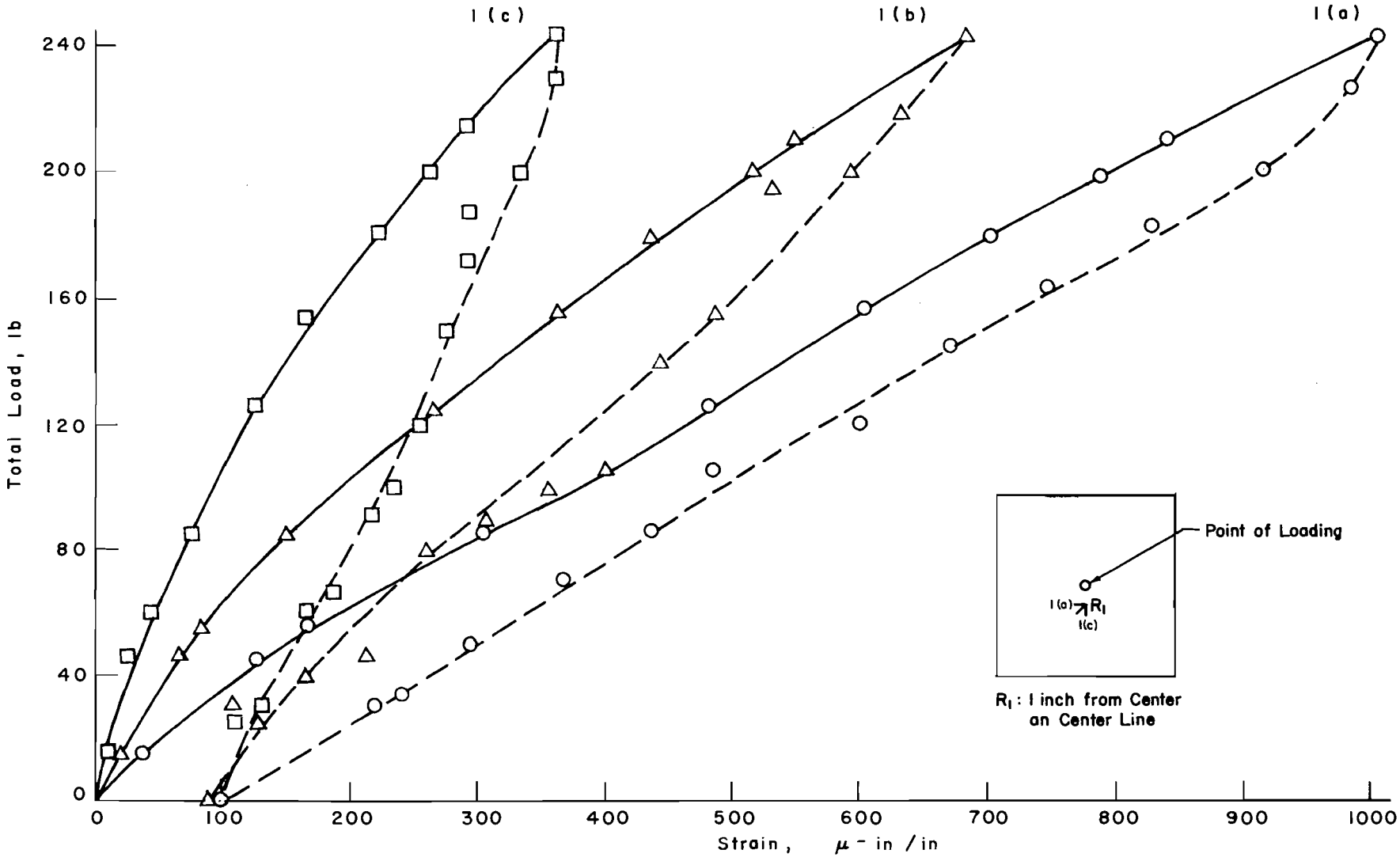

Fig A3.5. Load versus strain for rosette 1 for center load slab test.

y = distance from neutral axis = 1/16 inch,

I = moment of inertia/unit width.

For the slab under consideration Eq A3.4 reduces to

$$\sigma = 384M \tag{A3.5}$$

The largest principal stresses thus obtained are given in Ref 26.

Determination of Stresses Along the Edge

In the corner loads slab test, strains were measured along one edge at two locations, as shown in Fig 56. The stresses along the edge were found from strains.

For a plane stress case, the stresses can be calculated (Ref 47) in the x and y-directions, for an isotropic case, if the strains in the two directions and the elastic properties (E and ν) are known, i.e.,

$$\sigma_x = \frac{E}{1 - \nu^2} (\epsilon_x + \nu\epsilon_y) \tag{A3.6}$$

$$\sigma_y = \frac{E}{1 - \nu^2} (\nu\epsilon_x + \epsilon_y) \tag{A3.7}$$

For the case under consideration, strains in the y-direction ϵ_y, i.e., perpendicular to the edge, were neglected, and stresses along the edge were determined using the following equation:

$$\sigma_x = \frac{E}{1 - \nu^2} (\epsilon_x) \tag{A3.8}$$

Figure A3.6 shows the load versus strain curve for gage 5, and the corresponding stresses as calculated for different loads are shown in Fig 61.

In the DSLAB solutions, moments and stresses are calculated using half of the stiffness along the edge. To compare them with the experimental solutions, DSLAB solutions were multiplied by 2. They are given in Ref 26.

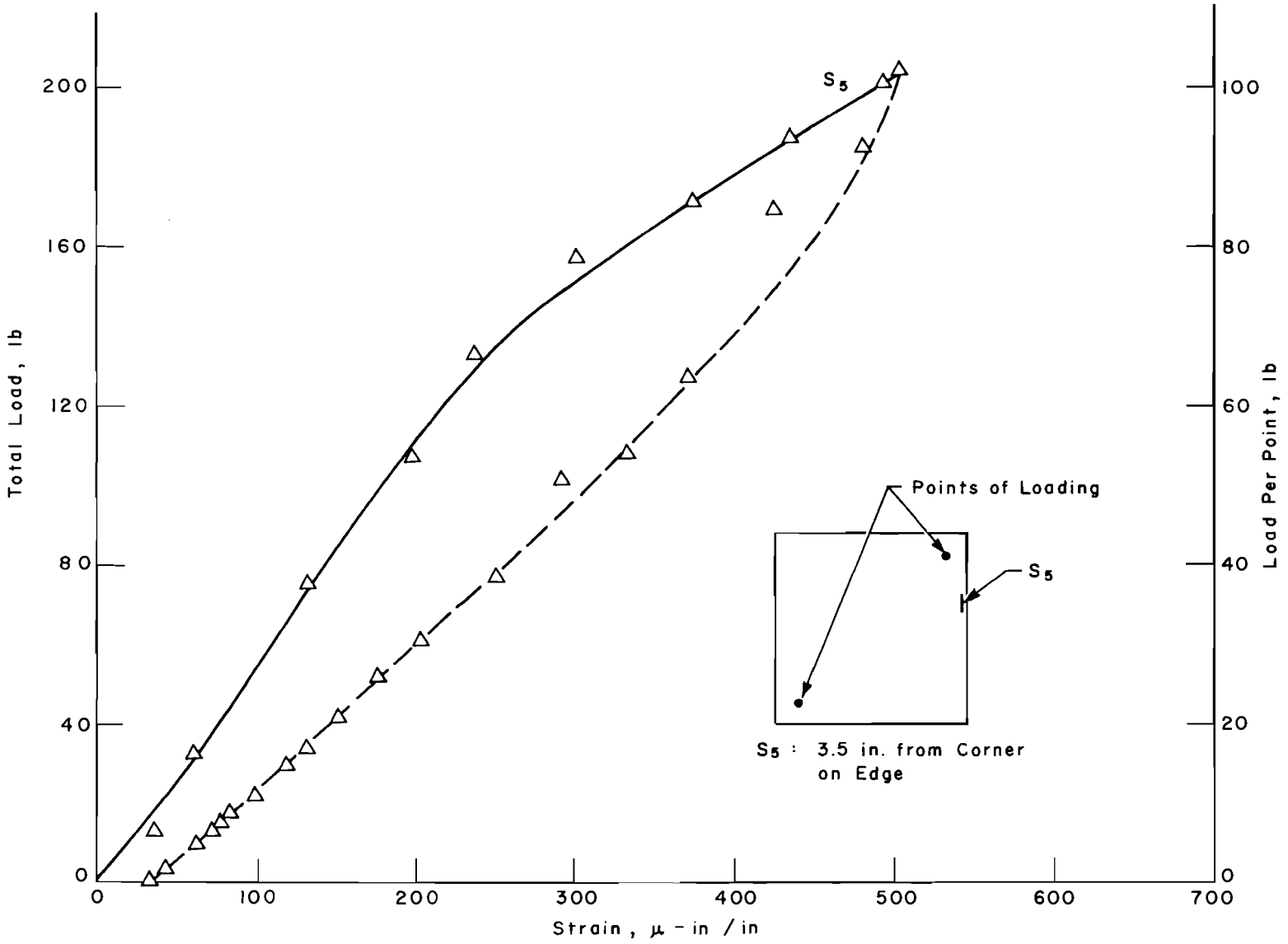

Fig A3.6. Load versus strain for strain gages along edge for corner loads slab test (series 340).

APPENDIX 4

SKEMPTON'S RECOMMENDATION TO PREDICT PRESSURE VERSUS DEFLECTION CHARACTERISTIC FROM STRESS-STRAIN RELATION OF SOIL

APPENDIX 4. SKEMPTON'S RECOMMENDATION TO PREDICT PRESSURE VERSUS DEFLECTION CHARACTERISTIC FROM STRESS-STRAIN RELATION OF SOIL

The method of soil representation used herein is based upon a theory of foundation deflection advanced by Skempton (Ref 40) in which strain in specimens of clay soil tested in triaxial compression is related to the deformation of a rigid foundation resting on the surface of a mass of the clay soil. This theory has been used by Reese and Matlock (Refs 37 and 24) for laterally loaded piles and by Lee (Ref 21) for slabs resting on plasteline, a plastic modeling clay.

Skempton's (Ref 40) derivation of a relationship between strain in compression tests and the deformation of a plate or foundation at the surface of a mass of soil is restated here for the convenience of the reader, with minor notation changes incorporated for consistency in this report.

From the theory of elasticity, the mean settlement of a rigid foundation of width or diameter B on the surface of a semi-infinite solid is given by the expression

$$y = pBI_w \frac{1 - \mu^2}{E} \qquad \text{(A4.1)}$$

where

y = deflection or settlement,

p = foundation pressure,

B = width of footing,

I_w = influence value which depends upon the shape and rigidity of the foundation,

μ = Poisson's ratio of the solid,

E = modulus of elasticity of the solid.

For saturated clays Eq A4.1 may be written as

$$\frac{y}{B} = \frac{p}{p_f} \frac{p_f}{c} I_w \frac{I - \mu^2}{\frac{E}{c}} \tag{A4.2}$$

where

p_f = ultimate bearing capacity,

c = apparent cohesion of the clay, or the shear strength under undrained loading conditions ($\phi = 0$) .

For such clays (i.e., no water content change under applied stress) and with $\mu = 0.5$, the ultimate bearing capacity (Ref 44) is

$$p_f = cN_c + q \tag{A4.3}$$

where

N_c = bearing capacity factor depending on ϕ , plan dimensions of the foundation and its depth;

q = overburden pressure at foundation level.

In the case of the foundation, at the surface, $q = 0$ so

$$N_c = \frac{p_f}{c} \tag{A4.4}$$

Lee, Skempton, and Timoshenko (Refs 21, 40, and 46) show that for a rigid circular footing at the surface

$$I_w = \frac{\pi}{4} \tag{A4.5}$$

Thus for a rigid circular plate at the surface

$$\frac{y}{B} = \frac{p}{p_f} N_c \frac{\frac{\pi}{4}\left[1 - (0.5)^2\right]}{\frac{E}{c}} \tag{A4.6}$$

From the undrained triaxial compression test, strain is defined as

$$\epsilon = \frac{\sigma_1 - \sigma_3}{E} \tag{A4.7}$$

where

ϵ = axial strain,

$(\sigma_1 - \sigma_3)$ = deviator stress,

E = secant Young's modulus at the stress $(\sigma_1 - \sigma_3)$.

Equation A4.7 may be rewritten

$$\epsilon = \frac{(\sigma_1 - \sigma_3)}{(\sigma_1 - \sigma_3)_f} \frac{(\sigma_1 - \sigma_3)_f}{c} \frac{1}{\frac{E}{c}} \tag{A4.8}$$

where

$(\sigma_1 - \sigma_3)_f$ = ultimate deviator stress.

For completely saturated clays with no water content change under applied stress, the failure is defined, as shown in Fig A4.1, by

$$(\sigma_1 - \sigma_3)_f = 2c$$

Thus Eq A4.8 reduces to

$$\epsilon = \frac{\sigma_1 - \sigma_3}{(\sigma_1 - \sigma_3)_f} \frac{2}{\frac{E}{c}} \tag{A4.9}$$

For a material, $\frac{E}{c}$ is the same whether the material is tested in triaxial compression or in bearing capacity, if the same proportion of ultimate strength is considered in either case; therefore,

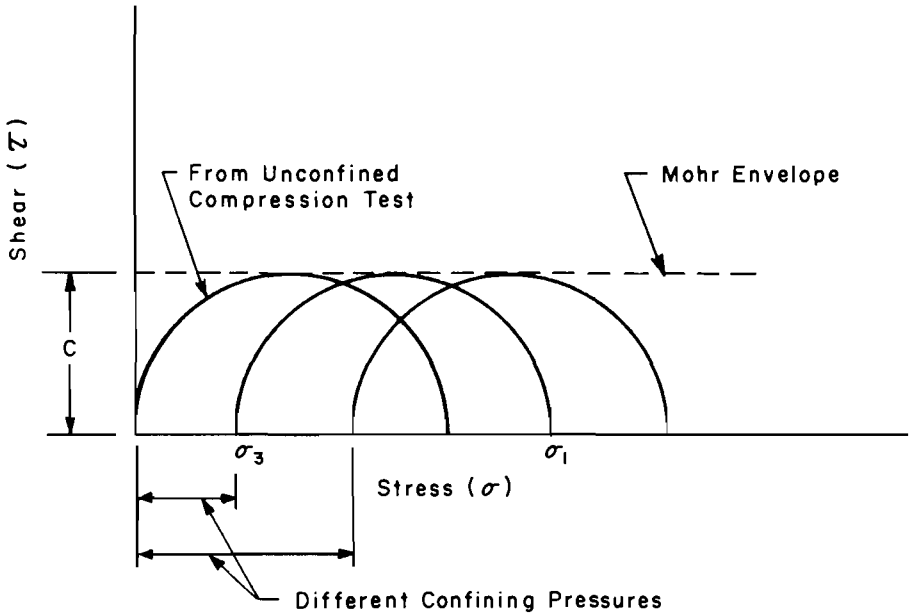

Fig A4.1. Mohr failure representation of saturated clays.

$$\frac{\sigma_1 - \sigma_3}{(\sigma_1 - \sigma_3)_f} = \frac{p}{p_f} \tag{A4.10}$$

and

$$\frac{\varepsilon}{2} = \frac{y}{B} \frac{1}{N_c} \frac{1}{\frac{\pi}{4}\left[1 - (0.5)^2\right]} \tag{A4.11}$$

Thus, for the same ratio of applied stress to ultimate stress, the deformation in a plate bearing test is related to the axial strain in a compression test by the equation

$$\frac{y}{B} = 0.2945\, N_c \varepsilon \tag{A4.12}$$

Equation A4.12 can be modified for other shapes by using appropriate values of I_w .

The stress-strain characteristics of the soil are determined by static loading in undrained triaxial or unconfined compression tests. The rate of loading can be kept the same in both the plate load test and the triaxial test. Assuming failure to occur at deflections negligibly small compared with breadth of the footing, the theoretical value of N_c should be 6.2 for circular footings with rough bases. Experimentally, when the full shear strength of the clay is mobilized and failure occurs, N_c is reported to be 6.8 by Lee (Ref 21).

The preceding theory leads to a procedure for predicting plate deflection from unconfined compression tests on a saturated clay, as shown in Fig A4.2, and the ultimate bearing capacity p_f by Eq A4.4 by

$$p_f = cN_c$$

If shear strength c is taken as half the unconfined compression strength σ_f then

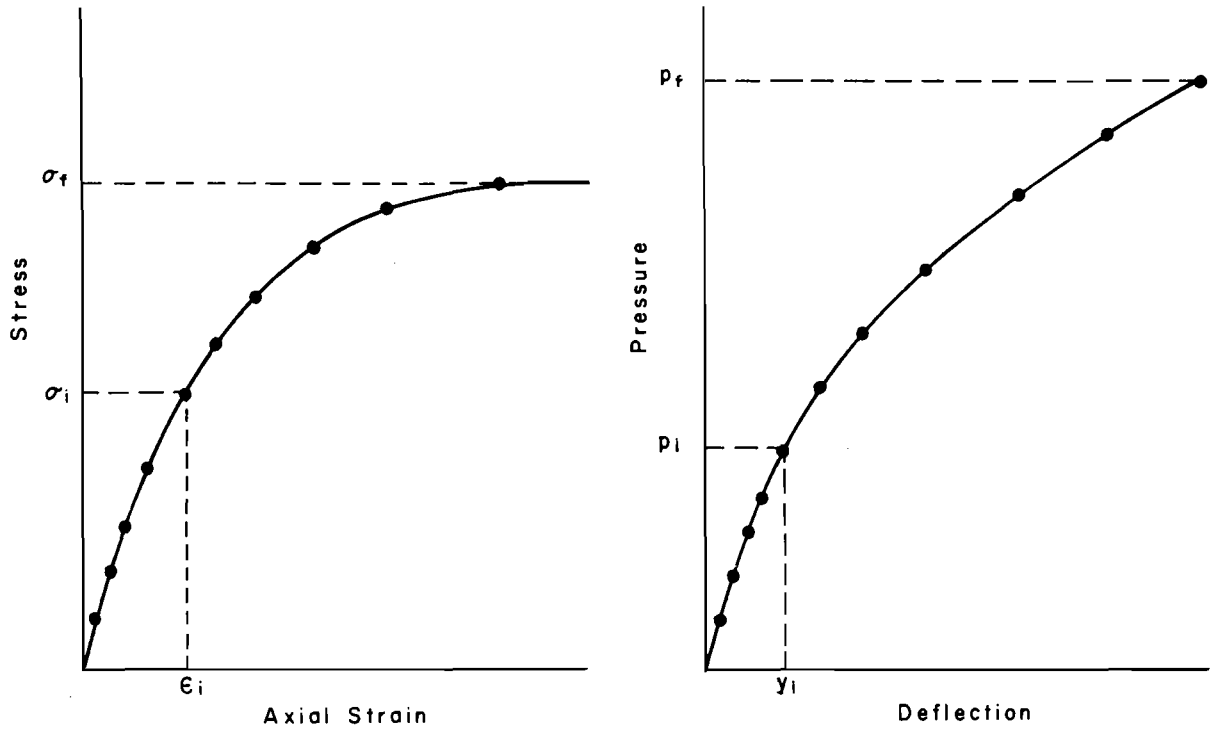

(a) Stress-strain characteristic from unconfined compression test.

(b) Pressure versus deflection relation for rigid plate.

Fig A4.2. Skempton's method of conversion from stress-strain characteristic of saturated clays to pressure-deflection relation.

$$p_f = N_c \frac{\sigma_f}{2} \tag{A4.13}$$

The following procedure can be adopted to predict the deflection of a rigid circular plate on the surface of a mass of clay (Fig A4.2):

(1) Select a stress σ_i from the compression test and find the corresponding strain ϵ_i as shown in Fig A4.2(a).

(2) Calculate the deflection y_i for an appropriate value of N_c, e.g., $N_c = 6.8$, using the relation

$$y_i = 0.2945\, N_c B \epsilon_i$$

(3) Plot the calculated value of y_i at a plate pressure

$$p_i = \frac{N_c}{2} \sigma_i$$

(4) Repeat the above process for enough points to define the curve as shown in Fig A4.2(b).

Using this procedure, the stress-strain relationships at many points along the curve from the unconfined compression test were converted to pressure versus deflection characteristic for a 9-inch-diameter plate as shown in Fig 46.

APPENDIX 5

CYCLIC TEST DATA

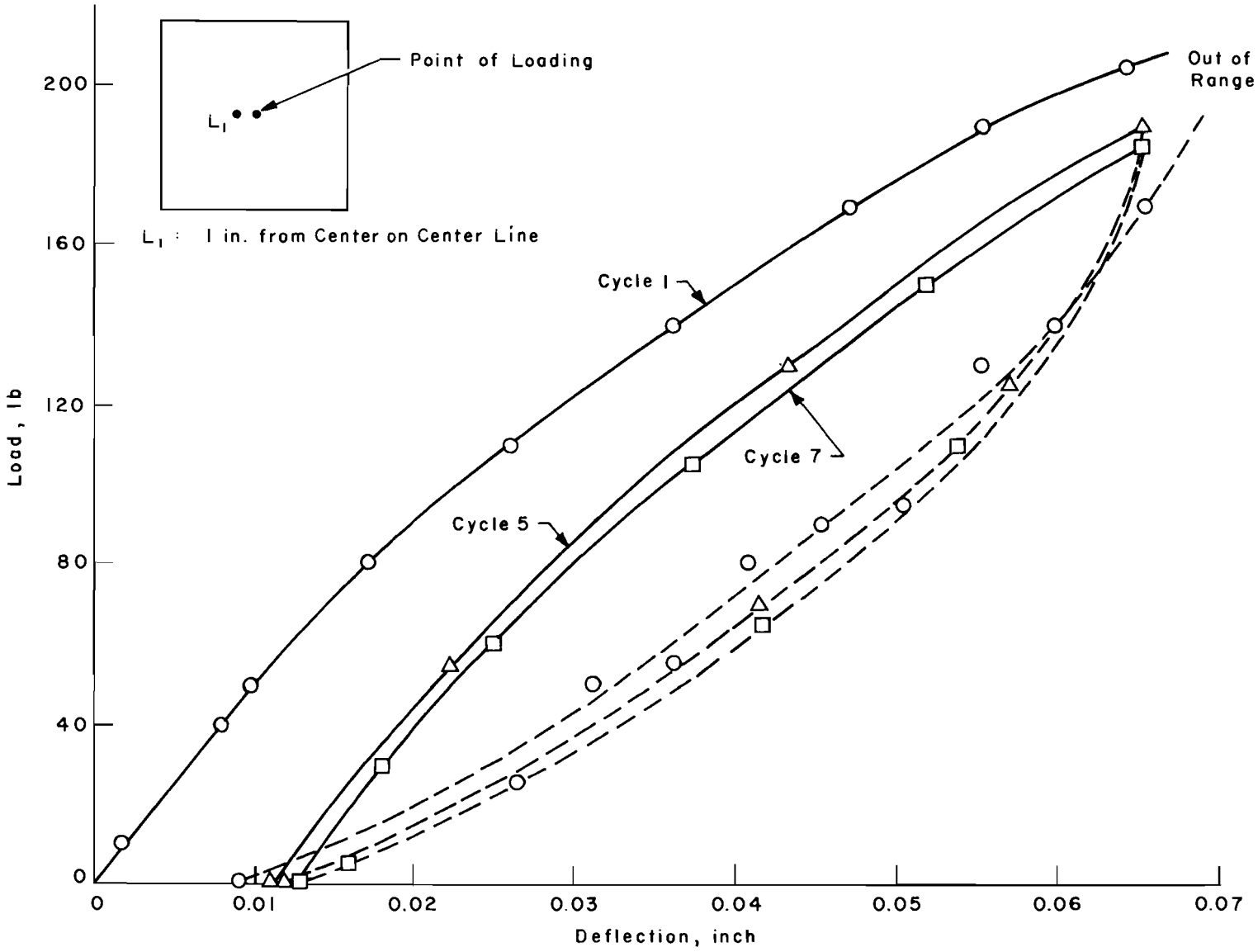

Fig A5.1. Load versus deflection for LVDT 1 for center cyclic load slab test (series 330).

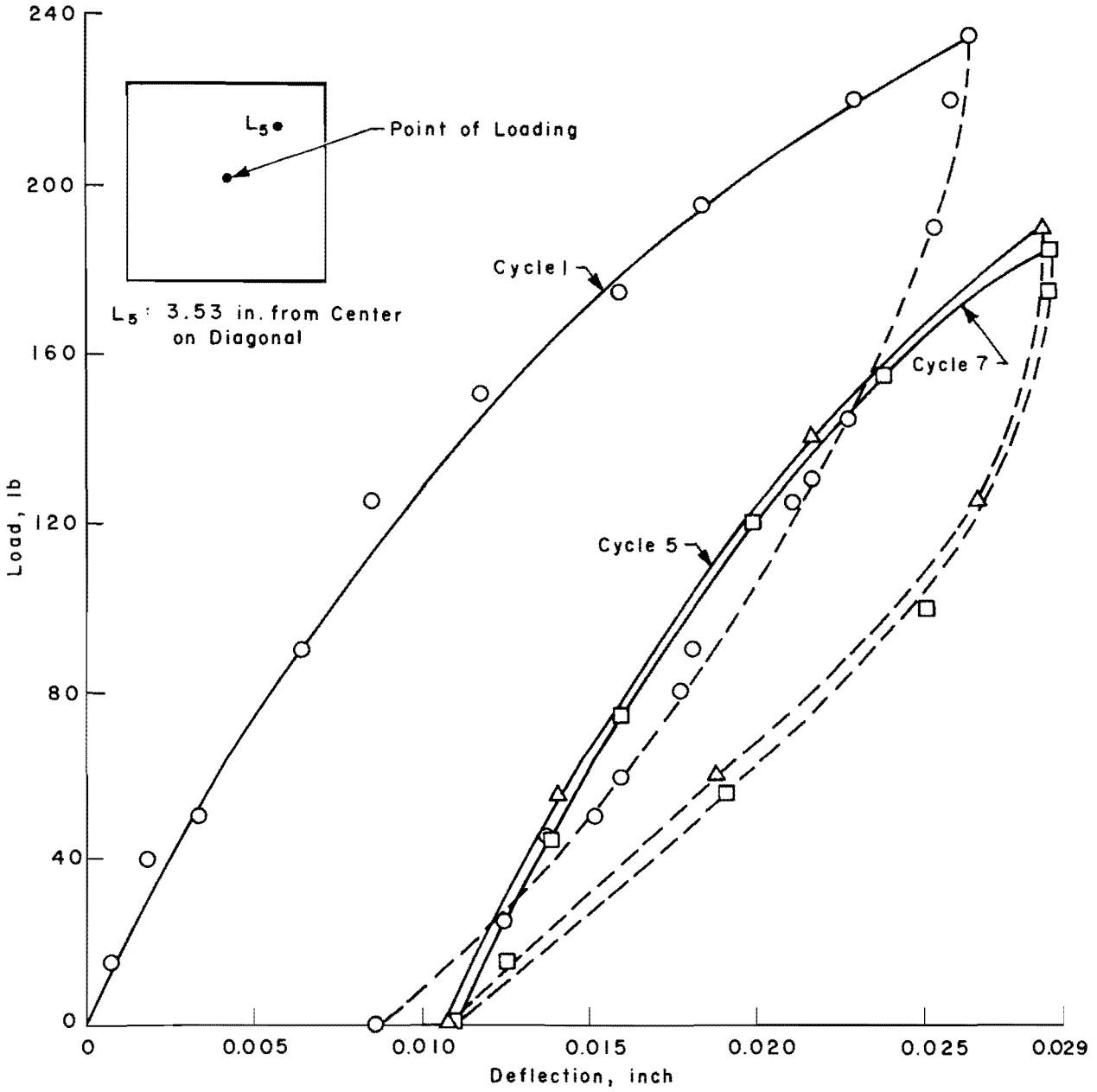

Fig A5.2. Load versus deflection for LVDT 5 for center cyclic load slab test (series 330).

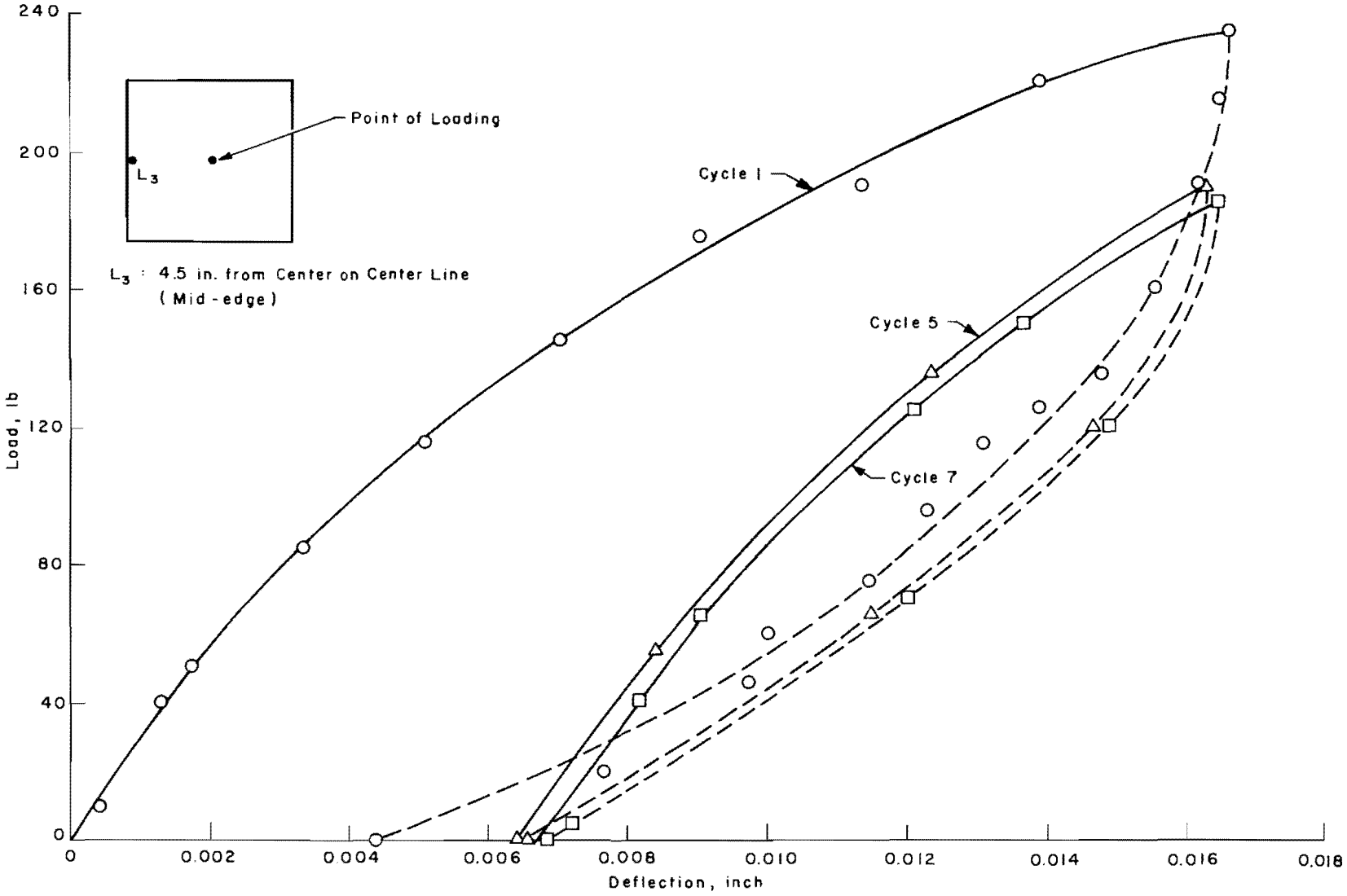

Fig A5.3. Load versus deflection for LVDT 3 for center cyclic load slab test (series 330).

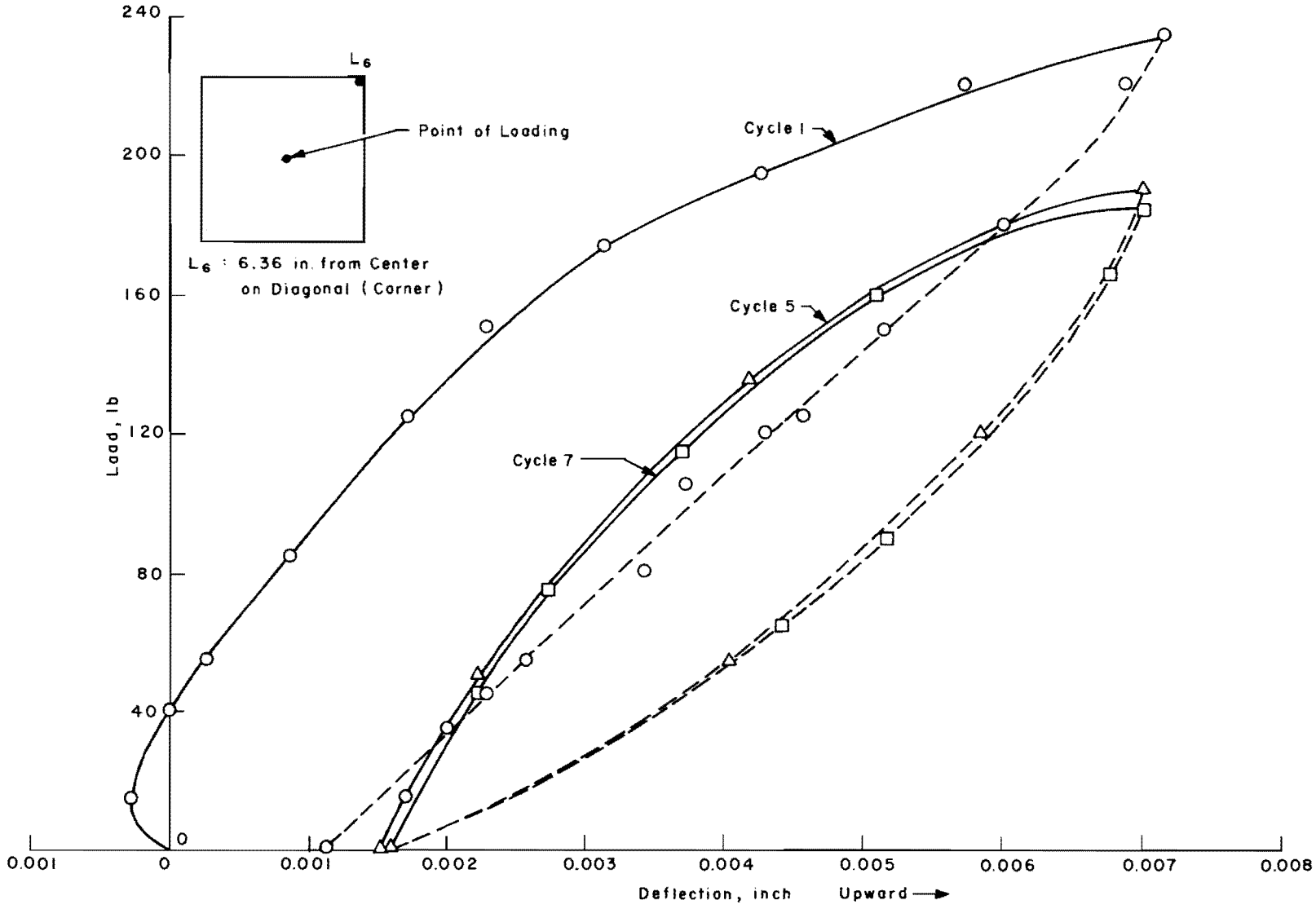

Fig A5.4. Load versus deflection for LVDT 6 for center cyclic load slab test (series 330).

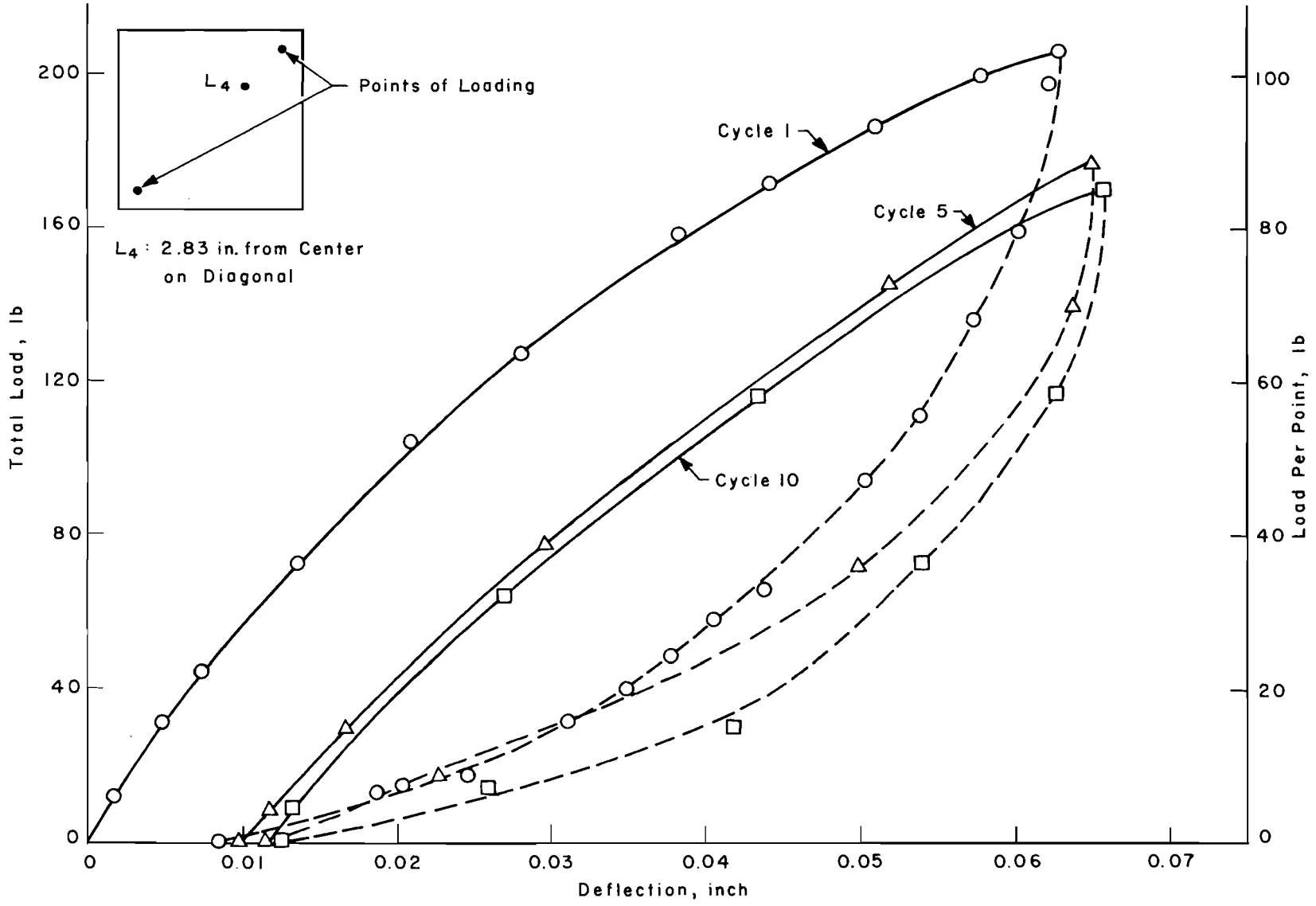

Fig A5.5. Load versus deflection for LVDT 4 for corner cyclic loads slab test (series 340).

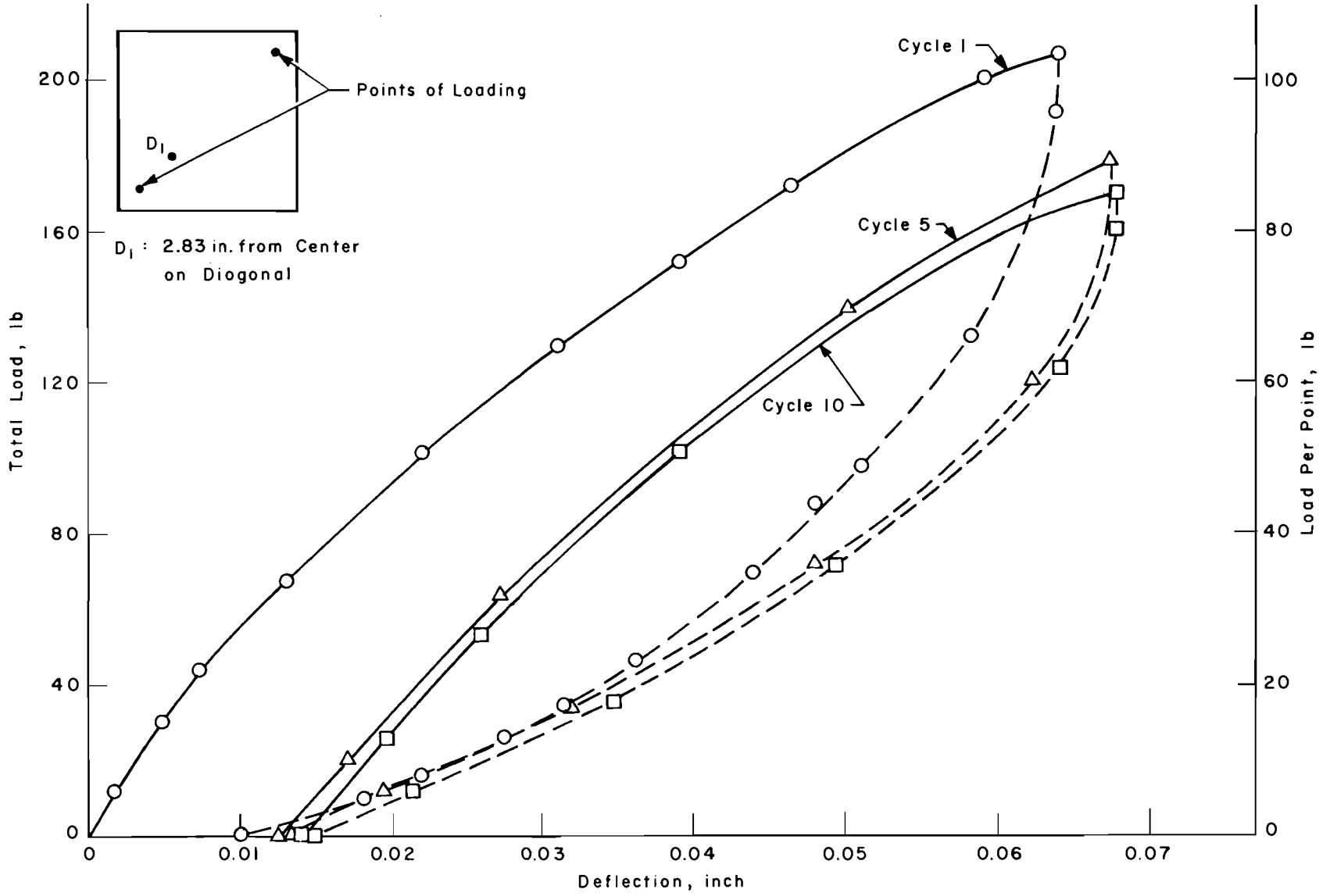

Fig A5.6. Load versus deflection for dial gage 1 for corner cyclic loads slab test (series 340).

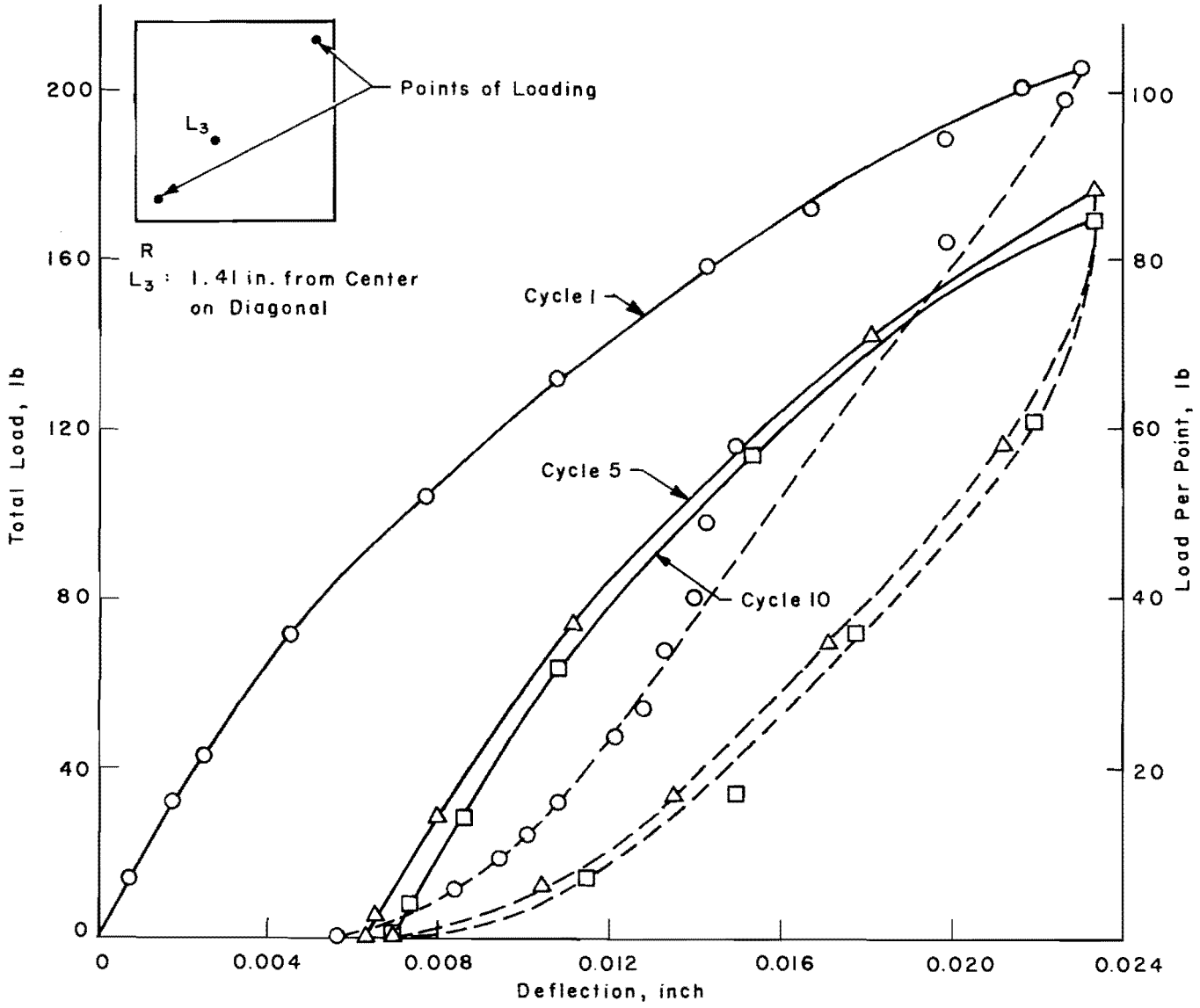

Fig A5.7. Load versus deflection for LVDT 3 for corner cyclic loads slab test (series 340).

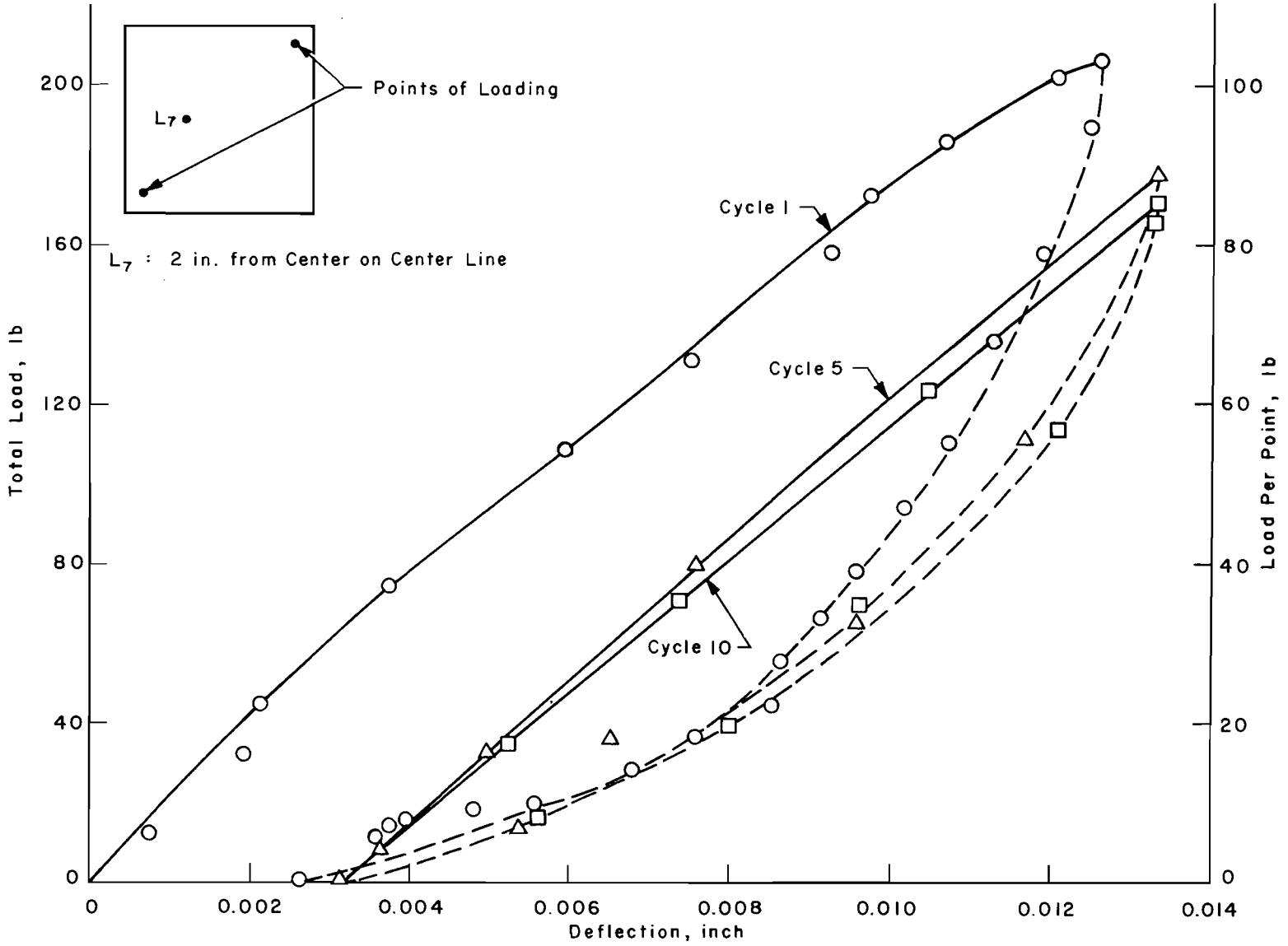

Fig A5.8. Load versus deflection for LVDT 7 for corner cyclic loads slab test (series 340).

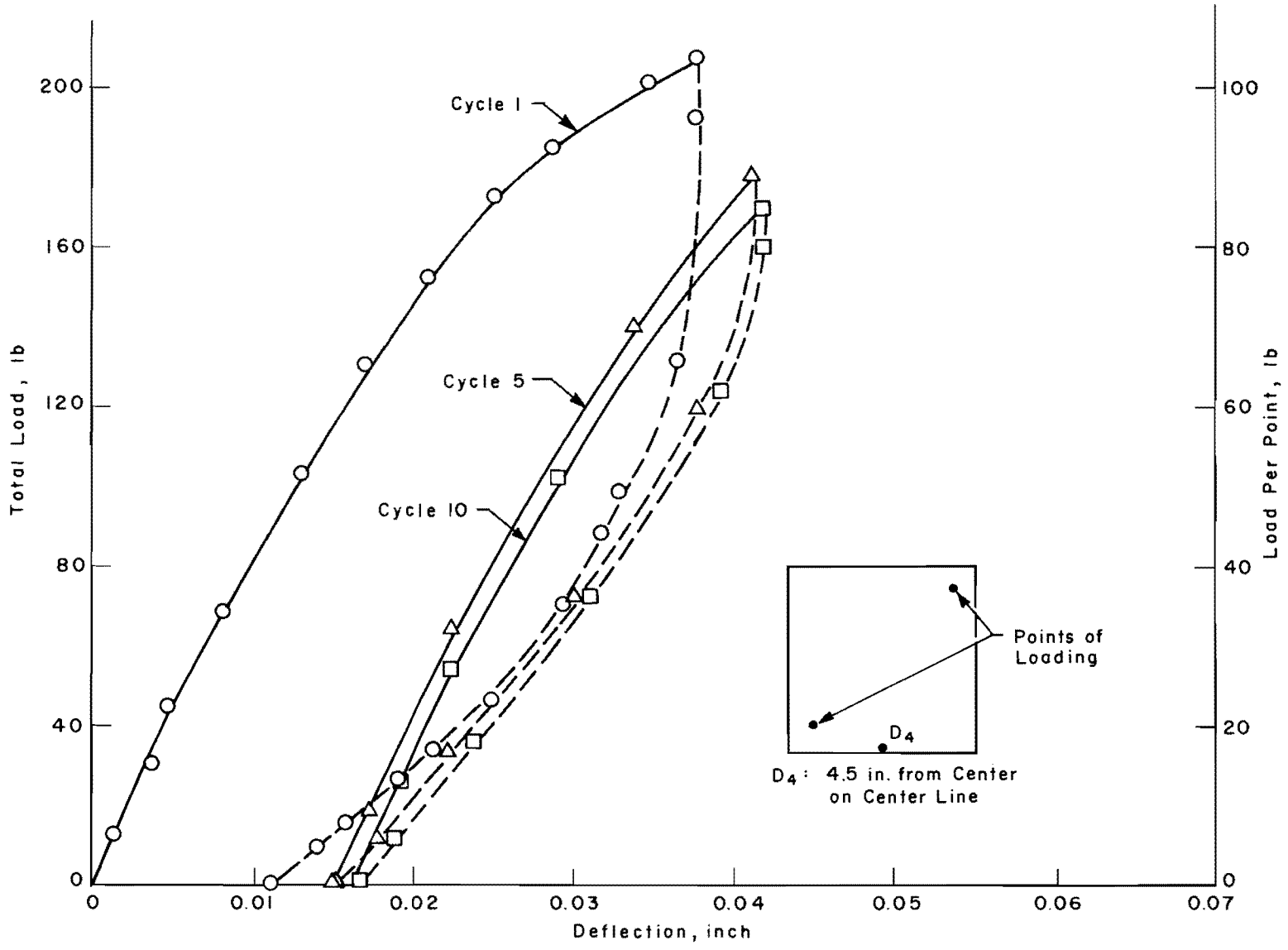

Fig A5.9. Load versus deflection for dial gage 4 for corner cyclic loads slab test (series 340).

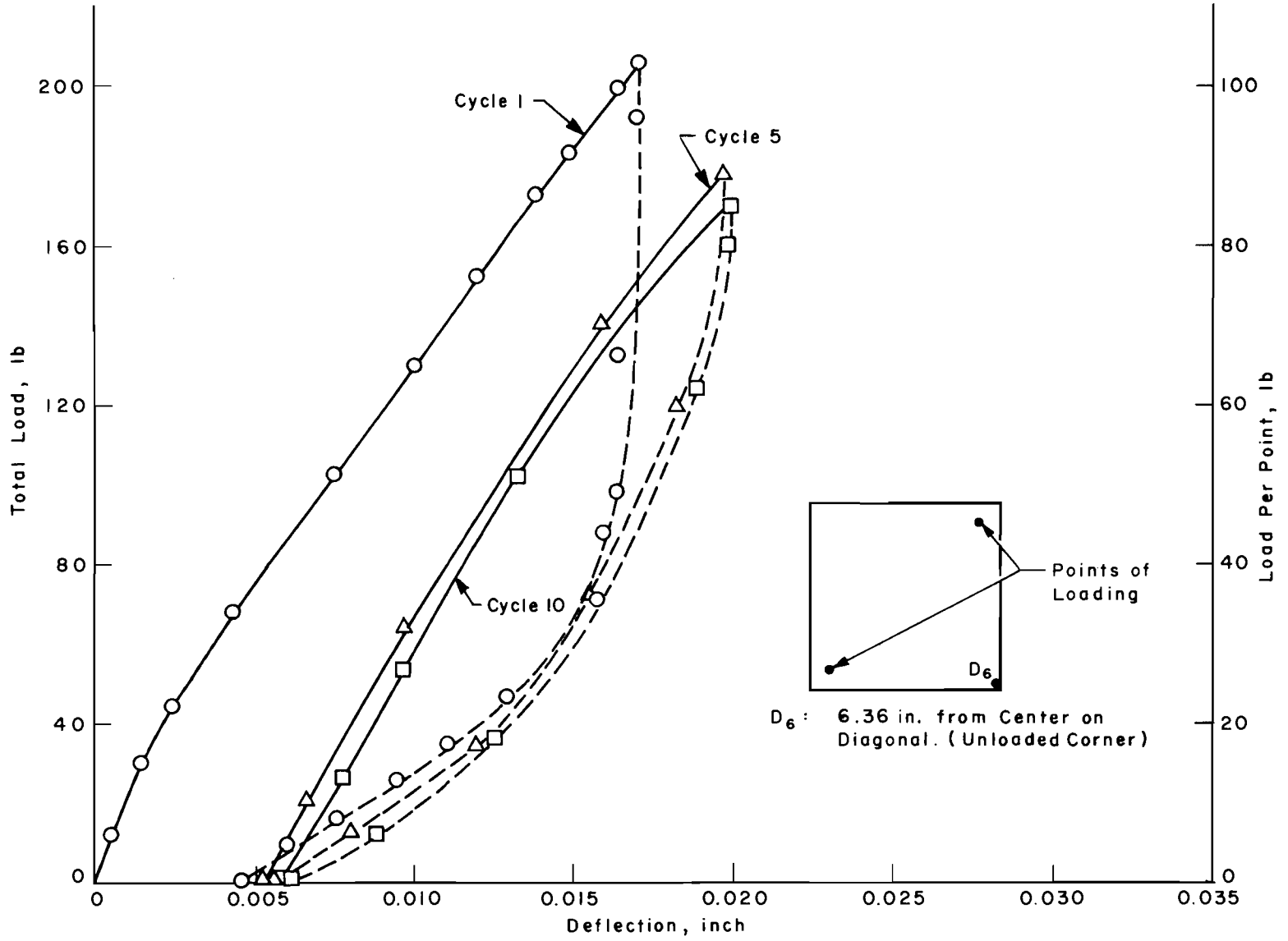

Fig A5.10. Load versus deflection for dial gage 6 for corner cyclic loads slab test (series 340).

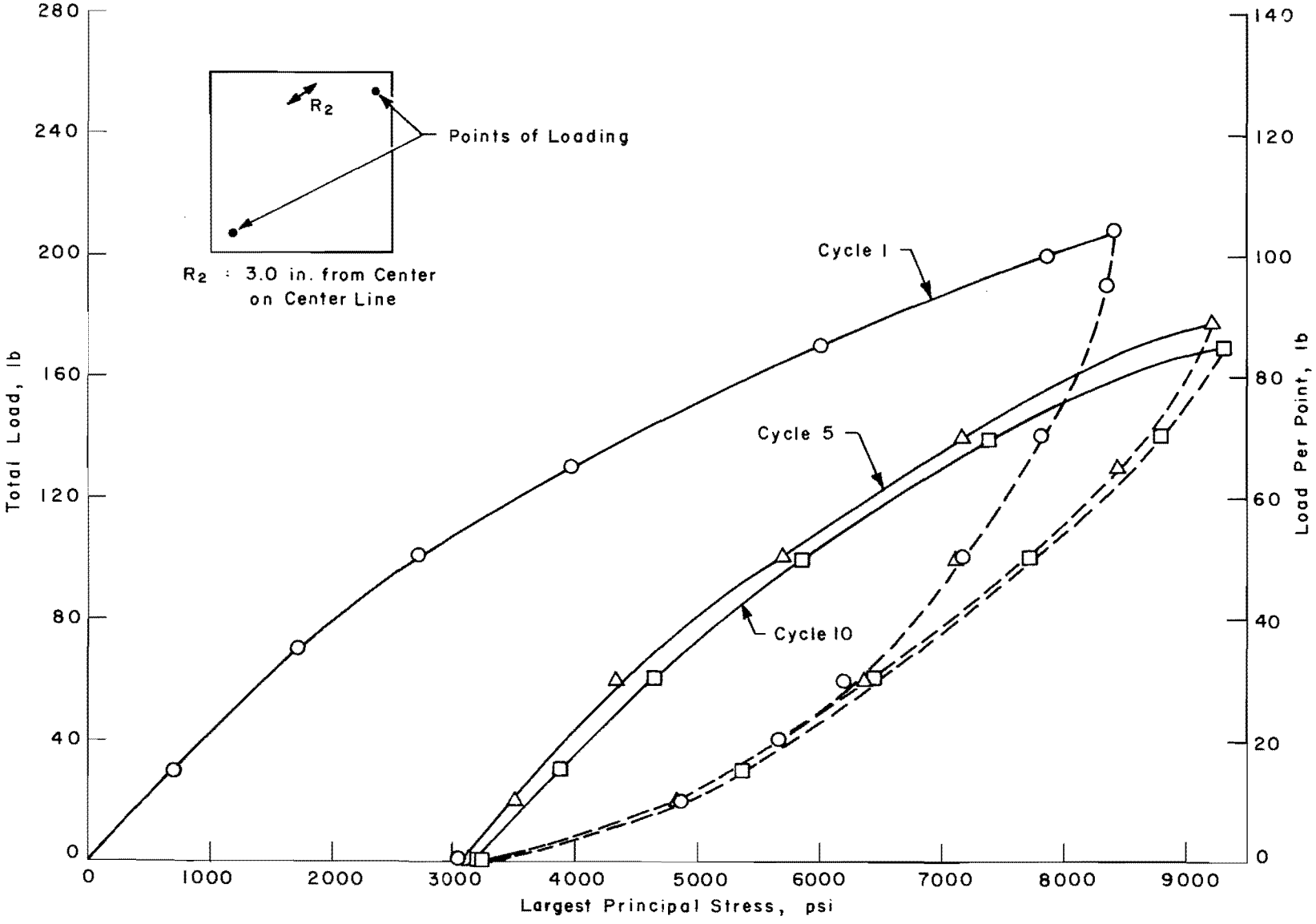

Fig A5.11. Load versus largest principal stress for rosette 2 for corner cyclic loads slab test (series 340).

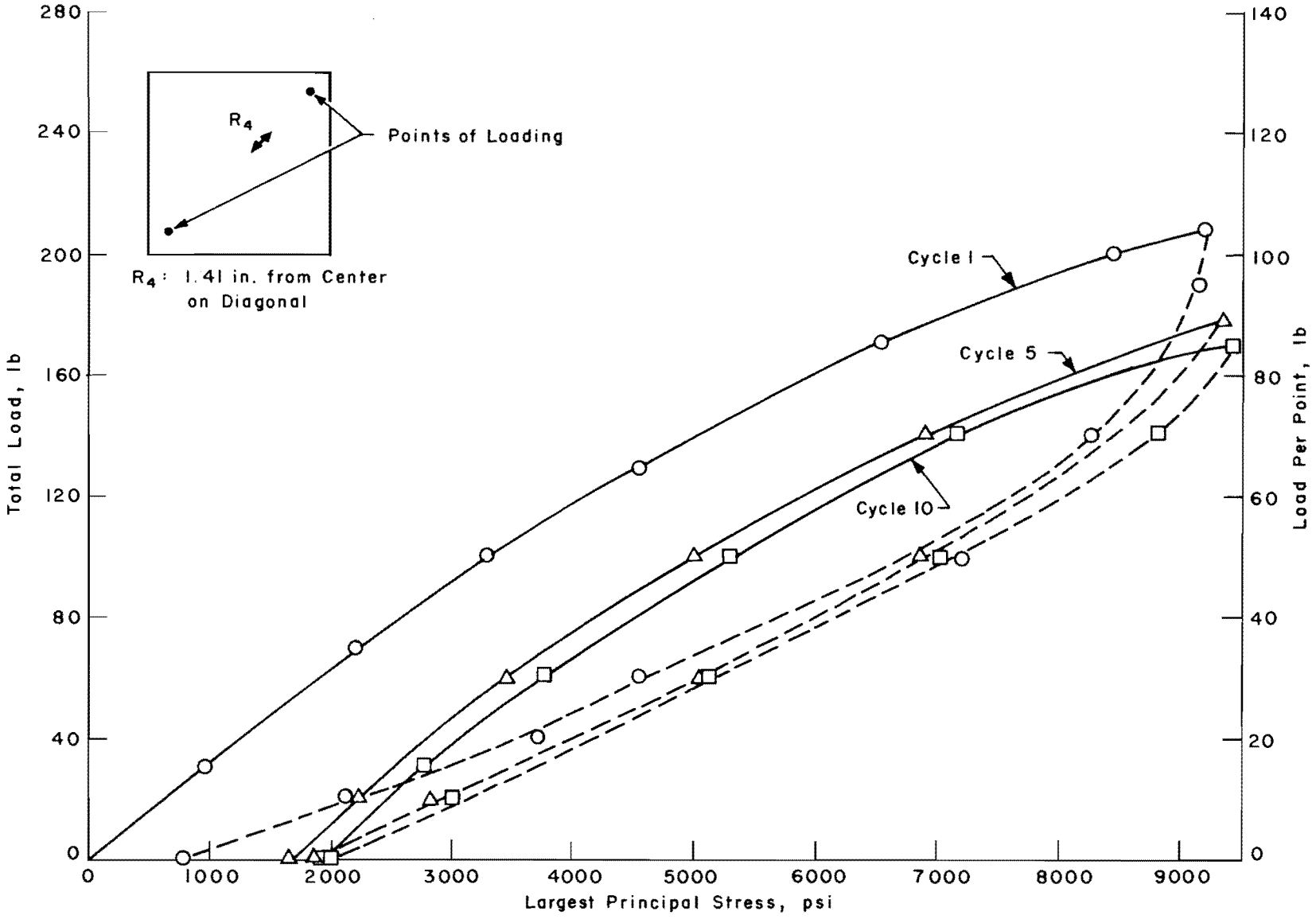

Fig A5.12. Load versus largest principal stress for rosette 4 for corner cyclic loads slab test (series 340).

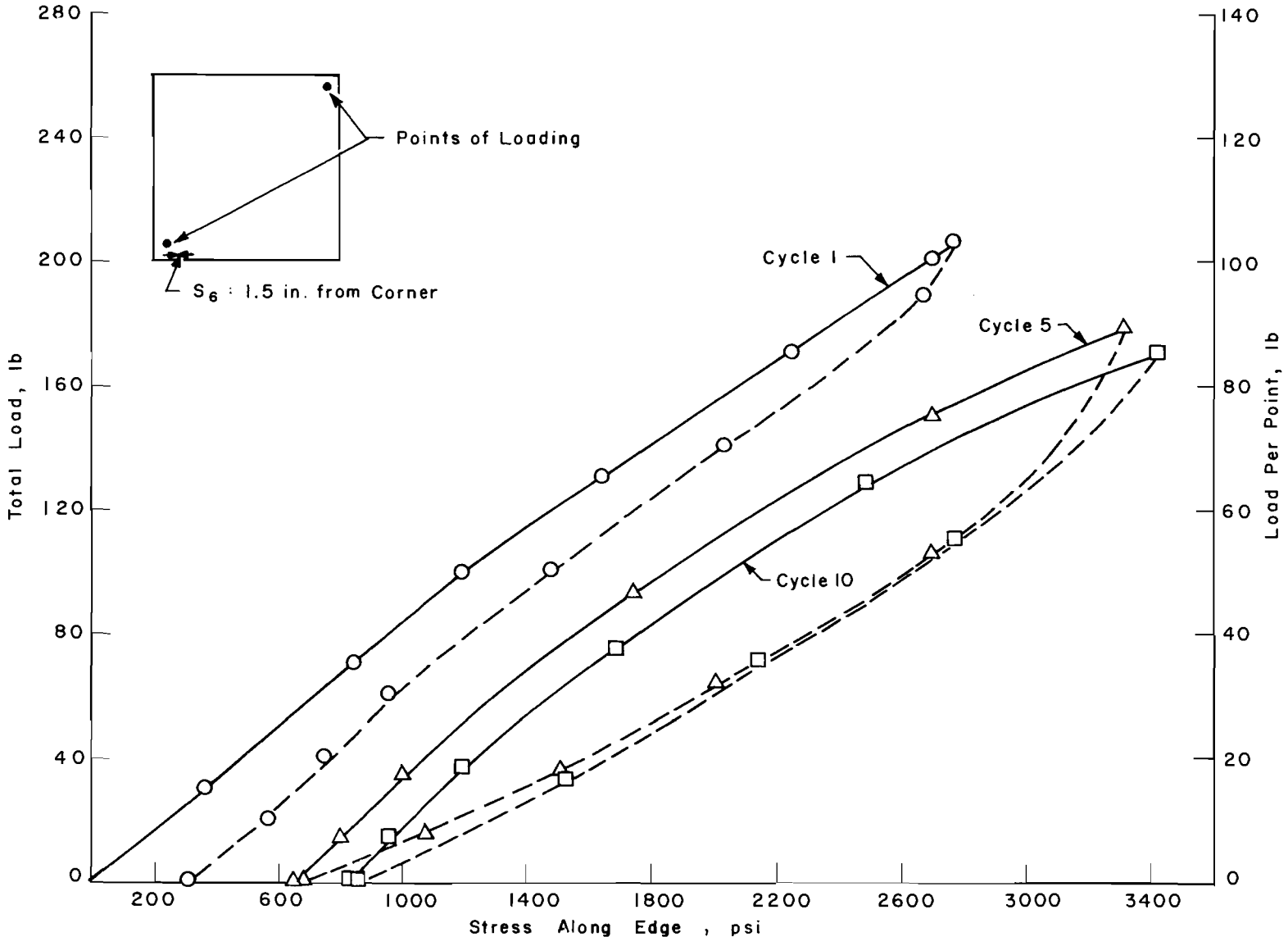

Fig A5.13. Load versus stress along edge for strain gages for corner cyclic loads slab test (series 340).

ABOUT THE AUTHORS

Sohan L. Agarwal

Assistant Professor of Civil Engineering, San Diego State College; formerly Research Engineer Assistant, Center for Highway Research, The University of Texas at Austin.

W. Ronald Hudson

Research Engineer, Center for Highway Research, The University of Texas at Texas; Associate Professor of Civil Engineering and Assistant Dean of Engineering, The University of Texas at Austin.